The Role of Cdx Genes in Normal and Malignant Hematopoiesis

Silvia Thöne

Munich 2011

Clinical Cooperative Group Leukemia

Helmholtz Center Munich – German Research Center for Environmental Health

and

University Hospital Grosshadern, Department of Internal Medicine III

Ludwig-Maximilian-University, Munich

THE ROLE OF CDX GENES IN NORMAL AND MALIGNANT HEMATOPOIESIS

Thesis Submitted for the Doctoral Degree in Natural Sciences

at the Faculty of Biology

Ludwig-Maximilian-University, Munich, Germany

By

Silvia Thöne

Munich, 24.01.2011

Klinische Kooperationsgruppe “Leukämie”

Helmholtz Zentrum München – Deutsches Forschungszentrum für Umwelt und Gesundheit

und

Klinikum der Universität München - Großhadern, Medizinische Klinik und Poliklinik III

Ludwig-Maximilians-Universität, München

DIE ROLLE VON CDX GENEN

IN DER NORMALEN UND MALIGNEN HÄMATOPOESE

Dissertation eingereicht zum Erwerb des Doktorgrades der Naturwissenschaften an der Fakultät für Biologie

Ludwig-Maximilians-Universität, München

Vorgelegt von

Silvia Thöne

München, 24.01.2011

Date of Submission: 24.01.2011

First Examiner: Prof. Dr. Dirk Eick

Second Examiner: PD Dr. Josef Mautner

Date of oral examination: 19.05.2011

Declaration

I hereby declare to have written this thesis myself and without any sources other than indicated herein. This work has not been submitted to any other examining body in this or any other form.

Munich, 24.01.2011

……

(Silvia Thöne)

The results of this study were partly published in the following publications:

Thoene S, Rawat VPS, Heilmeier B, Hoster E, Metzeler KH, Herold T, Hiddemann W, Goekbuget N, Hoelzer D, Bohlander SK, Feuring-Buske M, Buske C (2009) *The homeobox gene CDX2 is aberrantly expressed and associated with an inferior prognosis in patients with acute lymphoblastic leukemia*. Leukemia; 23(4):649-55.

Rawat VP, **Thoene S**, Naidu VM, Arseni N, Heilmeier B, Metzeler K, Petropoulos K, Deshpande A, Quintanilla-Martinez L, Bohlander SK, Spiekermann K, Hiddemann W, Feuring-Buske M, Buske C (2008) *Overexpression of CDX2 perturbs HOX gene expression in murine progenitors depending on its N-terminal domain and is closely correlated with deregulated HOX gene expression in human acute myeloid leukemia*. Blood; 111(1):309-19.

TABLE OF CONTENTS

ABBREVIATIONS & NOMENCLATURE

5-FU	5-flourouracil
AGM	aorta-gonad-mesonephros
ALL	acute lymphoblastic leukemia
AML	acute myeloid leukemia
Amp	ampicillin
AP	anterior-posterior
BFU-E	burst forming unit erythroid
BM	bone marrow
CC	cytokine cocktail
CFC	colony forming cell
CFU-E	colony forming unit erythroid
CFU-G	colony forming unit granulocyte
CFU-GEMM	colony forming unit granulocyte/ erythroid/ macrophage/ megakaryocyte
CFU-GM	colony forming unit granulocyte/ macrophage
CFU-M	colony forming unit macrophage
CI	confidence interval
CLP	common lymphoid progenitor
CMP	common myeloid progenitor
C_T	cycle threshold
DMSO	dimethyl sulfoxide
dNTP	deoxyribonucleotide triphosphate
eGFP	enhanced green fluorescent protein
eYFP	enhanced green fluorescent protein
ESC	embryonic stem cell
FACS	fluorescence activated cell sorting
FBS	fetal bovine serum
FISH	fluorescence *in situ* hybridization
HR	hazard ratio
HSC	hematopoietic stem cell
kb	kilobase
LB	Luria-Bertani
LC	liquid culture
LDA	low density array (TaqMan)

LM-PCR	linker-mediated PCR
LSC	leukemic stem cell
M	molar (mol/L)
MEP	megakaryocytic/erythrocytic progenitor
MPP	multipotent progenitor
MSCV	murine stem cell virus
NK	normal karyotype
NOD/SCID	non-obese diabetic severe combined immunodeficiency (mouse strain)
NPM	nucleophosmin
NPMc	cytoplasmatic nucleophosmin
n.s.	not significant
OS	overall survival
PB	peripheral blood
PI	propidium iodide
pMIG	MSCV-IRES-(e)GFP plasmid
qRT-PCR	quantitative reverse transcription PCR
RA	retinoic acid
RBC	red blood cell
rpm	revolutions per minute
mSCF	murine stem cell factor
SC	stem cell
SCID	severe combined immunodeficiency (mouse strain)
SD	standard deviation
SEM	standard error of mean
shRNA	short hairpin RNA
SNP	single nucleotide polymorphism
WBC	white blood cell
WT	wild type

Species	**Gene**	**Protein**
human	*CDX4*	CDX4
mouse	*Cdx4*	CDX4
zebrafish	*cdx4*	Cdx4

1. INTRODUCTION

1.1 Hematopoiesis

As the life span of most mature hematopoietic cells is limited, blood cells have to be regenerated by a process called hematopoiesis: the formation and development of blood cells in the body. In vertebrae, hematopoiesis occurs in two distinct phases: primitive (embryonic) and definitive (adult) hematopoiesis, both of which originate in the embryo (Liao *et al.*, 2002).

1.1.1 Blood Formation in the Embryo

Distinct regions of the embryonic primitive streak (PS) give rise to different mesodermal populations like blood, vasculature, kidney, cardiac and skeletal muscle (Tam and Beddington, 1987; Lawson *et al.*, 1991). Clustered homeobox (*Hox*) genes are involved in the anterior-posterior (AP) patterning of this mesodermal region and the establishing of cell identities by forming overlapping gradients along the AP axis (Favier and Dolle, 1997; Veraksa *et al.*, 2000). According to the "*Hox* code" hypothesis, a specific combinatorial expression of different *Hox* genes leads to the specification of a certain tissue type. Perturbation of this defined expression pattern by an alteration of the anterior expression boundaries results in a change in cell fate (Kessel and Gruss, 1991, Figure 1). Hemangioblasts, common progenitors for both the hematopoietic and the vascular lineage, are found at highest frequency at the posterior region of the primitive streak. After migration to the yolk sac, they give rise to both lineages in response to the interaction of the vascular endothelial growth factor (VEGF) with its receptor FLK-1 (Huber *et al.*, 2004; Choi *et al.*, 1998).

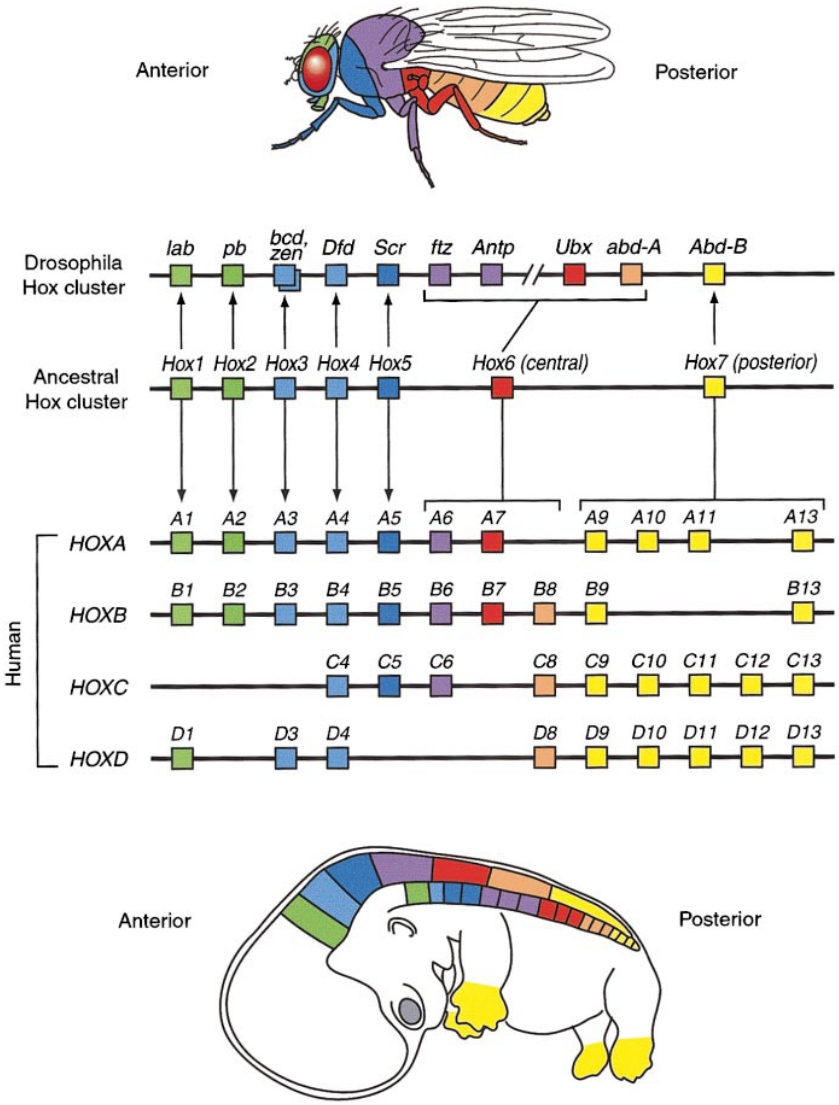

Figure 1: Genomic organization and expression patterns of *Hox* genes (Veraksa *et al.*, 2000).
Depicted are the four clusters and the expression patterns of mammalian *Hox* genes vertically aligned with their *Drosophila* orthologs. A hypothetical ancestral *Hox* cluster is presented in the middle, arrows indicate predicted evolutionary origins of both *Drosophila* and mammalian *Hox* genes. The four mammalian *Hox* clusters each contain eight to eleven genes and are located on four different chromosomes. Individual genes in different *Hox* clusters can be aligned into paralogous groups (indicated by identical colors) based on the sequence homology within their homeobox regions, and with the homeotic genes of the Drosophila *HOM-C* cluster.

Beside factors defining the AP axis, also signaling molecules involved in the dorsal ventral (DV) patterning collaborate in the embryonic blood formation. One important factor is BMP-4 which, as well as VEGF, TGF-β and FGF2, is considered a ventralizing factor in contrast to the dorsalizing factors TGF-α and EGF (Pardanaud and Dieterlen-Lievre, 1999, Figure 2). Whereas the latter antagonize hematopoietic induction, most ventralizing factors are thought to positively induce hematopoiesis (Faloon *et al.*, 2000; Winnier *et al.*, 1995).

BMP-4, for example, induces hematopoietic activity in developing murine embryonic HSCs in aorta-gonad-mesonephros (AGM) explants (Johansson and Wiles, 1995; Durand *et al.*, 2007). In contrast, deficiency of BMP-4 in the mouse generally leads to embryogenic lethality due to mesodermal defects (Winnier *et al.*, 1995).

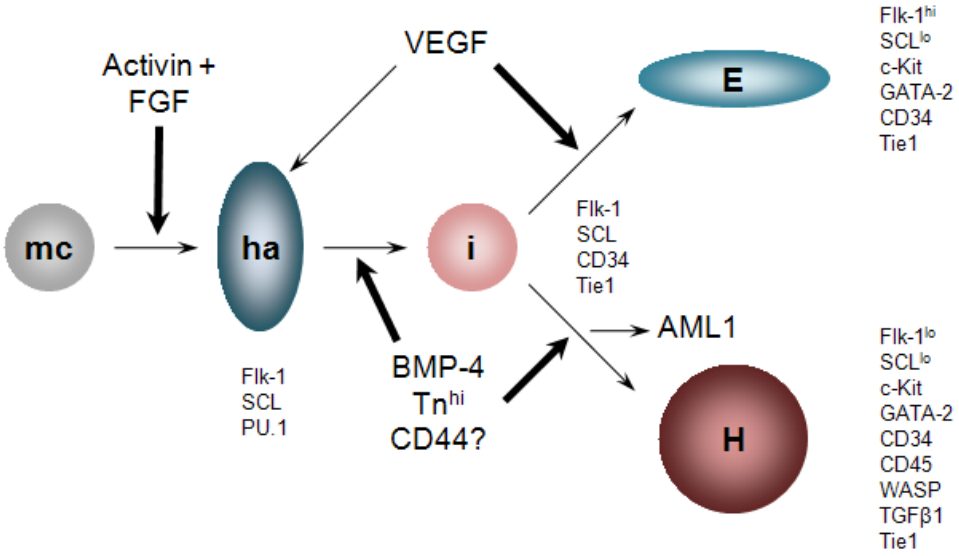

Figure 2: Model for the generation of hematopoietic cell from the embryonic mesoderm within the mammalian AGM region.
mc: mesenchymal cell, ha: hemangioblast, i: intermediate endothelial cell, E: committed endothelial cell, H: committed hematopoietic cell (modified from Marshall and Thrasher, 2001).

In the mouse conceptus, the first primitive hematopoietic cells can be found at day 7.0-7.5 after fertilization when primitive nucleated erythrocytes arise in the yolk sac. One day later myeloid progenitors can be detected (Palis and Yoder, 2001; Dzierzak and Speck, 2008, Figure 3). GATA-1 and PU.1 are key factors for this first primitive wave of hematopoiesis with the ratio of both determining the production of primitive erythroid and myeloid cells. Whereas a knockdown of pu.1 in the zebrafish leads to a shift towards the erythroid lineage, loss of gata-1 expression induces formation of myeloid cells (Galloway *et al.*, 2005; Berman *et al.*, 2005).

However, these first embryonic hematopoietic cells are a transitory population. Definitive adult hematopoietic stem cells (HSCs), with the capacity to reconstitute BM of lethally irradiated adult mice, can be found only at day 10.5 in the AGM region of the embryo. RUNX-1 is a pivotal regulator for this second hematopoietic wave, and lack of RUNX-1 results in complete absence of definitive HSCs in the AGM region as well as embryonic lethality (Chen and

Zon, 2009). At this time, other transcription factors such as c-MYB, LMO2, IKAROS and SCL are expressed in the AGM (de Jong and Zon, 2005). The contribution of yolk sac-derived progenitors to adult hematopoiesis is still uncertain and may vary between species (Orkin and Zon, 2002).

During the second half of embryogenesis, the fetal liver becomes the major site of blood formation. Importantly, HSCs in the fetal liver are not generated *de novo.* Starting at day 9.5 to 10.0, the liver is colonized by HSCs originating from the AGM as well as the yolk sac and the placenta, which undergo a massive expansion in the liver (Johnson and Moore, 1975; Kumaravelu *et al.*, 2002, Gekas *et al.*, 2005; Ottersbach and Dzierzak, 2005). Subsequently, other secondary hematopoietic organs such as spleen and thymus are seeded by HSCs derived from either their primary production sites or from fetal liver. Only shortly before birth definitive hematopoiesis shifts towards the BM (Figure 3).

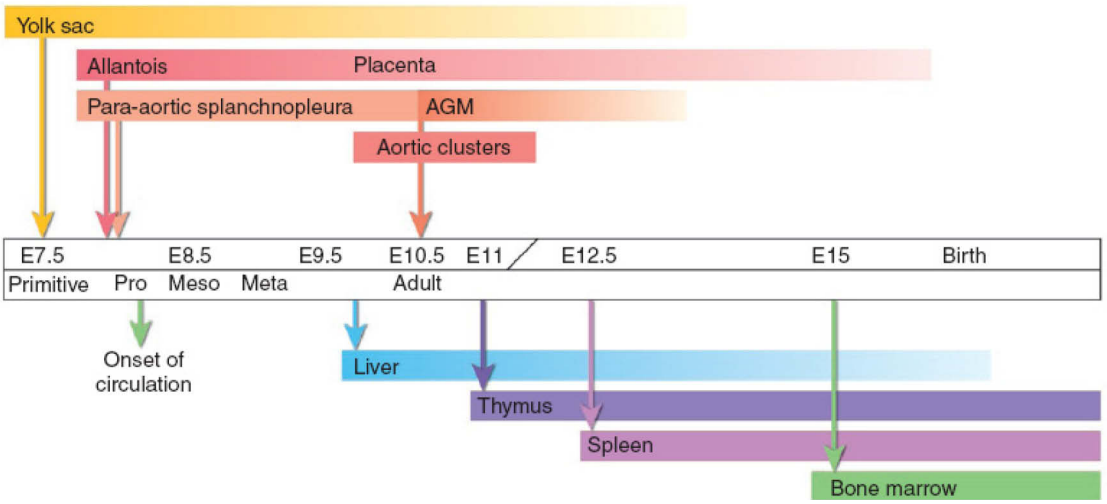

Figure 3: Timeline of hematopoietic events in the mouse conceptus.
Upper arrows indicate the onset of hematopoietic cell generation and/or appearance; lower arrows indicate the first colonization of secondary hematopoietic organs (Dzierzak and Speck, 2008).

1.1.2 Adult Hematopoiesis

Beside sporadic disease induced hematopoietic activity in extramedullary sites like spleen or liver, the BM is the exclusive site of blood formation in adult mammals (Wang *et al.*, 2009; Wolber *et al.*, 2002). The HSC population residing within the BM constitutes the top of the hematopoietic hierarchy and throughout life replenishes the pool of rapidly proliferating multipotent hematopoietic progenitors, which in turn give rise to the different hematopoietic lineages.

Blood cells can be divided into a myeloid-erythroid and a lymphoid compartment. The lineage restriction of the blood cells progressively increases with differentiation towards the mature cell types. The classical model of hematopoiesis suggests a branching point at which the multipotent progenitors become restricted to either one of the two branches. Source of all lymphoid cells hereby is the common lymphoid progenitor (CLP) whereas the common myeloid progenitor (CMP) gives rise to the myeloid and the erythroid lineage (Reya *et al.*, 2001, Figure 4). However, recently the existence of additional branching points in differentiation was described: With both granulocyte-monocyte and lymphoid potential, the lymphoid-primed multipotent progenitor (LMPP) and the granulocyte-monocyte-lymphoid progenitor (GMLP) are able to contribute to B- and T-lymphoid as well as to granulocyte/macrophage lineages (Adolfsson *et al.*, 2005; Lai *et al.*, 2005; Iwasaki and Akashi, 2007).

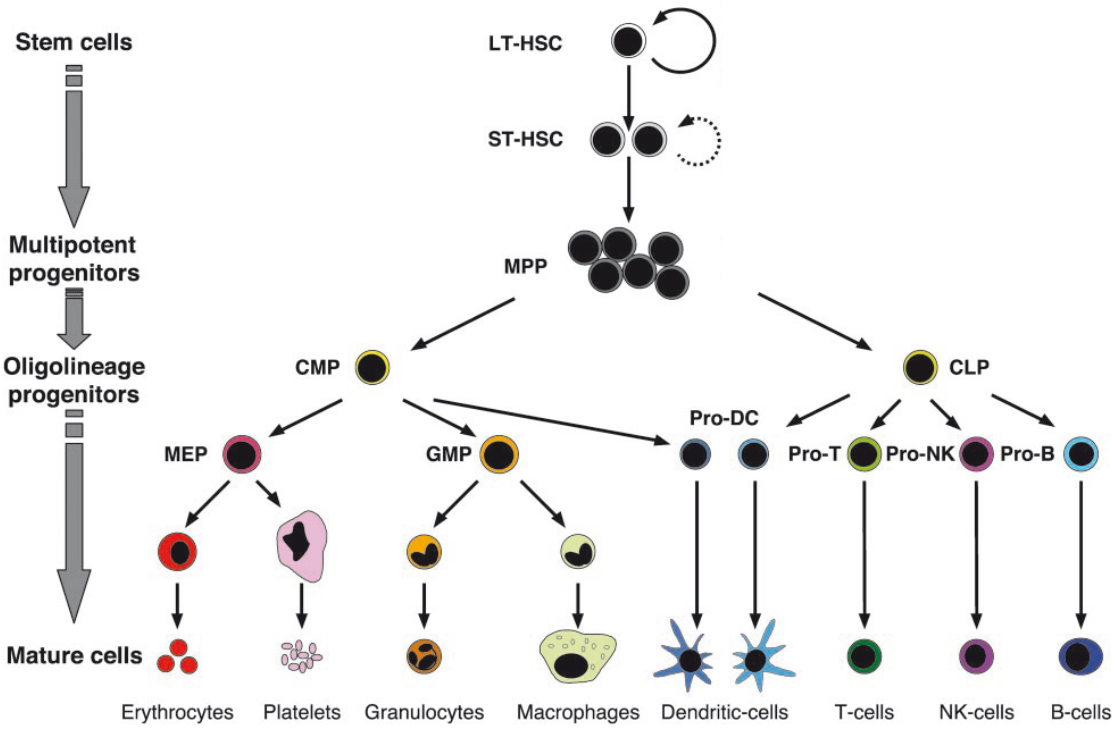

Figure 4: Classical model of hematopoietic differentiation.
Whereas long-term (LT) HSCs possess unlimited self-renewal, the ability to self-renew is limited in the short-term (ST) HSC population. Multipotent progenitors (MPP) do not self-renew or only briefly and give rise to the oligolineage-restricted progenitors CMP and CLP which in turn produce a progeny becoming more and more lineage-restricted (according to Passegue *et al.*, 2003).

Lymphoid Lineage

The two main types of lymphoid cells, T- and B-cells, constitute the adaptive immune system and are derived from a common lymphoid progenitor. Chromatin remodeling activities as well as a complex network of transcription factors leading to the expression of either myeloid or lymphoid transcripts is responsible for the initial step of lineage priming. The LEF/TCF-dependent WNT/β-Catenin pathway is one key regulatory component for the specification of the T- and B-cell lineages. Mice deficient for TCF1 and LEF-1 for example show a severe defect of the early thymocyte compartment with a reduced T-cell count (Verbeek *et al.*, 1995). NOTCH1 receptor signaling is critical for initiation of T-cell development by upregulating the transcription of TCF1 or GATA3 (Dias *et al.*, 2008).

Proper expression of LEF-1 furthermore is of importance for survival and proliferation in normal B-cell development (Bruhn *et al.*, 1997; Reya *et al.*, 2000). EBF1, its target PAX5, and FLT3 are also central to B-lymphopoiesis: Whereas early B-lymphopoiesis requires FLT3, with a knockout leading to severe reduction in the number of B-cell progenitors, FLT3 has to be repressed by PAX5 to allow further differentiation (Mackarehtschian *et al.*, 1995; Holmes *et al.*, 2006; Dias *et al.*, 2008). PAX5 on the other hand is critical for B-lymphoid commitment and loss of PAX5 expression leads to a differentiation block in early B-cells and de-differentiation of even mature B-lymphocytes (Urbanek *et al.*, 1994; Nutt *et al.*, 1997; Cobaleda *et al.*, 2007).

Myeloid Lineage

Myelocytes, including granulocytes, macrophages and megakaryocytes, play roles in different processes including blood clotting, the adaptive and the innate immunity. PU.1, whose expression is required both in the lymphoid and in the myeloid lineage, is crucial for the myeloid lineage specification. This protein acts dose-dependent with low levels promoting B-lymphoid differentiation of hematopoietic progenitors and high levels driving macrophage differentiation (DeKoter and Singh, 2000; Iwasaki *et al.*, 2003). In the myeloid lineage, the transcriptional activity of PU.1 is antagonized by C/EBPα and GFI-1, which are able to block monocytic differentiation and commit the progenitors to granulocytic differentiation (Dahl *et al.*, 2003; Dahl *et al.*, 2007, Figures 5 and

6). However, low levels of PU.1 are still required for proper granulocytic development (Friedman, 2007) and it cooperates with GATA-2 to induce mast cell differentiation (Walsh *et al.*, 2002).

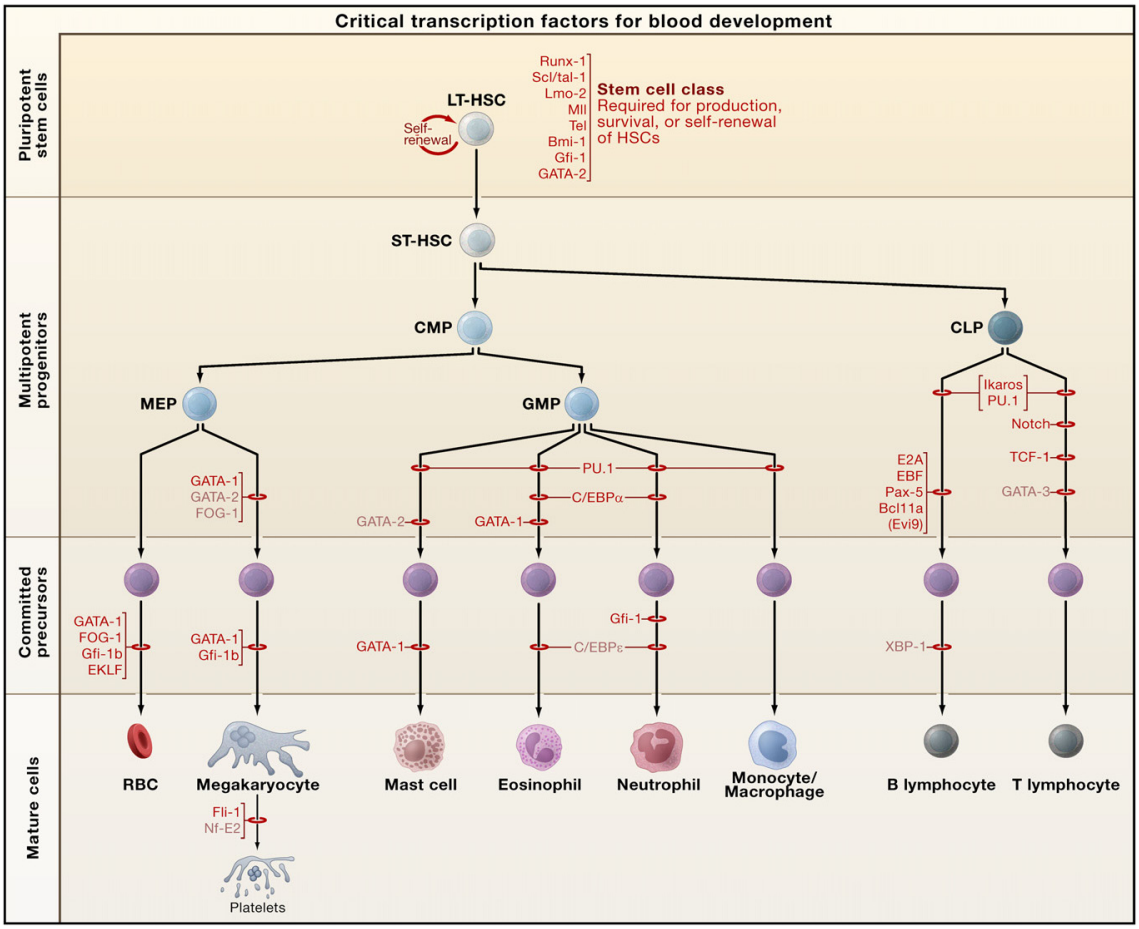

Figure 5: Transcription factors in hematopoiesis
Red circles indicate the stage at which the absence of a respective transcription factor blocks hematopoietic development. The red factors have been associated with oncogenesis whereby the light red factors have not been found to be translocated or mutated in hematopoietic malignancies yet (Orkin and Zon, 2008).

Erythroid Lineage

Erythroid cells, having the function to supply the body with oxygen, are derived from the same precursor as the myeloid lineage: the megakaryocytic/ erythrocytic progenitors (MEP). To allow erythroid differentiation, Gata-1 is indispensable. This factor antagonizes PU.1 and is highly expressed in this hematopoietic progenitor subtype (Rekhtman *et al.*, 2003; Rekhtman *et al.*, 1999). Deficiency of GATA-1 in the embryo leads to a block in the early proerythroblast stage and subsequent death due to severe anemia (Fujiwara *et*

al., 1996). As depicted in Figure 6, the balance between the erythroid-specific Kruppel-like factor (EKLF) and FLI-1 subsequently regulates the differentiation towards either the erythroid or the megakaryocytic lineage. Whereas FLI-1 is required for megakaryopoiesis and is able to activate the promoters of several megakaryocyte-specific genes, EKLF inhibits FLI-1 dependent transcription but induces erythroid differentiation (Starck *et al.*, 2003).

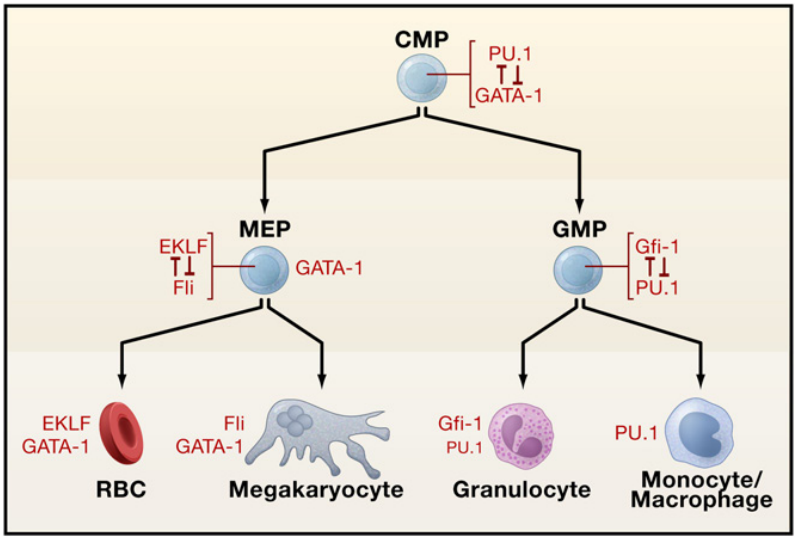

Figure 6: Transcriptional antagonism in myeloid lineage determination (Orkin and Zon, 2008).
CMP: common myeloid progenitor, MEP: megakaryocyte/erythroid progenitor, GMP: granulocyte/macrophage progenitor, RBCs: red blood cells.

1.1.3 Hematopoietic Stem Cells

Although the presence of different lineages within the hematopoietic system is well known, the stem cell concept of a few cells sitting on top of the hematopoietic pyramid and possessing the capacity to give rise to all the hematopoietic lineages is relatively new. In 1994 Morrison and Weissman were the first to isolate and characterize murine LT-HSCs, which they could highly enrich by fractionation according to their Thy-1.1^{lo}/Sca-1^{hi}/Lin^{-} phenotype. A few years later, in 1997, Bhatia *et al*. showed in the human system that hematopoietic stem cells reside within the Lin^{-}/CD34^{+}/CD38^{-} compartment. Due to their *in vivo* repopulating activity in severe combined immunodeficiency (SCID) mice these cells are also referred to as SCID repopulating cells. In the following years, the enrichment methods were refined and additional markers were identified for isolation of mouse and human HSCs, as depicted in Figure 7.

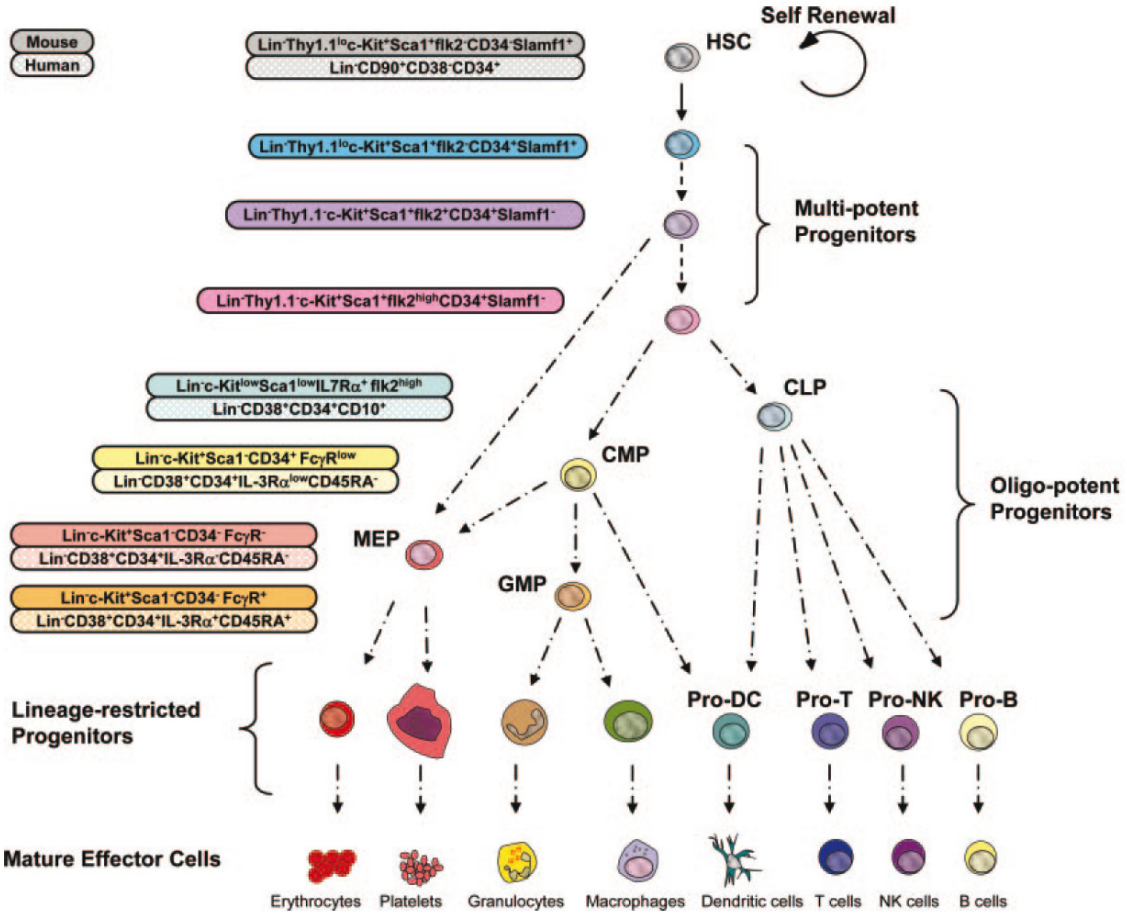

Figure 7: Hematopoietic subpopulations and their phenotype.
Surface markers used for isolation of the different populations from mouse (bottom) and human (top) are indicated. MPP: multipotent progenitors with limited self-renewal leading to transient but multilineage reconstitution, CMP: common myeloid progenitor, CLP: common lymphoid progenitor, Pro-T: T-cell progenitor, GMP: granulocyte/ macrophage progenitor, MEP: megakaryocyte/ erythroid progenitor (Weissman and Shizuru, 2008).

HSCs, like all stem cells, are characterized by two main properties: multipotency, which is the capacity to generate all cell types of the hematopoietic lineage, and the ability to self-renew, hereby allowing the maintenance of the HSC pool by asymmetric cell division. These characteristics allow one single donor HSC to reconstitute the whole blood system of a recipient animal and replenish its blood cell pool from thereon in. Besides long-term (LT-) HSCs with indefinite self-renewal potency there are also short-term (ST-) HSCs which possess limited self-renewal capacity. Multipotent progenitors (MPPs) show multipotency and have high proliferative potential but are not able to self-renew (Morrison *et al.*, 1997).

After birth, the number of HSCs in the BM is maintained at a steady state and the HSCs mainly remain quiescent. Not all of the cellular signals regulating self-

renewal and quiescence are known, however several candidate factors have been identified (Figure 8). One essential factor for maintaining the adult HSC pool is the ETS-related transcription factor TEL1/ETV6. Inactivation of this gene in the hematopoietic compartment leads to loss of HSCs (Hock *et al.*, 2004). A positive regulator of self-renewal is HOXB4 which, when overexpressed in the BM, leads to an expansion of the HSC population *in vitro* and *in vivo* (Sauvageau *et al.*, 1995). A knockout of HOXB4, however, leads to only mild defects in the proliferation of HSCs (Brun *et al.*, 2004), suggesting compensatory mechanisms by other members of the HOX family. BMI-1, a member of the Polycomb group of proteins, regulates self-renewing cell division, and a deficiency of BMI-1 leads to proliferation arrest, apoptosis and differentiation of leukemic cells (Park *et al.*, 2003).

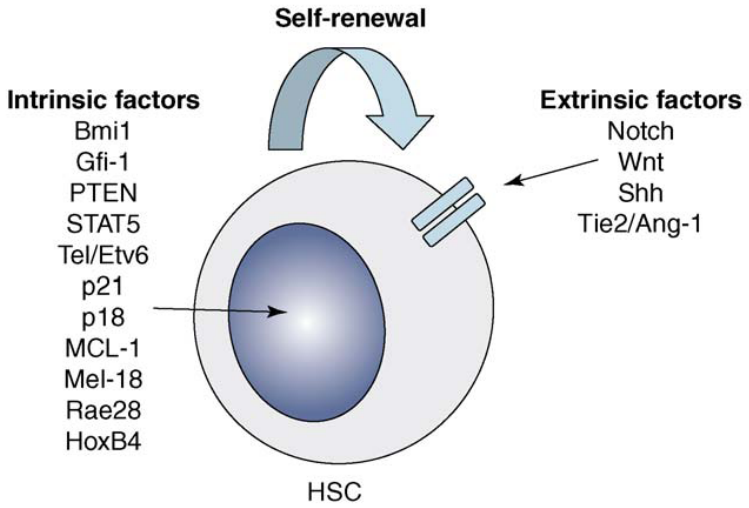

Figure 8: Known factors of HSC maintenance (Akala and Clarke, 2006).

Besides these intrinsic factors, HSC self-renewal also depends on extrinsic regulators provided by the microenvironment, i.e. the stem cell niche. Amongst those is the Notch signaling pathway, which is highly active in HSCs and downregulated with advancing differentiation. Inhibition of this pathway leads to enhanced differentiation and depletion of the HSC pool *in vivo* (Duncan *et al.*, 2005). The LEF/TCF-dependent WNT/β-Catenin pathway is also required for maintaining the HSC function (Reya *et al.*, 2003; Willert *et al.*, 2003). Whereas mice lacking β-Catenin expression do not show an altered number of HSCs, β-Catenin overexpression leads to accumulation of HSCs by blocking HSC differentiation (Cobas *et al.*, 2004; Scheller *et al.*, 2006; Kirstetter *et al.*, 2006).

1.2 Leukemia

In normal hematopoiesis self-renewal, proliferation and differentiation are delicately balanced. Genetic alterations affecting these processes can thus lead to deregulation of the normal hematopoietic program. Blocking differentiation of early hematopoietic progenitors and clonal expansion of neoplastic cells in the BM leads to an accumulation of the leukemic bulk, replacement of the remaining healthy hematopoietic system and finally to a deprivation of mature, functional hematopoietic cells.

Analysis of this cytogenetic and molecular heterogeneous group of diseases revealed that genetic alterations occurring in leukemia can be assigned to two different groups: one that promotes survival advantage and/or increased proliferative potential, and the other one that confers self-renewal properties to the affected cells (Dash and Gilliland, 2001; Gilliland *et al.*, 2004). Dash & Gilliland observed cooperation in particular between constitutively activated tyrosine kinase molecules and fusion of signal transduction genes. In these cases, activated tyrosine kinases led to enhanced proliferation and/or antiapoptotic activity whereas fused signal transduction genes disturbed hematopoietic differentiation and enabled the cells to self-renew.

1.2.1 Acute Myeloid Leukemia

AML is a malignant clonal disorder of the myeloid hematopoietic compartment. It is the most common form of acute leukemia in adults with an incidence of 3.5 cases per 100,000 people and year and a median age of 67 years at diagnosis (www.seer.cancer.gov). According to the World Health Organization (WHO), AML is defined by the presence of more than 20% of myeloid blasts in the BM (Gilliland and Tallman, 2002). There is massive evidence that, like many cancers, AML is a multistep disease with an accumulation of multiple mutations as well. Beside perturbation of the normal differentiation program, the leukemic clone additionally has to acquire enhanced self-renewal capacity as well as increased proliferative potential promoting clonal expansion.

Chromosomal Translocations in AML (Abnormal Karyotype)

40% to 45% of AML cases carry chromosomal abnormalities and are referred to as AML with abnormal karyotype. In 20-25% of AML, loss of function alterations of core binding factor (CBF) subunits can be found. The translocation t(8;12)(q22;q22) hereby results in the AML1-ETO fusion protein and correlates especially with AML M2, whereas the inversion inv(16)(p13q22) leads to expression of CBFβ-SMMHC which is associated with AML M4eo (Gilliland and Tallman, 2002). Other translocations, which impair hematopoietic differentiation, include rearrangements of the mixed lineage leukemia (*MLL*) gene. MLL rearrangements are mostly found in myelomonocytic, monoblastic, or monocytic leukemia (AML M4, M5a and M5b, respectively) and constitute up to 10% of *de novo* AML. The t(15;17) (PML-RARα) translocation strictly correlates with acute promyelocytic leukemia (AML M3) and is found in 95% of these cases. Both MLL-rearrangements and PML-RARα were shown to immortalize hematopoietic progenitors (Gilliland and Tallman, 2002; Cozzio *et al.*, 2003; Gilliland *et al.*, 2004; Krivtsov *et al.*, 2006, Figure 9A).

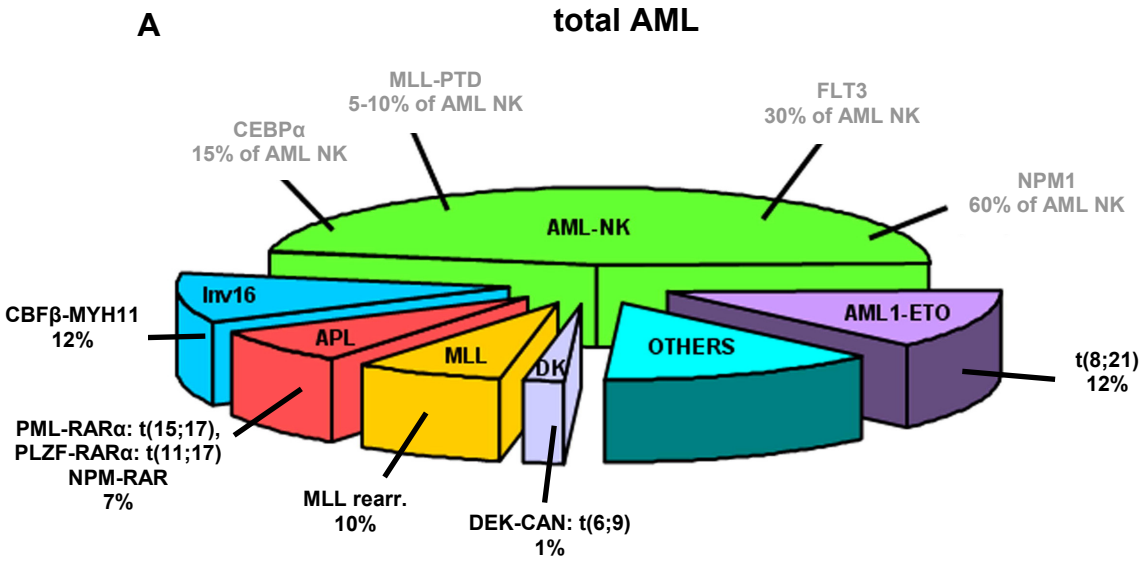

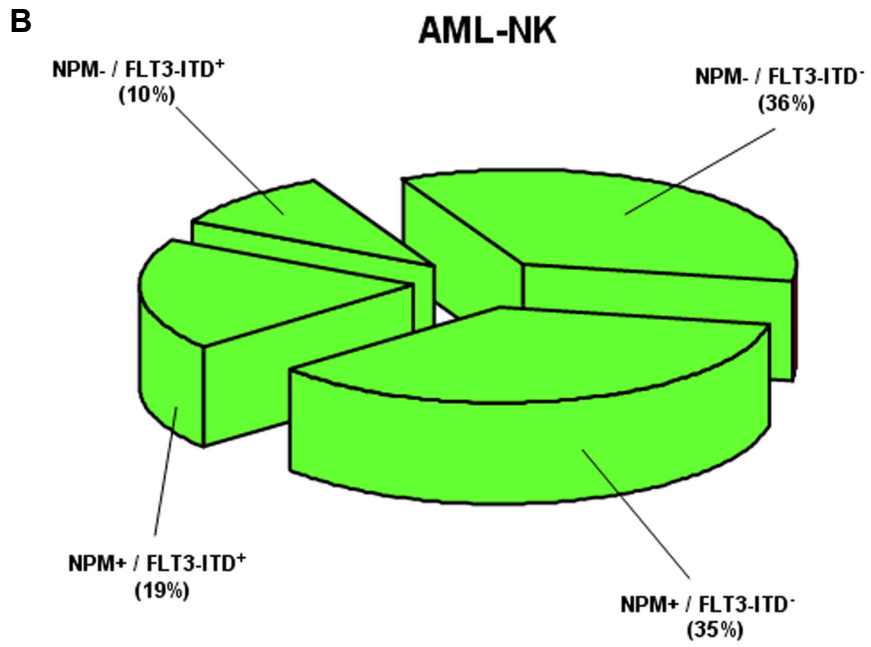

Figure 9: Genetic alterations in adult AML.
(A) Pie chart presenting cytogenetic alterations in adult AML and frequency of gene mutations in AML with normal karyotype (AML NK). (B) Pie chart showing the relationship between *NPM1* mutations and FLT3-ITD in AML-NK (modified from Falini *et al.*, 2007).

Mutations in AML (Normal Karyotype)

Mutations characterize the second group of AML. As these genetic alterations cannot be detected by fluorescence *in situ* hybridization (FISH), AML cases harboring these mutations are also referred to as AML with normal karyotype (AML NK). 25% to 30% of AML NK is associated with mutations of the tyrosine kinase *FLT3,* This tyrosine kinase is constitutively activated by internal tandem duplications (FLT3-ITD) or point mutations of the tyrosine kinase domain (FLT3-TKD). The resulting autodimerization and subsequent autophosphorylation is thought to promote proliferation by activating signaling pathways such as RAS/MAPK, STAT and AKT/PI3K. In about 35% of total AML and up to 60% of AML NK, mutated cytoplasmatic nucleophosmin (NPMc) can be found (Falini *et al.*, 2007, Figure 9). NPM-mutated cases are frequently associated with FLT3-ITD mutations, which can be detected in approximately 50-60% of the $NPMc^+$ patients (Falini *et al.*, 2007, Figure 9B). Other recurrent mutations occur in *CEBPα* or *RAS* with frequencies of 20% and 10% of AML, respectively (Rau and Brown, 2009).

Homeobox Gene Deregulation in AML

Deregulations of homeobox genes, as for example *PBX3*, *MEIS1* or *POU4F1*, are found in both AML with normal and abnormal karyotype (Miller and Stamatoyannopoulos, 2010). As reported in several gene expression profiling studies, the deregulation of *HOX* gene expression is a frequent observation (Debernardi *et al.*, 2003; Verhaak *et al.*, 2005; Miller and Stamatoyannopoulos, 2010). As shown in Figure 10, more than 60% of AML patients, particularly patients with normal karyotype, show aberrant expression of *HOX* genes. In a small subset of cases deregulation of MLL, a known upstream regulator of *HOX* genes, is responsible for the aberrant *HOX* gene expression. For the vast majority of patients, however, the cause for *HOX* gene deregulation is still unclear as most of the occurring mutations are not able to upregulate leukemogenic *HOX* genes.

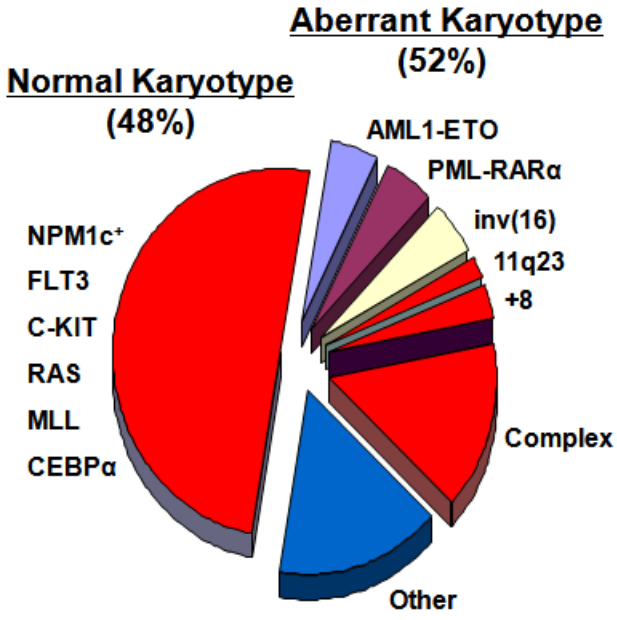

Figure 10: *HOX* gene deregulation in different subgroups of AML.
AML subgroups with deregulation of *HOX* genes are coloured red (frequency of genomic aberrations according to www.onkodin.de).

The largest group characterized by *HOX* gene deregulation is AML with normal karyotype, particularly AML with normal karyotype and mutated NPM, Figure 11). Again, the reason for *HOX* gene deregulation is not clear, as $NPMc^+$ is not able to deregulate *HOX* expression and the *HOX* upstream regulator MLL is not deregulated in the majority of cases. In addition, the differentiation stage of the

cells cannot explain this situation, as the leukemic blasts in cases with NPMc positive AML are negative for CD34 (Figure 11B).

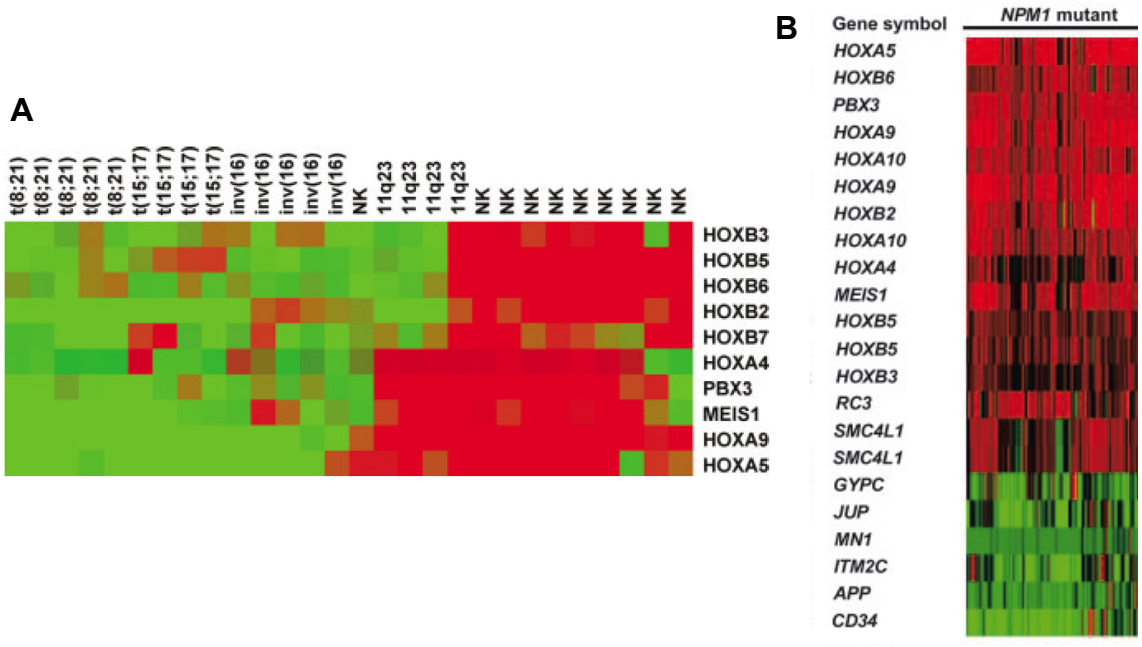

Figure 11: Homeobox gene expression in AML.
A) Hierarchical clustering of homeobox gene expression in 27 AML patients (Debernardi *et al.*, 2003) B) expression signature of NPMc$^+$ AML (Verhaak *et al.*, 2005). red: upregulation, green: downregulation, NK: normal karyotype.

1.2.2 Acute Erythroid Leukemia

Acute erythroid leukemia (AML M6), a subtype of AML, constitutes about 5% of AML. No specific genetic alterations are linked to AML M6, which is associated with an especially poor treatment outcome (Kasyan *et al.*, 2010). This subtype is characterized by the presence of a predominant erythroid population, which, in the case of AML M6a, is mixed with myeloid blasts. In contrast, in pure erythroid leukemia (AML M6b) the leukemic clone exclusively consists of erythroblasts. Commonly, erythroid markers such as glycophorin A (which correlates with Ter119 in the mouse) are used for classification of this subtype (Kina *et al.*, 2000). However, cases with more immature erythroid blasts and missing known erythroid markers have also been described. These abnormal cases are aptly called “cryptic erythroid leukemia” or “early erythroblastic leukemia” (Greaves *et al.*, 1983; Villeval *et al.*, 1986). The neoplastic clone found in these cases is derived from transformed c-Kit$^+$ BFU-E or c-Kit$^+$/CD71$^+$ CFU-E but does not show expression of mature erythroid markers (Shimizu *et al.*, 2008, Figure 12).

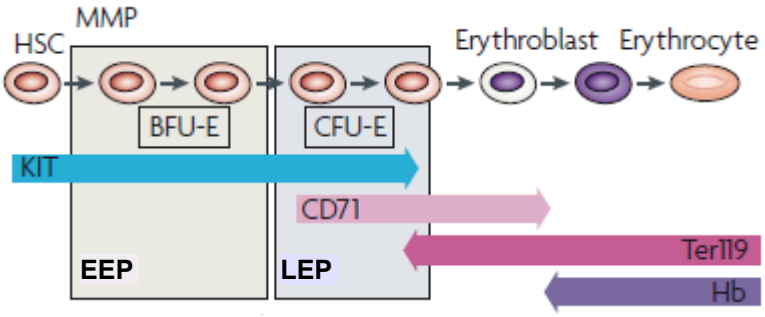

Figure 12: Expression of the lineage markers c-Kit, CD71 and Ter119 in different stages of murine erythroid differentiation.
EEP: early erythroid progenitor, LEP: late erythroid progenitor, BFU-E: burst-forming unit-erythroid, CFU-E: colony-forming unit-erythroid (according to Shimizu *et al.*, 2008).

1.2.3 Acute Lymphoblastic Leukemia

Acute lymphoblastic leukemia (ALL), a malignant disorder of the lymphoid compartment, derives from either the B- or the T-lineage. ALL affects both children and adults with a median age of 13 at diagnosis and an incidence rate of 1.6 per 100,000 people per year (www.seer.cancer.gov). Whereas more than 80% of childhood ALL can be cured, in the adult there is an increased number of molecular subtypes with poor prognosis (Teitell and Pandolfi, 2009).

Based on immunophenotyping, ALL of the B-cell lineage can be divided in common ALL (cALL), pro-B ALL, pre-B ALL and mature B-cell ALL. T-cell ALL subtypes comprise pro-T ALL, pre-T ALL, cortical T-ALL and mature T-cell ALL. Recurrent chromosomal abnormalities are one hallmark of ALL and can be found in 60-70% of the adults (Faderl *et al.*, 2003). With a prevalence of 20-30%, the most frequent of these chromosomal aberrations is the t(9;22) translocation, also known as the Philadelphia (Ph) chromosome. This translocation is found almost exclusively in $CD10^+$ precursor ALL and is associated with very high-risk ALL (Ottmann and Wassmann, 2005; Ravandi and Kebriaei, 2009). Patients with 11q23 (MLL) rearrangements have a poor prognosis as well, especially those with a MLL-AF4 translocation which has a 50% prevalence in adult pro-B ALL (Gleissner *et al.*, 2005; Pui *et al.*, 2008). Most characteristic for mature B-ALL are c-Myc rearrangements, whereas the most common genetic aberrations in mature T-ALL are T-cell receptor (TCR) rearrangements (Faderl *et al.*, 2003). However, in ALL, as in many other cancers, there is evidence that chromosomal aberrations alone are not sufficient to induce overt leukemia but have to cooperate with other genetic

lesions. Indeed, by genome-wide analyses, genetic alterations have been identified in a number of genes regulating lymphoid development. For example, affected in almost one third of ALL cases is *PAX5*, but *TCF3*, *LEF1*, *IKAROS* or *NOTCH1* are also frequently targeted by mutations (Weng *et al.*, 2004; Mullighan *et al.*, 2007).

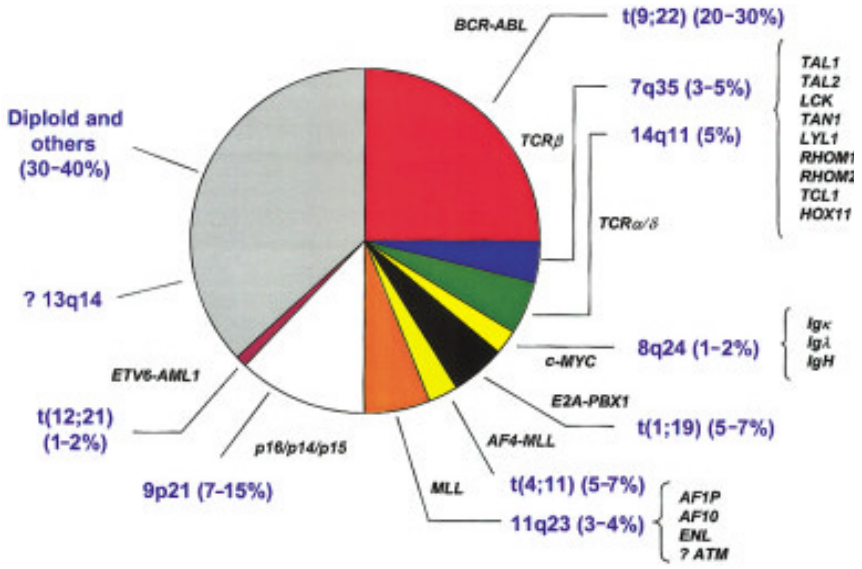

Figure 13: Cytogenetic abnormalities in adult ALL (Faderl *et al.*, 2003).

Furthermore, deregulated expression of *HOX* genes is a recurrent event in ALL. Deregulation of the whole *HOXA* gene cluster can be observed in inv(7) positive T-ALL cases where the distal part of the *HOXA* cluster is juxtaposed to the *TCRβ* locus (Soulier *et al.*, 2005). In the affected patients, particularly high levels of *HOXA10* and *HOXA11* are found (Speleman *et al.*, 2005). Deregulation of *HOXA* cluster genes as well as *HOXC6* was reported in MLL and CALM-AF10 positive T-ALL cases (Ferrando *et al.*, 2003; Soulier *et al.*, 2005).

1.2.4 Cancer Stem Cells and the Leukemic Stem Cell Model

The different subtypes of leukemia are well characterized by means of their genetic and morphological phenotype. Already at the beginning of the last century, leukemia was classified into chronic lymphocytic leukemia, chronic myeloid leukemia, acute lymphocytic leukemia and acute myeloid leukemia/ erythroleukemia (Reschad and Schilling-Torgau, 1913). Despite this, the origin of the neoplastic clone remained unclear for a long time. Although Arthur

Pappenheim postulated the existence of HSCs already in 1917 (Pappenheim, 1917), the existence of cancer stem cells (CSCs) as a population with similar properties was only proven in the late 20th century. In 1994 it was shown that an immature subset of leukemic cells derived from AML patients was able to engraft SCID or non-obese diabetic severe combined immunodeficiency (NOD/SCID) mice and exhibited the same phenotype observed in patients (Lapidot *et al.*, 1994; Bonnet and Dick, 1997). Since that time, CSCs have been identified for several types of cancer including breast cancer and glioma (Al-Hajj *et al.*, 2003; Singh *et al.*, 2003). Due to the establishment of different functional *in vitro* and *in vivo* assays, CSCs are especially well analyzed within the hematopoietic system where they are also referred to as leukemic stem cells (LSCs) (Warner *et al.*, 2004).

CSCs are cells within a tumor which possess the capacity to self-renew and, by definition, fulfill three criteria: CSCs are enriched for tumorigenic ability, serially propagate tumor growth *in vivo* and are able to regenerate the whole phenotypic diversity of the tumor (Reya *et al.*, 2001).

Based on gene expression analysis and *in vivo* studies, the capacity to self-renew was identified as one key property of both normal HSCs and LSCs, an ability that is normally lost during the process of cell differentiation. Therefore, an important question to answer is if LSCs are derived directly from normal adult HSCs, which escaped regulation networks, or from a more mature hematopoietic cell, e.g. a committed progenitor cell, which acquired the capacity to self-renew by genetic alterations. Due to the shared attribute of self-renewal capacity of both normal and leukemic stem cells, it was first suggested that leukemia originates from transformed HSCs by accumulation of multiple mutations. This was supported by the fact that the cells capable of initiating AML in the NOD/SCID mouse model (SCID leukemia-initiating cell, SL-IC) were highly enriched in the CD34-positive compartment (Lapidot *et al.*, 1994; Bonnet and Dick, 1997). However, more and more evidence indicates that leukemia can also arise from more committed progenitors in which the self-renewal program is reactivated due to the activation of appropriate oncogenes (Figure 14). Krivtsov *et al.* (2006) for example described that committed granulocyte/monocyte progenitors (GMPs) expressing the fusion gene MLL-AF9 undergo leukemic transformation. Another example is the CALM/AF10 murine

BM transplantation model, where the leukemia propagating cell was found to reside within the progenitor compartment positive for the lineage marker B220 (Deshpande *et al.*, 2006).

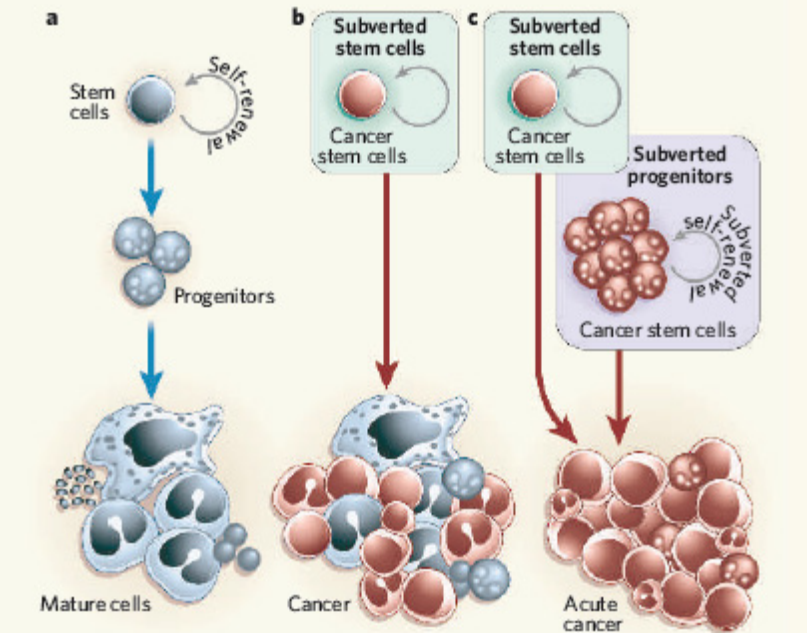

Figure 14: Origin of CSCs.
CSCs can either be derived from normal stem cells (a) with intrinsic self-renewal properties or from progenitor cells (b & c) which reacquired self-renewal properties by genetic lesions (Passegue, 2006).

The fact that both leukemic and normal stem cell share the capacity to self-renew leads to the assumption that the self-renewal capacity of both cell types is driven by equal pathways. Indeed, overlapping pathways were identified (Figure 15): BMI-1 for example is essential for the self-renewal of the normal HSC but is also indispensable to maintain the self-renewal properties of the LSC in the murine model of HOXA9 and MEIS1 coexpressing AML (Lessard and Sauvageau, 2003; Park *et al.*, 2003). Frequently observed in cancer is also a deregulation of genes associated with embryonic development like SCL or RUNX1, which were initially identified because of their aberrant expression in leukemia (Izraeli, 2004; Ben-Porath *et al.*, 2008).

Another critical regulator of self-renewal is the WNT pathway, which was shown to regulate *Hox* expression in the embryo (Lohnes, 2003). Besides being required for normal stem cell function, this pathway also leads to leukemic transformation when deregulated (Reya *et al.*, 2003; Petropoulos *et al.*, 2008). Interestingly, in many tissues in which stem cells are regulated by the WNT

cascade, the cancer cells are strictly dependent on this pathway (Reya *et al.*, 2003).

Another example is MLL, which regulates developmental processes during embryogenesis as a master regulator of *Hox* gene expression and is found to be a fusion partner of various proteins in leukemia.

Also *Hox* genes themselves are able to induce leukemia when ectopically expressed (Owens and Hawley, 2002). Many of the lesions identified in AML in the murine model do not cause leukemia on their own and some of them, as for example AML1-ETO, have even been detected in cells of healthy individuals (Nucifora *et al.*, 1993). In contrast, many *HOX* genes possess a strong oncogenic potential with their aberrant expression leading to induction of leukemia (Perkins *et al.*, 1990; Thorsteinsdottir *et al.*, 2002; Fischbach *et al.*, 2005).

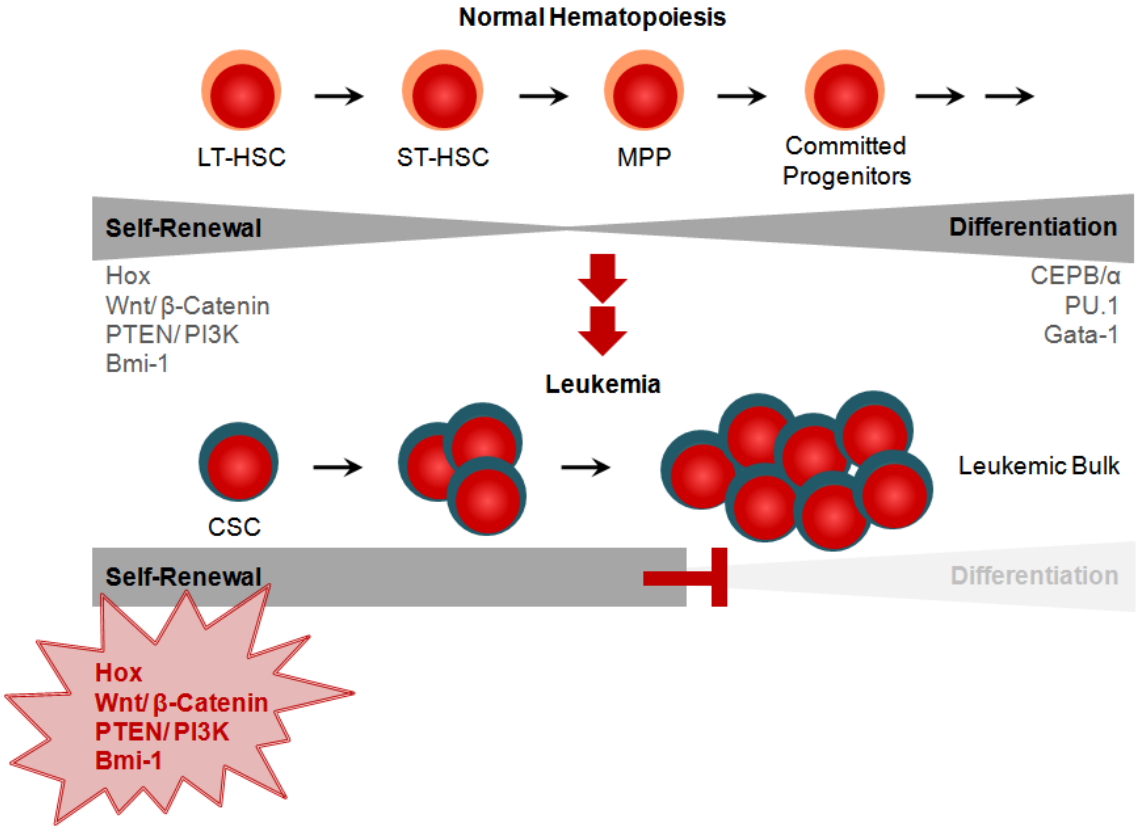

Figure 15: Deregulation of genes involved in stem cell self-renewal can cause induction of leukemia.
LT-HSC: long-term hematopoietic stem cell, ST-HSC: short-term HSC, MPP: multipotent progenitor, CSC: cancer stem cell.

1.3 Homeobox Genes

Members of the homeobox family are transcription factors characterized by a 180 bp long homeobox sequence coding for a helix-turn-helix (HTH) motif. This region is called the homeodomain. By this highly conserved 60 amino acid (AA) region, homeodomain containing transcription factors bind to DNA and regulate the expression of their target genes which commonly are involved in development and differentiation (Billeter *et al.*, 1993; Wintjens and Rooman, 1996).

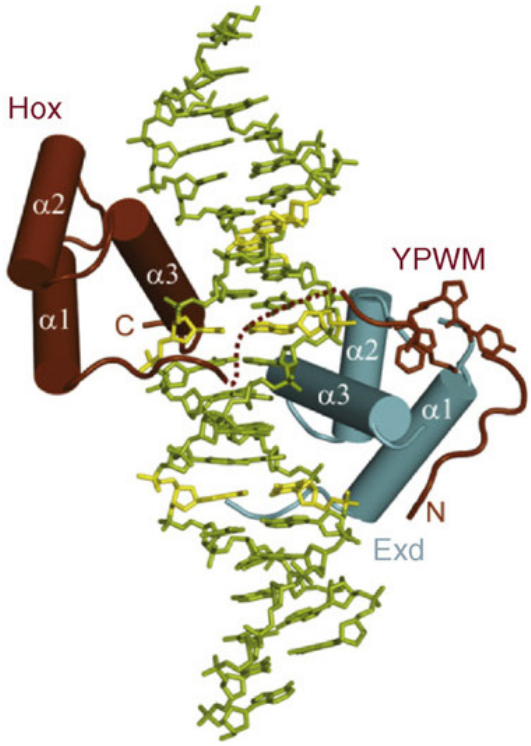

Figure 16: Crystal Structure of two homeodomain peptides bound to DNA.
Depicted are the two homeodomains of the HOX protein SCR (red) and the HOX-cofactor EXD (blue, homolog of the vertebrate PBX) in complex with DNA (Wang *et al.*, 2009 PDB database entry 2r5y). The HOX protein interacts with the EXD cofactor via its N-terminal pentapeptide sequence, which is shown here in the binding pocket of EXD.

HOX genes, as well as *CDX* genes belong to the ANTP (*antennapedia*) class of homeobox genes, which comprises 119 of 300 currently known (pseudo-) homeobox genes in the human. Members of the PAX family on the other hand belong to the second largest group, the PRD (paired) class containing 74 genes. This classification groups eleven different families according to the homology to their *Drosophila melanogaster* counterparts (www.homeodb.cbi.pku.edu.cn/families. php?og=Human). However, homeobox genes can also be subgrouped depending on their chromosomal organization

into clustered homeobox or *HOX* genes, which are physically linked on a chromosome, and non-clustered homeobox genes, which are dispersed throughout the genome. Members of the CDX family are classified as non-clustered homeobox genes.

1.3.1 *Hox* Genes

The clustered homeobox genes of the HOX family are well characterized. This conserved system can be found in all higher metazoans and is derived from one common ancestral cluster (Graham *et al.*, 1989). Whereas most invertebrates like *Drosophila* possess only one *Hox* cluster, the cluster was amplified throughout evolution and as a result mammals, such as mouse and human possess four different *Hox* clusters (*HOXA*, *HOXB*, *HOXC* and *HOXD*) with 39 different *Hox* genes. The position and order of homologous genes are preserved between the *Hox* clusters of different species (Figure 1) They are closely correlating with their spatial and temporal sequence of activation along the anterior-posterior axis of the embryo, a characteristic also termed “colinearity” (Gaunt, 1988; Duboule and Dolle, 1989; Duboule, 1994). In the embryo, expression of *Hox* genes was reported to be regulated by MLL as well as members of the CDX family (Subramanian *et al.*, 1995; Ernst *et al.*, 2004, Davidson *et al.*, 2003; Chawengsaksophak *et al.*, 2004).

In the adult, *Hox* gene expression can be found in different organs such as kidney, colon and liver, each with a specific expression pattern (Cillo *et al.*, 1992; De Vita *et al.*, 1993). The same applies to *Hox* gene expression in the hematopoietic tissue, where hematopoietic progenitors show the expression of *HoxA* and *HoxB* genes, but only a few genes of the *HoxC* cluster and none of the *HoxD* cluster are expressed (Sauvageau *et al.*, 1994). Comparable to the embryonic development, expression of 3’ *Hox* genes can be observed mainly in the earliest hematopoietic progenitors. With advancing differentiation towards the committed progenitor stage, the expression shifts towards the more 5’ *Hox* genes (Magli *et al.*, 1991; Giampaolo *et al.*, 1994; Sauvageau *et al.*, 1994).

Hox genes are involved in the self-renewal of HSCs as well as the specification of the hematopoietic lineages. A knock down of *HOXA5* in human BM cells for example leads to a shift from the granulocytic/monocytic hematopoiesis towards the erythroid lineage whereas an overexpression of *HOXB4* leads to the

expansion of HSCs (Sauvageau *et al.*, 1995; Fuller *et al.*, 1999). In the mouse, *Hoxa9* deficiency results in reduced granulocyte and lymphocyte counts (Lawrence *et al.*, 1997).

To allow final maturation of the hematopoietic cells, *Hox* gene expression needs to be silenced. An aberrant expression of *Hox* genes can lead to perturbation of hematopoietic differentiation and the induction of leukemia which was reported amongst others for *Hoxa9*, *Hoxa10*, *Hoxb6* or *Hoxb8* (Perkins and Cory, 1993; Borrow *et al.*, 1996; Thorsteinsdottir *et al.*, 1997; Fischbach *et al.*, 2005; Bach *et al.*, 2010, Figure 17).

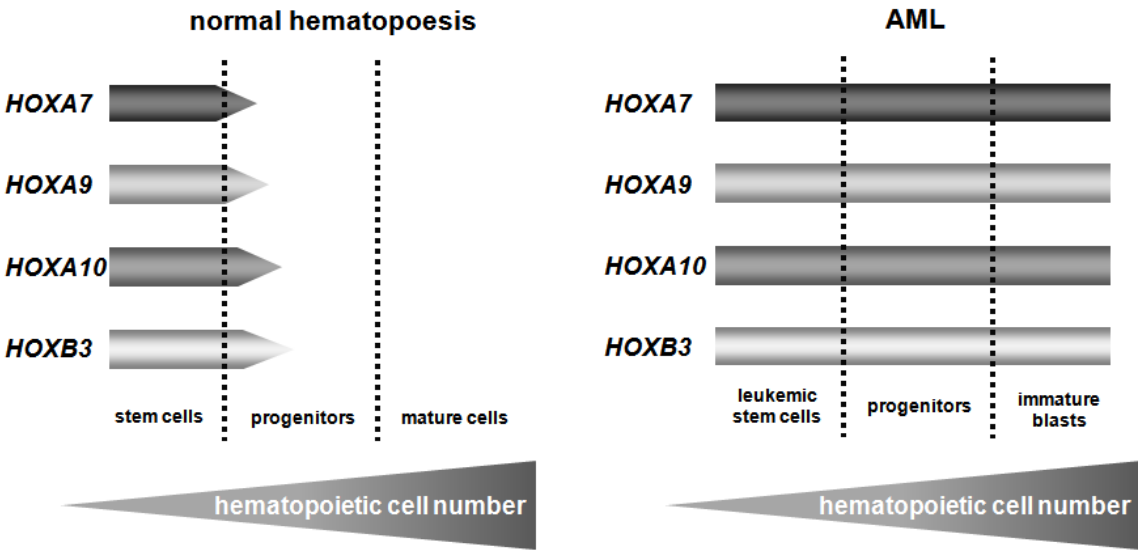

Figure 17: Deregulation of *HOX* genes in AML.
Whereas the expression of most *HOX* genes is silenced in adult normal hematopoiesis, aberrant *HOX* gene expression is a frequent event in acute myeloid leukemia and leads to a block of differentiation.

As mentioned in section 1.2.1, deregulation of *HOX* genes can be observed in a major subset of human leukemia. However, in only 5-10% of patients this aberrant expression can be explained by deregulation of the *HOX* upstream regulator MLL (Falini *et al.*, 2007, Figure 9). The reason for aberrant *HOX* gene expression in human leukemia in many cases still remains to be solved.

1.3.2 *Cdx* Genes

Evolutionary, the *Caudal-type* or *Cdx* genes are most closely related to the posterior *Hox* genes (Figure 18) and are equally important for the AP patterning during embryogenesis. *Caudal* genes contribute to posterior segmentation and

deficiency of these genes leads amongst others to posterior truncation of the embryo, shown for example in zebrafish or mouse (Hammerschmidt *et al.*, 1996; van den Akker *et al.*, 2002).

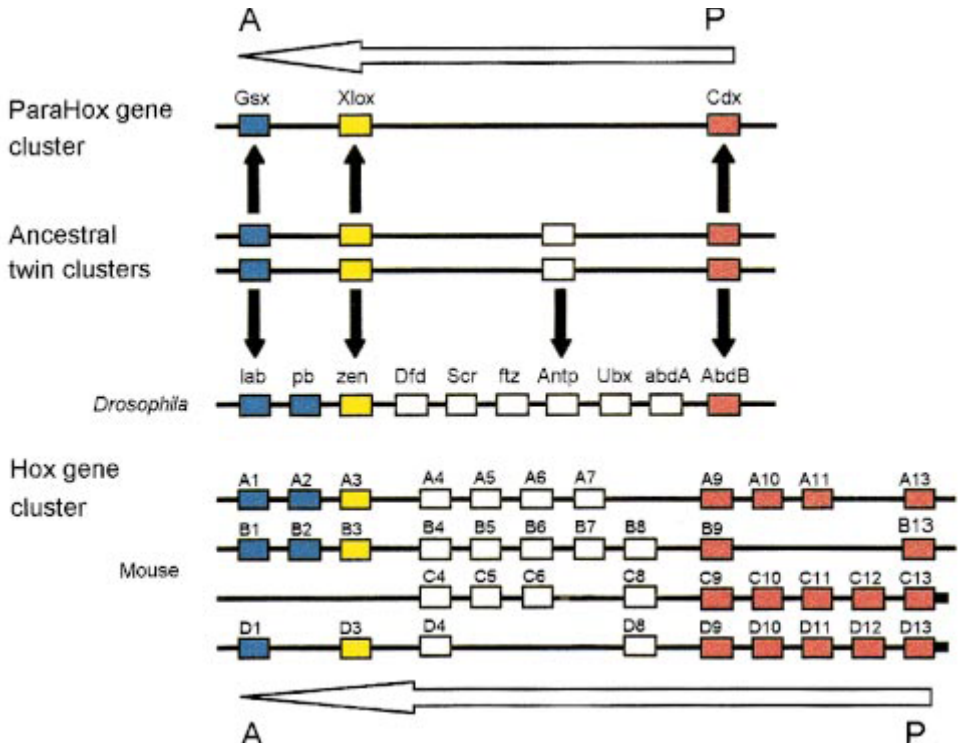

Figure 18: *Hox* and *ParaHox* gene clusters originate from a common ancestral cluster.
Whereby *Gsx* genes are related to anterior and *Xlox* genes to group 3 *Hox* genes, *Cdx* genes and posterior *Hox* genes are derived from the same common ancestor (Brooke *et al.*, 1998).

Whereas the *Drosophila* Cad is involved in segment specification in a HOX-like manner, vertebrate CDX proteins act upstream of *Hox* genes as transducers of positional information (Charite *et al.*, 1998; Lohnes, 2003). Members of the vertebrate CDX family act as master regulators of *Hox* gene expression through conserved CDX binding sites, which were identified in the cis-regulatory elements of several *Hox* genes (Subramanian *et al.*, 1995; Gaunt *et al.*, 2004; Tabaries *et al.*, 2005). Like most homeobox proteins, CDX members possess a conserved YPWM motif (also called hexa- or pentapeptide) as well, which allows binding of PBC proteins like PBX.

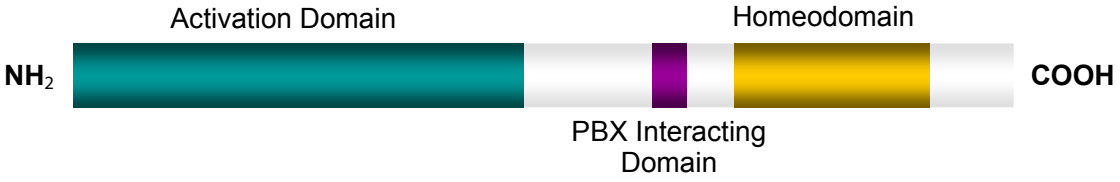

Figure 19: Domain structure of *Cdx* genes.
Green: N-terminal transactivation domain, yellow: homeodomain, violet: PBX interacting motif.

CDX1

Cdx1 was the first *Cdx* gene isolated from mouse (Duprey *et al.*, 1988) where it is expressed starting from day 7.5 post coitum (p.c.). Embryos deficient for CDX1 expression show an anterior homeotic transformation accompanied by a posterior shift of *Hox* expression (Subramanian *et al.*, 1995).

In the adult, CDX1 is known to be involved in the intestinal differentiation and the development of intestinal metaplasias (Wong *et al.*, 2005; Bonhomme *et al.*, 2008). In normal adult hematopoietic tissue, however, no expression of this homeobox gene has been reported.

CDX2

A knock out of *Cdx2*, which is the only *Cdx* member expressed in the extra-embryonic ectoderm, results in trophoectodermal defects and leads to embryonic lethality at day 3.5 due to implantation failure (Chawengsaksophak *et al.*, 1997). The expression of the trophoectodermal marker *Cdx2* was suggested to be positively regulated by RAS/ERK signaling (Lu *et al.*, 2008).

Cdx2$^{+/-}$ mice are viable, but show a phenotype similar to *Cdx1*$^{-/-}$ animals with an anterior homeotic shift (Chawengsaksophak *et al.*, 1997). A combination of *Cdx2* heterozygocity with a heterozygous mutation of *Cdx1* leads to AP patterning defects with a higher penetrance and more severe than the sum of defects observed in both the single *Cdx* mutant mice. Furthermore, an exchange of *Cdx2* by *Cdx1* in a knock-in mouse model was able to fully substitute for CDX1 function and thus suggests a certain redundancy between members of the *Cdx* family (van den Akker *et al.*, 2002; Savory *et al.*, 2009).

From day 12.5 on as well as in the adult, expression of *Cdx2* is restricted almost exclusively to the intestine like gut epithelium (James and Kazenwadel, 1991) and to the α-cells of the pancreas where it activates expression of proglucagon (Liu *et al.*, 2006). There is substantial evidence suggesting CDX2 acts as a tumor suppressor in the intestine. Mice heterozygous for *Cdx2* for example show a high incidence of colorectal tumors and in human colorectal carcinomas *Cdx2* expression was shown to be downregulated as well as to inversely correlate to the tumor grade (Chawengsaksophak *et al.*, 1997; Tamai *et al.*, 1999). Ectopic *Cdx2* expression in the stomach or esophagus, on the other

hand, has been attributed to the development of intestinal metaplasias (Silberg *et al.*, 2002; Almeida *et al.*, 2003; Eda *et al.*, 2003). Interestingly, in colorectal carcinoma *Cdx2* expression has been shown to be downregulated by a hyper-activated RAS/ERK pathway, hereby highlighting the differential regulation of *Cdx2* in adult intestine compared to embryonic tissue (Krueger *et al.*, 2009).

Cdx2 furthermore is supposed to be targeted by FGF4-FRS2α signaling and to induce expression of *Bmp4* upon stimulation by this pathway (Murohashi *et al.*, 2009). Murohashi *et al.* also found *Cdx2* to be a downstream target of ERK in trophoblast stem cells and are hereby in line with the results of Lu *et al.* (2008). As described for CDX1, CDX2 positively regulates its own expression. Additionally, it is able to cross-regulate the expression of *Cdx1* (Xu *et al.*, 1999; Mutoh *et al.*, 2009).

CDX4

The third member of the caudal family, *Cdx4*, shows a peak of expression during the late streak stage of murine embryonic development (Gamer and Wright, 1993) and promotes the differentiation of the hemangioblast towards the hematopoietic lineage compared to the endothelial lineage (Wang *et al.*, 2005; McKinney-Freeman *et al.*, 2008). Interestingly, compared to CDX1 and CDX2, which both suppress hematopoietic factors like GATA-1, PU.1 or RUNX1 and inhibit embryonic hematopoietic activity by blocking progenitor differentiation, CDX4 strongly induces hematopoietic progenitor formation and confers multilineage engraftment potential to embryonic stem cell-derived hematopoietic cells (Wang *et al.*, 2005; McKinney-Freeman *et al.*, 2008, Figure 20).

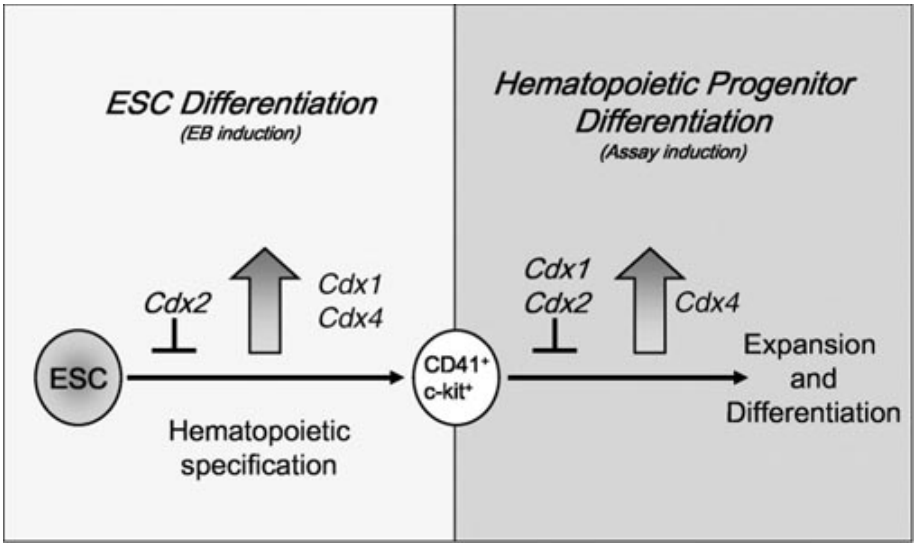

Figure 20: Differential effect of CDX proteins on ESC-derived hematopoiesis.
According to McKinney-Freeman *et al*. (2008) *Cdx* genes affect both the formation of hematopoietic progenitors and also the hematopoietic potential of already specified progenitors.

Overexpression of CDX4 in murine ES cells furthermore leads to an effect similar to the one observed with HOXB4 with an expansion of stem and progenitor cells. Hereby, CDX4 revealed an even stronger stem cell amplificatory potential than HOXB4 (Davidson *et al.*, 2003).

As demonstrated in zebrafish, Cdx4 is important for embryonic blood formation, especially for specifying erythroid lineage (Davidson *et al.*, 2003). In this model, a loss-of-function mutation of Cdx4 led to perturbation of early hematopoiesis mainly due to a severe reduction of hemoglobin-expressing erythroid cells. This bloodless phenotype went along with tail defects and an altered expression pattern of posterior *hox* genes suggesting that the deficiency for Cdx4 led to an aberrant mesodermal patterning. The phenotype was rescued by overexpression of *hoxb7a* or *hoxa9*. An additional knock down of *cdx1* in a *cdx4* deficient background resulted in a complete failure to specify blood precursors and led to a deficiency in forming definitive HSCs as well (Davidson and Zon, 2006). Also in the latter case, embryonic erythropoiesis as well as HSC specification was rescued by *hoxa9* overexpression, indicating that the effect of Cdx4 in particular is mediated via regulation of *hox* gene expression. The more severe effects of compound *Cdx* mutants compared to single Cdx mutants again suggest partial redundancy of Cdx members (Davidson and Zon, 2006; Faas and Isaacs, 2009).

Similar to CDX1, CDX4 is also involved in retinoic acid (RA) signaling and was shown to regulate expression patterns of *raldh2* and the RA catabolizing *cyp26a1* (Wingert *et al.*, 2007). Both *Cdx* genes are targets of WNT signaling, and are positively regulated by BMP4 and suppressed by Noggin. CDX1 and CDX4 were shown to indirectly crossregulate each other by upregulation of *Wnt3a* expression, suggesting WNT3A as well as CDX1 and CDX4 to be part of a positive feedback loop (Lengerke *et al.*, 2008; Faas and Isaacs, 2009). Furthermore, FGF signaling has been linked to the expression of *Cdx4* (Pownall *et al.*, 1996; Keenan *et al.*, 2006; Shimizu *et al.*, 2006).

CDX2 in Leukemia

Usually, chromosomal translocations involve and activate genes which encode proteins controlling cell differentiation, developmental processes and important transcriptional pathways (Armstrong and Look, 2005). The developmental gene *CDX2* was found to be targeted by such a translocation, which was reported by Chase *et al*. in 1999. In a patient with chronic myeloid leukemia, a t(12;13)(p13;q12) translocation was identified resulting in the *ETV6-CDX2* fusion gene. The fusion partner, ETV6/TEL1 is an important regulator of hematopoietic stem cell survival and frequently affected by translocations (Hock *et al.*, 2004). However, Rawat *et al*. (2004) showed that in the case of the *ETV6-CDX2* positive leukemia it was the ectopic expression of the protooncogene *Cdx2,* and not the expression of the fusion gene, that led to induction of AML in the murine BM transplantation model. The coexpression of the fusion gene hereby did not accelerate the course of disease (Figure 21).

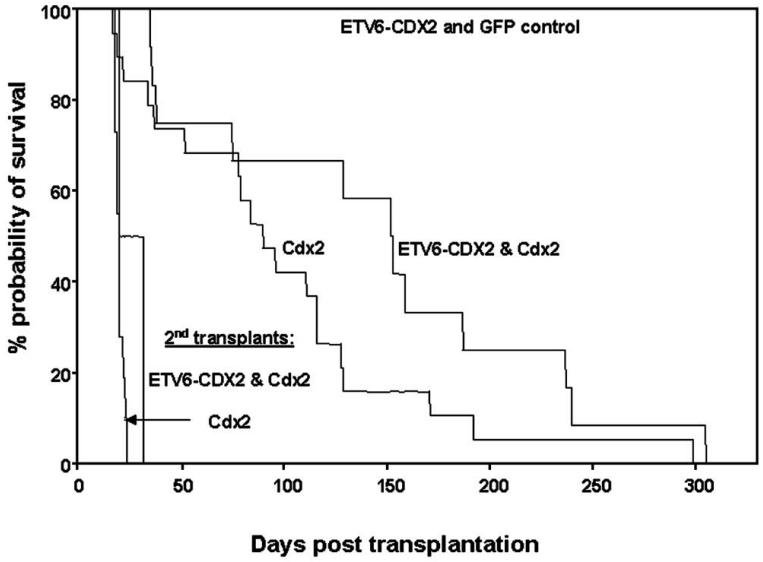

Figure 21: Ectopic expression of *Cdx2* is the transforming event in a mouse model of t(12;13)(p13;q12) acute myeloid leukemia (Rawat *et al.*, 2004).

2. AIM OF THE STUDY

Deregulation of *HOX* genes is a frequently observed phenomenon in acute leukemia, especially in acute myeloid leukemia with normal karyotype. So far, only in a small subset of these cases the cause for the aberrant *HOX* expression is known. For the vast majority of patients the reason for *HOX* gene deregulation remains unclear. From embryogenesis, members of the CDX family are known to be upstream regulators of *HOX* genes. Based on a single case observation in human AML, our lab previously demonstrated that ectopic expression of CDX2 induces AML in the murine BM transplantation model (2004). However, the role of *CDX* genes in murine normal and human malignant hematopoiesis remained largely unknown.

One intention of this study therefore was to analyze the role of *CDX* genes in acute leukemia patients with *HOX* gene deregulation. Furthermore, it was to be functionally tested if CDX factors possess the ability to regulate *HOX* gene expression in adult hematopoiesis as well. In contrast to the leukemogenic CDX2, Davidson *et al.* (2003) described another CDX family member, CDX4, to possess stem cell amplificatory potential, thereby leading to the expansion of hematopoietic progenitors during murine embryonic development. Like the stem cell amplificatory HOXB4, CDX4 also seemed to play a role in stem cell self-renewal. Based on this finding, one major focus of this work was to investigate the role of CDX4 in adult murine hematopoiesis *in vitro* and *in vivo* by establishing and analyzing a murine BM transplantation model.

3. MATERIAL

3.1 Reagents

1 kb plus ladder	New England BioLabs, Ipswich, MA, USA
100 bp DNA ladder	New England BioLabs, Ipswich, MA, USA
5-fluorouracil	TEVA-GRY-Pharma GmbH, Kirchzarten, Germany
Agar	Sigma-Aldrich, Taufkirchen, Germany
Agarose	Sigma-Aldrich, Taufkirchen, Germany
β- Mercaptoethanol	Sigma-Aldrich, Taufkirchen, Germany
Bromphenol blue	Sigma-Aldrich, Taufkirchen, Germany
Calcium chloride	Sigma-Aldrich, Taufkirchen, Germany
Cholorquine	Sigma-Aldrich, Taufkirchen, Germany
DNAzol reagent	Invitrogen, Carlsbad, CA, USA
Ethanol	Sigma-Aldrich, Taufkirchen, Germany
Ethidium bromide	Sigma-Aldrich, Taufkirchen, Germany
Formaldehyde 40%	Sigma-Aldrich, Taufkirchen, Germany
Giemsa's azur eosin-methylene blue	Merck, Whitehouse Station, NY, USA
HEPES	GIBCO, Karlsruhe, Germany
Isopropanol	Sigma-Aldrich, Taufkirchen, Germany
Luria agar	Gibco/ Invitrogen, Carlsbad, CA, USA
Luria broth base	Gibco/ Invitrogen, Carlsbad, CA, USA
May-Grünwald's eosine-methylene blue (mod.)	Merck, Whitehouse Station, NY, USA
Methanol	Sigma-Aldrich, Taufkirchen, Germany
Methylcellulose M3434	Stem Cell Technologies, Vancouver, BC, Canada
Methylcellulose M3630	Stem Cell Technologies, Vancouver, BC, Canada
PCR enhancer system	Gibco/ Invitrogen, Carlsbad, CA, USA
Propidium iodide	Sigma-Aldrich, Taufkirchen, Germany
Protease inhibitor cocktail I & II	Sigma-Aldrich, Taufkirchen, Germany
SDS	Sigma-Aldrich, Taufkirchen, Germany

Sodium chloride	Sigma-Aldrich, Taufkirchen, Germany
TaqMan Universal PCR Master Mix NoUNG	Applied Biosystems, Foster City, CA, USA
Trizol reagent	Invitrogen, Carlsbad, CA, USA

3.2 Consumables

6-well plates	Sarstedt, Newton, NC, USA
15 ml tubes	Sarstedt, Newton, NC, USA
96-well plates	Sarstedt, Newton, NC, USA
Blunt end needles	Stem Cell Technologies, Vancouver, Kanada
Cell culture dishes 100 mm	Corning, NY, USA
Cell culture dishes 150 mm	Corning, NY, USA
Cell scraper	Sarstedt, Newton, NC, USA
Cell strainer	Becton Dickinson, Franklin Lakes, NJ, USA
Cryo tubes	Nunc, Rochester, NY, USA
FACS tubes	Becton Dickinson, Franklin Lakes, NJ, USA
Filtercards for cytospin	Thermo Shandon, Runcore, Chesire, England
Microspin S-300 HR columns	Amersham Biosciences, Uppsala, Sweden
Microvettes	Sarstedt, Newton, NC, USA
PCR softtubes	Biozym, Oldendorf, Germany
Petri dishes 100 mm	Becton Dickinson, Franklin Lakes, NJ, USA
Protran nitrocellulose transfer membrane	Schleicher & Schuell, Dassel, Germany
Hybond N membrane	Amersham Biosciences, Uppsala, Sweden
Sterile cover sheets	Hartmann, Heidenheim, Germany
Syringe filters 45 and 22 µm	Millipore, Billerica, MA, USA

3.3 Media and Supplements for Cell Culture

ACl	Stem Cell Technologies, Vancouver, Kanada
Ciprobay 400	Bayer, Leverkusen, Germany
Chloroquine	Sigma-Aldrich, Taufkirchen, Germany
DMEM	PAN Biotech, Aidenbach, Germany
DMSO	Sigma-Aldrich, Taufkirchen, Germany
Fetal bovine serum	PAN Biotech, Aidenbach, Germany
IMDM	Gibco/ Invitrogen, Carlsbad, CA, USA
Methocult M3434	Stem Cell Technologies, Vancouver, Canada
Methocult M3630	Stem Cell Technologies, Vancouver, Canada
mIL-3	ImmunoTools, Friesoythe, Germany
mIL-6	ImmunoTools, Friesoythe, Germany
mSCF	ImmunoTools, Friesoythe, Germany
PBS	PAN Biotech, Aidenbach, Germany
Penicillin/ Streptomycin	PAN Biotech, Aidenbach, Germany
Protamine sulfate	Sigma-Aldrich, Taufkirchen, Germany
RPMI	PAN Biotech, Aidenbach, Germany
Terasaki Park medium	BAG Healthcare, Lich, Germany
Trypan blue	Gibco/ Invitrogen, Carlsbad, CA, USA
Trypsin/ EDTA	Gibco/ Invitrogen, Carlsbad, CA, USA

3.4 Enzymes

DNA ligase T4	New England BioLabs, Ipswich, MA, USA
Restriction enzymes	New England BioLabs, Ipswich, MA, USA

Enzymes for PCR and radioactive labeling were purchased as components of Kits (see chapter 3.6)

3.5 FACS α-Mouse Antibodies

All antibodies were purchased from BD Pharmingen, Franklin Lakes, USA.

Tag	Antigen	Clone	BD Cat.	Target
PE	Sca-1 (Ly-6A/E)	D7	553108	Hematopoietic stem and progenitor cells
	Gr-1 (Ly-6C/ Ly-6G)	RB6-8C5	553128	Granulocytes
	CD19	1D3	553786	B-lymphocytes
	CD8a (Ly-2)	53-6.7	553033	T-lymphocytes
	Ter119 (Ly-76)	TER-119	553673	Erythroid cells
	CD45.1 (Ly-5.1)	A20	553776	Hematopoietic cells of PEB
APC	c-Kit/ CD117	2B8	553356	Hematopoietic stem and progenitor cells
	Mac-1/ CD11b	M1/70	553312	Myelomonocytic cells
	B220/ CD45R	RA3-6B2	553092	B-lymphocytes (+ lymphoid dendritic cells)
	CD4 (L3T4)	RM4-5	553051	T-lymphocytes
	NK-1.1 (NKR-P1B, NKR-P1C)	PK136	550672	Natural killer cells

3.6 Kits

Kit	Company
GenElute Plasmid Miniprep Kit	Sigma-Aldrich, St. Louis, MO, USA
GenElute HP Plasmid Maxiprep Kit	Sigma-Aldrich, St. Louis, MO, USA
GenElute HP Endotoxin-Free Plasmid Maxiprep Kit	Sigma-Aldrich, St. Louis, MO, USA
illustra GFX PCR DNA and Gel Band Purification Kit	GE Healthcare, Waukesha, WI, USA
Megaprime DNA labeling system	Amersham Biosciences, Uppsala, Sweden
Mycoplasma Detection Kit	Roche, Basel, Switzerland
Platinum Taq Polymerase Kit	Invitrogen, Carlsbad, CA, USA
QickChange II XL Site-Directed Mutagenesis Kit	Stratagene, La Jolla, CA, USA
RNeasy Micro Kit	Quiagen, Hilden, Germany
ThermoScript RT-PCR System (cDNA synthesis for PCR)	Invitrogen, Carlsbad, CA, USA

3.7 Kits, Material and Reagents for Microarray

Acetylated BSA	Invitrogen
cDNA Synthesis System (cDNA synthesis for microarray)	Roche Applied Science, Basel, Switzerland
GeneChip® Expression 3'-Amplification Reagents Hybridization Control Kit	Affymetrix, Santa Clara, CA USA
GeneChip® Sample Cleanup Module	Affymetrix, Santa Clara, CA USA
GeneChip® IVT cRNA Cleanup Kit	Affymetrix, Santa Clara, CA USA
GeneChip® Expression 3'-Amplification Reagents for IVT Labeling	Affymetrix, Santa Clara, CA USA
Herring Sperm DNA	Promega, Madison, WI, USA
R-Phycoerythrin-conjugated Streptavidin	Jackson ImmunoResearch, West Grove, PA, USA

3.8 Oligonucleotides

Primer for Standard PCR and Sequencing

PCR Primer Sequence 5' → 3'	$T_{ann.}$ [°C]	Product Length [b]	Comment
Murine			
pMSCV.for/ MIG_Seq.rev			
for CAG CCC TCA CTC CTT CTC TA rev CCT AGG AAT GCT CGT CAA G	58	100 (w/o insert)	
HPRT_fuxa			
for GGG GGC TAT AAG TTC TTT GC rev TCC AAC ACT TCG AGA GGT CC	59	312	
Cdx4end			
for CAG CCA ATC GAG ATA CAG CA	59	-	for sequencing
Cdx4			
rev TTA CAG GGA CCT CAG GAT GG	59	222 bp with Cdx2.FP	exon 2

PCR Primer Sequence 5' → 3'	$T_{ann.}$ [°C]	Product Length [b]	Comment
Cdx4			
FP AGT GCC CAT GAA TGA CAT GA RP CCA GCT CTG ACT TCC TCC TG	59	344	exon 1 - exon 2
Human			
hsCDX4 full length			
for ATG TAC GGA AGC TGT CTT TTG rev TCA TTC GGA GAC TAT AAC CTG CT	57	855	
CDX2_hum_clon			
for CGG GAA TTC ATG TAC GTG AGC TAC CTC CTG rev GGC CTC GAG TCA CTG GGT GAC GGT GGG GTT	58	924	Contains EcoRI and XhoI restriction sites
CDX2 Exon1.for/ Exon2.rev			
for ACG TGA GCT ACC TCC TGG AC rev TGT CTT TCG TCC TGG TTT TCAa	58	558	
CDX2 Exon2.for/ Exon3.rev			
for TGA AAA CCA GGA CGA AAG ACA rev TAC TCC CCA CTT CCC TTC AC	58	1261	
CDX2 Exon1neu.for/ Exon3neu.rev			
for CAG ACT ACC ATC CGC ACC AC rev TGC GGT TCT GAA ACC AGA TT	58	708	
ACTB_hu			
for CTT CAA CAC CCC AGC CAT rev TAA TGT CAC GCA CGA TTT CC	55	260	not intron-spanning
Others			
pGL3 basic.rev (= GLprimer2, Promega)			
rev CTT TAT GTT TTT GGC GTC TTC CA			sequencing of pGL3

Mutagenesis Primer

Cdx4 W157A		
for CAC AGC CCC TAC GCA GCG ATG CGC AAA ACT GTG rev CAC AGT TTT GCG CAT CGC TGC GTA GGG GCT GTG		mutagenesis of Pbx-binding site

Cdx4 N51S

for	T CTG GTT TCA GTC TCG CAG AGC CAA GGA GAG G	mutagenesis of homeodomain
rev	C CTC TCC TTG GCT CTG CGA GAC TGA AAC CAG A	

Cdx4 S153M

for	GC AGG AGC CGT CAC ATG CCC TAC GCA TGG ATG	introduction start codon for deltaN
rev	CAT CCA TGC GTA GGG CAT GTG ACG GCT CCT GC	

Cdx4 deltaN EcoRI.for/ XhoI.rev neu

for	GAA TTC ATG CCC TAC GCA TGG ATG C	introduction restriction sites for deltaN
rev	GCA GGT CAT AGT TTC TGA ATG ACT CGA G	

shRNAs

shRNA Sequence 5' → 3' (mature siRNA sequence is underlined)

sh_Cdx4_759

TGCTGTTGACAGTGAGCGACCGGAGAACTGCCTAACGCTTTAGTGAAGCCACAGATGTAA
AGCGTTAGGCAGTTCTCCGGGTGCCTACTGCCTCGGA

sh_Cdx4_628

TGCTGTTGACAGTGAGCGACCTTTCTGAGAGACAGGTGAATAGTGAAGCCACAGATGTATT
CACCTGTCTCTCAGAAAGGCTGCCTACTGCCTCGGA

sh_Cdx4_112

TGCTGTTGACAGTGAGCGATCTGCCTGCCTCCAACTTTACTAGTGAAGCCACAGATGTAGT
AAAGTTGGAGGCAGGCAGAGTGCCTACTGCCTCGGA

sh_Cdx4_719

TGCTGTTGACAGTGAGCGCGGAGGTTCCGTGCAAAGTGACTAGTGAAGCCACAGATGTAG
TCACTTTGCACGGAACCTCCATGCCTACTGCCTCGGA

sh_CDX2_487

TGCTGTTGACAGTGAGCGAGCGGAACCTGTGCGAGTGGATTAGTGAAGCCACAGATGTAA
TCCACTCGCACAGGTTCCGCCTGCCTACTGCCTCGGA

sh_CDX2_673

TGCTGTTGACAGTGAGCGAGCTCTCTGAGAGGCAGGTTAATAGTGAAGCCACAGATGTATT
AACCTGCCTCTCAGAGAGCCTGCCTACTGCCTCGGA

sh_CDX2_672

TGCTGTTGACAGTGAGCGAGGCTCTCTGAGAGGCAGGTTATAGTGAAGCCACAGATGTAT
AACCTGCCTCTCAGAGAGCCCTGCCTACTGCCTCGGA

sh_CDX2 698

TGCTGTTGACAGTGAGCGATTTCAGAACCGCAGAGCAAAGTAGTGAAGCCACAGATGTAC
TTTGCTCTGCGGTTCTGAAACTGCCTACTGCCTCGGA

Oligonucleotides for Linker Mediated PCR

PstI-Linker

for CTCTCCCTTCTCGTCCTCTCCTTCCTGCA

rev GGAAGGAGAGGACGCTGTCTGTCGAAGGTAAGGAACGGACGAGAGAAGGGAGAG

PCR A (Vectorette/ GFP-A)

for CGAATCGTAACCGTTCGTACGAGAATCGCT

rev ACTTCAAGATCCGCCACAAC

PCR B (Nested Vectorette/ GFP-C)

for TACGAGAATCGCTGTCCTCTCCTT

rev ACATGGTCCTGCTGGAGTTC

Assays for qRT-PCR

All assays for qRT-PCR, which were performed using the TaqMan 7900HT system, were purchased from Applied Biosystems, Foster City, CA, USA.

Gene Symbol	Assay ID/ Product No
Murine	
Cdx1	Mm00438172_m1
Cdx2	Mm01212280_m1
Cdx4	Mm00432452_m1
Gapdh (housekeeping gene)	4352932E
Hoxa5	Mm00439362_m1
Hoxa7	Mm00657963_m1
Hoxa9	Mm00439364_m1
Hoxa10	Mm00433966_m1
Hoxb3	Mm00650701_m1
Hoxb6	Mm00433970_m1
Hoxb8	Mm00439368_m1
Hoxb9	Mm01700220_m1

Gene Symbol	Assay ID/ Product No
Human	
CDX1	Hs00156451_m1
CDX2	Hs01078080_m1
CDX4	Hs00193194_m1
GSH1	Hs00793699_g1
GSH2	Hs00370195_m1
HOXA5	Hs00430330_m1
HOXA7	Hs00600844_m1
HOXA9	Hs00365956_m1
HOXA10	Hs00172012_m1
HOXB3	Hs00231127_m1
HOXB6	Hs00980016_m1
HOXB8	Hs00256885_m1
LEF1	Hs01547248_m1
PDX1	Hs00236830_m1
TBP (housekeeping gene)	4333769F

3.9 Buffers and Stock Solutions

Cytokine Cocktail (100x)	10 mg/ ml mSCF 1 mg/ ml mIL6 600 ng/ ml mIL3 dissolved in DMEM, stored at -20°C
Freezing medium	90% FBS 10% DMSO
HBS (hepes buffered saline, ½ x)	50 mM hepes 280 mM NaCl 0.75 mM Na_2HPO_4 0.75 mM NaH_2PO_4 adjust pH to 7.2/ 7.0 (depending on cell type) stored at 4°C
FACS buffer (1x)	5 µg/ ml propidium iodide

	2% FBS in PBS, stored in dark at 4°C
Hybridization solution for Southern Blot	4.0 g fat free milk powder 40.0 g dextran sulphate 120.0 ml 20x SSC 40.0 ml formamide 20.0 ml 20% SDS 1.6 ml 500 mM EDTA ad 500 ml aqua dest.
5x loading buffer for SDS page	31.35 ml 1 M Tris/HCl pH 6.8 10 g SDS 25 ml Glycerol 250 mg Bromphenolblue 5 ml β-Mercaptoethanol ad 100 ml aqua dest.
Neutral buffered formalin 4%	55 mM Na_2HPO_4 (water free) 12 mM NaH_2PO_4 x 2 H_2O ad 900 ml aqua dest. 100 ml formaldehyde 40% stored in dark at RT
20x SSC	525.9 g NaCl 264.6 g NaCitrate ad 3,000 ml aqua dest. pH adjusted to 7.0
TB buffer (1x)	10 mM hepes 15 mM $CaCl_2$ x 2 H_2O 250 mM KCl 35 mM $MnCl_2$ ad 125 ml aqua dest. sterile filtrated, always made fresh
TAE buffer (50x)	2 M Tris

	50 mM EDTA-Na_2 x $2H_2O$ 1 M Acetic Acid pH adjusted to 8.5
TE buffer (100x)	1 M Tris 100 mM EDTA-Na_2 x 2 H_2O pH adjusted to 8.0

3.10 Technical Equipment

7900HT real-time PCR System	Applied Biosystems, Foster City, CA, USA
^{137}Cs source Gammacell 40	Atomic Energy of Canada Limited, Missisauga, Ontario, Kanada
Cyclone 25 PCR Cycler	PeqLab, Erlangen, Germany
FACSCalibur	Becton Dickinson, Franklin Lakes, NJ, USA
FACSVantage	Becton Dickinson, Franklin Lakes, NJ, USA
NanoDrop 1000 spectrophotometer	Thermo Fisher Scientific, Waltham, MA, USA
Shandon Cytospin 2 Centrifuge	Thermo Fisher Scientific, Waltham, MA, USA
UV GS gene linker.	Bio-Rad, Hercules, CA, USA

3.11 Bacteria Strains

XL10-Gold® ultracompetent *E.coli* (TetrΔ(mcrA)183 Δ(mcrCB-hsdSMR-mrr)173 endA1 supE44 thi-1 recA1 gyrA96 relA1 lac Hte [F´ proAB lacIqZDM15 Tn10 (Tetr) Amy Camr], Stratagene, La Jolla, CA, USA) were purchased in combination with the QuikChange Kit and were used for the transformation of the mutated plasmids. For all other purposes DH5α (fhuA2 Δ(argF-lacZ)U169 phoA glnV44 Φ80 Δ(lacZ)M15 gyrA96 recA1 relA1 endA1 thi-1 hsdR17) were used.

3.12 Cell Lines

293T	human embryonic kidney cell line
32D	mouse myeloid cell line
NIH-3T3	mouse embryonic fibroblast cell line
GP+E-86	ecotropic packaging cell line for retroviral gene transfer, derived from NIH-3T3
Phoenix Eco	helper-virus free packaging cell line, derived from 293T; highly transfectable by calcium phosphate- or lipid-based transfection

4. METHODS

4.1 Molecular Biology Methods

4.1.1 RNA Extraction

Cell pellets were resuspended in 1 ml Trizol and incubated 5 min at RT. After addition of 200 µl chloroform per 1 ml Trizol, the mixture was vortexed for 10 s and incubated 10 min at RT. By a 15 min centrifugation step at 12000 rpm and 4°C, the RNA containing aqueous phase was separated from the lower phenol phase. The aqueous phase was transferred to a new tube and mixed with an equal volume of isopropanol by inverting several times. The mixture was incubated for 10 min at RT and afterwards centrifugated 10 min at 12000 rpm and 4°C to precipitate the RNA. The resulting pellet was washed twice with 500 µl EtOH. To remove residual ethanol, the pellet was dried at RT for several minutes. RNA was dissolved in DEPC-treated, RNase free H_2O and heated 10 min at 55°C to completely dissolve the RNA pellet. Dissolved RNA was stored at -80°C.

4.1.2 DNA Extraction

Cells were resuspended in DNAzol (1 ml per 10 cm dish) and lysed by careful pipetting. After 10 min centrifugation at 10.000 g and 4°C, the supernatant was transferred into a fresh tube. For precipitation of DNA, 500 µl of 100% EtOH was added per 1 ml DNAzol and was then mixed well by vigorous shaking. After taking off the supernatant, the DNA pellet was washed twice with 1 ml 75% EtOH and after drying resuspended in an appropriate volume of H_2O. Dissolved genomic DNA was stored at 4°C.

4.1.3 Quantification of RNA and DNA

RNA and DNA concentrations were photometrically measured using a Nanodrop 1000 spectrophotometer (Thermo Fisher Scientific) at a wavelength of 260 nm, which is the absorption peak of nucleic acids. By simultaneously measuring the absorption at 280 nm (absorption peak of aromatic amino acids

in proteins), the purity of the extract can be estimated. The ratio of A_{260} to A_{280} therefore should be as high as possible and normally is between 1.8 (when measured against water) and 2.1 (when measured against Tris buffer). A third measuring point at 230 nm can give information about other impurities such as salts or phenolic residues.

4.1.4 Polymerase Chain Reaction (PCR)

Reverse Transcription PCR

During reverse transcription (RT), RNA is transcribed into complementary cDNA. Besides reverse transcriptase and dNTPs, $MgCl_2$ as a cofactor is also needed and is included in the reaction buffer. Random hexamers were used to synthesize a complete cDNA library of the total RNA sample. Per 20 µl reaction 1 µg of RNA was used and filled up to 9 µl with DEPC treated H_2O. After addition of dNTPs and hexamers, the sample was heated 5 min at 65°C for complete denaturation of RNA, then rapidly cooled down on ice to prevent new formation of secondary structures. The remaining reagents were added to the sample and the mixture successively incubated 10 min at 25°C for primer annealing, 50 min at 50°C for synthesis of the DNA strand and 5 min at 85°C for inactivation of the reverse transcriptase. For detection of contaminations with genomic DNA, RT controls - containing RNA but no enzyme - were performed. Until further usage, cDNA samples were stored at -20°C.

	Volume [µl]
total RNA ad 10 µl DEPC H_2O [µl]	10.0
10 mM dNTP mix [µl]	2.0
Random hexamers (50 ng/µl) [µl]	1.0
5 x cDNA synthesis buffer	4.0
dTT 0.1 M [µl]	1.0
RNaseOut 40 U/µl [µl]	1.0
ThermoScript RT (15 U/µl)	1.0
Total Volume	20.0

Tab. 1: Reaction components for RT-PCR.

Standard PCR

For PCR, two specific primers are used to amplify one defined DNA region. The primers anneal to the complementary DNA sequence and enable the polymerase to attach to the DNA. Normally *Taq* DNA polymerase is employed, an enzyme isolated from the thermophilic bacterium *thermus aquaticus.* For amplification of longer transcripts, special high fidelity polymerases are used.

The standard PCR consists of a number of cycles, each containing three steps: For *denaturation* of the double-stranded DNA, the sample is heated at 95°C for 30 s. To enable the *annealing* of both primers, in the next step the sample is cooled down to 55-65°C, with the exact temperature depending on the length and GC content of the primer pair in use. Last, in the *extension* step, the new strand is synthesized at the temperature optimum of the polymerase, which for example is 72°C for the Platinum® *Taq* DNA polymerase (Invitrogen) routinely used in this study. Ideally, each newly synthesized strand will act as template in the next cycle, which would lead to a doubling of PCR products in each cycle with a number of 2^n products after n cycles. In fact, the PCR efficiency is lower and generally is around 1.80-1.85.

The following reaction components and conditions were used:

	Volume [µl]
10x buffer -Mg	2.50
$MgCl_2$ 50 mM	0.75
dNTP mix 10 mM	0.50
Forward primer	0.50
Reverse primer	0.50
Taq polymerase 5 U/µl	0.10
Template DNA	1.0
PCR-H_2O	ad 25.0

Table 1: Reaction components for standard PCR.

Step	No Cycle(s)	Target Temp. [°C]	Time [s]
Denaturation	1	94	120
Denaturation		94	30
Annealing	ps	ps	30
Extension		72	ps
Extension	1	72	120

Table 2: Cycler program for standard PCR.
ps = product-/ primer-specific parameter, Table 3.

Primer	Annealing [°C]	No Cycles	Elongation Time [s]
Hprt	60	35	30
Cdx4 FP/rev	59	35	30
MSCV.for/MIG.Seq.rev	58	30	30
β-Aktin	58	28	30
hsCDX4 fl	58	30	60
Cdx2_hum_clon	62	30	60
CDX2 E1.for/E2.rev	58	30	30
CDX2 E2.for/E3.rev	58	30	90
CDX2 E1short.for/E2short.rev	60	35	20
CDX2 E2short.for/E3short.rev	60	35	20

Table 3: Product-/ primer specific parameters for standard PCR.

To reamplify PCR products, either the whole PCR product, diluted or undiluted, or the gel-purified product was used as template for a new PCR reaction. In the latter case, the band was either purified using the *illustra GFX PCR DNA and Gel Band Purification Kit* according to manufacturer's instruction or the band was cut and crushed in a 1.5 ml tube with about 50 µl of PCR-grade H_2O. 1 µl of the supernatant was transferred in the new reaction as template.

Site Directed Mutagenesis PCR

For introduction of point mutations or deletions of a few bases into plasmid DNA, the "*QickChange II XL Site-Directed Mutagenesis Kit*" (Stratagene) was used. In brief, after denaturation of the plasmid, the mutagenic primers containing the desired mutation anneal to the single strand DNA. Both

oligonucleotides cover the same region of the DNA strand and are designed using following formula:

$$T_M = 81.5 + 0.41 \times \%GC - 675/N - \%mismatch$$

N: length of primer, between 25 and 45 b with mutation in the middle, $T_M \geq 78°C$

The primers then are elongated by the high fidelity polymerase PfuUltra™, featuring especially high accuracy and processivity compared to normal Taq polymerase. To avoid introduction of random mutations during PCR, only 18 cycles are run. Unmutated plasmid DNA subsequently is digested by DpnI, a endonuclease specifically cutting methylated or semi-methylated DNA and competent bacteria were transformed with the plasmid DNA (see section 4.2.2).

Linker Mediated PCR

For the linker-mediated PCR (LM-PCR), integrated long-terminal repeats (LTRs) and flanking genomic sequences were amplified and subsequently isolated using a modification of the bubble LM-PCR strategy (Riley *et al.*, 1990).

1 µg genomic DNA from diseased mice was digested overnight with *PstI* (New England Biolabs) in a volume of 50 µl. The DNA fragments were purified by precipitation with Na-Acetate, redissolved in 12 µl H_2O and ligated overnight at 16°C to the double-stranded bubble *PstI* linker in a total reaction volume of 100 µl. Subsequently, a nested PCR was performed with the first PCR (PCR A) using a primer pair consisting of vectorette primer A and GFP-A primer, followed by a nested PCR (PCR B) using the nested vectorette primer B and the GFP-C primer.

Component	Volume [µl]
10x buffer –Mg [µl]	2.50
$MgCl_2$ 50 mM [µl]	0.75
dNTP mix 10 mM [µl]	0.50
Vectorette primer	0.50
GFP-A primer	0.50
Taq polymerase 1 U/µl [µl]	0.25
Ligation template [µl]	10.00
PCR-H_2O [µl]	10.30
Total Volume [µl]	25.30

Table 4: Reaction components for PCR A.

Component	Volume [µl]
10x buffer –Mg [µl]	2.50
$MgCl_2$ 50 mM [µl]	0.75
dNTP mix 10 mM [µl]	0.50
Vectorette primer	0.50
GFP-A primer	0.50
Taq polymerase 1 U/µl [µl]	0.25
PCR product PCR A [µl]	1.00
PCR-H_2O [µl]	19.30
Total Volume [µl]	25.30

Table 5: Reaction components for PCR B.

Step	No Cycle(s)	Target Temp. [°C]	Time [s] PCR A/ B
Denaturation	1	94	120
Denaturation		94	30
Annealing	30	65	30
Extension		72	120/ 300
Extension	1	72	120/ 300

Table 6: Cycler program for LM-PCR A and B.

To each 25 µl PCR B reaction 2.5 µl 10x loading dye were added and 12 µl of this mixture were loaded on a 1.5% agarose gel. Gel bands were excised and purified using the *illustra GFX PCR DNA and Gel Band Purification Kit* (GE Healthcare). Fragments of sufficient size were sequenced directly using one of the primers of PCR B, smaller fragments were first subcloned into pGM-T easy.

Real-Time Quantitative Reverse Transcription PCR

Real-time quantitative reverse transcription PCR (real-time qRT-PCR) allows the quantitative determination of PCR products generated during PCR. For real-time qRT-PCR, fluorescent dyes are used and the increase of fluorescence, which is proportional to the number of transcripts, is measured at the end of every PCR cycle, i.e. in *real-time*. The most specific chemistry is based on hybridizing probes, which is also employed in the TaqMan method (7900HT fast real-time PCR system, Applied Biosystems) used for this study. The gene specific assay, which is available predesigned for a large number of different

genes, beside the primers also contains the probe, which is designed to hybridize with the target sequence. This probe is labeled with 6-FAM at the 5' end and a nonfluorescent quencher at the 3' end. By the nuclease activity of the DNA polymerase, the probe is cleaved during the elongation step leading to a separation of the quencher from the reporter dye and hereby to an increase of fluorescence.

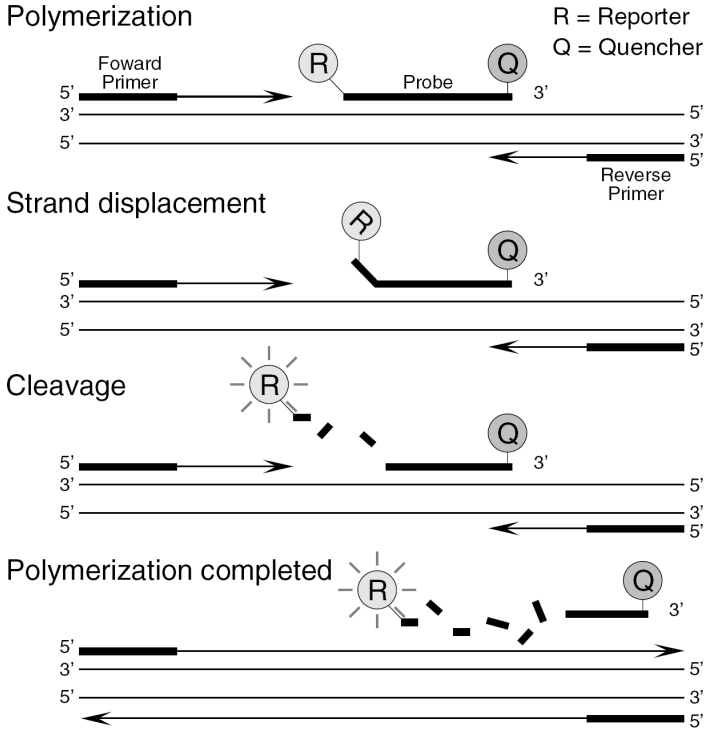

Figure 22: 5´–3´ Nuclease Activity of the DNA Polymerase System.
By the nuclease activity of the polymerase the fluorescent dye is separated from the quencher and starts to emit light (source: protocol TaqMan® Gene Expression Assays, Applied Biosystems).

The point at which the fluorescence signal of one sample reaches a predefined level above the background fluorescence is referred to as *threshold cycle* (C_T) and is used to calculate the initial sample concentration. This can be done either in an absolute way, by comparing the C_T of the target sample with a standard curve, or by relative quantification when the C_T of the target sample is compared to an internal control. The absolute quantification gives information about the effective molecule concentration in the sample of interest. However, the DNA for the standard curve, e.g. recombinant DNA or RT-PCR product, does not undergo the same processing as the unknown mRNA samples which have to be reverse transcribed first, thus leading to a certain inaccuracy. More robust is the relative quantification, as the expression of the gene of interest is

compared to the expression of one or more endogenous controls, mostly called *housekeeping genes*, within the same sample and parameters such as RNA quantity or RT efficiency thus lose their relevance.

Assuming the same efficiency for both target and housekeeping control primers, which is given for primers designed by Applied Biosystems, the expression height can be calculated using the $\Delta\Delta C_T$ method. First, the ΔC_T is calculated by normalization to the housekeeping gene. In this study, the housekeeping gene *Gapdh* was used for normalization of murine genes and the gene encoding the TATA-box binding protein (*TBP*) for normalization of human genes.

$\Delta C_T = C_{T(target)} - C_{T(reference)}$ with the standard deviation $s = \sqrt{s_{target}^2 + s_{reference}^2}$.

It is important to note that ΔC_T values are inversely correlated to the expression height of a gene. For a better understanding, i.e. to achieve a positive correlation, ΔC_T values were subtracted from the maximum cycle number of 40 cycles.

The fold change between a test sample (e.g. treated sample) and a calibrator sample (e.g. untreated sample) subsequently can be calculated by $2^{-\Delta\Delta C_T} = 2^{-(\Delta C_{T(test\ \ sample)} - \Delta C_{T(calibrator\ \ sample)})}$ with a range of $2^{-(\Delta\Delta C_T + s)}$ to $2^{-(\Delta\Delta C_T - s)}$.

Reactions were run in triplicates with 1 µl of cDNA containing the equivalent of 50 ng total RNA and in a total volume of 20 µl. Because of less material, patient samples were run only once.

	Volume [µl]
TaqMan Universal PCR Master Mix No UNG (2x)	10.00
DEPC-H_2O [µl]	8.00
Assay (primer & probe) 20x [µl]	1.00
cDNA [µl]	1.00
Total Volume	20.00

Table 7: Reaction components for TaqMan qRT-PCR.

All PCR reactions were run with the standard program and 40 to 45 cycles.

Step	Cycles	Target T [°C]	Time [s]
Activation AmpErase UNG	1	50	120
Activation AmpliTaq Gold	1	95	600
Melting	40-45	95	15
Annealing/ Extension		60	60

Table 8: Standard program for TaqMan qRT-PCR.

Methylation Specific PCR and Bisulfite Sequencing

Methylation specific PCR and successive bisulfate sequencing was performed commercially by Varionostic GmbH, Ulm, Germany.

4.1.5 Agarose Gel Electrophoresis

Preparative and analytical separation of PCR products or plasmids was done by agarose gel electrophoresis. For this, 10 µl of PCR product was mixed with 1 µl 10x probe buffer and loaded on an agarose gel containing 0.005% ethidium bromide. Depending on the size of the expected PCR product, gels of 0.8% to 2.0% were used. For electrophoresis of plasmids, the samples were loaded on 0.5% agarose gels. As marker, 0.5 µg of a 100 bp or 1 kb ladder (both NEB, see chapter 3.1) were loaded. The electrophoretic separation was carried out for 60 min at 80-100 V.

4.1.6 Purification of PCR Products out of Agarose Gel

To purify PCR products from interfering byproducts for reamplification or sequencing, the corresponding bands were cut out of the agarose gel and purified using the *illustra GFX PCR DNA and Gel Band Purification Kit* according to manufacturer's specifications.

4.1.7 Cloning of DNA Fragments

For retroviral gene transfer into primary BM cells, the different constructs were cloned into the multiple cloning site of the modified murine stem cell virus (MSCV) vector (Pineault *et al.*, 2003) upstream of the internal ribosomal entry

site (IRES) and the enhanced green or yellow fluorescent protein (eGFP/ eYFP) gene. For this, the PCR product as well as the plasmid were digested with *EcoRI* and *XhoI* for at least 3 h or overnight at 37°C. Subsequently, the plasmid was gel-purified to remove the excised fragment. 20 to 100 ng of the digested and purified vector were ligated to a 2- to 5-fold excess of the digested PCR product in a total reaction volume of 10 µl by incubation over night at 16°C. Competent bacteria were transformed with 5 µl of the ligated plasmid according to chapter 4.2.2.

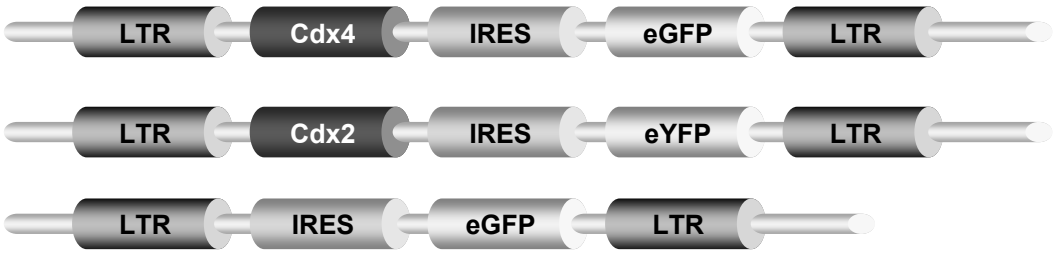

Figure 23: Schematic view of retroviral constructs.
The *MSCV-Cdx4-IRES-eGFP* construct kindly was provided by Keith Humphries.

4.1.8 Restriction Analysis

To test for successful ligation of a insert into a plasmid, the plasmid was cut with appropriate restriction enzymes and analyzed via agarose gel electrophoresis. Control digestions were performed at 37°C for 3 h in a total volume of 10 µl and with the same enzymes applied for cloning.

4.1.9 Southern Blot

Southern blot analyses to assess proviral integration were performed using genomic DNA isolated from bone marrow, spleen and peripheral blood of leukemic mice by DNAzol reagent according to manufacturer' instructions (see chapter 4.1.2).

Southern blot was performed using standard protocols (Buske *et al.*, 2001): 10 µg of genomic DNA were digested over night with *PstI* in a total volume of 60 µl to release a fragment specific to the proviral integration site. After a reduction of the volume to approximately 40 µl by speed vac (30-40 min at 55°C), the DNA was loaded on a medium size 0.8% agarose gel with 0.5 µg/ml

ethidium bromide and separated with 70 V for several hours. Subsequently, the DNA was depurinated by incubating the gel in 0.2 N HCL for exactly 10 minutes and denatured for 45 minutes in denaturation solution. Overnight, the DNA was transferred to a Hybond N membrane (Amersham Biosciences) by capillary action using 10x SSC buffer. Cross-linking of the DNA with the membrane was performed by incubating the damp membrane at 150 mJ in a UV GS gene linker (Bio-Rad). The membrane was transferred in a prewarmed glass hybridization tube and after addition of 25 ml prehybridisation buffer incubated for 15 min at 65°C. After addition of 100 µl salmon DNA, the membrane was incubated for additional 2 h to block unspecific binding.

In the meantime the probe, a 700 bp eGFP-fragment cut out of the pEGFP-C1 plasmid (Clontech), was labeled with $4x10^7$ DPM α-32P dCTP, using the *Megaprime DNA labeling System* (Amersham Biosciences) and afterwards purified using *Microspin S-300 HR* columns (Amersham Biosciences). The hybridization with the labelled eGFP-probe was performed over night at 62°C for eYFP samples and at 65°C for eGFP samples. After two wash steps with 2x SSC + 0.2% SDS, each for 15 min, and one wash step with 0.2x SSC and 0.2% SDS for 30 min, the membrane was sealed in plastic wrap and X-ray film was exposed to the radioactive labelled membrane.

4.1.10 Sequencing

PCR products and plasmids were commercially sequenced by Sequiserve (Vaterstetten, Germany).

4.2 Bacteria

4.2.1 Preparation of Competent Cells

Bacteria (for example DH5α) were plated on LB plates and incubated over night at 37°C. 10-12 colonies were picked and used for inoculation of a 50 ml starter culture, which again was incubated at 37°C over night. 250 ml of LB medium were inoculated with this starter culture to an OD600 of 0.1 and incubated at 18°C and 200-250 rpm until a OD of 0.6 was reached (ca. 5 h). The bacteria suspension was cooled 10 min on ice and, after distribution into five 50 ml

tubes, centrifuged 15 min at 3000 rpm and 4°C. Pellets were resuspended in 80 ml ice cold fresh and sterile filtered TB buffer, incubated 10 min on ice and centrifuged 15 min at 3000 rpm and 4°C. Pellets were resuspended in 20 ml ice cold TB buffer and, after mixing with 1.5 ml DMSO, incubated on ice again for 10 min. The competent bacteria cells were aliquoted in pre-cooled 1.5 ml tubes and quick-frozen in liquid nitrogen. For storage cells were kept at -80°C.

4.2.2 Transformation of E.coli

For transformation, competent bacteria were thawed on ice. 50 µl of bacteria suspension were mixed with 5 µl of plasmid DNA, then incubated at RT for 10 min. The transformed bacteria were streaked on an appropriate, prewarmed agar plate and incubated at 37°C over night.

4.2.3 Isolation of Plasmid DNA (Miniprep, Maxiprep)

Depending on the amount of plasmid DNA needed, 5 ml (miniprep) or up to 200 ml (maxiprep) of LB medium supplemented with 100 µg/ml ampicillin were inoculated with transfected bacteria and incubated shaking at 200 rpm and 37°C over night. The isolation of plasmid DNA from E.coli cultures of 1-5 ml was performed with *GenElute Plasmid Miniprep Kit,* for larger amounts the *GenElute HP Plasmid Maxiprep Kit* or for endotoxin free preparations, the *GenElute HP Endotoxin-Free Plasmid Maxiprep Kit* (all by Sigma-Aldrich) were used. All isolations were performed according to manufacturer's specifications. Determination of concentration and purity of isolated DNA was performed photometrically (see chapter 4.1.3).

4.3 Culture of Eukaryotic Cell Lines

4.3.1 General Culture Conditions

Eukaryotic cell lines were cultured in DMEM supplemented with 10% inactivated FBS. When necessary, cells were passaged at ratios of 1:3 to 1:5. All cell lines were cultivated at 37°C, 5% CO_2 in a humified atmosphere.

4.3.2 Freezing and Thawing of Cells

For freezing, cells were trypsinized if necessary and after pelleting resuspended in freezing medium, which was slowly added to the cells. 1 ml of freezing medium was used per $5x10^5$ to $5x10^7$ cells and the cell suspension was transferred to cryotubes in aliquots of 1 ml. Cells were stored at -80°C for short term and in liquid nitrogen for long term storage.

Frozen cells were rapidly thawed by incubation at 37°C in a water bath. Directly after thawing cells were washed two times with warm medium to remove traces of DMSO and seeded in a fresh 10 cm dish.

4.3.3 Determination of Cell Number and Vitality

For assessment of cell number and vitality of the cells, trypan blue exclusion was performed. This acid diazo dye penetrates the cell membrane of dead cells which subsequently appear blue under the light microscope, vital cells in contrast shine brightly. To count only living cells, an aliquot of the cell suspension to be analyzed was mixed with trypan blue at a ratio of 1:1, pipetted in the reservoir of a Neubauer-counting chamber and a defined volume was counted using the given grid. The cell number per ml was calculated as follows: average cell number per main square x chamber factor 10^4 x 2 (dilution factor).

4.3.4 Generation of Packaging Cell Line

For preparation of ecotropic retrovirus, Phoenix Eco cells were transiently transfected using the $CaCl_2$ method. For this, cells were grown in 10 cm dishes to a density of around 80% and pretreated 5 min before transfection with 25 µM chloroquine. Subsequently, cells were transfected by dropwise addition of the transfection mix consisting of 16 µg plasmid DNA, 122 µl 2 M $CaCl_2$ and 1 ml HBS buffer pH 7.0 in a total volume of 2 ml. Because of the toxicity of chloroquine to the cells, the medium was changed 9-10 h (latest 12 h) after transfection. 48 h after the transfection, continuing for the next two days with time intervals of 8 h, the virus conditioned medium (VCM) was collected and filtered through a 0.45 µm filter. After addition of 5 to 10 µg/ml protamine sulfate the VCM was used for transduction of the ecotropic cell line GP+E86 to

establish a stable high-titer packaging cell line. Transduced GP+E86 were sorted by FACS according to their eGFP or eYFP expression 48 h after transduction.

To determine the virus titer, $5x10^4$ NIH-3T3 cells were seeded in wells of a 6-well plate. 16 h after seeding, VCM of a fully confluent GP+E86 dish was harvested, filtered and pipetted on the NIH-3T3 in dilutions of 1/1, 1/3 and 1/10 in a total volume of 500 µl and with addition of 1 µl 5 mg/ml protamine sulfate stock. Protamine sulfate prevents aggregation of virus particles, and hereby increases the efficiency of transduction. Four hours later new medium was added to a total volume of 5 ml. After 48 h eGFP or eYFP expression was assessed and the titer (infectious particles per ml) calculated: the percentage of eGFP/ eYFP positive cells was multiplied with the number of NIH-3T3 cells at the beginning of virus exposure and divided by 500 µl (volume of VCM applied to the cells).

4.4 Mice and Murine Primary Cells

4.4.1 Mouse Strains and Progenitor Enrichment by 5-FU Injection

Parental strain mice were bred and maintained at the animal facility of the Helmholtz Center Munich. Donors of primary BM cells were ≥ 8 week old animals of the strain (C57Bl/ 6Ly-Peb3b x C3H/ HeJ) F1 (PebC3). For enrichment of hematopoietic progenitors, the mice were injected intravenously (*i.v.*) or intraperitoneally (*i.p*). with 150 mg 5-FU per kg body weight. The pyrimidine analog 5-FU, 5-flourouracil, removes a large proportion of actively cycling, more differentiated, cells and thereby enriches the BM for primitive hematopoietic progenitors, which are non-cycling or quiescent in nature. 8–12 week old (C57Bl/ 6J x C3H/ HeJ) F1 (B6C3) mice were used as recipients.

4.4.2 Collection of Murine BM

Four days post injection 5-FU mice were euthanized with CO_2 and after death sterilized in 70% EtOH. Femures, tibiae, hips and sternum of the animals were removed and cleaned properly with scissors and tissue paper to remove adherent tissue. The cleaned bones subsequently were crushed with mortar

and pestle in 3% FBS PBS. The BM cell containing supernatant was harvested and filtered through a 40 µm filter unit to remove bone chips and other impurities. For lysis of RBCs, cells were pelleted by centrifugation, resuspended in 1 ml of DMEM and, after addition of 4 ml ammonium chloride (ACl) 3%, incubated on ice for 30 min. After lysis cells were washed with PBS.

No RBC lysis was performed if later on the BM cells were to be transduced retrovirally.

4.4.3 Cultivation of Murine BM

To induce cell cycling, murine 5-FU BM progenitors were stimulated for 48 h in complete BM medium (DMEM supplemented with 15% FBS and cytokine cocktail (CC) with an end concentration of 10 ng/ml mIL-6, 6 ng/ml mIL-3 and 100 ng/ml mSCF). BM cells were cultivated at 37°C, 5% CO_2 within a humified incubator.

4.4.4 Retroviral Transduction

For transduction BM cells were co-cultured for 48 h with irradiated (40 Gy) GP+E86 virus producing cells in complete medium and with addition of 5 µg/ml protamine sulfate. Loosely adherent and non-adherent BM cells were harvested from the feeder 48 h after the end of transduction by thorough rinsing with PBS. To allow expression of eGFP or eYFP, BM cells were further cultured in fresh complete BM medium for 48 h. By fluorescence activated cell sorting (FACS) successfully transduced BM cells were sorted using eGFP or eYFP as marker. In the following, experiments performed on *pMIG*-, *Cdx2*-, and *Cdx4*-transduced cells will be termed pMIG, CDX2, and CDX4 arm, respectively. Examples for achieved titers are shown in Figure 24.

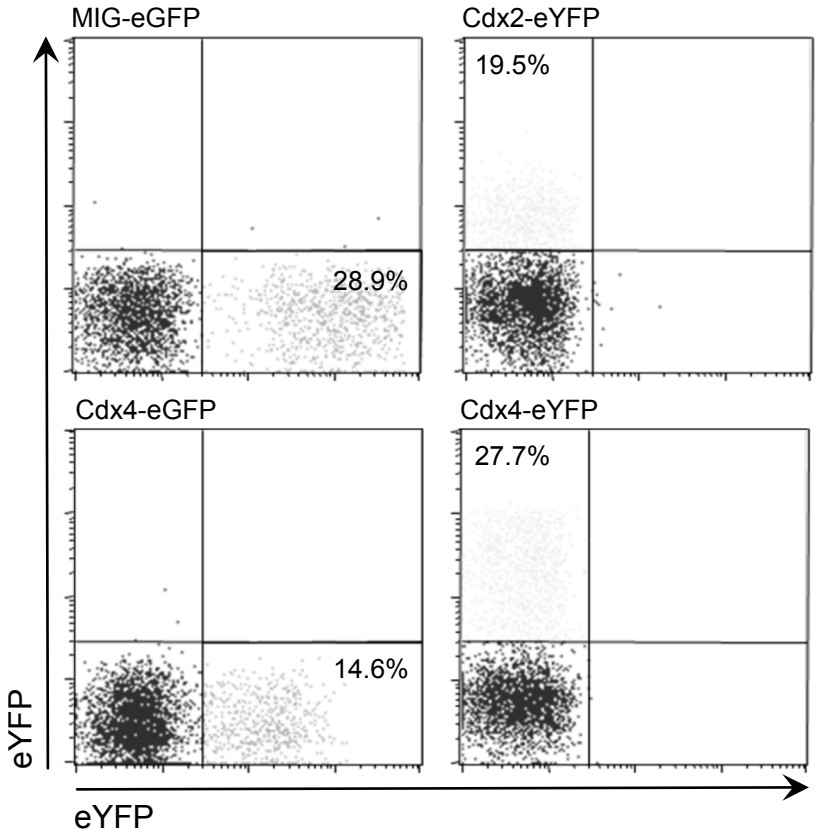

Figure 24: Transduction efficiency of retrovirally transduced 5-FU BM cells.
Cells were transduced following the above described method and 48 h after transduction sorted by FACS Vantage according to fluorescence marker expression.

4.4.5 Establishment of a Retroviral Packaging Cell Line for *Cdx4*

For transduction of murine hematopoietic cells the retroviral *MSCV-IRES-eGFP* vector was used which is known to be able to efficiently transduce primary BM cells. The *pMIG-Cdx4* construct was kindly provided by RK Humphries (Terry Fox Laboratory, Vancouver, Canada). The ecotropic packaging cell line GP+E86 was stably transduced with this *Cdx4* construct and a high titer clone was selected (Figure 24, methods section).

The expression level of *Cdx4* did change only slightly during *in vitro* culture as well as during *in vivo* experiments with e.g. a ΔC_T of 2.5 ± 0.2 SEM 72 h after transduction and a ΔC_T of 3.3 ± 0.4 SEM in BM of diseased mice.

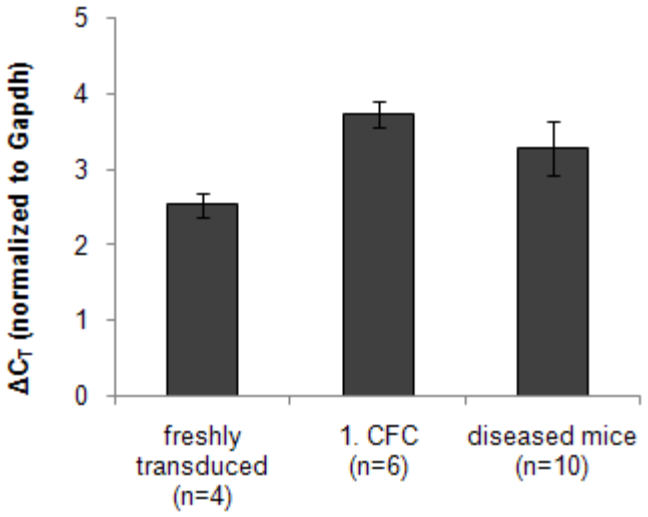

Figure 25: Expression levels of *Cdx4* in transduced BM cells.
Expression levels of *Cdx4* in BM cells 72 h after transduction, after 1st CFC assay and in diseased mice which were transplanted with transduced BM cells were determined by TaqMan qRT-PCR. The diagram shows average ΔC_T ± SEM, and the numbers of analyzed *Cdx4* transduced samples.

4.4.6 shRNA-Mediated Knock Down

Short hairpin RNA against CDX2 (NM_001265) were designed using the *RNAi oligo retriever* tool at http://www.cshl.org/public/SCIENCE/hannon.html. Four different shRNAs were obtained and cloned into the MSCV/LTRmiR30-PIG retroviral vector (pLMP, kindly provided by Scott W Lowe, Howard Hughes Medical Institute, New York, USA). Cell lines were retrovirally transduced as described in Chapter 4.4.4. Knock-down of CDX2 was confirmed by Western Blot (Figure 26).

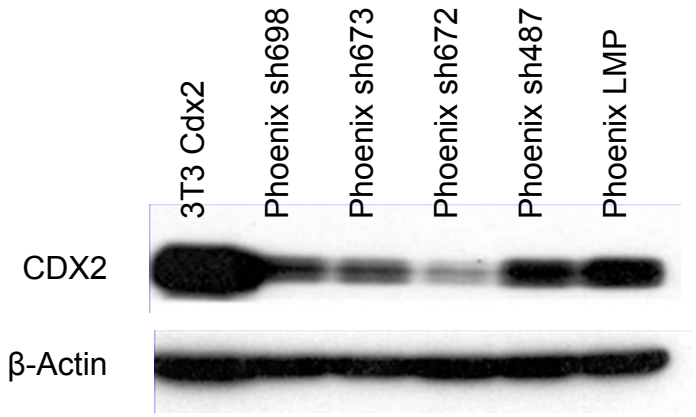

Figure 26: shRNA-mediated knock-down of CDX2 expression by retroviral transduction.

4.4.7 Immunophenotyping by Fluorescence Activated Cell Sorting

Lineage distribution and differentiation stage of cells were analyzed by fluorescence activated cell sorting (FACS). For this purpose, cells were washed with PBS and stained with PE- or APC-conjugated antibodies (see chapter 3.4, 0.0625 µg antibody per $1x10^6$ cells). After incubation on ice or at 4°C for 20 minutes and in the dark, cells were washed with PBS and resuspended in FACS buffer (2% FBS and 2 µg/ml propidium iodide in PBS). Cells were analyzed using the FACS Calibur system or sorted using the FACS Vantage cell sorter.

4.4.8 Proliferation Assay

For determination of the proliferative potential of BM cells *in vitro*, $2.5x10^4$ transduced BM cells were plated directly after sorting in 6-well suspension plates using complete BM medium. Every week, cells were subcultured in appropriate dilutions and viable cells were counted using trypan blue exclusion.

To generate IL-3 dependent cell lines, sorted cells were additionally plated in DMEM containing 15% FBS and 10 ng/ml IL-3 only. As above, every seven days an appropriate amount of cells was subcultured.

Left over cells regularly were immunophenotypically and morphologically analyzed by cytospin.

4.4.9 Colony Forming Cell Assay

For quantification of committed myeloid hematopoietic progenitors, colony forming cell (CFC) assays were performed using methylcellulose supplemented with cytokines (*MethoCult GF M3434*, Stem Cell Technologies) which supports growth of erythroid (BFU-E, CFU-E), granulocyte/macrophage (CFU-GM, CFU-M, CFU-G) and multi-potential granulocyte-erythroid-macrophage-megakaryocyte (CFU-GEMM) progenitors.

For this assay, 500 highly purified cells per dish, transduced with the gene of interest, were resuspended in 300 µl of plain DMEM and added to 3 ml of methylcellulose. After vortexing, 1.1 ml of the mixture was transferred into a 35 mm Petri dish using 3 ml syringes and blunt end needles. Per sample, two

dishes were plated and placed into a 10 cm dish together with one open 35 mm dish filled with water to avoid desiccation. CFC assays were incubated at 37°C in a humified incubator and 5% CO_2. After 7-9 days of incubation colony number and morphology was microscopically assessed using standard criteria. Subsequently, cells were harvested and the total cell number was determined. To test the colony forming/ clonogenic capacity, the cells were serially replated in appropriate dilutions up to three times.

4.4.10 Delta CFC Assay

During *in vitro* culture, normal BM cells rapidly lose their clonogenic potential. To analyze whether progenitors cells expanded in the proliferation assay lost their clonogenic potential, CFC-assays were set up at the end of a proliferation assay by plating 3,000 to 5,000 BM cells in methylcellulose. After 7 to 9 days of culture, colony number and morphology were assessed.

4.4.11 BM Transplantation of Mice

Directly after the end of transduction, $1.4x10^4$ – $1.1x10^6$ total BM cells (average of 16.25% ± 5.9 % SEM eGFP positivity) were transplanted into primary mice lethally irradiated with 800-850 cGy. One small aliquot of the BM cells was retained and further cultivated for 48 h to assess the percentage of successfully transduced cells by eGFP or eYFP expression with FACS. Lethally irradiated secondary recipients were injected with 10^6 BM cells from a diseased primary mouse together with $5x10^5$-$1x10^6$ untransduced BM helper cells of a normal syngenic animal.

4.4.12 Retroviral BM Transplantation Model

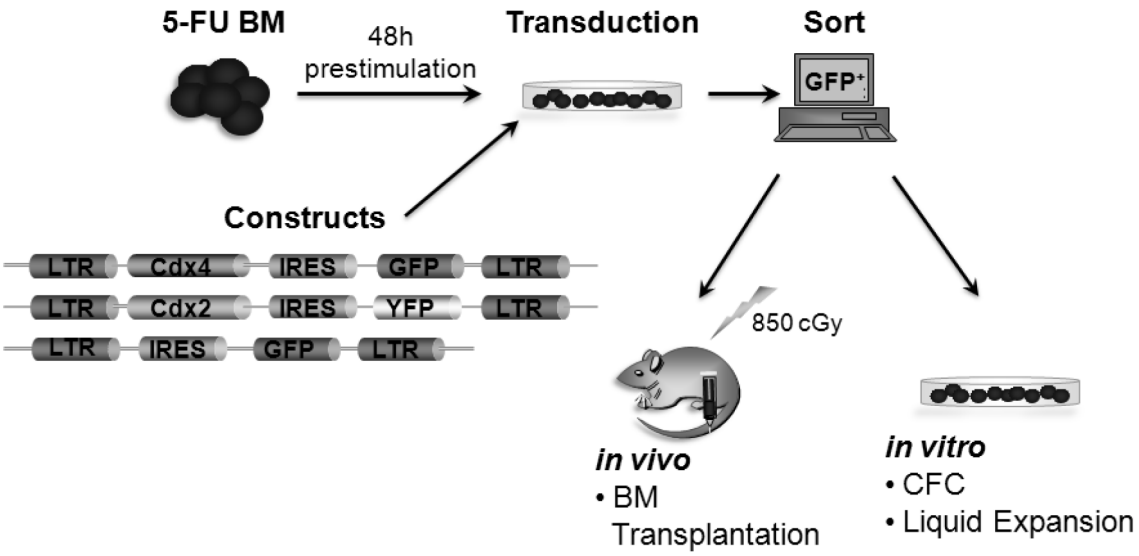

Figure 27: Experimental scheme applied for retroviral BM transplantation experiments. 5-FU treated BM was prestimulated in complete BM medium to induce cycling of HSCs and subsequently retrovirally infected by co-culture with virus producing E86 cell lines. Successfully transduced cells were highly purified by FACS and *in vitro* and *in vivo* experiments were performed.

4.4.13 Peripheral Blood Analysis

Peripheral blood (PB) of experimental mice was collected every four to eight weeks by tail incision. Directly after, several blood smears were made which after drying were stained as described in chapter 4.4.14.

The RBC count was determined after dilution of 1 µl PB in 5 ml of PBS. For evaluation of the WBC count 5 µl of PB were resuspended in 45 µl ACl for disruption of RBC and counted after 5 min lysis at RT. For immunophenotyping, the rest of the blood was resuspended in 200 µl ACl and for RBC lysis left on ice for 30 min. After washing with PBS, cells were stained as described in chapter 4.4.7.

4.4.14 Preparation and Staining of Cytospins

For cytomorphological analysis of the BM cells, $1x10^5$ cells were resuspended in 200-250 µl of PBS and loaded into the sample chamber of a Shandon Cytospin 2 centrifuge. By 10 min centrifugation at 450 rpm, cells were

transferred to a glass slide as a single layer with the cellular structure kept intact.

For Pappenheim's staining, dried slides were stained with undiluted May-Gruenwald eosine-methylene blue for exactly 3 min, washed 5 min in water and transferred to freshly diluted Giemsa solution (4 ml stock solution + 200 ml aqua dest.) for 1 h. After two times washing with water for 5 min each, slides were ready for assessment of cell morphology.

4.4.15 Histopathology

Histopathologic analysis of mice and organs fixed in formalin was performed by Dr. Leticia Quintanilla-Fend (Institute for Pathology, Tuebingen).

4.4.16 Analysis of Sacrificed Experimental Mice

Sick mice, characterized by cachexia, shortness of breath and lethargy, were euthanized using CO_2 and PB was taken immediately and directly from the heart using a 1 ml syringe and heparin to avoid coagulation of the blood. The blood was analyzed according to section 4.4.13. BM was obtained as described in chapter 4.4.2. Additionally, the spleen was removed, measured in size and half of it was homogenized using a 40 µm filter unit to obtain a single cell suspension. The other half of the spleen was fixed in formalin for histophatological analysis.

RNA as well as DNA were prepared from hematopoietic organs and immunophenotyping was performed (section 4.4.7). If necessary, *ex vivo* CFC assays and *ex vivo* proliferation assays were set up and secondary mice were transplanted. The rest of the cells was stored at -80°C.

4.5 Patient Samples

For analysis, mononuclear cells prepared from diagnostic bone marrow or peripheral blood samples were used. The AML cases were classified according to the French-American-British criteria and the World Health Organization classification (Bennett *et al.*, 1985). The study was approved by the ethics committees of all participating institutions, and informed consent was obtained

from all patients before they entered the study in accordance with the Declaration of Helsinki (http://www.wma.net/e/policy/b3.htm). As a control, bone marrow mononuclear cells (BMMCs; CellSystem, St Katharinen, Germany) from healthy individuals were analyzed. Cytomorphology, cytochemistry, cytogenetics, and molecular genetics were applied in all cases as described.

4.6 Microarray Analyzes

4.6.1 Preparation of Microarrays

First and second-strand cDNA synthesis were carried out using the *cDNA Synthesis System* (Roche Applied Science) and an input of 1-8 µg RNA according to manufacturer's instructions. After clean-up of the cDNA using the *GeneChip Sample Cleanup Module* (Affymetrix), biotin-labeled cRNA synthesis was performed in a final reaction volume of 40 µl employing the *GeneChip IVT Labeling Kit* (Affymetrix), the labeled cRNA was again purified and additionally fragmented using the *GeneChip Sample Cleanup Module* (Affymetrix, both kits were used according to manufacturer's instructions). Hybridization of *GeneChip Mouse Genome 430 2.0 Arrays A+B* (Affymetrix) was performed for 16 hrs. Array post-hybridization, washing and scanning were performed following detailed protocols provided in the *GeneChip Expression Analysis Technical Manual* (Affymetrix).

4.6.2 Evaluation of Microarray Data

Data were obtained from Mo430 v2.0 chips and acquired raw data (*.CEL files) were normalized using an R statistical package implementation of GCRMA (Gene Chip Robust Multi Array) algorithm (R version 2.8.1 and Bioconductor version 2.5). Normalized data was subjected to Linear Models for Microarray Data (limma) package (Bioconductor version 2.5) to assess genes that are differentially regulated or, for a more stringent assessment of differentially regulated genes, the R implemented twilight package was used. Probe sets that showed statistically significant differential expression at 95% confidence interval (p value <0.05, adjusted for multiple hypothesis testing with the Benjamini and

Hochberg's method) were selected. Heatmaps were built using the heatmap function in R (R version 2.8.1 and Bioconductor version 2.5).

4.7 Statistical Analyzes

Data were analyzed using the students t-test (Microsoft Office Excel 2007, Microsoft Cooperation, Redmond, WA, USA). Differences with p-values of 0.05 and less were considered as significant.

5. RESULTS

5.1 CDX2 in Human AML

Rawat *et al*. (2004) previously showed that ectopic expression of *Cdx2* in adult hematopoietic cells leads to induction of AML in the murine BM transplantation model. Human AML, especially AML with normal karyotype, is characterized by overexpression of a number of *HOX* genes. As CDX members were shown to upregulate *Hox* gene expression in murine early hematopoiesis, we intended to examine if aberrant expression of *CDX* genes could be responsible for the aberrant *HOX* gene expression observed in human AML patients.

5.1.1 *CDX2* is the Only CDX Member Aberrantly Expressed in Patients with Normal Karyotype AML

For the determination of the expression of *CDX2* and *CDX4* in normal hematopoietic tissues, total normal bone marrow (BM) and cord blood (CB) were analyzed by TaqMan real-time qRT-PCR. As Figure 28 depicts, neither *CDX4* nor *CDX2* are expressed in these hematopoietic populations. The specificity of the *CDX4* assay was confirmed in two different human ES cell lines where its expression was readily detected.

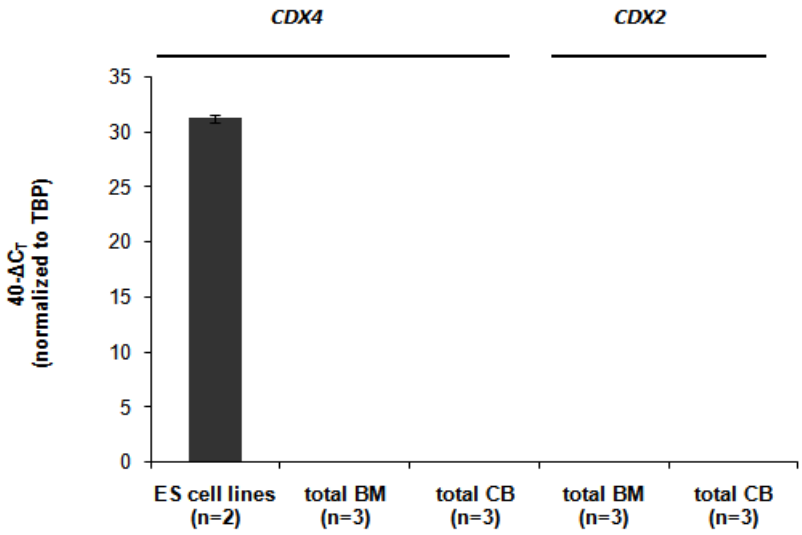

Figure 28: Expression of *CDX2* and *CDX4* in total normal BM and CB.
The expression of *CDX2* and *CDX4* was determined by TaqMan qRT-PCR and the ΔC_T values calculated by normalization to the *TATA-box binding protein* gene (*TBP)*.

To analyze if an aberrant expression of *CDX2* can be observed in AML with deregulated *HOX* expression, diagnostic BM or PB samples of 71 adult AML patients with normal karyotype were analyzed by qRT-PCR for expression of *CDX2*. In contrast to normal BM and CB where no *CDX2* transcript was detected, 89% of the 71 tested AML patients with normal karyotype proved to be positive for *CDX2* expression (Figure 29). No significant difference was observed between $NPMc^+$ and $NPMc^-$ patients.

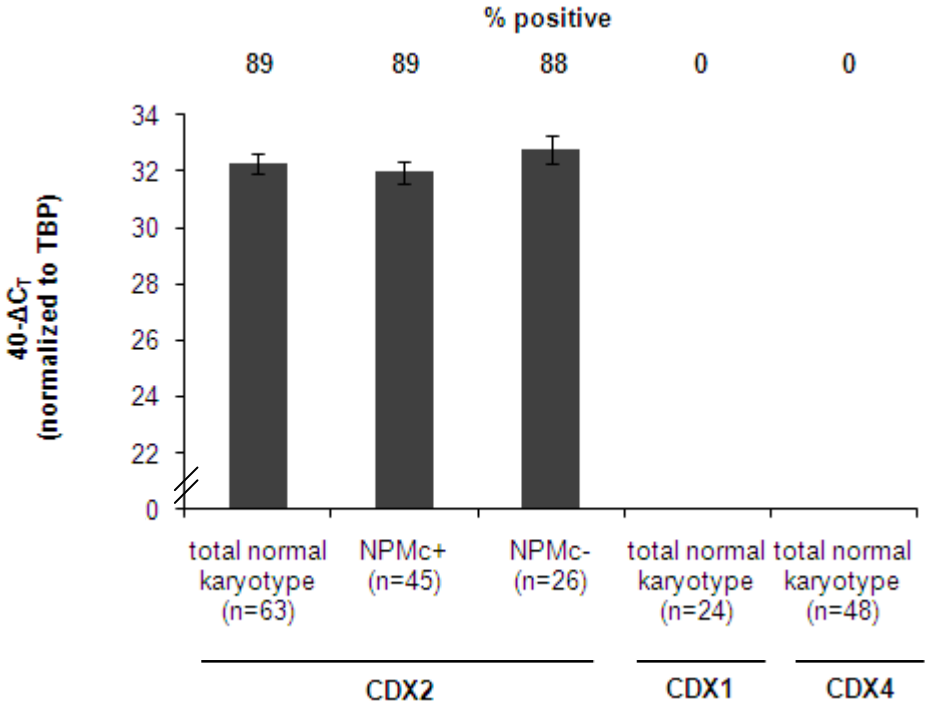

Figure 29: Expression of *CDX2* in AML with normal karyotype.
ΔC_T values were obtained by normalizing for *TBP* expression. Columns represent average expression level of *CDX2* ± SEM.

Furthermore, twenty-four patients ($NPMc^+$: 10, $NPMc^-$: 14) were tested for expression of *CDX1* and 48 patients ($NPMc^+$: 22, $NPMc^-$: 26) for the expression of *CDX4*. However, none of these patients showed any expression of these homeobox genes (Figure 29).

5.1.2 *CDX2* Is Expressed in 64% of AML with Abnormal Karyotype

Expression of *CDX2* was detected not only in patients with normal karyotype, but also the majority of patients with abnormal karyotype showed aberrant expression. When 44 patients with AML1-ETO, PML-RARα, MLL translocations or inv(16) were tested for *CDX2* expression, in 64% of these patients

expression of the transcript was detected (Figure 30). The positivity for *CDX2* expression varied considerably. Whereas in the AML1-ETO and MLL subgroups only half of the patients expressed *CDX2*, all of the ten tested patients harboring the PML-RARα translocation were positive for *CDX2* expression.

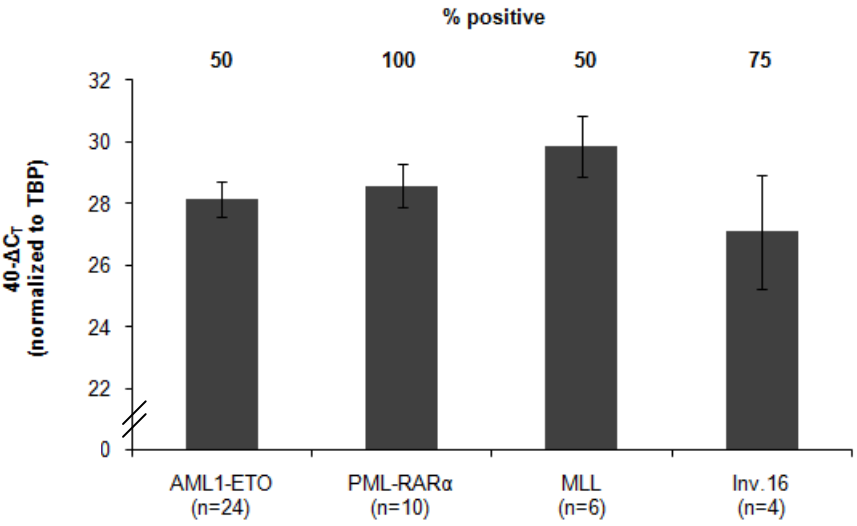

Figure 30: Expression of *CDX2* in different subgroups of AML with abnormal karyotype. Forty-four patient samples with abnormal karyotype, confirmed by FISH, were analyzed. Columns represent average ΔC_T expression values for each AML subgroup ± SEM.

5.1.3 *CDX2* Is Higher Expressed in AML with Normal Karyotype Compared to Abnormal Karyotype

Interestingly, a comparison of *CDX2* expression between patients with normal (n=63 of 71 total) and patients with abnormal karyotype (n=28 of 44 total) revealed a significantly higher *CDX2* expression in patients with normal karyotype of more than 15-fold ($p<0.001$).

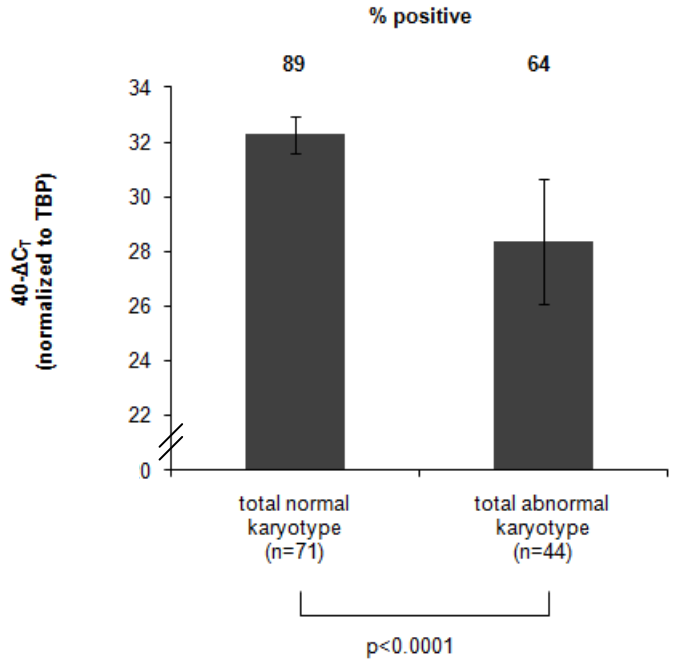

Figure 31: Expression of *CDX2* in AML with normal and abnormal karyotype.
Columns represent average ΔC_T values ± SEM. Only positive patients are shown.

5.1.4 High *HOX* Gene Expression Is Common in Patients with Normal Karyotype

As CDX2 is an important upstream regulator of *HOX* genes, the pattern of *HOX* expression within different AML subgroups was determined by analysis of microarray data. Those data were available for 12 of the patients with NPMc$^+$, 12 patients with NPMc$^-$, and 14 patients with AML-ETO translocation, which were tested for *CDX2* expression as described before. All of the NPMc$^+$ patients and 11 of 12 NPMc$^-$ patients were positive for *CDX2* expression whereas of the AML-ETO positive patients only 50% showed expression of the *CDX2* transcript. In order to allow a better comparison, data of six more AML-ETO positive patients as well as 20 PML-RARα positive patients and 10 healthy controls (each with unknown *CDX2* status) were included.

Clearly visible is the high expression level of all six analyzed *HOX* genes within the patient group with normal karyotype - not only within the NPMc$^+$ patients but also in the group of those patients lacking the *NPM* mutation. In contrast, patients with abnormal karyotype did not display an elevated expression of *HOX* genes but, as for example in the case of *HOXA9*, even showed a lower expression compared to normal BM.

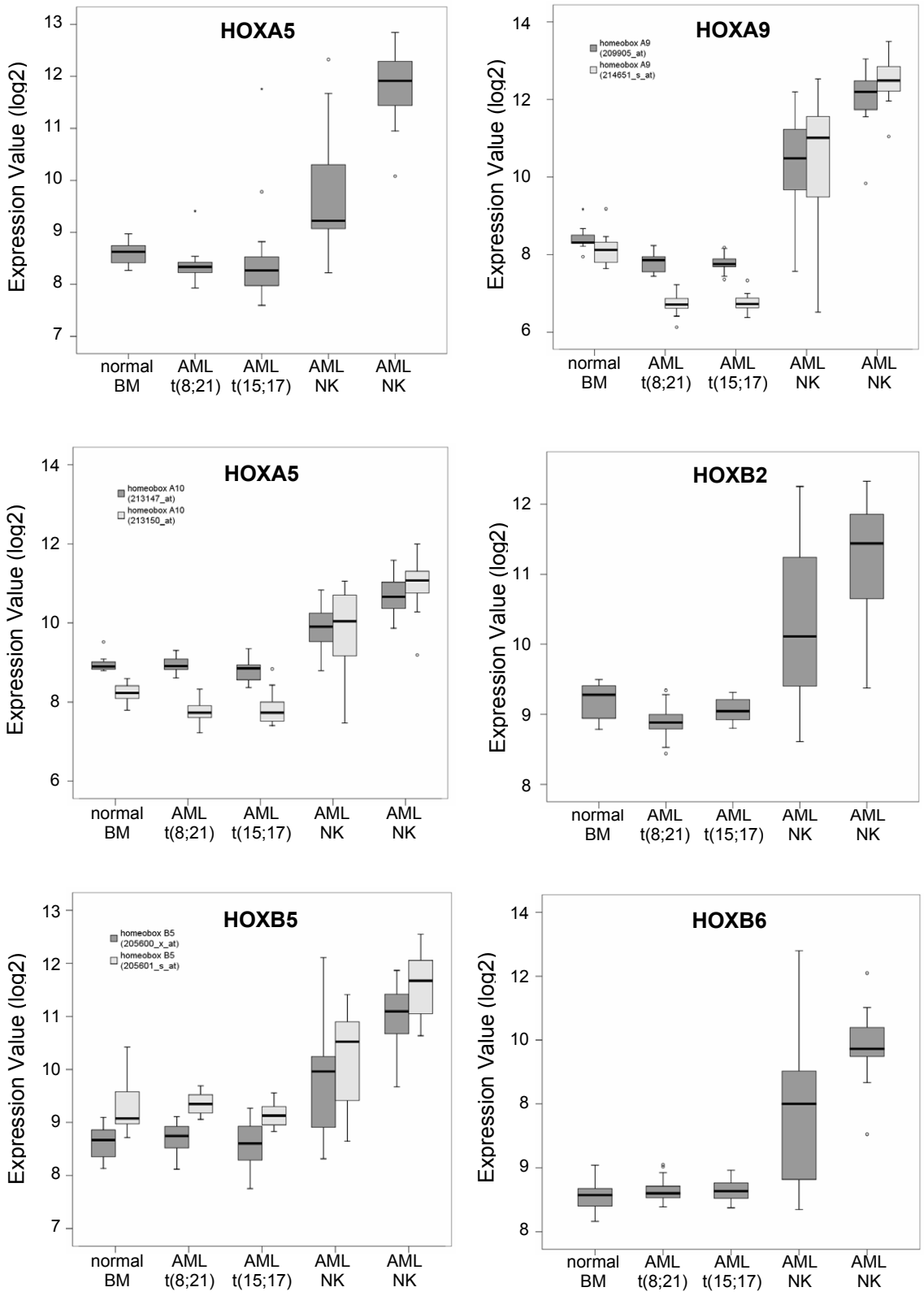

Figure 32: Expression of individual *HOX* genes in *CDX2* positive samples with normal and abnormal karyotype.
Log2 expression levels of six different *HOX* genes are shown in box-and-whisker plots. Bars indicate median expression levels and boxes show 25th and 75th percentiles, while whiskers indicate maximum and minimum values. Outliers (values that are more than 1.5 interquartile ranges above the 75th or below the 25th percentile) are represented by open circles.

Previously, *HOX* deregulation was reported only for AML cases with $NPMc^+$ normal karyotype. By performing this analysis, we now show an association of aberrant *HOX* gene expression with AML NK lacking NPM1 mutations. Although *HOX* gene expression in this subtype is not as high as in AML NK and $NPMc^+$, it is clearly elevated compared to normal BM and AML with abnormal karyotype.

5.1.5 *CDX2* Expression Levels Positively Correlate with Aberrant *HOX* Gene Expression in AML

As described above, aberrant *CDX2* expression was also detected in AML with aberrant karyotype, i.e. in those patient groups in which according to Figure 32 no significant elevated levels of *HOX* gene expression was observed. Therefore, it was tested if not positivity or negativity for *CDX2* expression but the level of *CDX2* gene expression would be connected to high levels of *HOX* gene expression. For this, the microarray data used for Figure 32 were analyzed by unsupervised hierarchic clustering.

The resulting heat map depicted in Figure 33 is composed of two main clusters. One cluster consists of patients with normal karyotype and the other comprises both patients with abnormal karyotype and normal BM. Compared to AML patients with t(8;21) or t(15;17) as well as normal BM, there is a striking elevated level of *HOX* gene expression within the cluster of normal karyotype AML. Notably, the high *HOX* gene expression is not dependent on the expression of the *HOX* regulating MLL. Another interesting fact is that the three normal karyotype patients showing no difference in their *HOX* expression when compared to healthy BM fall into the same cluster as normal BM and aberrant karyotype. These patients either show only weak expression of *CDX2* ($40\text{-}\Delta C_T$ 28.5 and 29.4) or have a *CEBPα* mutation which is assumed to inversely correlate with *HOX* gene expression (Roche *et al.*, 2004, Kirstetter *et al.*, 2008).

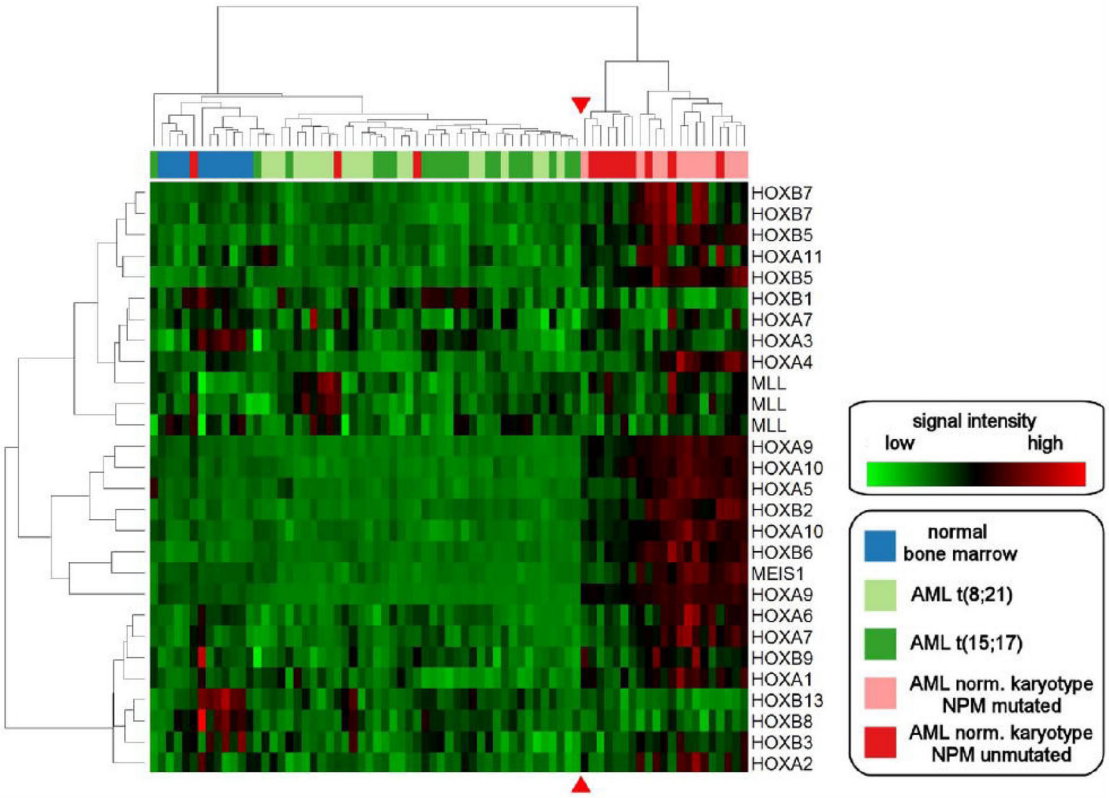

Figure 33: Hierarchic clustering of *CDX2*-positive AML samples according to *HOX* gene expression.
Unsupervised hierarchic clustering according to *HOX* gene expression demonstrates *HOX* gene deregulation in patients with normal karyotype with or without *NPM* mutation compared with samples with abnormal karyotype or normal bone marrow samples. Normal BM samples n=11, AML with t(8;21) n=20, AML with t(15;17) n=20, AML with normal karyotype n=12 and without *NPM* mutation (n=12). Red arrows highlight the boundary between the two main clusters. Genes and samples were permutated.

The NK cluster itself also can be subdivided into two subclusters of which one consists mainly of NPMc$^+$, the other of NPMc$^-$ patients. NPMc$^+$ patients generally show stronger deregulation of *HOX* expression, which is a common feature of this AML type (Debernardi *et al.*, 2003; Alcalay *et al.*, 2005; Verhaak *et al.*, 2005).

To determine if deregulated *HOX* gene expression might also be associated with *CDX1* or *CDX4*, 52 patients with normal karyotype (22 NPMc$^+$, 26 NPMc$^-$) were tested for *CDX4* expression and 22 patients (10 NPMc$^+$, 14 NPMc$^-$) for *CDX1* expression. Unlike *CDX2*, neither transcripts of *CDX1* nor *CDX4* were detectable by qRT-PCR (Figure 29), indicating a possible key role of CDX2 in this type of AML.

5.1.1 *CDX2* Expression Does Not Correlate with Mutations of *FLT3*

One gene frequently affected in patients with NK is *FLT3*, which is mutated in about 30% of all the cases of AML NK (Falini *et al.*, 2007). The most common mutation of this gene is the internal tandem mutation or FLT3-ITD, which was present in 31.0% of the analyzed patients, followed by point mutations present in 8.5%. As it was previously reported that *FLT3* mutations correlate with *HOX* expression (Roche *et al.*, 2004), four different subgroups of AML NK with or without $NPMc^+$ as well as with or without *FLT3* mutation were analyzed for *CDX2* expression.

As Table 9 indicates, no significant differences were found between any of the four groups. In the case of $NPMc^-$ patients, this could be due to the low number of patients with *FLT3* mutation. However, there was still no major difference observed between the larger groups of 23 $NPMc^+$ patients with *FLT3* mutation and 22 $NPMc^+$ without *FLT3* mutation (see Table 9), nor when only the *FLT3* mutation status was considered. Therefore, it is unlikely that the correlation between *CDX2* and *HOX* expression is influenced by the presence of *FLT3* mutations.

AML NK subgroup	median 40-ΔC_T ± SEM	p-Value		
		$NPM^+/FLT3^+$	$NPM^+/FLT3^-$	$NPM^-/FLT3^+$
NPM+/FLT3+	30.6 ± 0.56	-	-	-
NPM+/FLT3-	31.6 ± 0.53	0.26	-	-
NPM-/FLT3+	32.9 ± 0.88	0.45	0.76	-
NPM-/FLT3-	32.9 ± 0.75	0.91	0.43	0.49

Table 9: *CDX2* expression in NK patients with and without *FLT3* mutation.
18 of the patients with NPMc+ had a *FLT3 ITD*, 5 patients a *FLT3 D835* mutation. Of the NPMc- 4 patients were positive for *FLT3 ITD*, one for *FLT3 D835*.

5.2 CDX2 Is Able to Deregulate *Hox* Gene Expression in Adult Murine BM *in vitro*

It is known that *Cdx* genes are involved in the regulation of *Hox* genes during murine embryonic development. To confirm that CDX2 also possesses this capacity for *Hox* gene upregulation in adult hematopoiesis, murine 5-FU enriched BM cells were transduced with *Cdx2*. 48 h after transduction

successfully transduced, eYFP-positive cells were sorted and analyzed for *Hox* gene expression by qRT-PCR.

Although no significant changes were seen for the expression of *Hoxa1* and *Hoxb4*, CDX2 was able to induce the expression of *Hoxb6*, *Hoxb8* and *Hoxd13*, which were not expressed in BM cells transduced with the empty vector alone. As shown in Figure 34, CDX2 furthermore significantly upregulated *Hoxa5* (15.3-fold), *Hoxa7* (12.0-fold), *Hoxa9* (3.8-fold), *Hoxa10* (10.1-fold) and *Hoxb3* (10.5-fold) compared to the control and therefore CDX2 does indeed possess the capacity for *Hox* gene deregulation in adult murine BM cells.

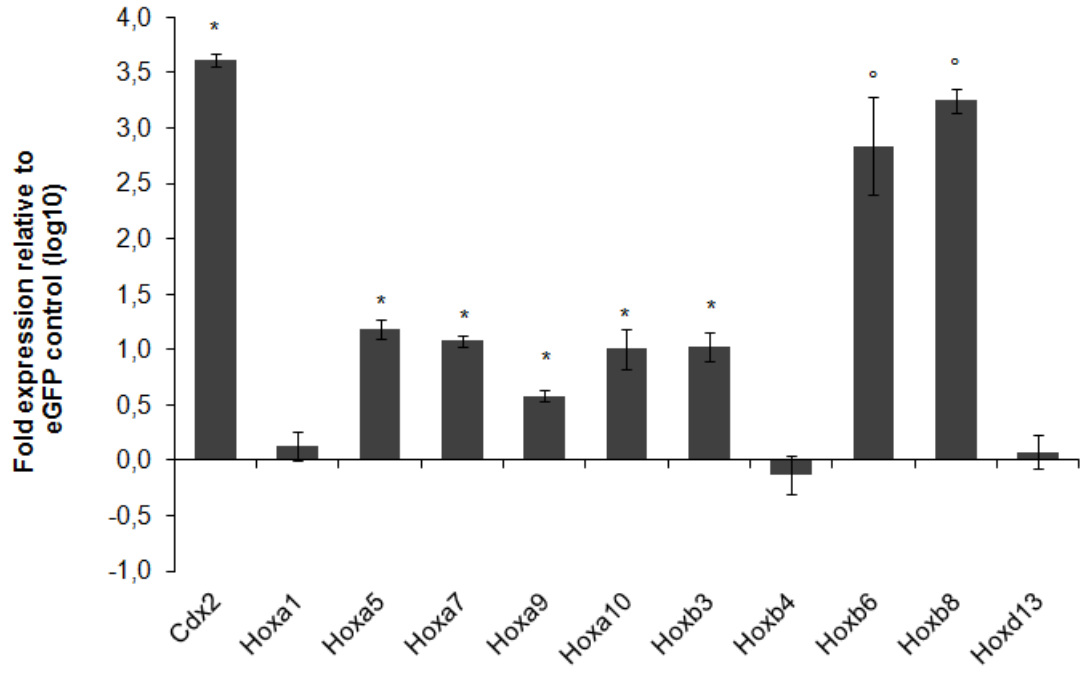

Figure 34: Overexpression of *Cdx2* in murine BM progenitors leads to *Hox* gene deregulation.
Murine progenitor enriched 5-FU BM cells were transduced with *Cdx2* or empty *pMIG* for control and 48h after transduction sorted for eYFP and eGFP expression, respectively. ΔC_T values were obtained by normalizing to *Gapdh* and fold-expression compared to *pMIG* was calculated. The diagram shows average expression levels of three independent experiments ± SD. ° marks calculated values, as *pMIG*-transduced cells were negative for *Hox* expression.

5.3 *CDX2* in Human ALL

As with more than 79% of all AML patients were positive for *CDX2* expression, we subsequently were interested if this aberrant expression of *CDX2* is restricted to AML or if it would be a more common feature and observable in other kinds of leukemia, as well.

5.3.1 *CDX2* Is Aberrantly Expressed in the Majority of Patients with ALL

To address this question, samples from 57 adult patients of different ALL subgroups were analyzed for expression of *CDX2* by TaqMan qRT-PCR.

In 81% of these patients the *CDX2* transcript was detected. The expression of *CDX2* showed high variation between the different ALL subgroups with highest median expression in pre-T ALL followed by cALL and pro-B ALL. ALL patients positive for the Philadelphia Chromosome translocation (Ph^+) expressed *CDX2* at a median level whereas patients with B-ALL/ Burkitt lymphoma and thymic T-ALL exhibited only low *CDX2* expression. Also the number of patients aberrantly expressing *CDX2* differed considerably between ALL subtypes, with 100% positivity in patients with pro-B ALL, c-ALL and Ph^+ ALL versus only 40% positivity in B-ALL/ Burkitt lymphoma, 70% in thymic T-ALL and 71% in pre-T ALL.

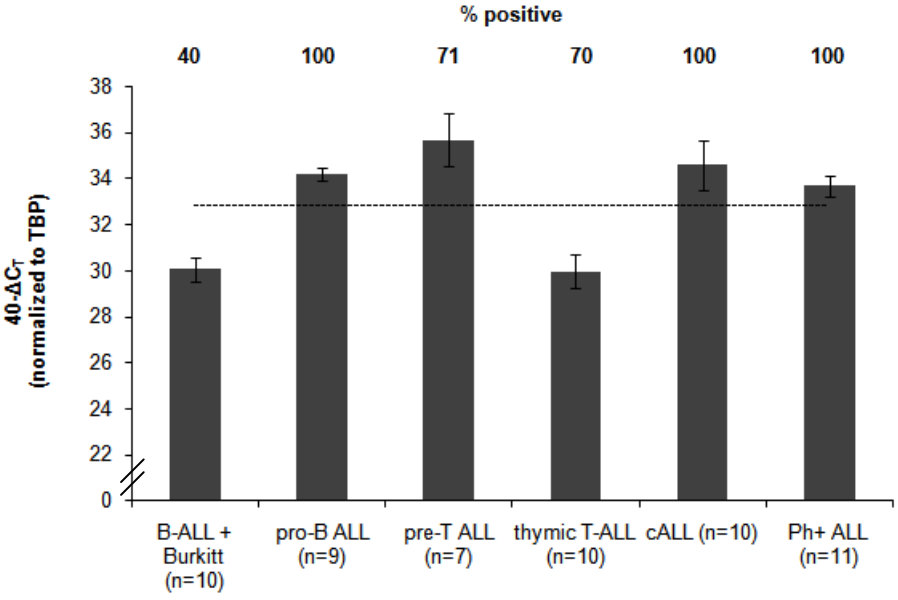

Figure 35: Expression of *CDX2* in 57 patients with ALL.
The diagram shows median *CDX2* expression of each ALL subgroup ± SEM. The dashed line represents the median *CDX2* expression of total ALL (40-ΔC_T of 32.8). Values were obtained by normalization against *TBP* expression.

In ALL, 50 of 57 patients were tested for expression of *CDX4* as well. However, the gene was undetectable in all the patients.

The ALL patients were classified according to the median *CDX2* expression level of total ALL (40-ΔC_T 32.8) in two groups with either high *CDX2* expression or low/absent *CDX2* expression. None of the patients with B-ALL/ Burkitt

lymphoma of thymic T-ALL showed high *CDX2* expression, whereas all patients with pro-B ALL showed high *CDX2* expression. With a p-value <0.001 the *CDX2* expression level significantly correlated with the ALL subtype (Figure 36).

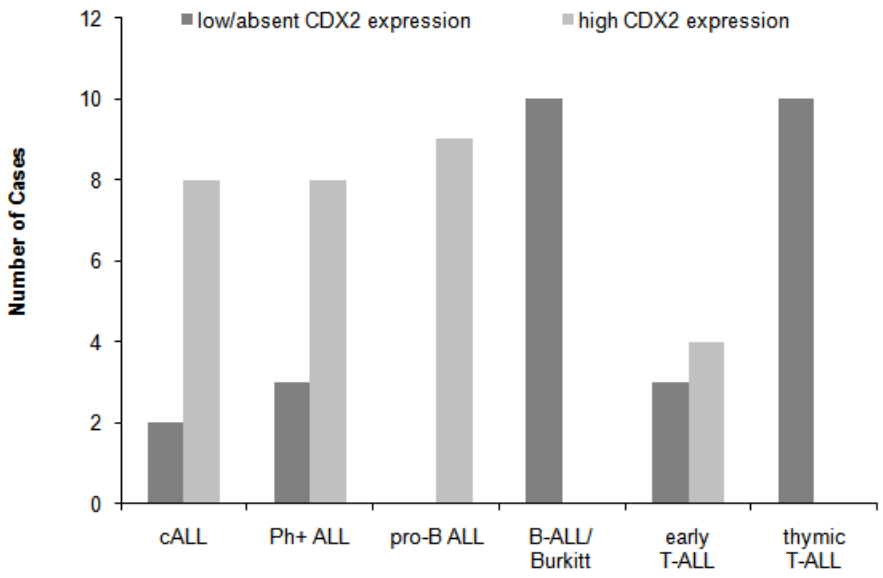

Figure 36: Distribution of patients with low/absent versus high *CDX2* expression levels in different ALL subgroups.
Patients with no *CDX2* expression or expression below the median (40-ΔC_T 38.2) were considered as low/absent, patients with *CDX2* expression equal to or above the median as high.

In total, with a median expression level of 32.8, ALL patients showed a significant higher expression of *CDX2* than AML patients (Figure 37, p<0.0001). Furthermore, the expression of *CDX2* in ALL was even higher than in normal karyotype AML which, with a median *CDX2* expression of 32.4, was the subgroup with highest *CDX2* expression in AML.

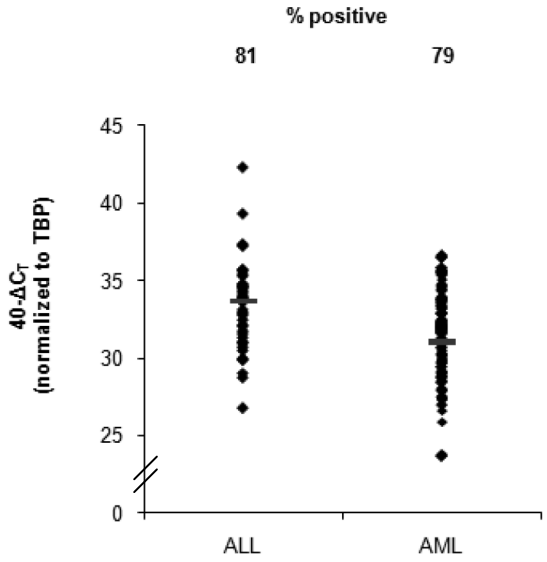

Figure 37: Comparison of *CDX2* expression in AML and ALL.
Shown are relative expression values for each single patient. The red line indicates the median *CDX2* expression. ΔC_T values were obtained by TaqMan qPCR and normalized to *TBP* expression.

5.3.2 High *CDX2* Expression Levels Are Associated with Poor Treatment Outcome in ALL

For 30 of the above analyzed ALL patients complete data sets were available. Following statistical analyses these patients were classified as "*CDX2* high" if their expression was above the median ALL expression or defined as "*CDX2* low/negative" if they showed *CDX2* expression lower than the median (Figure 36). The resulting subgroups each consisted of 15 patients.

When the *CDX2* expression within different risk groups of ALL (classified according to Raff *et al.*, 2007) was analyzed, most very high risk and high risk patients showed high *CDX2* expression. In contrast, the standard risk group consisted mainly of patients expressing low levels of *CDX2* (p=0.007 according to Fisher's exact test, Figure 38).

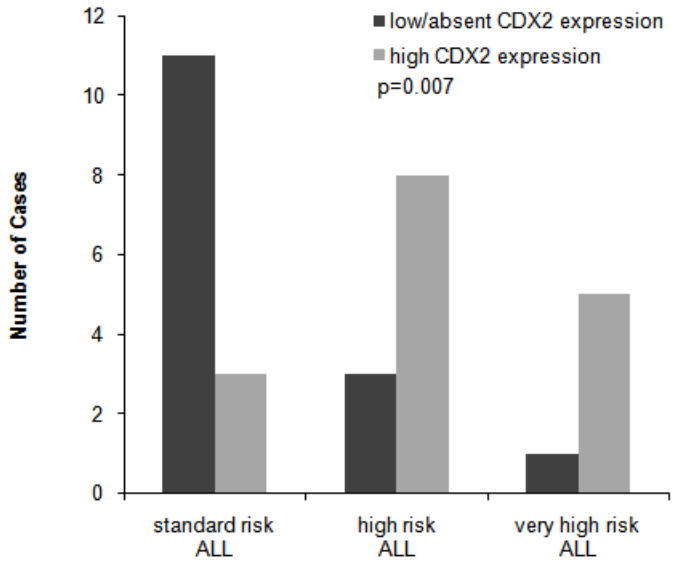

Figure 38: Expression of *CDX2* according to risk groups.
High and low/ absent *CDX2* expression were determined as expression above and below the median of total ALL.

Besides a significant correlation of the *CDX2* expression level with risk group and ALL subtype as already mentioned above, a significant correlation with blast percentage in the BM was also observed (p=0.047). No correlation was detected between *CDX2* expression and presence of molecular aberrations, age or karyotype. An overview of the correlation between high *CDX2* expression and different patient characteristics is given in Table 10.

Variable	P-*value*	*High* CDX2 *expression*	%	*Median value in high vs low/absent* CDX2 *expression groups*
ALL subtype	<0.001			
c-ALL		8 of 10	80	
Ph^+ ALL		8 of 11	73	
Pro-B ALL		9 of 9	100	
Mature B-ALL/Burkitt lymphoma		0 of 10	0	
Early T-ALL		4 of 7	57	
Thymic T-ALL		0 of 10	0	
Menigeosis leucemica	0.343			
Not present		12 of 22	55	
Present		1 of 4	25	
Risk[13]	0.007			
SR		3 of 14	21	
HR		8 of 11	73	
VHR		5 of 6	83	
Age (years)	0.303			48 vs. 40 years
Molecular aberrations[a]	0.790			
Present		11 of 23	48	
Not present		18 of 34	53	
Gender	0.111			
Female		16 of 25	64	
Male		13 of 32	41	
Karyotype	1.000		52	
Normal		6 of 11	55	
Aberrant		22 of 43	51	
Blasts in BM (in % of cells)	0.047			95 vs. 95%
Blasts in PB (in % of WBC)	0.188			95 vs. 90%
Leukocytes at presentation	1.000		52	
<30 000/µl		11 of 22	50	
>30 000/µl		17 of 32	53	

Table 10: Correlation of high *CDX2* expression levels with patients characteristics.
SR: standard risk, VHR: very high risk. The correlations between different patient characteristics and high *CDX2* expression are indicated.

In a univariate analysis, high *CDX2* expression levels were significantly associated with inferior overall survival (hazard ratio (HR) 4.2, 95% CI: 1.1–15.7, Figure 39). The survival rate two years after diagnosis was 86% of patients with low/absent and 52% of patients with high *CDX2* expression levels (p=0.019, log rank test). The hazard ratio for *CDX2* did not change substantially after adjusting for age (HR for *CDX2* 3.3, 95% CI: 0.86–12.85), presence of molecular aberrations (HR for *CDX2* 4.0, 95% CI: 1.07–15.13), ALL subtype (HR for *CDX2* 1.8, 95% CI: 0.36– 8.96), ALL risk category (HR for *CDX2* 2.9, 95% CI: 0.69–12.25), presence of karyotype aberrations (HR for *CDX2* 4.7, 95% CI: 0.99–12.45), gender (HR for *CDX2* 6.2, 95% CI: 1.58–24.24) or leukocytes at presentation (HR for *CDX2* 3.8, 95% CI: 0.97–15.18) by bivariate Cox regression. In all the cases, *CDX2* expression level remained an independent risk factor.

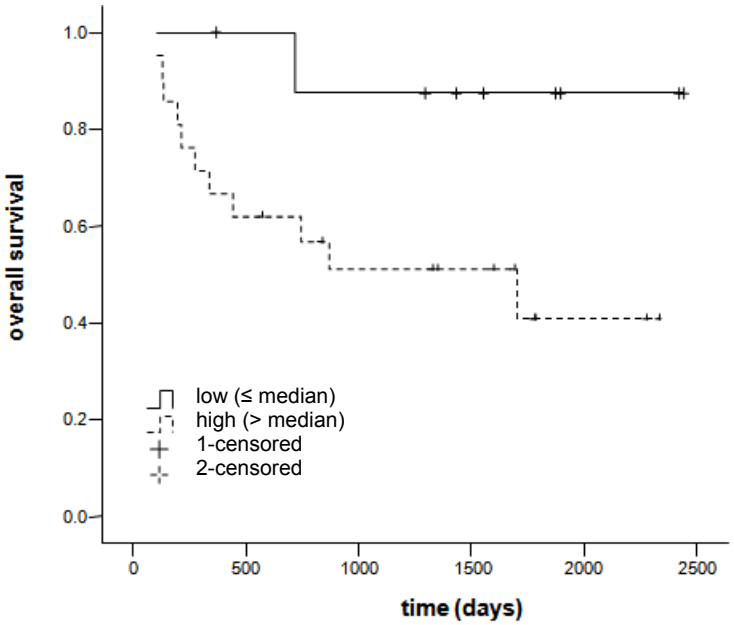

Figure 39: High expression of *CDX2* is associated with poor treatment outcome in ALL. Kaplan-Meier plot for overall survival of patients with high versus low/absent *CDX2* expression levels.

5.3.3 Knock Down of *CDX2* Leads to a Decrease in the Clonogenic Potential of the Pre-B Leukemia Cell Line Nalm-6

The importance of CDX2 for the clonogenic potential of leukemic cells was tested in the CDX2-positive human pre-B ALL cell line Nalm-6. For this, Nalm-6 cells were retrovirally transduced with two validated pLMP-shRNA constructs as well as with empty pLMP. Successfully transduced cells expressing eGFP were isolated by cell sorting. As determined by qRT-PCR, Nalm-6 cells expressing shRNA Hu_672_CDX2 showed a 49% reduction of *CDX2* expression levels whereas the control shRNA Hu_673_CDX2 did not lead to any change of *CDX2* expression (Figure 40).

The clonogenic potential of the transduced Nalm-6 cells was determined in the CFC assay. Nalm-6 cells transduced with shRNA Hu_672_CDX2 showed a significant, 31% reduction in colony formation compared to both the empty vector control and the non-active shRNA Hu_673_CDX2 (n=3, p=0.019 and 0.018, respectively). These results show the importance of CDX2 expression for the clonogenic capacity of the Nalm-6 cell line.

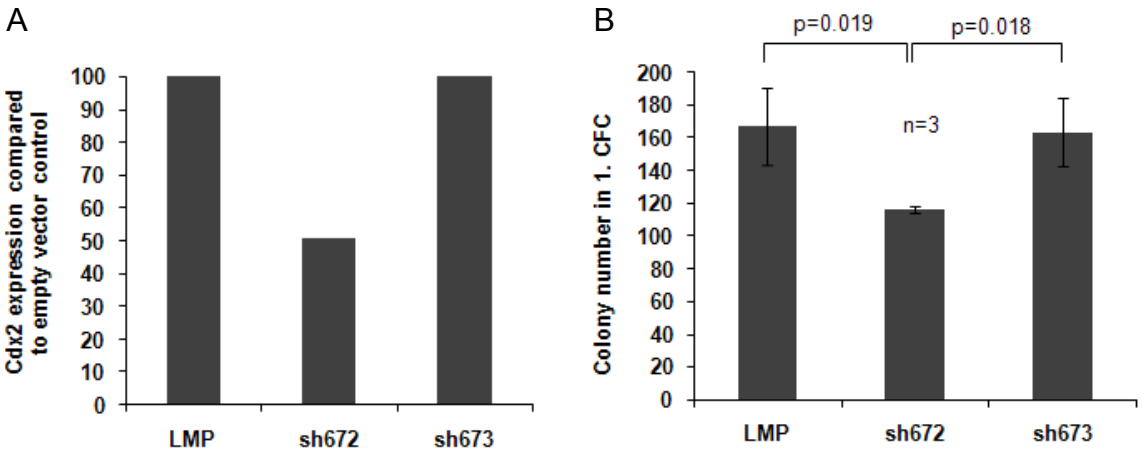

Figure 40: Knockdown of *CDX2* in Nalm6.
A) Compared to the empty vector, transduction with sh672 lead to a 49% reduction of the *CDX2* expression level. No effect was observed for sh673. B) Only transduction with sh672 lead to a decrease in colony formation, no change of colony number was detected in the inactive sh673 compared to the empty vector control. Knockdown on protein level was confirmed in Phoenix cells (Chapter 4.4.6).

5.3.4 Aberrant Expression of *CDX2* Does Not Depend on Promoter Methylation

One explanation for high expression levels of *CDX2* as observed in lymphoid leukemia might be epigenetic changes as promoter demethylation. To determine if this would be the case, the methylation status of the *CDX2* promoter region (-181 to +163 relative to the transcription start site (Yuasa *et al.*, 2005) was quantitatively analyzed by pyrosequencing. Nine patients, six positive and three negative for *CDX2* expression, were included in this analysis.

As already demonstrated for AML by Scholl *et al*. (2007), there was no detectable difference in the methylation level of *CDX2*-positive and -negative ALL patients (see Tables 11 and 12). Both groups exhibited a high variation of the methylation levels within the promoter region between 7% and 82%. Therefore, differential methylation of this CpG rich region as cause for high *CDX2* expression could be excluded. However, one interesting observation was that all four T-ALL samples (3x early T-ALL, 1x thymic T-ALL) showed a promoter methylation above 60% whereas the methylation levels of all other ALL samples were below 30%.

Patient No	CDX2	No of CpG site																							
		1	2	3	4	5	6	7	8	9	10	11	12	13	14	15	16	17	18	19	20	21	22	23	24
1	+	29	45	24	57	60	17	15	10	38	18	10	12	49	34	24	28	22	21	16	21	80	52	7	18
3	+	31	30	39	37	15	2	4	3	3	4	5	4	34	33	25	35	8	33	11	41	8	30	2	19
22	+	3	3	3	33	7	1	2	0	3	3	2	1	16	11	3	3	3	6	3	40	7	7	0	2
27	+	5	4	13	9	5	1	1	0	5	4	3	3	29	36	13	42	40	33	17	51	63	10	0	5
42	+	67	63	78	76	75	62	66	62	80	72	82	60	72	79	59	77	80	70	67	92	35	70	52	56
43	+	88	80	98	93	92	82	89	81	95	90	91	58	78	93	70	91	91	82	77	100	5	80	74	79
32	-	7	4	4	8	14	1	2	1	39	39	14	26	42	15	9	14	21	9	9	12	79	13	4	9
44	-	84	77	94	88	87	79	86	77	91	84	93	71	78	90	69	90	92	83	74	100	25	81	61	76
52	-	54	47	60	74	82	70	69	32	79	61	82	64	71	81	62	82	86	74	79	71	11	17	33	66

Patient No	CDX2	ALL subtype	Avg	SD
1	+	cALL	**29**	**19**
3	+	cALL	**19**	**14**
22	+	pro-B ALL	**7**	**10**
27	+	pro-B ALL	**16**	**18**
42	+	early T-ALL	**69**	**12**
43	+	early T-ALL	**82**	**19**
32	-	B-ALL	**16**	**18**
44	-	early T-ALL	**80**	**15**
52	-	thymic T-ALL	**63**	**21**

Tables 11 and 12: Methylation analysis of ALL samples
Quantitative analysis of the % methylation status of CpG islands surrounding the transcription start site of *CDX2* from the position -181 to +163 in six ALL patients positive and three patients negative for *CDX2* expression. Table 11 indicates the methylation level per site and Table 12 the average methylation level of all 24 CpG sites located within the analyzed region.

5.3.5 *CDX2* and *HOX* Expression Do Not Correlate in ALL

As microarray data demonstrated a correlation between *HOX* deregulation and *CDX2* expression level in AML, ALL patients were examined for the existence of a similar relationship via qRT-PCR. 30 ALL patient samples as well as three samples from both normal BM mononuclear cells (MNCs) and BM $CD34^+$ were screened for the expression of *HOXA7*, *HOXA9*, *HOXB6* and *HOXB8*.

Whereas almost all patient samples revealed *HOXA7* and *HOXA9* expression and two third of the samples showed expression of *HOXB6*, only two of the 30 ALL patients were positive for *HOXB8* expression. Clearly visible is an upregulation of the MLL-AF4 target gene *HOXA9* within the MLL-AF4 positive pro-B ALL group compared to healthy controls. However, whereas in AML

CDX2 expression was clearly associated with *HOX* gene deregulation, no significant correlation between *CDX2* expression and expression of *HOXA7, A9* or *B8* was found in ALL samples. Only a borderline significance between expression of *CDX2* and *HOXB6* (p= 0.048, Mann–Whitney U-test) was detected.

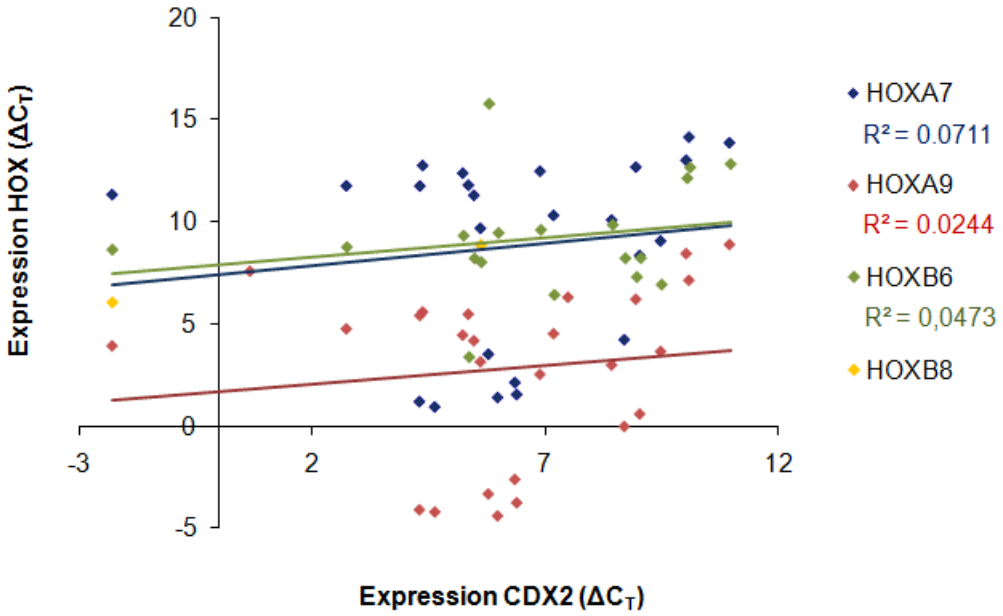

Figure 41: Expression of *HOX* genes in *CDX2*-positive ALL patients and BM of healthy individuals.
Correlations of *HOX* gene expression with high or low *CDX2* levels (according to median expression level in ALL) were calculated using the Mann-Whitney-U-test. ΔC_T values were obtained by qPCR and normalized to *TBP* expression. Whereas a weak positive correlation can be observed for *HOXA7*, *HOXA9* and *HOXB6,* a significant correlation only was detected between the expression levels of *CDX2* and *HOXB6*.

	HOXA7	HOXA9	HOXB6	HOXB8
CD34$^+$	3/3	3/3	3/3	-
MNC	3/3	3/3	3/3	2/3
c-ALL	5/6	6/6	5/6	1/6
cort. T-ALL	4/5	5/5	4/5	-
Ph$^+$ ALL	6/6	6/6	5/6	1/6
pre-T ALL	3/4	3/4	1/4	-
pro-B ALL	6/6	6/6	3/6	-
B-ALL	3/3	3/3	3/3	-

Table 13: Number of samples positive for *HOX* gene expression.
The table supplements Figure 41 and indicates the number of samples positive for *HOX* gene expression vs. total sample number.

5.3.6 CDX2 Deregulates Genes Involved in Lymphopoiesis

Unlike AML, in which CDX2 is able to influence the self-renewal and proliferative potential of the leukemic clone by its ability to activate *HOX* gene expression, *CDX2* expression in ALL did only weakly correlate with the expression levels of analyzed *HOX* genes. To test if ectopic expression of CDX2 in BM progenitors would also perturb the expression of other genes involved in stem cell function, TaqMan Low Density Array (LDA) was performed. For this analysis, 92 genes involved in hematopoietic self-renewal, proliferation and differentiation were selected and the expression of these genes was analyzed in 5-FU BM samples 48 h after transduction with empty vector control or *Cdx2*.

The results of this assay demonstrated that CDX2 was able to significantly upregulate a number of genes involved in self-renewal. Amongst these genes were, as expected, *Hox* genes - including the *Hox* genes known to be deregulated in ALL such as *Hoxa10* or *Hoxa5* (Figure 42). However, genes involved in stem cell function were also differentially expressed, amongst others *Slamf1* or the Abc transporter coding *Abcb1b*.

In accordance with the important function of CDX2 during embryogenesis, *Cdx2* transduced BM cells also showed an upregulation of different genes involved in embryogenic development like *Ddx4*, which is involved in the germ cell specification of the embryo or *Wnt2*, which is regulating the differentiation of the hemangioblast.

Interestingly, besides these genes several genes involved in lymphoid lineage determination were deregulated. For example, *Flt3a* was upregulated 4-fold. FLT3 is a marker in hematopoietic stem cell differentiation, but is also crucial for B-cell lineage commitment. A 4-fold upregulation was also detected for *Lef-1*, which affects proliferation and apoptosis in B-cell precursors but, as our group previously showed, can induce B-lymphoblastic leukemia in the murine model when aberrantly expressed. *Id3* and *Tcf3* both were more than 10-fold upregulated. *Tcf3* is a gene frequently affected by translocations especially in childhood ALL, whereas overexpression of ID3 blocks B-cell specification at an early B-cell stage. These results suggest that CDX2 in ALL, unlike in AML,

exerts its leukemogenic effect by deregulation of lymphoid pathways rather than by deregulation of *HOX* genes.

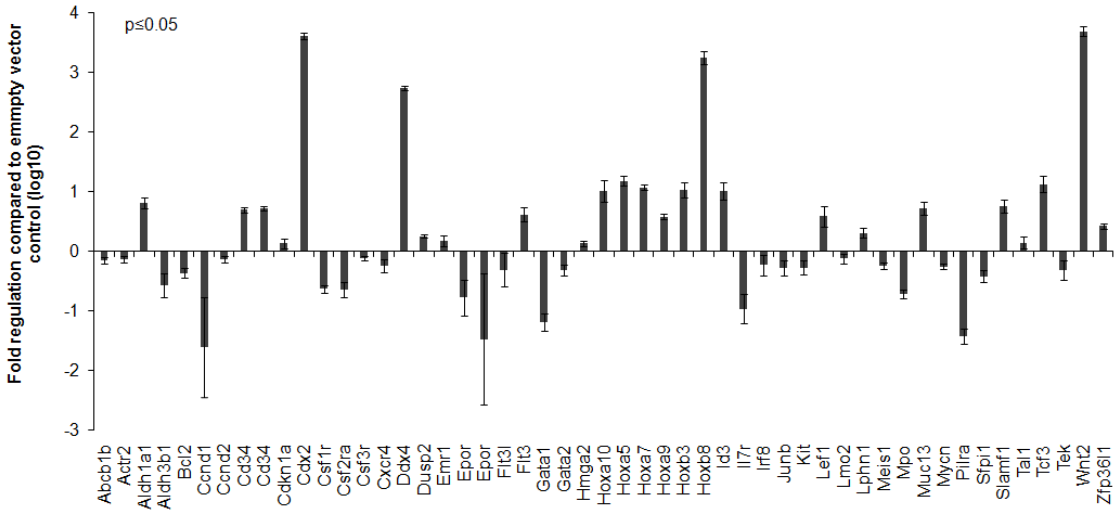

Figure 42: Differential gene expression in *Cdx2*-transduced bone marrow.
Differential gene expression in *Cdx2*-transduced-bone marrow cells. Fold expression levels of different genes in murine progenitor enriched 5-FU bone marrow after ectopic expression of *Cdx2*. RNA was extracted 72 h after stopping the transduction. Fold expression difference compared with empty vector-transduced bone marrow cells was calculated by averaging three independent experiments. Only genes with significant up- and downregulation are shown.

5.4 *Cdx4* in the Murine Transplantation Model

As reported by Davidson *et al*., CDX4 plays an important function in embryonic hematopoiesis (2003) and is expressed in murine adult hematopoiesis as well. However - and unlike *CDX2* - no expression of *CDX4* was detected in human acute leukemia. In contrast, overexpression of CDX4 was reported to result in an expansion of hematopoietic progenitor cells and its effect seemed more likely to equal that of HOXB4, a HOX member with known stem cell amplificatory potential. Using the BM transplantation model, it therefore was analyzed, what relevance overexpression of CDX4 would have on HSC function and maintenance.

5.4.1 *Cdx4* Is Highly Expressed in Murine BM Progenitors

To test this, the expression of *Cdx4* was determined in different adult hematopoietic subpopulations of the mouse by TaqMan qRT-PCR. The highest expression of *Cdx4* was detected in early hematopoietic cells, i.e. in KSL cells, followed by progenitor enriched 5-FU BM cells. Both populations showed a

significantly higher expression of *Cdx4* compared to BM MNCs with a more than 1,700-fold difference between normal BM and KSL and an almost 400-fold difference between normal BM and 5-FU BM (p=0.008 and 0.005, respectively). The same was true for spleen, where the expression level of *Cdx4* was more than 200-fold lower in total spleen than in 5-FU enriched splenic cells. This is consistent with data of Bansal *et al*. (2006) who reported high expression of *Cdx4* in early hematopoietic populations, especially in HSCs and CLPs.

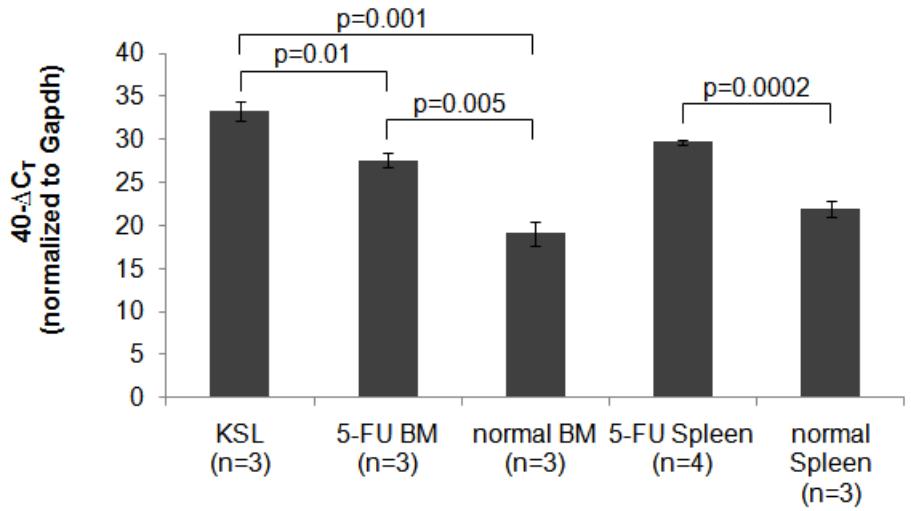

Figure 43: Expression of *Cdx4* in hematopoietic populations.
Expression of *Cdx4* in highly purified KSL cells as well as 5-FU enriched and total BM and spleen cells was analyzed by TaqMan qRT-PCR and normalized to the housekeeping gene TBP.

Importantly, in human samples no expression of *CDX4* was detected, neither in normal hematopoietic tissue nor in AML or ALL patients. The *CDX4* primers were tested successfully using the two human ES cell lines H9 and CA for positive control (see chapter 5.1.1).

5.4.2 CDX4 Confers Proliferative Potential to Murine BM Progenitors *in vitro*

For assessment of the influence of CDX4 on the proliferative potential of hematopoietic cells, progenitor enriched 5-FU BM cells were retrovirally transduced with the *Cdx4*-containing construct or the empty vector for control and proliferation assays were performed.

BM cells transduced with empty *pMIG* were not able to proliferate in the *in vitro* liquid culture (LC) over a time longer than one week but turned into mast cells.

In contrast, CDX4 was able to confer proliferative potential to the transduced cells with a cell number of $1.8x10^{11}$ after four weeks of culture in complete medium supplemented with cytokines. The same applied to the culture of *Cdx4*-transduced cells in medium supplemented with IL-3 only. CDX4 was able to induce IL-3 dependent growth, and after two weeks showed an average cell number of $3.7x10^{9}$ (n=6). Within the four weeks of IL-3 supplemented liquid culture, CDX4 promoted a more than $2x10^{6}$-fold expansion of the initial input cell number.

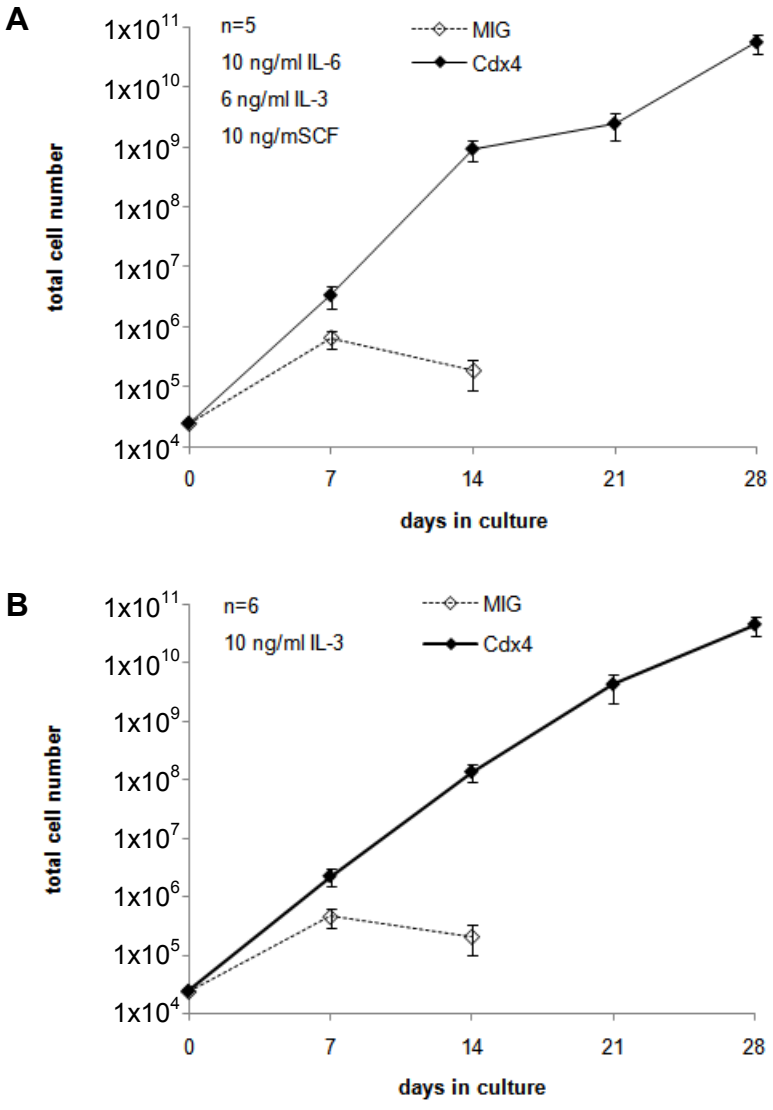

Figure 44: Proliferation assays of 5-FU murine BM cells transduced with *pMIG* and *Cdx4*. Transduced cells were sorted for eGFP expression and proliferation assays were set up with $2.5x10^{4}$ cells per plate. Cells were cultivated in DMEM 15% FBS supplemented with either A) cytokine cocktail (100 ng/ml mSCF, 10 ng/ml IL-6 and 6 ng/ml IL-3) or B) 10 ng/ml IL-3 only. Every week a half-medium change was performed, the cell number was determined by trypan exclusion and fresh cytokines were added to the culture. The diagram shows average cell numbers ± SEM.

5.4.3 CDX4 Does Not Block the Differentiation Program of Murine BM Progenitors *in vitro*

As CDX4 expressing BM cells show high proliferative potential, it was analyzed if this could be due to a block in differentiation. To investigate this, immunophenotyping of *Cdx4*-transduced murine BM cells was performed. In IL-3 only conditions, the fraction of the different myeloid subpopulations remained almost unchanged with 38.2% myeloid cells after one week and 41.0% after three weeks of culture (Figure 45C). After one week in culture supplemented with cytokine cocktail, overexpression of CDX4 resulted in increased differentiation into the myeloid lineage: 51.5% of the cells were positive for the myeloid markers Gr-1 and/or Mac-1 in the CDX4-overexpressing arm vs. 43.8% in the control arm. This difference was mainly due to an increased percentage of Gr-1$^-$/Mac-1$^+$ cells (p=n.s., Figures 45A and B). Although after three weeks of culture 50.2% myeloid cells were present, the ratio of the myeloid subpopulations changed in favor of Gr-1$^+$/Mac-1$^-$ granulocytes (Figure 45B). The presence of cells with these marker combinations indicate that CDX4 overexpressing BM progenitor cells were not blocked in their differentiation ability but were able to give rise to mature hematopoietic cells.

In none of the two arms growth of B220$^+$ B-lymphoid cells or CD4 or CD8 positive T-lymphoid cells was detected by immunophenotyping.

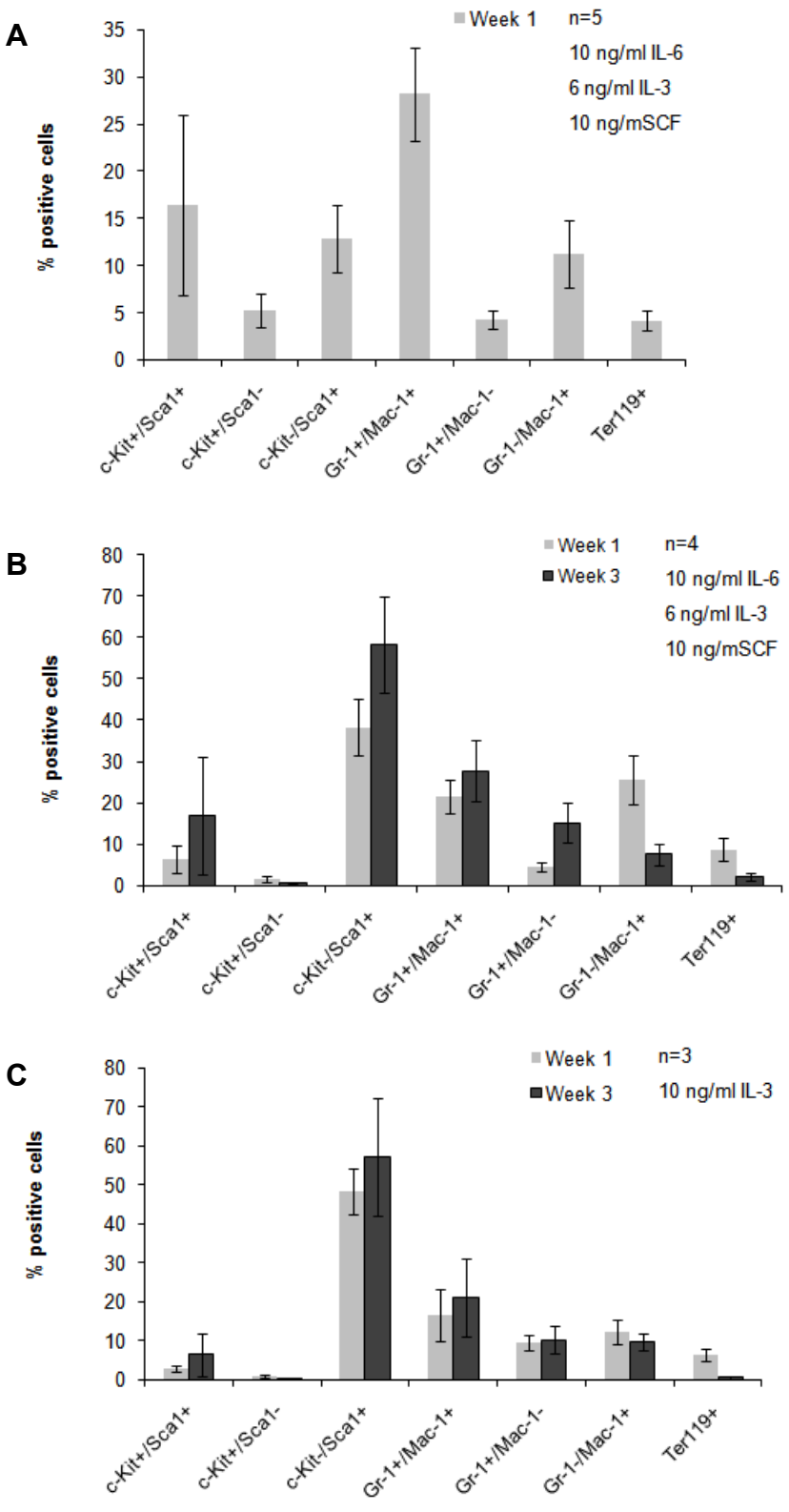

Figure 45: Immunophenotypic analysis of BM cells after three weeks of LC.
5-FU BM cells were transduced with *Cdx4* or empty *pMIG* and immunophenotypically analyzed by FACS Calibur each week A) *pMIG*-transduced cells in cytokine supplemented culture B) *Cdx4*-transduced cells in cytokine supplemented culture C) *Cdx4*-transduced cells in IL-3 only supplemented culture.

Transduction of BM cells with *Cdx4* additionally resulted in an increase of c-Kit$^+$/Sca-1$^+$ blast forming cells. After three weeks in CC supplemented medium 16.9% of the cells were positive for this marker combination, with addition of only IL-3 6.5% positive cells were detected. An increase was also observed for the population of c-Kit$^-$/Sca-1$^+$ cells, which constituted almost 60% of the cells after three weeks of culture in both arms. Although this population is not well defined, it was shown that it harbors clonogenic capacity *in vitro* (Metcalf *et al.*, 2009).

Additionally, a small fraction of Ter119$^+$ erythroid cells was observed after one week of culture in both arms. Whereas this fraction was almost lost after three weeks in IL-3 only conditions, a small percentage of Ter119$^+$ cells was still present in CC supplemented culture.

5.4.4 CDX4 Confers Serial Replating Capacity to Murine BM Progenitors *in vitro* without Blocking Differentiation

To examine the effect of *Cdx4* overexpression on committed hematopoietic progenitors, CFC assays were performed using M3434 methylcellulose, which supports growth of myeloid colonies.

CDX4 showed a strong effect on the replating capacity of the transduced BM cells. As depicted in Figure 46A, CDX4 was able to confer a significantly higher proliferative potential to the transduced progenitors in first plating compared to pMIG and resulted in a 1.6-fold higher colony number (p=0.01). In contrast to *pMIG*-transduced BM cells, which were not replatable, CDX4 was able to confer replating capacity to the BM cells up to the 4th plating. After four weeks, an average colony number of 8.3x10^9 per dish was achieved.

The same was observable in total cell number. After one week of culture, the number of *Cdx4*-transduced BM cells was significantly increased compared to the control (p=0.003). On average, one CDX4$^+$ colony consisted of 2.7x10^4 cells whereas the median colony size of the pMIG control was 7.9x10^3.

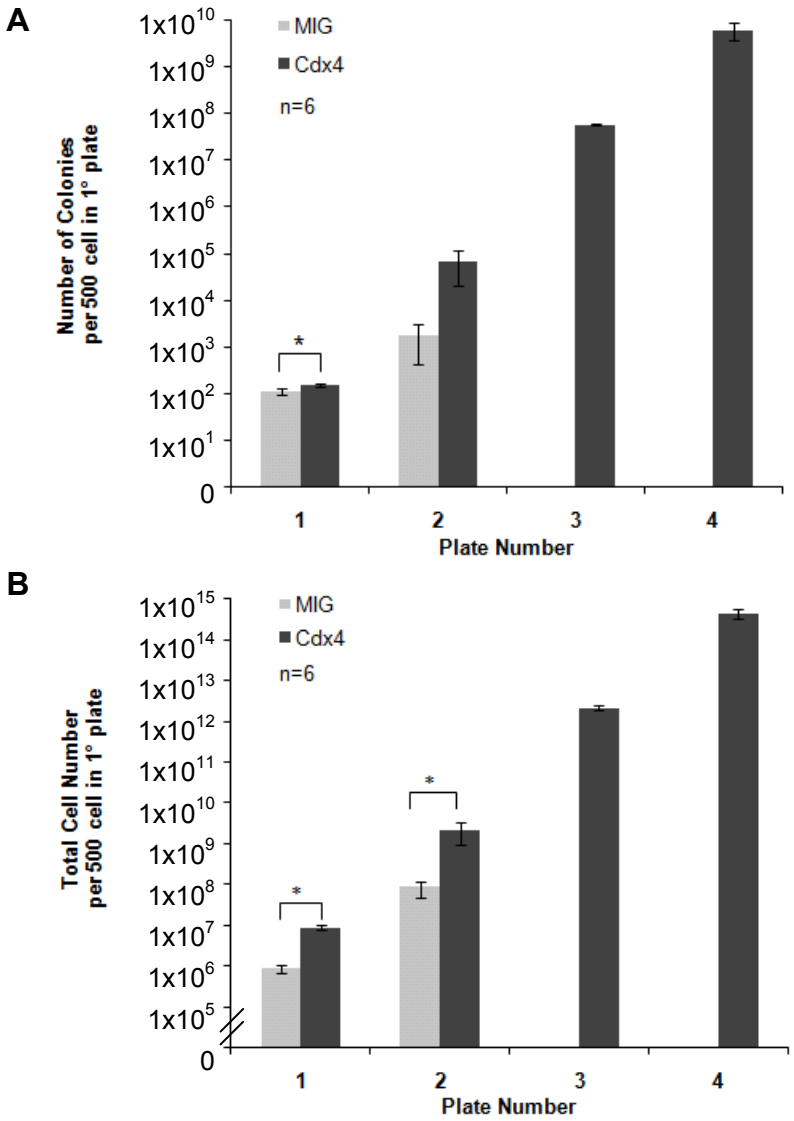

Figure 46: Total number of cells per 500 cells in 1st plating.
Cells were transduced with *pMIG*- and *Cdx4*-constructs, sorted for eGFP expression and plated in methylcellulose with 500 cells per dish. For replating, cells were diluted in an appropriate dilution. A) Columns represent average total colony numbers ± SEM. B) Columns represent average total cell numbers ± SEM.

Figure 47 displays the colony type distribution of BM cells transduced with *Cdx4* and the empty vector control. Whereas 27.4% of the CFUs in *pMIG*-transduced BM cells were of the G type, no significant number of CFU-G was present in the CDX4 overexpressing arm. Instead, *Cdx4*-transduction led to a significant increase in the number of both CFU-M and CFU-blast in first plating compared to the control (CFU-M: p=0.02; CFU-blast: p=0.03). The number of blast colonies reached its maximum after 2nd plating with 43.1% of total colony number and then subsequently decreased. Over the four weeks of culture an increase of CFU-M was observed with a final percentage of 31.4% in 4th plating.

pMIG-transduced cells were not replatable and after the 1st week produced almost exclusively mast colonies.

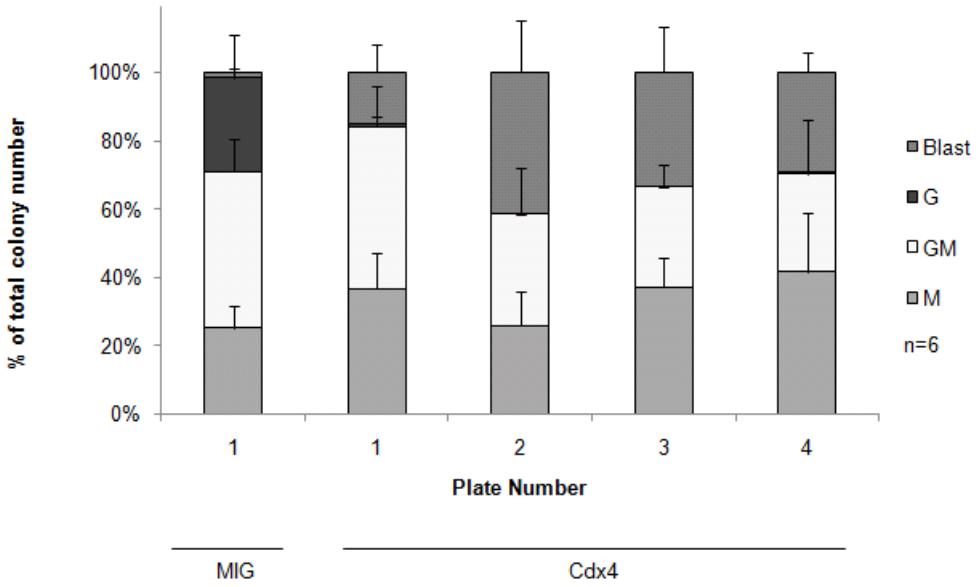

Figure 47: Colony distribution of *pMIG*- and *Cdx4*-transduced BM cells in CFC assay.
The diagram shows the average percentage of the different colony types in proportion to the total colony number. Errors are SEM-based.

The observations were confirmed by H&E staining of cells derived from CFC assay after 3rd plating. Whereas cells from the control arm revealed a mast cell-like phenotype, CDX4-overexpressing cells phenotypically were identified as either undifferentiated progenitors or mature cells. The presence of terminally differentiated cells, especially macrophages, indicated the ability of *Cdx4*-transduced progenitor cells to undergo terminal differentiation (Figure 48B).

pMIG **Cdx4**

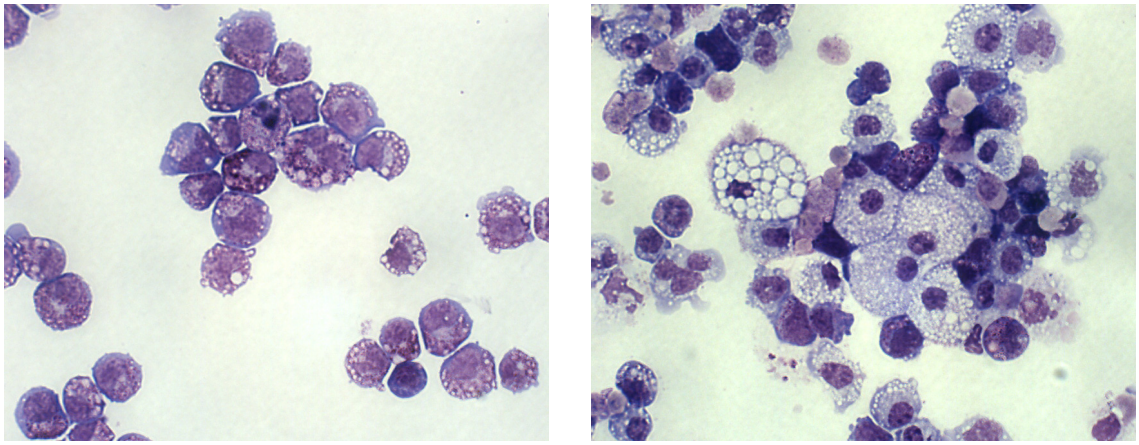

Figure 48: Pictures of cell morphology after 3rd plating of CFC assays.
For assessment of cell morphology, cells were plated on glass slides using the cytospin method and stained with H&E. Pictures were taken with 400-fold amplification.

To determine the lineage distribution, harvested BM cells were immunophenotypically analyzed after each round of CFC assay. One week after the beginning of the experiment, *Cdx4*-transduced BM cells showed a significant increase of c-Kit$^-$/Sca-1$^+$ clonogenic cells (p=0.023) as well as mature macrophages (p=0.015) compared to empty vector transduced cells (Figure 49). Similar to LC, overexpression of CDX4 led to a decrease in the number of myeloid progenitors and committed progenitors in the CFC assay. After the first week of CFC culture, the Ter119$^+$ cell population was significantly increased in the CDX4 arm (6.2-fold increase, p=0.020).

As in LC, the Ter119$^+$ population decreased over time in the CFC assay but Ter119 positive cells still were present after 3rd plating. Overexpression of CDX4 was able to maintain this erythroid population up to 5th plating. After the 3rd plating, approximately one quarter of the cells showed blast-like c-Kit$^-$/Sca-1$^+$ immunophenotype. However, compared to the first plating, a pronounced expansion of the c-Kit$^+$/ Sca-1$^-$ progenitors was observed with 13.1% of the cells displaying this marker combination.

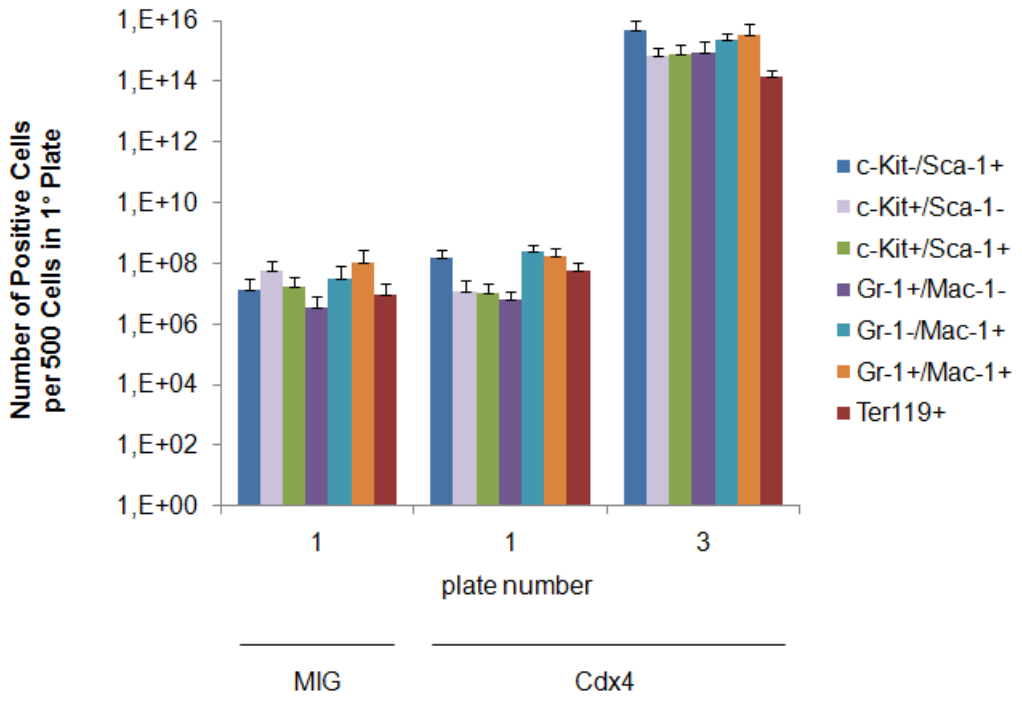

Figure 49: Immunophenotyping of CFCs.
Depicted are the results of the immunophenotypic analysis after 1st week of CFC assay for pMIG-transduced cells and after 1st and 3rd week of CFC assay for *Cdx*4-transduced cells. The columns represent the number of positive cells per 500 cells in 1° plate ± SEM.

BM cells from five different CFC experiments (2nd to 4th plating) were transplanted into lethally irradiated mice (n=16). In none of these cases any long-term engraftment was detected.

5.4.5 CDX4 Overexpressing BM Progenitor Cells Possess Short-Term Proliferation Advantage *in vivo*

The previous *in vitro* results suggest that overexpression of CDX4 in murine BM progenitor cells enhances their proliferative and clonogenic potential without blocking the differentiation capacity. Subsequently it was investigated if also *in vivo* overexpression of *Cdx4* in BM progenitor cells would enhance the self-renewal properties of HSCs without affecting their differentiation program. To test this, lethally irradiated mice were transplanted with *Cdx4*-transduced progenitor enriched 5-FU BM cells and analyzed regularly by PB immunophenotyping.

Cdx4-transduced progenitor cells readily engrafted all the transplanted experimental mice. Additionally, *Cdx4*-transduced cells had an obvious advantage in short-term engraftment compared to non-transduced 5-FU BM cells, at week four. Whereas at the time of transplantation on average only 16.3% of the transplanted BM cells were positive for eGFP-expression, four weeks post transplantation 41.8% of the PB WBCs showed expression of eGFP. After this time point, the number of eGFP-positive cells declined, before slowly increasing again from week 12 on, indicating that CDX4 has also some effect on long-term stem cells. At week, 36, the percentage of eGFP positive cells reached almost 70%.

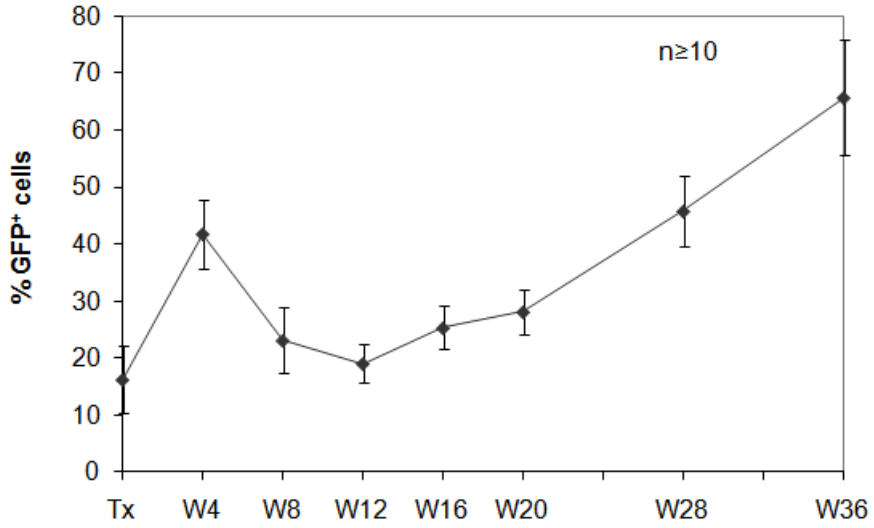

Figure 50: Engraftment of *Cdx4* transduced 5-FU BM cells.
5-FU BM cells were transduced with *Cdx4* by cocultivation with stable virus expressing GP+E86 feeder cells. After 72 h transduction the BM progenitor cells either were sorted for eGFP$^+$ cells and transplanted together with mock BM cells (n=1) or transplanted without sorting (n=10). The diagram displays average engraftment of mice (at least 10 mice per time point) with eGFP$^+$ cells ± SEM.

Despite the bias due to myeloid growth conditions before transplantation, the *Cdx4*-transduced BM progenitors were able to give rise to all lineages *in vivo*. As Figure 51 demonstrates, the PB analysis revealed multilineage engraftment of the transplanted BM progenitor cells already in week 4, which was maintained up to week 28 after transplantation. This indicates the potential of *Cdx4*-transduced cells to undergo long-term multilineage engraftment. The lineage distribution in week 28 hereby resembled that of untransduced BM cells with 23.0% (eGFP$^-$, week 4) vs. 17.6% (eGFP$^+$, week 28) expressing the erythroid marker Ter119, 33.5% vs. 29.3% the myeloid markers Gr-1 and/or Mac-1, and 10.8% vs. 9.5% the T-lymphoid markers CD8 or CD4. Only the B220$^+$ B-lymphoid compartment turned out to be diminished in the CDX4-overexpressing compartment (25.3% vs. 7.0%).

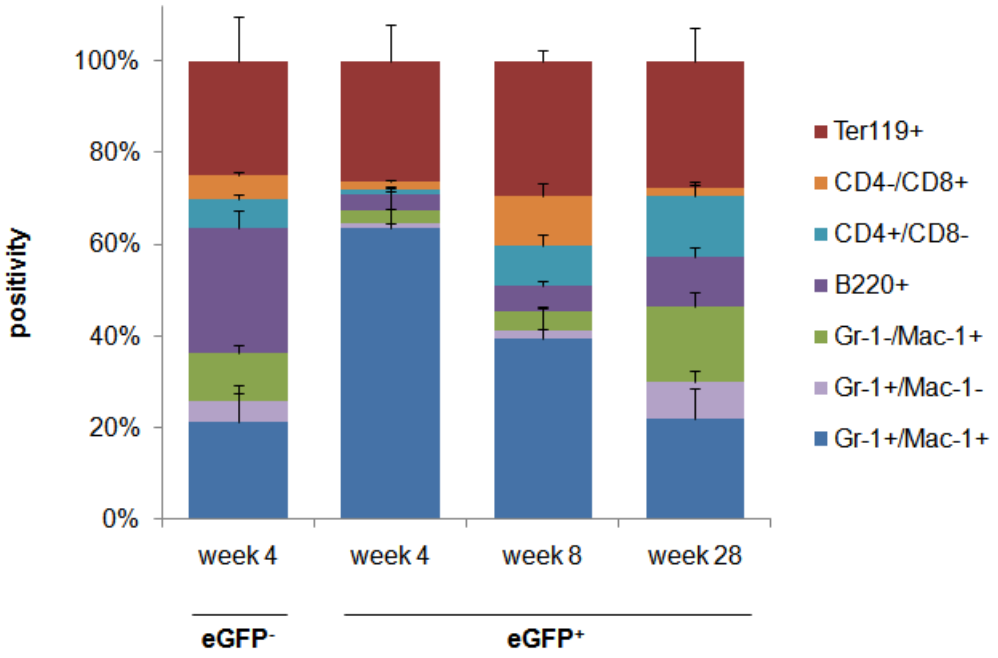

Figure 51: Immunophenotypic PB analysis of mice transplanted with unsorted *Cdx4*-transduced BM progenitors.
PB WBCs were analyzed at 4 weeks (n=8), 8 weeks (n=9) and 28 weeks (n=8) after transplantation. For week 4 the percentages of both the $eGFP^-$ (=untransduced) and $eGFP^+$ (=*Cdx4*-transduced) compartments are shown.

Within this time span, the number of RBCs constantly declined, starting at an average cell number of $1.1x10^{10}$/ml and reaching an RBC count of $4.7x10^9$/ml in week 36 post transplantation (Figure 52). The WBC count in contrast remained nearly on the same level during the first 28 weeks with cell counts between $4.0x10^6$ and $1.0x10^7$. However, after week 28 the WBC number rapidly increased and on average reached a concentration of $2.0x10^8$/ml.

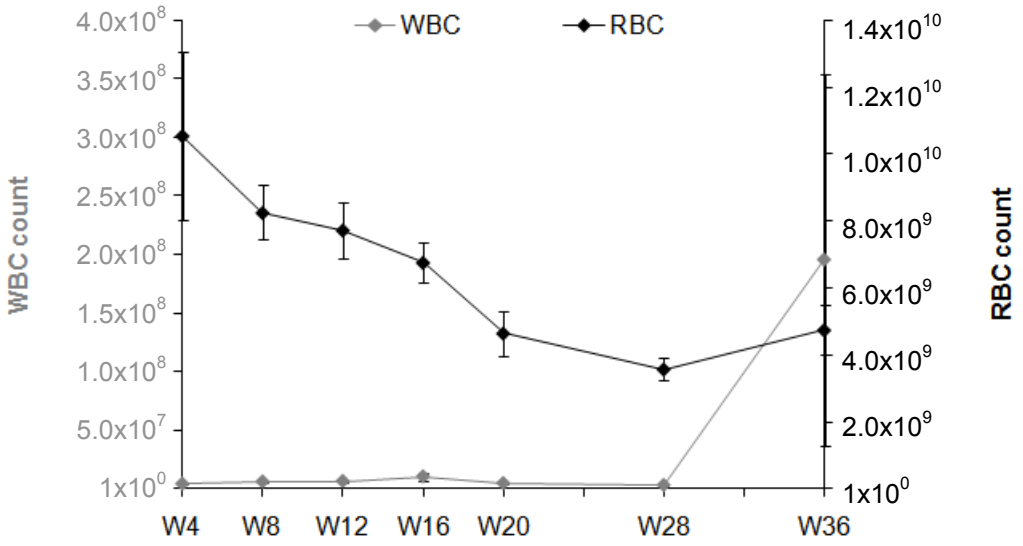

Figure 52: Hematological parameters of CDX4 engrafted mice.
Peripheral blood was regularly taken from engrafted mice, transplanted with *Cdx*4-transduced 5-FU BM cells (n=12) and RBC as well as WBC counts were determined.

5.4.6 CDX4 Induces Myeloid Leukemia with Long-Latency

As depicted in Figure 53, all mice transplanted with *Cdx4*-transduced BM progenitors succumbed to disease (n=12) with a median latency of 309 days post transplantation (range 154 – 504 days).

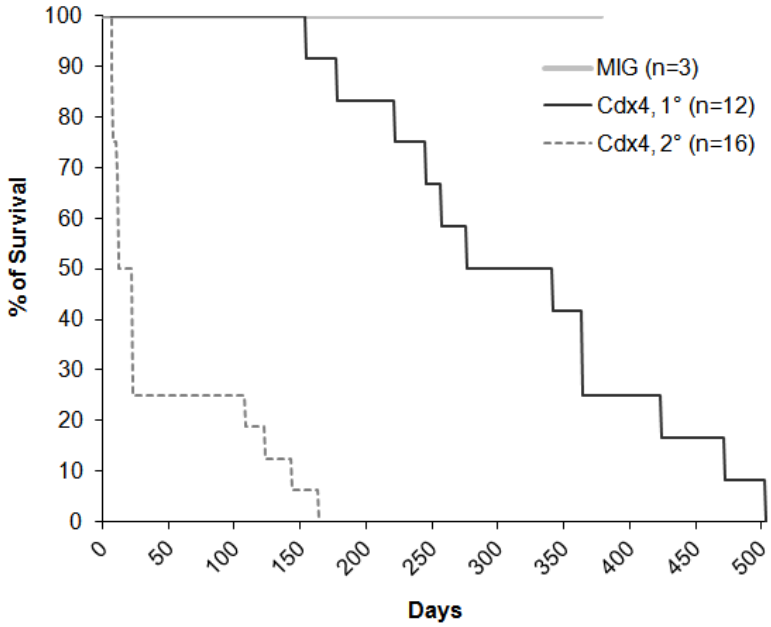

Figure 53: Survival curve of mice transplanted with 5-FU BM cells expressing CDX4 or pMIG.
Primary mice were transplanted with either *Cdx4*-transduced 5-FU BM cells (n=12, black line) or 5-FU BM cells transduced with empty *pMIG* for control (n=3, grey line). BM of four different diseased, CDX4-transplanted primary mice was transplanted into each four secondary recipients. The dashed line represents secondary transplanted mice (total number of 16).

All sacrificed mice (with the exception of mice 4513/A1 and 4513/A2, which were sacrificed in an early stage of disease) showed signs of anemia with an average RBC count of $5.0x10^9$ and leukocytosis with a WBC count of $3.8x10^6$ on average. The majority of the analyzed mice additionally displayed splenomegaly with an average weight of 313 mg.

As confirmed also by Wright-Giemsa staining and demonstrated in Figure 54, myeloid blasts were present in PB, BM and spleen of all diseased mice.

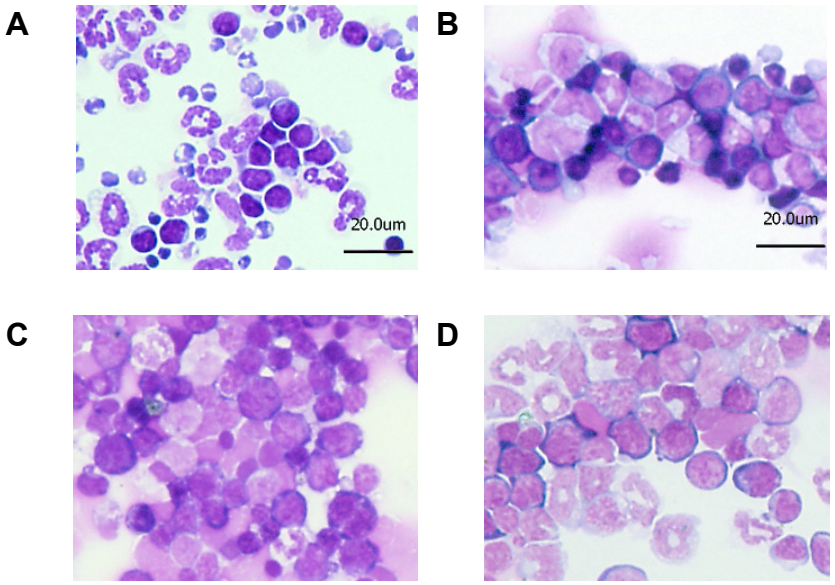

Figure 54: Wright-Giemsa stained cytospins of PB, BM and spleen of representative mice demonstrate the presence of erythroblasts.
A) PB of experimental mouse 4698/2, B) spleen of 4698/2, C) spleen of 4468/1, D) BM of 4468/1.

All experimental mice sacrificed in a terminal stage of disease showed a blast count above 20% in the BM (44% on average) and an equally high blast count of 44% in PB, thus confirming the presence of acute myeloid leukemia (Figure 54 and Table 14). The highest percentage of blasts was detected in the spleen with an average 62% of the cells showing blast-like features. Both experimental mice 4513/A1 and 4513/A2, which were sacrificed in an early stage of disease, revealed an elevated BM blast count with 20% and 11%, respectively. All animals had a lymphoid/myeloid ratio below 1.0. Already the animals sacrificed in an early stage of disease showed a decreased ratio of 0.8 and 0.9. All other animals with more progressed stages of leukemia showed even lower ratios of 0.01 and less.

Construct	Mouse No	Survival [d]	RBC/ml	WBC/ml	Spleen Weight [mg]	Blasts BM [%]	Blasts Spleen [%]	Blasts PB [%]	L/M
eGFP	1	90	$6.0x10^9$	$4.5x10^6$	150	0	0	0	5
eGFP	2	90	$4.8x10^9$	$3.2x10^6$	200	0	0	0	2
eGFP	3	90	$5.0x10^9$	$3.6x10^6$	200	0	0	0	2
Cdx4	4329/3	423	$1.5x10^9$	$2.3x10^6$	164	57	>95	56	<0.01
Cdx4	4401/2	178	$7.3x10^8$	$1.1x10^7$	449	>95	>95	61	0.02
Cdx4	4456/1	222	$1.3x10^{9}$*	$2.5x10^{6}$*	n.d.	n.d.	n.d.	52*	<0.01*
Cdx4	4468/1	504	$5.9x10^8$	$1.2x10^6$	401	35	62	52	<0.01
Cdx4	4513/A1	364	$1.8x10^{10}$	$1.6x10^7$	129	20	35	52	0.8
Cdx4	4513/A2	364	$1.4x10^{10}$	$8.3x10^6$	134	11	39	29	0.9
Cdx4	4513/A3	341	$8.5x10^{8}$*	$8.5x10^{7}$*	n.d.	n.d.	n.d.	63*	0.02*
Cdx4	4513/B1	276	$2.7x10^{9}$*	$3.4x10^{6}$*	n.d.	n.d.	n.d.	50*	0.1*
Cdx4	4513/B2	257	$2.3x10^9$	$2.3x10^7$	505	27	39	2	<0.01
Cdx4	4513/B3	472	$6.1x10^{9}$*	$5.5x10^{6}$*	345	65	75	25	<0.01
Cdx4	4621/3	245	$1.0x10^{10}$*	$4.0x10^{6}$*	398	n.d.	n.d.	66*	0.1*
Cdx4	4698/2	154	$1.0x10^9$	$5.3x10^6$	296	43	55	24	<0.01

Table 14: Hematological parameters of experimental mice.
*As spleen, BM and PB of some mice could not be analyzed due to sudden death of the animals, the results of the respective last PB analysis are indicated; n.d.: not determined, RBC: red blood cell, WBC: white blood cell, L/M: lymphoid/myeloid ratio in PB. Healthy control mice were sacrificed at day 90 post transplantation.

To assess the lineage distribution within the hematopoietic system, BM, spleen and PB cells from euthanized leukemic mice were harvested and immunophenotypically analyzed by FACS Calibur. Figure 55 displays the immunophenotypic profile of a representative CDX4-transplanted mouse (4698/2). The leukemic *Cdx4*-overexpressing cells did not completely displace the healthy, $eGFP^-$ BM cells but still contributed to all lineages clearly more than 1% at time of death. These untransduced, eGFP negative cells show differentiation patterns similar to healthy BM. Compared to the $eGFP^-$ compartment, in the $eGFP^+$ compartment of all organs a profound increase of the myeloid cell population was observed. This effect went along with a severe decline of the B-lymphoid as well as T-lymphoid lineages, indicating the presence of acute myeloid leukemia.

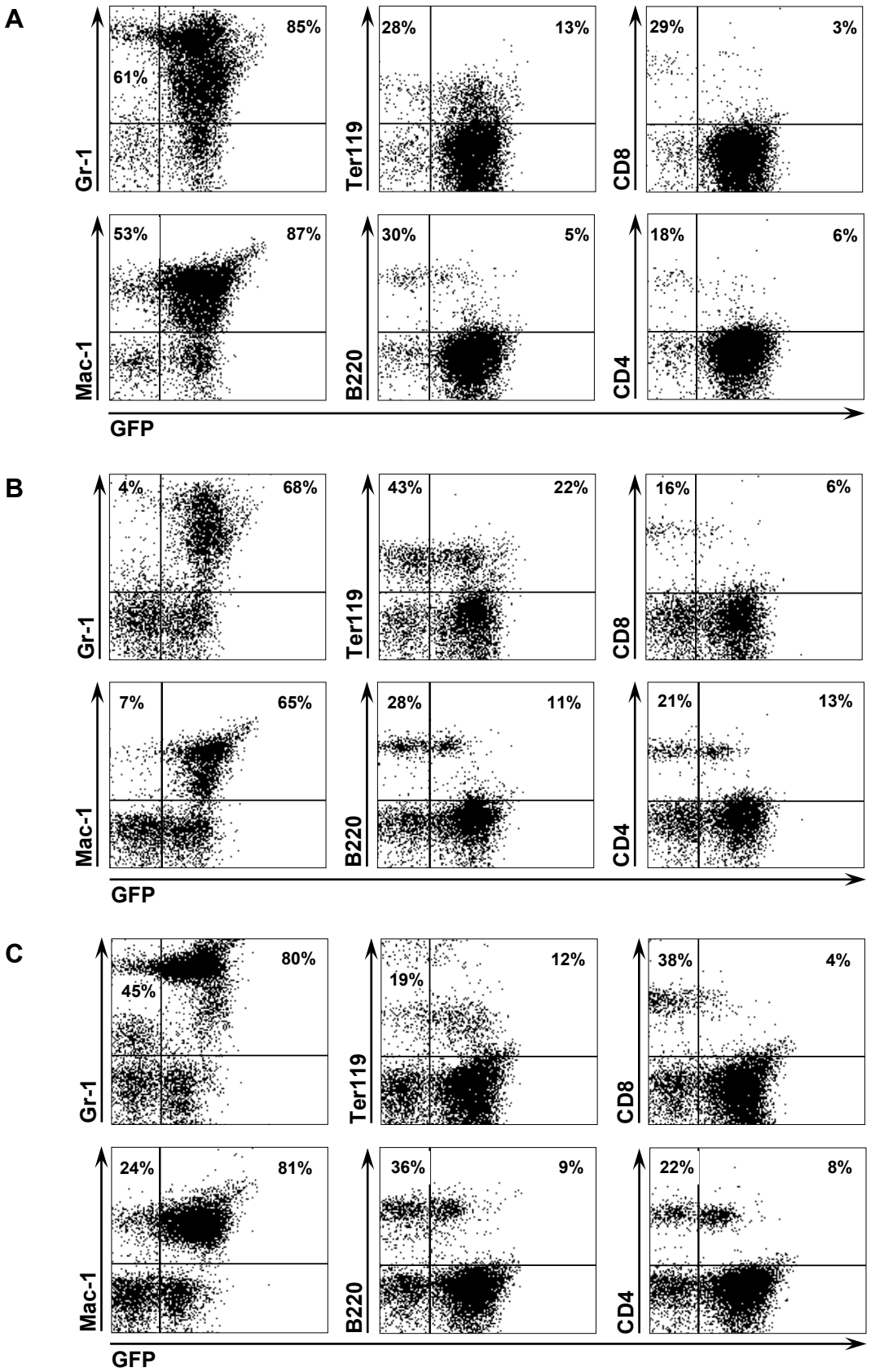

Figure 55: Immunophenotype of hematopoietic cells.
Expression of the myeloid markers Gr-1 and Mac-1, the B-lymphoid marker B220, the erythroid marker Ter119 and the T-lymphoid markers CD4 and CD8 on cells isolated from A) BM B) spleen and C) PB of a representative CDX4-transplanted animal (4698/2). The proportions of positive cells within the $eGFP^-$ and $eGFP^+$ compartments are indicated. The untransduced,

eGFP$^-$ compartment equals normal hematopoiesis whereas the eGFP$^+$ compartment demonstrates the leukemic engraftment.

As depicted in Figure 56, similar results were found for all animals analyzed. All organs showed a considerable increase of Gr-1$^+$/Mac-1$^+$ myeloid progenitors within the eGFP$^+$ myeloid compartment compared to the eGFP$^-$ myeloid compartment (PB: p=0.001, spleen: p=0.02). In contrast, the percentages of T-cells (CD4$^+$ and CD8$^+$) as well as B-cells (B220$^+$) were massively declined within the *Cdx4*-overexpressing compartment. A significant reduction of both the CD4$^+$ and the CD8$^+$ T-lymphoid lineage in PB and spleen was observed (spleen CD4$^+$: p=0.002, CD8$^+$: p=0.03; PB CD4$^+$: p=0.003, CD8$^+$: p=0.01). Also the percentage of B-lymphoid cells was severely reduced in PB and spleen (PB: p=0.02, spleen: p=0.0008). No significant change was observed in the erythroid compartment although the percentage of Ter119$^+$ cells was slightly decreased in *Cdx4*-overexpressing cells of the spleen.

In BM, the same trend as in PB and spleen was observed. However, the change in lineage distribution were not significant due to the lower number of analyzed samples.

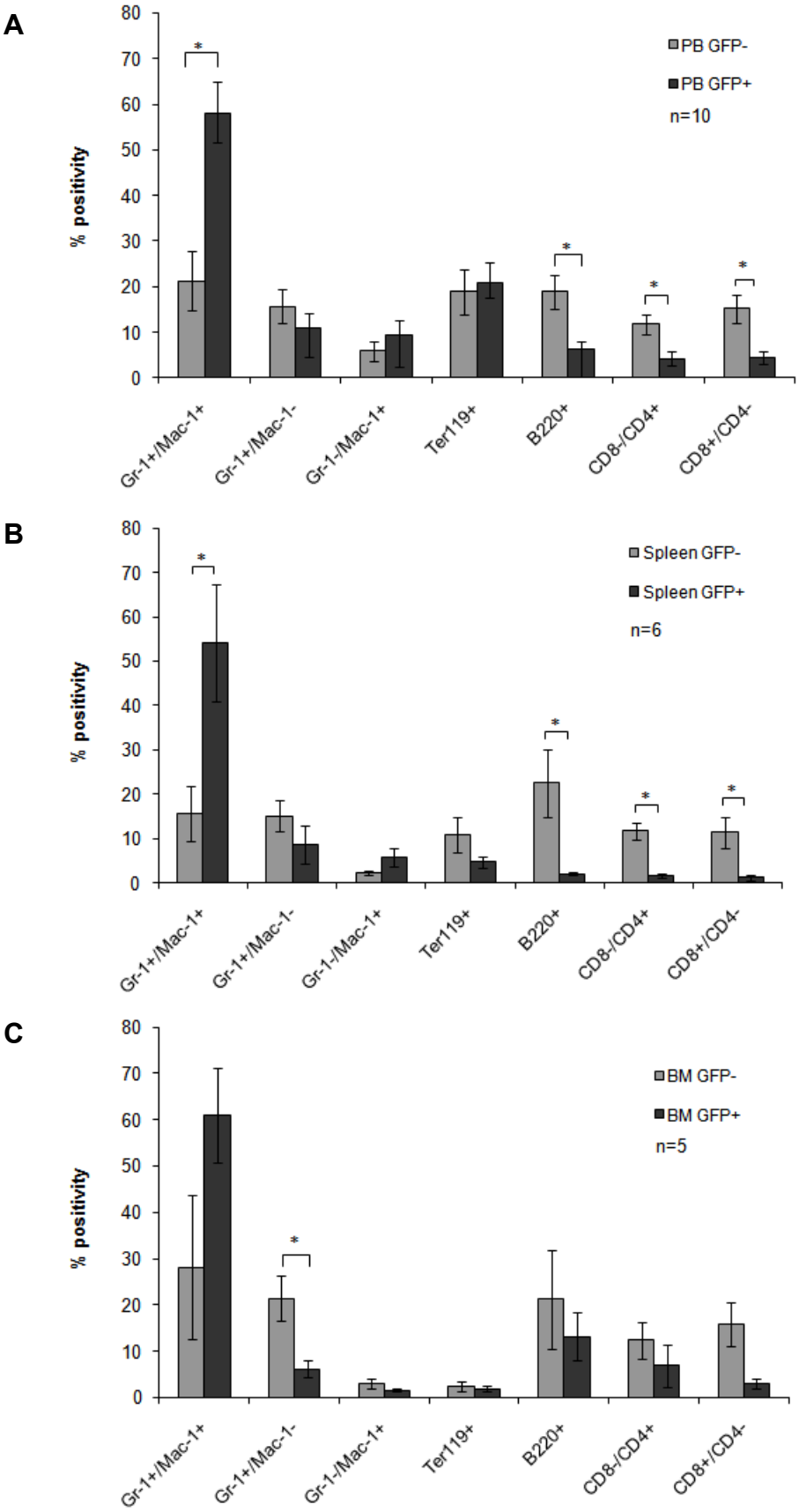

Figure 56: Immunophenotypic analysis of diseased CDX4-transplanted mice.
Mice were transplanted with 5-FU BM cells retrovirally transduced with *Cdx4*. Upon signs of disease, mice were sacrificed and the hematopoietic organs A) PB, B) spleen and C) BM were immunophenotypically characterized by FACS Calibur.

To test for the transplantability of the disease, secondary transplantation experiments were performed with BM isolated from four different diseased mice (out of four independent experiments. Each $1x10^6$ BM cells from each of the four different diseased primary mice, in combination with $5x10^5$ helper cells were transplanted into four secondary mice. All these secondary mice were deceased with a median of 74 days post transplantation, five times shorter survival compared to primary animals, indicating the presence of transplantable leukemia.

As depicted in Figure 57, all secondary mice revealed severe splenomegaly with an average spleen weight of 681 mg as well as leukocytosis with an average WBC count of $1.1x10^7$. With an RBC count of $7.2x10^9$ on average, no major change within the erythroid compartment was observed.

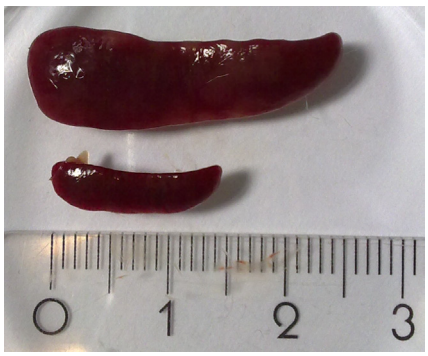

Figure 57: Splenomegaly of a secondary CDX4-transplanted mouse.
The spleen of a CDX4-transplanted mouse diseased of leukemia is shown in comparison to the spleen of a control mouse transplanted with *pMIG*-transduced BM cells.

As depicted in Figure 58 and similar to the primary mice, an increased fraction of Gr-1 and/or Mac-1 myeloid cells was observed in secondary mice.

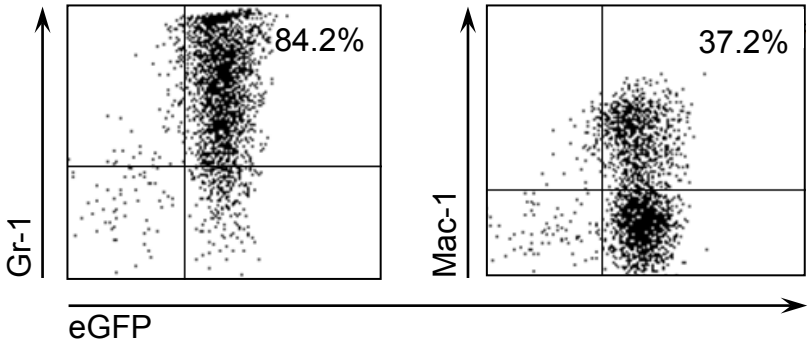

Figure 58: Immunophenotypic analysis of a secondary CDX4-transplanted mouse.
Immunophenotypic blot of a sacrificed secondary mouse were stained for Gr-1 and Mac-1.

5.4.7 CDX4 Induces Erythroid Leukemia in All Transplanted Mice

The subtype of the AML was specified by (immuno-) histophatological analyses according to the 'Bethesda proposals for classification of nonlymphoid hematopoietic neoplasms in mice' (Kogan *et al.*, 2002). Six primary animals were examined by H&E, Ter119, CD3 and B220 staining. According to their high percentage of erythroid precursors cells, all six animals were diagnosed with erythroleukemia. One of the mice (4468/1) was in an early stage of disease whereas all other five had full-blown erythroleukemia (Table 15, Figure 59). All secondary animals were histophatologically diagnosed with erythroleukemia, likewise.

Interestingly, in two out of the six analyzed primary animals older than 40 weeks, additionally adenocarcinomas of the colon were detected.

Exp.	Histopathology	Diagnosis
	1° Transplanted Mice	
4329/3	enlarged spleen with massive erythroid proliferation, few groups of MPO+ myeloid precursors; in red pulp proliferation of erythroid precursors in all stages of maturation; no other organ is infiltrated tumor around the bladder infiltrating the muscular tissue; adenocarcinoma of the caecal area	erythroleukemia
4401/2	diffuse infiltrate in spleen, liver, kidney, lymph nodes, BM and lung, characterized by the presence of large cells with blastic chromatin, prominent nucleolus and moderate amount of cytoplasm without any sign of maturation; blastic cells are infiltrating the sinusoidal and periportal spaces of the liver as well as kidneys and lungs; the vast majority of cells is positive for myeloperoxidase; hyperplasia of the erythroid cells in the spleen	erythroleukemia
4468/1	spleen enlarged by a diffuse infiltrate composed mainly of erythroid cells in all stages of maturation; only minority of the cells positive for MPO, vast majority positive for Ter119 ; all other organs free of infiltration	early erythroleukemia.
4513/B2	diffuse infiltrate in spleen, liver, and lung characterized by the presence of large cells with blastic chromatin, prominent nucleolus and moderate amount of cytoplasm alternating with numerous erythroid precursors in all stages of differentiation; atypical red cells with abnormal mitosis; in the liver blastic cells and erythroid components are infiltrating the sinusoidal and periportal spaces; presence of blasts positive for MPO, however vast majority positive for Ter119 granulosa cell tumor of the ovary; adenocarcinoma of the colon	erythroleukemia
4513/B3	enlarged spleen. red pulp congested and shows proliferation of erythroid precursors in all stages of maturation together with proliferation of megakaryocytes; massive infiltration of erythroid precursors in all stages of differentiation intermingled with megakaryocytes; only residual groups of myeloid precursors; no other organ infiltrated	erythroleukemia
4698/2	spleen enlarged by diffuse infiltrate composed mainly of erythroid cells in all stages of maturation and large cells with blastic chromatin, prominent nucleolus and moderate amount of cytoplasm; blastic cells are positive for MPO, erythroid precursors are Ter119+; all other organs are free of infiltration, only for MPO+ cells are in the vessels of sinusoids in lung, liver and kidney, suggesting circulation of leukemic cells	erythroleukemia

Exp.	Histopathology	Diagnosis
	2° Transplanted Mice	
4537/2 2° of 4401/2	diffuse infiltrate in multiple organs, characterized by the presence of large cells with blastic chromatin, prominent nucleolus and moderate amount of cytoplasm; blastic cells are infiltrating the sinusoidal and periportal spaces of liver, kidneys and lungs; vast majority of cells is positive for myeloperoxidase; hyperplasia of the erythroid cells in the spleen	erythroleukemia
4730/3 2° of 4513/B2	spleen and liver infiltrated by mostly erythroid precursors in all stages of maturation with picnotic nuclei and abundant basophilic cytoplasm, atypical red cells with abnormal mitosis; minority of the cells is MPO+, vast majority of cells is Ter119+	erythroleukemia
4955/A3 2° of 4468/1	spleen, liver, lung, heart, pancreas, testis, intestine, lymph nodes and thymus show a diffuse infiltrate characterized by the presence of large blastic cells alternating with numerous erythroid precursors in all stages of differentiation; blastic cells and the erythroid components	erythroleukemia
4955/B4 2° of 4698/2	are infiltrating the sinusoidal and periportal spaces of the liver; presence of blasts positive for MPO, vast majority of erythroid precursors positive for Ter119; both components are observed in all organs	erythroleukemia

Table 15: Results of histophatological analyses of diseased mice.
Mice fixed in formalin were histophatologically analyzed by staining with H&E, Ter119 or MPO staining.

The spleens of all mice showed diffuse to massive infiltration with myeloid blasts and erythroid precursors at different ratios. Whereas in mouse 4513/B2 both MPO^+ and $Ter119^+$ blasts were present in almost equal amounts (Figure 59A), in most of the other mice, especially in the secondary animals, the vast majority of blasts stained positive for Ter119 (Figure 59B).

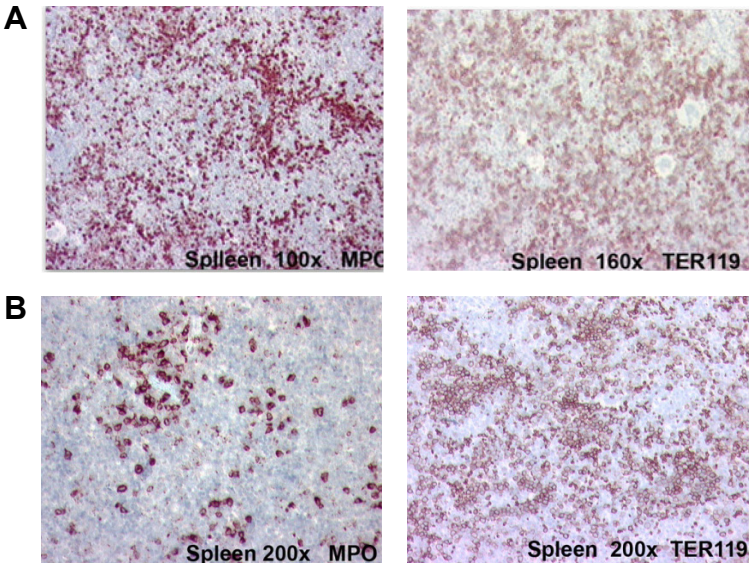

Figure 59: Histophatological analyses of spleens of diseased mice transplanted with $CDX4^+$ 5-FU BM.
Spleens of analyzed mice show different ratios of MPO^+ myeloid blasts and $Ter119^+$ erythroid precursors A) 4513/B2: in spleen both myeloblasts and erythroid precursors are present B) 4730/3 (4513/B2 2°): only a small portion of cells are positive for MPO, however the vast majority are $Ter119^+$.

None of the animals stained abnormally for the B-lymphoid marker B220 or the T-lymphoid marker CD3.

Only in few of the primary animals leukemic blasts were present in organs other than BM and spleen. Of those animals, 4513/B2 showed liver and lung to be infiltrated with blasts. In mouse 4698/2, the infiltration of MPO^+ cells in the sinusoids of lung, liver and kidney suggested circulation of the myeloid blasts. The organs, excluding BM and spleen, of the other four primary animals were free of MPO^+ or $Ter119^+$ blasts.

In contrast, infiltration of blasts was detected in all secondary animals. Mice 4573/1 and 4730/3 additionally showed infiltration of the liver, and in both 4955/A3 and 4955/B4 multiple organ infiltration was present targeting practically every single organ except the brain.

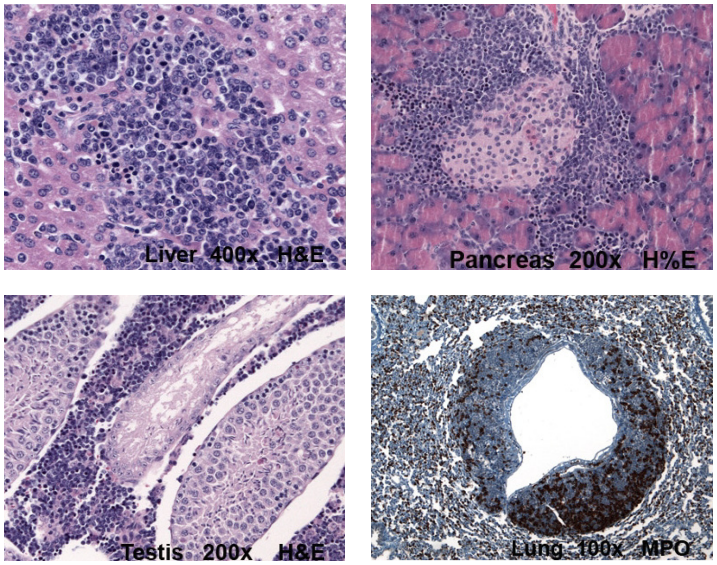

Figure 60: Infiltration of different organs by leukemic cells in 2° transplanted mice.
Leukemic cells are infiltrating liver, pancreas, testis and lung of 4955/A3 (4468/1 2°) and 4955/B4 (4698/2 2°).

5.4.8 The Latency of CDX4-Induced Leukemia Does Not Depend on the Number of Transplanted Cells

With a correlation coefficient (R^2) of 0.07, Figure 61 demonstrates that there was no correlation between the number of transplanted cells and the survival time of primary transplanted experimental mice. Whereas mouse 4698/2 for example was transplanted with only $1.4x10^4$ *Cdx4*-transduced BM cells and died after 22 weeks, all three mice of the 4513/A experiment, which were transplanted each with $8.1x10^5$ BM cells, survived for more than 48 weeks.

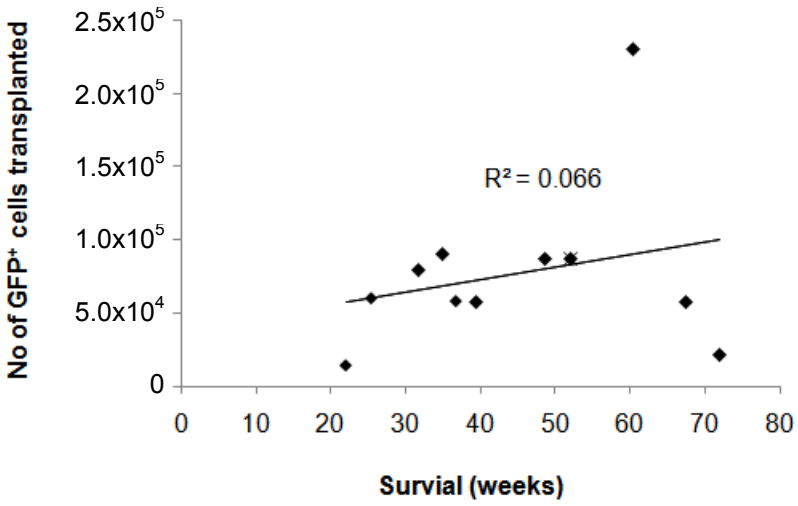

Figure 61: Correlation plot of transplanted cell number and survival.
Diamonds indicate individual CDX4-transplanted mice, crossed diamond indicates two animals.

Standard PCR and subsequent sequencing of the PCR products confirmed the presence of the full-length, wild type *Cdx*4 transcript in all transplanted mice. All mice showed overexpression of *Cdx4* compared to total normal BM – which was negative for *Cdx4* expression with the PCR conditions applied below – and expressed WT *Cdx4*.

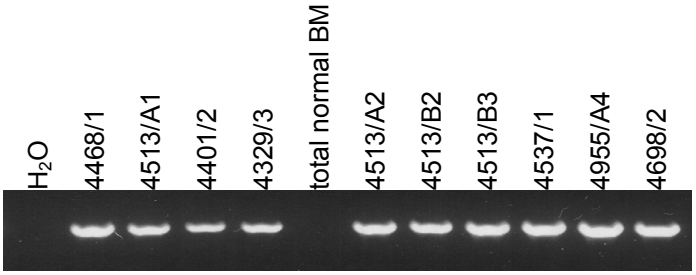

Figure 62: PCR to detect *Cdx4* expression in diseased mice.
The PCR was performed with a cDNA input equivalent to 50 ng total RNA isolated from spleen, PB or BM of diseased mice or total normal BM for control.

5.4.9 CDX4-Induced Leukemia Is of Oligoclonal Nature

To determine the clonality of CDX4-induced leukemia, Southern blot analyses were performed on hematopoietic tissues of leukemic mice.

The results of this analysis show that the disease in all four primary animals was of oligoclonal nature as revealed by the presence of multiple bands of different intensities within one sample (Figure 63). In BM and spleen of the secondary animal 4955/A4 bands of equal strength were visible, which normally

indicates monoclonal disease. However, in this case BM and spleen of the secondary animals were infiltrated with different clones. In each case, only one band corresponded with one band in the primary animal, and in both BM and spleen an additional second integration occurred.

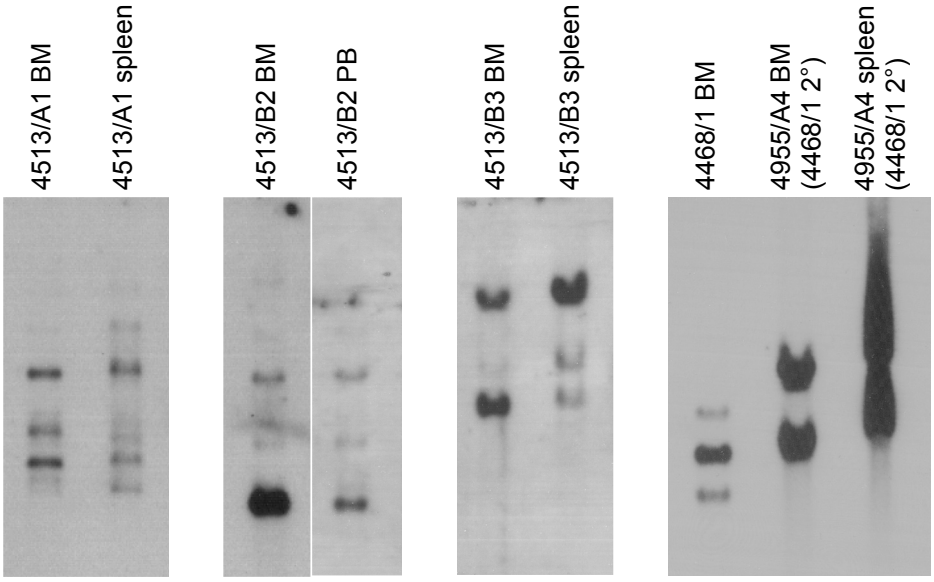

Figure 63: Southern blot of samples of CDX4-transplanted leukemic mice.
Genomic DNA of BM, PB or spleen of diseased mice was digested with *PstI* and hybridized with a ^{32}P labelled eGFP-probe.

5.4.10 Transformation of *Cdx4*-Transduced BM Progenitors Does Not Depend on Common Retroviral Integration Sites

To test the influence of retroviral insertion mutagenesis on leukemic transformation, linker mediated integration PCR was performed. The analysis in most cases revealed only one integration band per sample, as in samples from mice 4513/A2, 4698/2 or 4468/1 (Figure 64). Also in the spleens of mice 4513/A1 and 4513/B2 only one band was visible. However, BM and PB showed a second faint band in both cases. All integration bands from the different organs of one animal were of the same size and corresponded to at least one of the bands detected by Southern blot. Where possible, the bands were sequenced and a control digestion was performed using *KpnI*, which resulted in a drop out of a 550 bp vector band in all the samples.

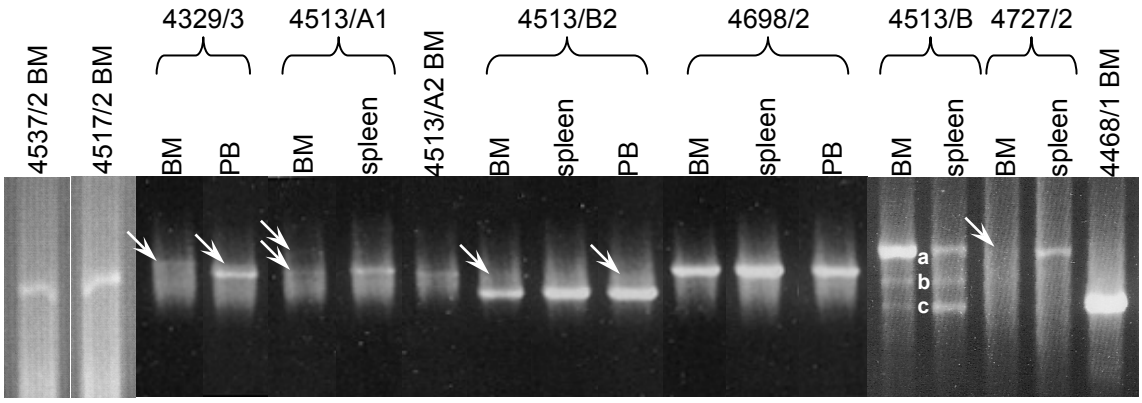

Figure 64: Results of the linker-mediated integration PCR.
Arrows indicate faint bands.

In three cases (4513/B2, 4513/B3b, 4468/1) the sequencing showed the provirus to be integrated upstream of repetitive elements, in all other cases one integration site was located. In mice 4329/3 and 4513/AS an integration occurred in introns of the zinc finger protein genes *Zfp407* and *Zfyve28*, both genes of unknown function. However, many of the zinc finger proteins are transcription factors. The secondary transplanted animals of 4329/2, 4517/2, and 4537/1 showed an integration about 600 bases upstream of *Opa3*, a gene associated with optic atrophy (Reynier *et al.*, 2004). In the case of 4513/A1, the integration was located approximately 600 bases upstream of *Akap1*, which codes for a membrane protein of the mitochondrial and endoplasmatic reticulum (Rogne *et al.*, 2009). The proviral integration site found in 4513/B3a was located between two genes, 15 kb downstream of *Coq2*, which is involved in the biosynthesis of CoQ (Forsgren *et al.*, 2004), and 80 kb upstream of *Plac8*, a gene of an unknown function as well but with high expression in hematopoietic tissues (Rissoan *et al.*, 2002; Forsgren *et al.*, 2004). In the case of 4698/2 the provirus integrated within an intron of the leukocyte activation antigen *Sema4D* (CD100), which is highly expressed in hematopoietic cells and involved in the activation of B- and T-cells (Shi *et al.*, 2000). The integration found in mouse 4727/2 is located upstream of two genes: about 10 kb upstream of the *Pkd1* gene coding for a transmembrane protein, which is suggested to be involved in renal tubulogenesis, and 4 kb upstream of *Rab26*, a member of the RAB family of small G-proteins which regulate intercellular vesicle trafficking.

Mouse No.	Genomic Location	Gene	Description
4329/3	18qE4	intron of Zfp407	zinc finger protein 407
4517/2 (4329/3 2°)	7qA3	intergenic (upstream Opa3)	optic atrophy 3
4537/1 (4401/2 2°)	7qA3	intergenic (upstream Opa3)	optic atrophy 3
4513/A1	11qC	intergenic (upstream Akap1)	a-kinase (PRKA) anchor protein 1
4513/A2	5qB2	intron of Zfyve28 (between exons 6 and 7)	zinc finger, FYVE domain containing 28
4513/B2	-	(repetitive elements)	-
4513/B3 a	5qE4	intergenic (downstream Coq2, upstream Plac8)	coenzyme Q2 homolog placenta-specific 8
4513/B3 b	-	(repetitive elements)	-
4698/2	13qA5	intergenic/ upstream Sema4d (depending on splice variant)	semaphorin 4D
4727/2	17qA3.3	intergenic (upstream of Rab26, Pkd1)	member RAS oncogene family polycystic kidney disease 1 homolog
4468/1	-	(repetitive elements)	-

Table 16: Genomic integrations in hematopoietic cells of mice transplanted with *Cdx4*-transduced BM cells.
Genomic DNA extracted from BM, spleen and/or PB cells of diseased mice was analyzed for retroviral integration by linker-mediated PCR. Per mouse, only one integration was found by this method. However, none of the identified locations have thus far been described in the *Retrovirus Tagged Cancer Gene (RTCGD) database* (www.rtcgd.ncifcrf.gov).

None of the integration sites identified in this analysis have been described in the *Retrovirus Tagged Cancer Gene (RTCGD) database* (www.rtcgd.ncifcrf.gov). This database comprises a collection of retroviral integration sites observed in murine tumors.

5.5 Differential Effects of CDX2 and CDX4

Our data demonstrated that aberrant expression of *CDX2* is a widespread event not only in acute myeloid but also in acute lymphoid leukemia. While this supports a possible involvement of CDX2 in the induction of human leukemia, no expression of its family member *CDX4* was found in leukemic patients. In contrast, whereas ectopic expression of *Cdx2* in the murine BM transplantation

model leads to induction of an aggressive form of AML (Rawat *et al.*, 2004), overexpression of *Cdx4* in hematopoietic cells resulted in expansion of hematopoietic progenitors *in vitro* (Davidson *et al.*, 2003). In the BM transplantation model used in this study, CDX4 induced leukemia only after long latency.

To characterize possible mechanisms for the higher leukemogenicity of CDX2, the influence of both genes on murine hematopoiesis was compared and differences as well as similarities between the two genes were analyzed.

5.5.1 CDX2 Possesses a Higher Leukemogenic Potential than CDX4 *in vivo*

As reported by Rawat *et al*. (2004), CDX2 leads to induction of leukemia with a median latency of 116 days *in vivo* (Figure 65). The latency of CDX2-induced disease thus is significantly lower than that of CDX4-transplanted mice, which in median survived more than 353 days ($p<0.001$).

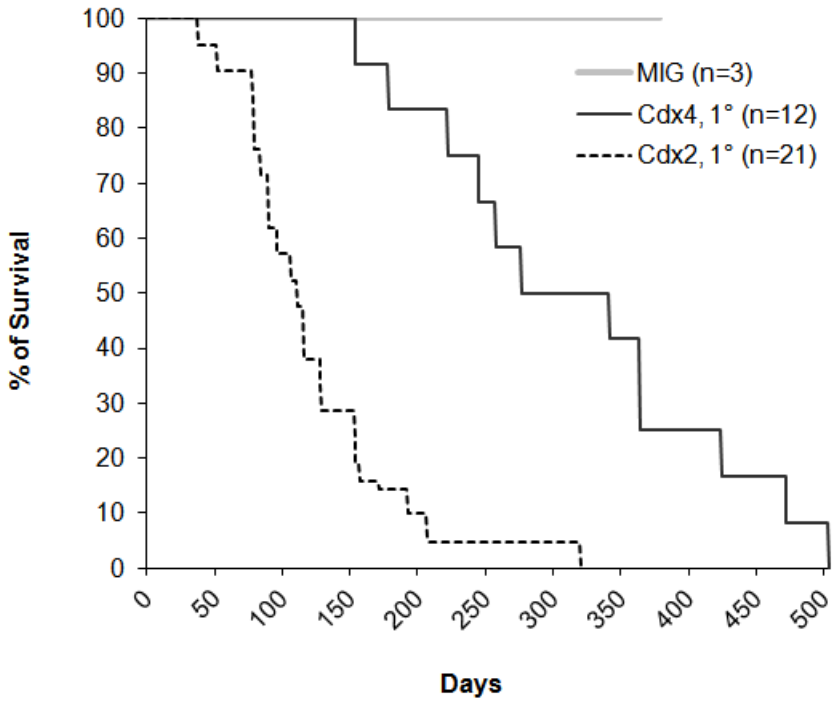

Figure 65: Survival diagram of CDX2- and CDX4-transplanted mice.
Primary mice were transplanted with either *Cdx4*-transduced 5-FU BM cells (n=12, black line) or 5-FU BM cells transduced with *Cdx2* (n=16, dashed line).

Whereas no significant difference of the WBC count was observed, CDX2-transplanted mice showed an RBC number significantly decreased compared to

CDX4-transplanted mice with (p=0.03). A significant difference also was observed in the spleen weights, as spleens of $CDX2^+$ mice in median had more than the double weight than those of CDX4-transplanted mice (p<0.0001).

Interestingly, the blast cell count of spleen and PB was significantly higher in $CDX4^+$ animals, which additionally showed a much more drastic inversion of the lymphoid/ myeloid ratio.

Construct	Survival [d] (range)	RBC/ml	WBC/ml	Spleen weight [mg]	Blasts BM [%]	Blasts spleen [%]	Blasts PB [%]	L/M
eGFP	123.5 (85-127)*	$5.7x10^9 \pm 9.3x10^8$	$3.4x10^6 \pm 2.6x10^6$	156 ± 59**	0	0	0	5
Cdx4	353 (154-504)	$5.0x10^9 \pm 1.8x10^9$	$1.4x10^7 \pm 7.0x10^6$	313 ± 43	44 ± 27	62 ± 24	44 ± 20	0.17
Cdx2	111 (37-229)	$6.8x10^8 \pm 1.4x10^8$	$1.2x10^7 \pm 3.8x10^6$	629 ± 68	45 ± 15	38 ± 15	18 ± 10	2

Table 17: Comparison of hematological parameters of CDX2- and CDX4-transplanted mice.
*a total of 4 (out of 6) healthy eGFP mice were killed for analysis. 2 out of the 6 control mice were analyzed by BM biopsy and bleeding. Values are given as average ± SD **Average weight of 4 eGFP mice, L/M: lymphoid/myeloid ratio in PB.

Whereas primary CDX4-transplanted mice in most cases did not show any presence of blasts outside the hematopoietic organs, in the case of CDX2 multiorgan infiltration with myeloid blasts was common (Figure 66).

CDX2- as well as CDX4- transplanted animals displayed a similar immunophenotypic profile. In both experimental arms, a pronounced increase of the myeloid compartment was observed whereas both the B-lymphoid and the T-lymphoid compartments were severely decreased.

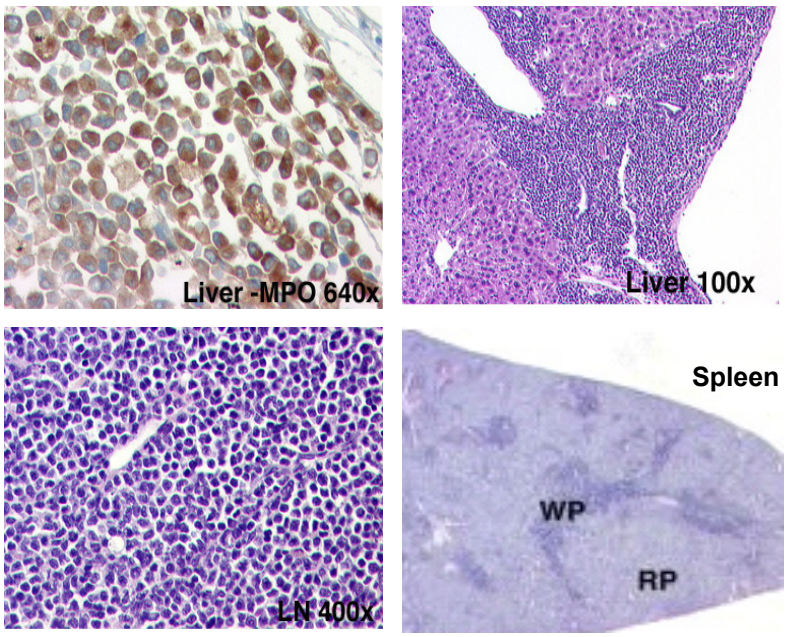

Figure 66: Histopathologically analyzed tissue sections of CDX2-transplanted mice (Rawat *et al*., 2004).
Liver, lymph nodes (LN) and spleen were immunohistochemically analyzed by H&E and MPO staining.

5.5.2 CDX2 and CDX4 Differentially Regulate Expression of *Hoxb6* and *Hoxb8 in vitro*

One possibility for the different oncogenic potential of CDX2 and CDX4 could be a differential regulation of *Hox* genes, which are able to confer self-renewal capacities to murine BM progenitors (see introduction, section 1.3.1). To analyze if a differential regulation of *Hox* genes could be responsible for the differing leukemogenicity of the two CDX members, 5-FU BM progenitors were transduced with CDX2, CDX4 and an empty vector control. The resulting effect on *Hox* gene expression was analyzed using TaqMan LDA 48 h after transduction.

As diagram 67 displays, no significant difference was detected between CDX2- and CDX4-transduced BM progenitors in the expression of the analyzed *HoxA* cluster genes. Both genes induced an upregulation of the analyzed *HoxA* genes, which was especially pronounced in the more anterior *Hox* genes *Hoxa5* and *Hoxa7*. Transduction with *Cdx2* and *Cdx4* led to a significant upregulation of both genes with a more than 55-fold higher expression of *Hoxa5* and a more than 65-fold increased expression of *Hoxa7* compared to the empty vector control (*Hoxa5*: $p<0.0001$, *Hoxa7*: $p=0.006$). Furthermore, upregulation of

Hoxb3 was detected (CDX4: 5.2-fold, CDX2: 4.4-fold). Deregulation of *Hoxb4* was only observed in *Cdx4*-transduced BM cells where a 2.3-fold higher expression of *Hoxb4* was measured. However, with a p-value of 0.06 this effect was of borderline significance. A 6.8-fold difference between the two CDX members was detected for *Hoxb6* expression, where CDX2 induced a significantly stronger effect compared to CDX4 (p=0.002). Additionally, only CDX2 was able to induce *Hoxb8* expression, as this gene was not expressed in the control nor in *Cdx4*-transduced BM cells.

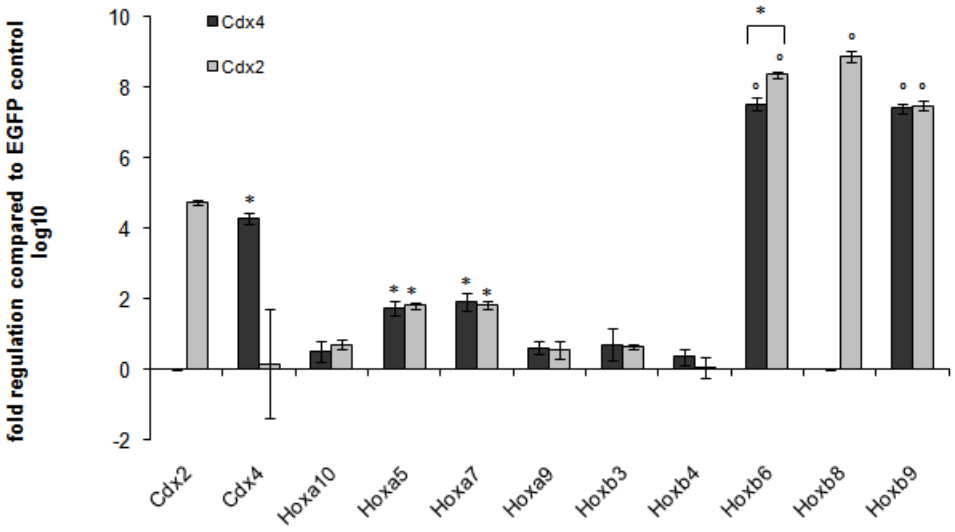

Figure 67: LDA analysis of *Cdx2*- and *Cdx4*-transduced BM cells.
Murine progenitor enriched 5-FU BM cells were transduced with *Cdx2*, *Cdx4* or empty *pMIG* for control and 48 h after transduction sorted for eYFP and eGFP expression, respectively. ΔC_T values were obtained by normalizing to *Gapdh* and fold expression compared to *pMIG* was calculated. The diagram shows average expression levels of three independent experiments ± SD.° marks calculated values as *pMIG*-transduced cells were negative for *Cdx2* expression. *: significant difference towards *pMIG* and between *Cdx2* and *Cdx4* respectively.

Also in mice that died of AML after transplantation with *Cdx2*- or *Cdx4*-transduced BM, *Hox* expression was analyzed. Here, the only differentially expressed *Hox* gene was *Hoxb4*, which was significantly 6.0-fold upregulated in CDX4-transplanted mice (p=0.04).

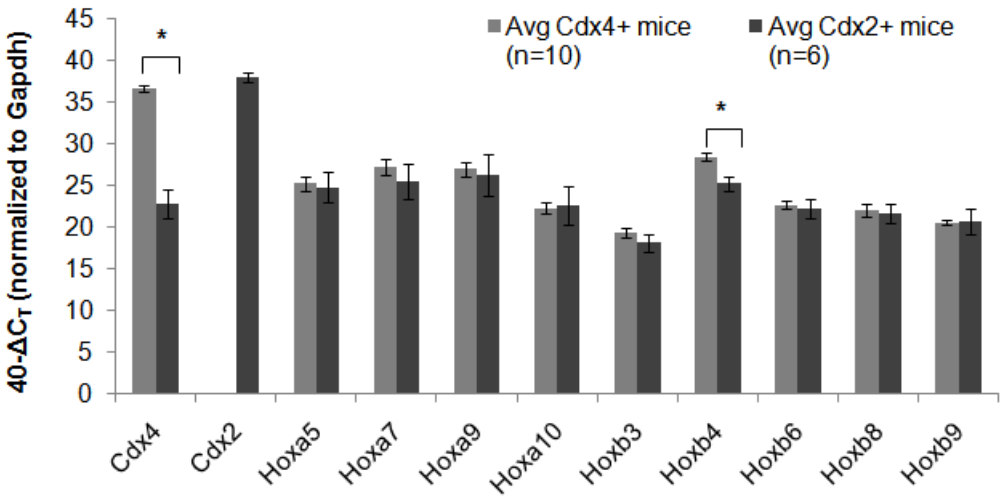

Figure 68: Expression of *Hox* genes in diseased, CDX-transplanted mice.
Mice which died of AML after transplantation with *Cdx2*- or *Cdx4*-transduced BM were analyzed for expression of *Hox* genes by TaqMan qRT-PCR.

5.5.3 CDX4 Is More Potent than CDX2 *in vitro*

Although CDX2 compared to CDX4 is more leukemogenic *in vivo*, overexpression of the two *Cdx* genes leads only to small differences in differential *Hox* gene expression. To analyze if the different leukemogenicity of CDX2 and CDX4 would depend on a different clonogenic and proliferative potential, *in vitro* experiments were performed.

First, the effect of an overexpression of both genes on the proliferative potential of BM progenitors was analyzed. Therefore, 5-FU BM cells were transduced with both constructs as well as empty vector control and liquid expansion assays were performed. As mentioned in section 5.4.2 as well as by Rawat *et al*. (2004), both genes are able to confer proliferative potential to BM progenitors. However, the average cell number of *Cdx2*-transduced cells was only 8.1×10^7 after four weeks of culture in complete medium (supplemented with cytokines), when CDX4 was able to expand the cells to a final number of 1.8×10^{11}. CDX4 hereby showed an almost 2,300-fold higher activity than CDX2 ($p=0.04$, Figure 69A). The same is true for culture in medium supplemented with IL-3 only. In this assay, both constructs were able to induce IL-3 dependent growth and after one week both constructs showed a significantly higher cell number compared to pMIG ($p<0.001$, Figure 69B). After four weeks CDX4

promoted a 1,700-fold higher expansion of the transduced BM progenitor cells than CDX2 ($p<0.001$).

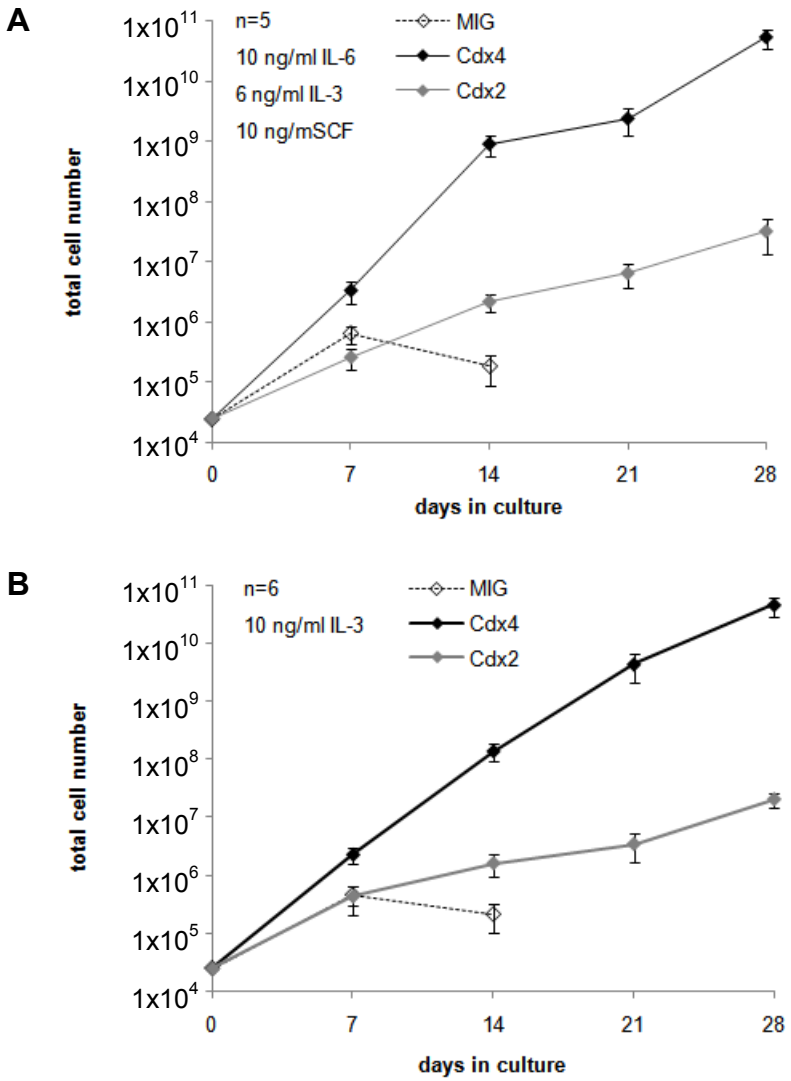

Figure 69: Proliferation assays of 5-FU murine BM cells transduced with *pMIG*, *Cdx2* and *Cdx4*.
Transduced cells were sorted for eYFP and eGFP expression, respectively and proliferation assays were set up with $2.5x10^4$ cells per plate. Cells were cultivated in DMEM 15% FBS supplemented with either cytokine cocktail (Figure A, 100 ng/ml mSCF, 10 ng/ml IL-6 and 6 ng/ml IL-3) or 10 ng/ml IL-3 only (Figure B). The diagram shows average cell numbers ± SEM.

Also, results from CFC assays show both constructs have a strong effect compared to empty *pMIG*-transduced cells and were able to confer replating capacity to the transduced cells up to fourth plating. As in LC, CDX4 demonstrated a strong effect and led to a significantly increased colony number compared to CDX2 ($p=0.019$).

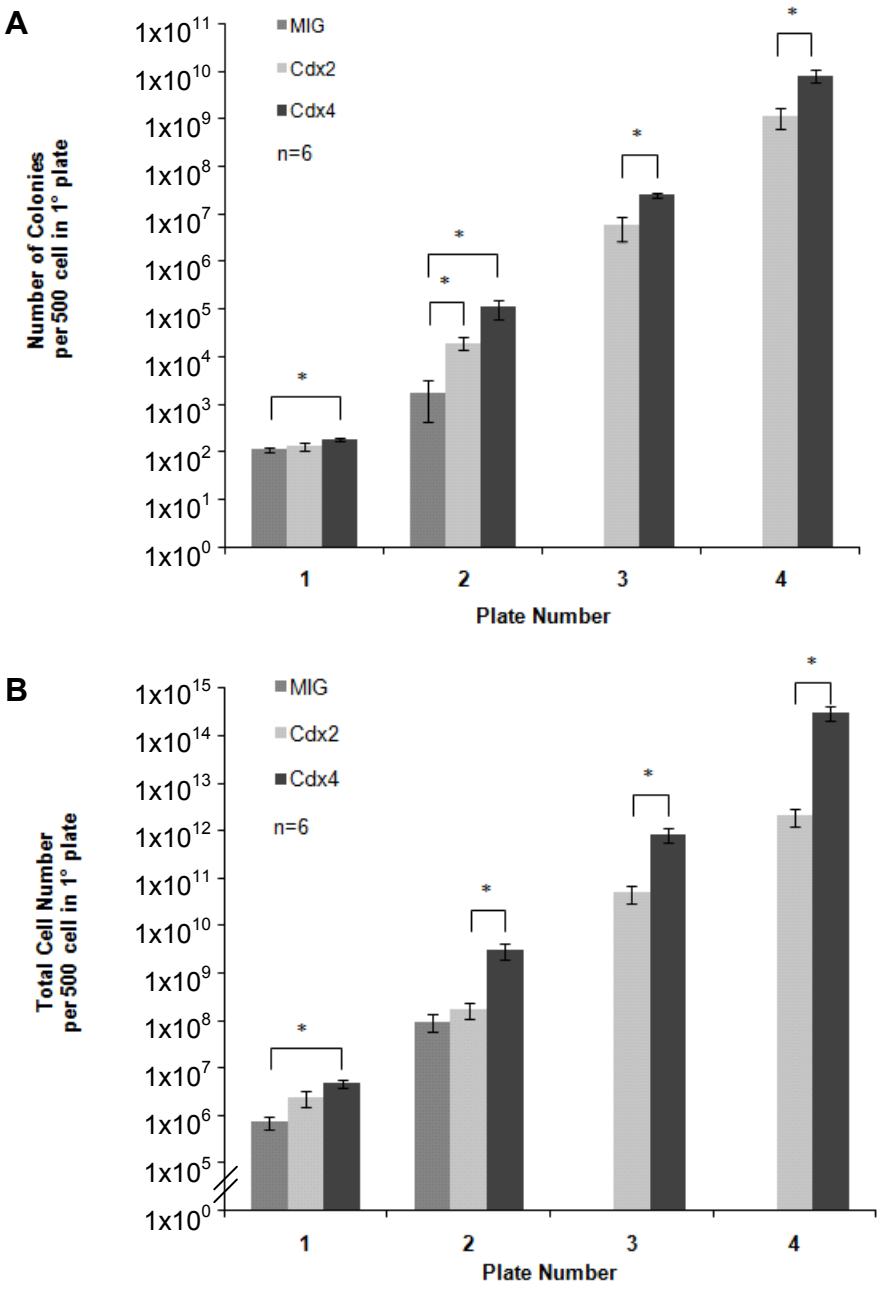

Figure 70: Total number of colonies per 500 cells in 1st week of CFC assay.
Cells were transduced with *pMIG*-construct, sorted for eYFP and eGFP expression, respectively and plated in methylcellulose with 500 cells per dish. For replating, cells were diluted in an appropriate dilution. A) Columns represent average total colony numbers ± SEM. B) Columns represent average total cell numbers ± SEM.

This difference was even more obvious in total cell number, where after 4th plating the cell number of *Cdx4*-transduced cells was 161.6-fold increased compared to *Cdx2*-transduced cells (p=0.03). The higher fold-difference in total cell number compared to total colony number between both constructs is due to a 22.5 times higher colony size within the *Cdx4*-transduced arm. Whereas colonies in the *Cdx2*-transduced arm after 4th plating contained on average

1.7x10^3 cells, *Cdx4*-overexpressing colonies at the same time-point on average contained 3.8x10^4 cells.

This result reflects the different colony morphology of both arms. The CDX4 arm had 2.1-fold higher number of CFU-M than the CDX2 arm (p=0.0001, Figure 71, Figure 72A). On the other hand, *Cdx2*-transduced cells gave rise to a higher percentage of CFU-GM (p=0.001). Interestingly, CDX4$^+$ CFU-GM generally were bigger in size than CFU-GM derived from *Cdx2*-transduced BM cells. With 44.0% versus 33.5%, the percentage of blast colonies was significantly higher in *Cdx2*-transduced BM cells compared to *Cdx4*-transduced cells as well (p=0.02). No significant number of CFU-G was observed.

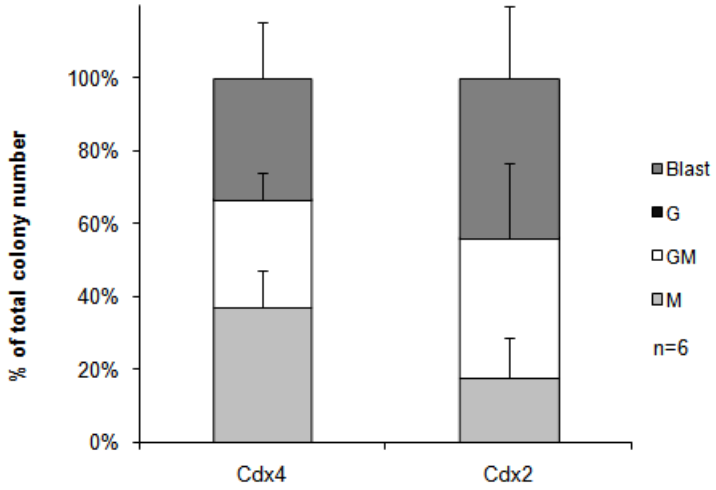

Figure 71: Colony distribution after 3rd plating of CFC assay.
The diagram shows the average percentage of the different colony types in proportion to the total colony number. Errors are SEM-based.

This observation was confirmed by H&E staining of cells derived from CFC assay after 3rd plating. Whereas the majority of *Cdx4*-overexpressing cells phenotypically were identified as differentiated macrophages, a high fraction of the cells derived of the CDX2 arm revealed a primitive blast-like phenotype (Figure 72B). The same was seen concerning colony morphology. As indicated by Figure 72, a higher percentage of primitive blast-like colonies was present in the CDX2 arm after 3rd and 4th plating. Whereas after 4th plating there were almost exclusively blast-like colonies in the CDX2 arm, *Cdx4*-transduced cells still were able to generate a high number of CFU-GM and CFU-M.

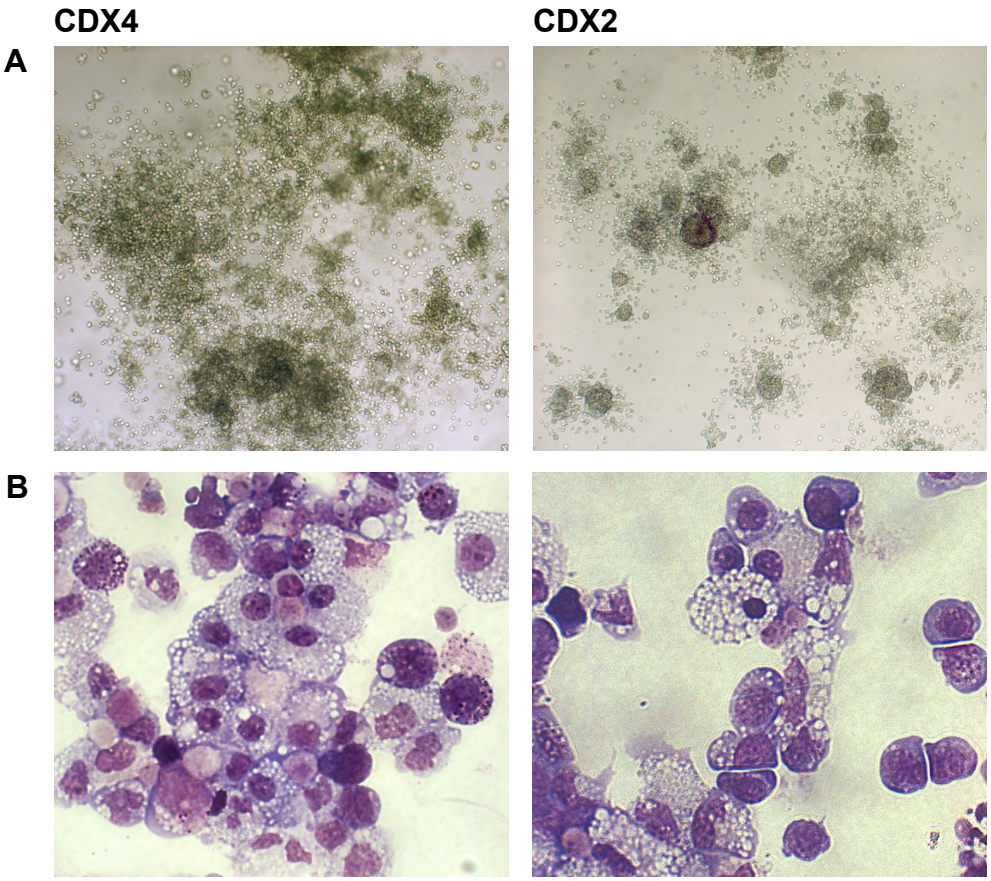

Figure 72: Picture of representative colony cell morphology.
A) Pictures of the colonies were taken with 50-fold amplification after 4th plating of CFC. B) For assessment of cell morphology, cells of 3rd plating were spread on glass slides using the cytospin method and stained with H&E. Pictures were taken in 400-fold amplification.

As depicted in Figure 73, immunophenotypical analysis of *Cdx2*- and *Cdx4*-transducd cells after 3rd plating revealed the majority of cells to express the myeloid markers Gr-1 and Mac-1. The positivity for these markers generally was higher in the CDX2 arm.

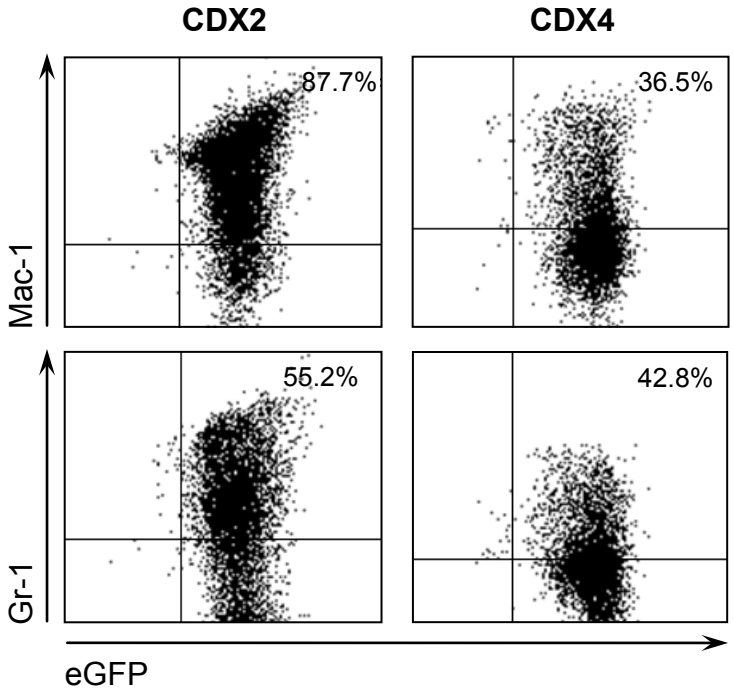

Figure 73: Immunophenotypic analysis of *Cdx2*- and *Cdx4*-transduced cells after 3rd plating of CFCs.
Transduced BM cells were harvested after 3rd CFC plating and analyzed by FACS Calibur for expression of myeloid markers.

5.5.4 Aberrant Expression of *Cdx2* Has a Considerably Higher Effect on Differential Gene Expression than *Cdx4*

Although both homeobox genes confer clonogenic potential and high proliferation capacity to murine BM progenitors, only CDX2 possesses a high oncogenic potential whereas CDX4 has a weak oncogenic effect. The DNA-binding homeodomain of both CDX members is strongly conserved, whereas the N-terminus is divergent (see attachment, Figure 76). Therefore, it would be interesting to know which targets both CDX members would have in common and could be responsible for their high clonogenic and proliferative potential. On the other hand, those genes deregulated only in *Cdx2*-transduced BM cells might allow finding pathways particularly critical for leukemogenesis.

The effects of *Cdx2*- and *Cdx4*-overexpression on hematopoietic progenitor cells were analyzed by microarray experiments. 5-FU enriched BM progenitor cells were transduced with both genes as well as empty pMIG for control and total RNA was extracted 72 h after transduction.

By a first approach differentially regulated genes were obtained using the R implemented LIMMA package. The ectopic expression of CDX2 led to a differential expression of 2919 genes whereas by retroviral enhanced expression of CDX4 only 1246 differentially regulated genes were identified. Furthermore, as depicted in the intersection of the Venn-Diagram, more than half of the genes differentially regulated by CDX4 also were found to be differentially regulated by CDX2. When those genes were analyzed more closely, almost all of these genes were more strongly deregulated by CDX2 than by CDX4. This indicates a much stronger effect of CDX2 on transcriptional gene regulation compared to CDX4.

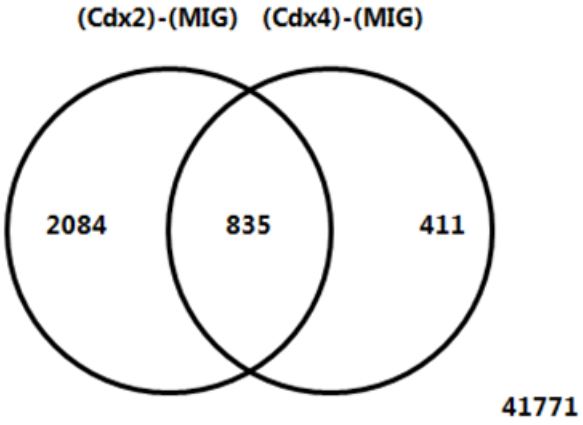

Figure 74: Venn-Diagram displaying the number of genes differentially regulated in the CDX2 and CDX4 arm compared to *pMIG*-transduced cells.
Data obtained with Affymetrix Mouse Genome 430 2.0 microarrays were data normalized using the GCRMA package of R. Differentially regulated genes were determined using the R implemented LIMMA package. 41.771 genes of 43.431 genes in total were not affected by overexpression of *Cdx2*, *Cdx4* or the empty *pMIG* vector.

A more stringent approach, using the R twilight package to exclude false positive findings, led to a similar result. As before, transduction with *Cdx2* showed a considerably higher effect on differential gene expression when compared to the empty vector control than *Cdx4*. Via this approach, 130 differentially regulated genes were identified in the CDX2 arm whereas in the CDX4 arm only 15 genes were detected. Thus, an 8.7-fold higher number of genes were deregulated in *Cdx2*-transduced BM cells compared to *Cdx4*-transduced cells. Furthermore, eight out of the 15 identified genes differentially regulated by overexpression of *Cdx4* were also deregulated in the CDX2 arm.

By the Panther Classification System (http://www.pantherdb.org) the list of differentially regulated genes identified by twilight were classified according to the ontologies of biological processes, pathways and molecular function. CDX2 and CDX4 differentially regulated52 and 9 genes, respectively. Signal transduction processes were most affected by aberrant CDX2 and CDX4 expression, followed by protein metabolism, immunity and developmental processes.

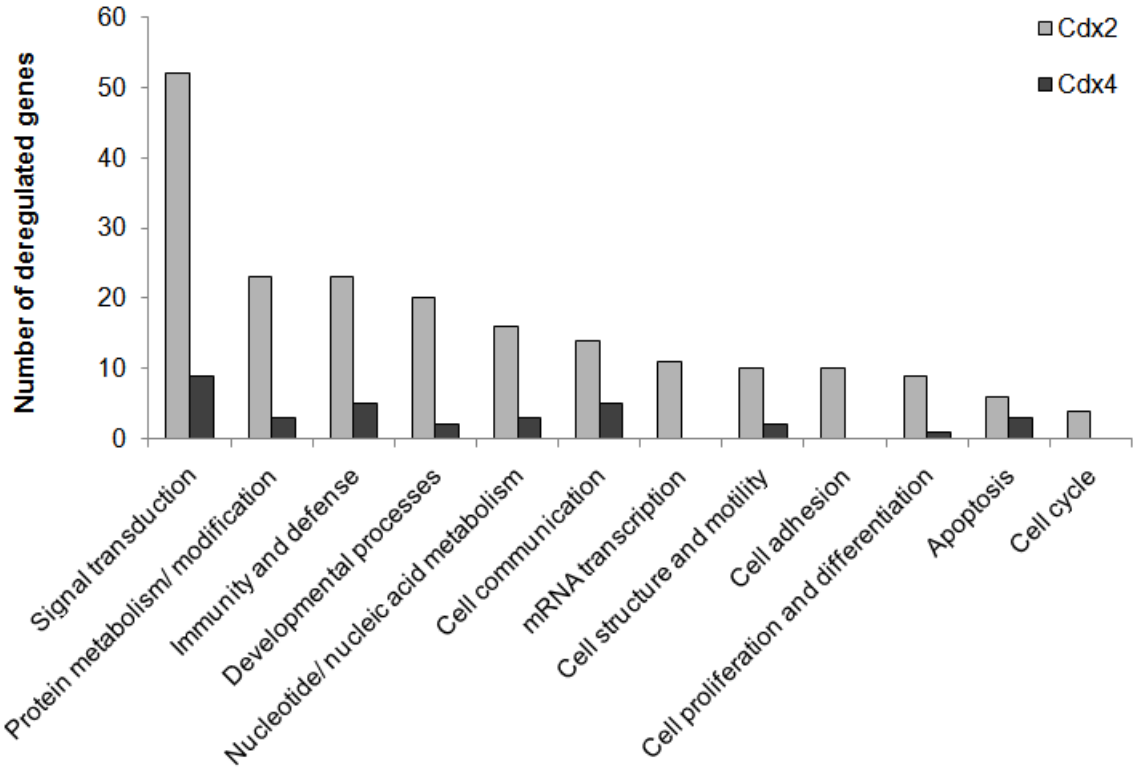

Figure 75: Genes differentially regulated by CDX2 and CDX4 compared to *pMIG*-transduced cells.
5-FU enriched BM progenitor cells retrovirally transduced with *Cdx2*, *Cdx4* or empty *pMIG* and highly purified by sorting for eYFP and eGFP expression, respectively. 72 h after the end of transduction successfully transduced cells were highly purified by FACS sorting and after an additional 24 hours of culture, total RNA was extracted. Affymetrix Mouse Genome 430 2.0 microarrays were used to compare differential gene expression of *Cdx2*- and *Cdx4*-overexpressing BM cells to *pMIG* only expressing cells. Data were normalized using the GCRMA algorithm and differentially regulated genes were detected using the R twilight package. The Panther Classification System was used to classify differentially regulated genes (http://www.pantherdb.org).

The CDX4 data did not show deregulation of specific pathways due to the low number of differentially regulated genes. Within the CDX2 arm the pathways for angiogenesis (number of deregulated genes =8), chemokine-mediated inflammation and cytokines signaling (n=7) as well as WNT signaling (n=7) were found to be significantly deregulated ($p<0.001$).

Interestingly, with a 4.6-fold increase, one of the highest differentially regulated genes within the CDX2 arm compared to the eGFP-transduced control was *Dlk1*, a gene which was shown to be upregulated in 61% of all AML cases, especially in AML M6 (Sakajiri *et al.*, 2005; Khoury *et al.*, 2010). Other significantly upregulated genes were *Chi3l4*, a chitinase of unknown function but high concentration in leukemic mice (Marchesi *et al.*, 2006), the fetal germ cell marker *Ddx4* as well as the ncRNA *Meg3* which was shown to induce p53 expression and is suggested to function as a tumor suppressor (Zhang *et al.*, 2009). Furthermore, aberrant CDX2 expression induced a differential upregulation of a number of signaling molecules including *Wnt2* (4.1-fold), *Il2ra* (3.1-fold), *Map3k8* (1.5-fold) or *Tgfbr3* (1.4-fold). Downregulated expression was found especially for genes associated with differentiated (hematopoietic) cells as for example *Mgl2* (2.9-fold), coding for a lectin expressed on antigen presenting cells, *Ebi2*, a G-protein coupled receptor which is expressed in mature B-cells, or *Ffar2*, encoding for a polymorphonuclear leukocytes expressed receptor (both 1.6-fold). Amongst the *Hox* genes, only *Hoxb3* was found to be significantly deregulated (1.6-fold upregulation).

Within the CDX4 arm, the highest differentially regulated genes, with a 3.8-fold increase compared to the *eGFP*-transduced control, were *Peg9*/*Dlk1*, *Chi3l4*, *Ddx4* and *Meg3/Gtl2*. However, in all cases the deregulation of the above-mentioned genes by CDX4 was less pronounced than by transduction with CDX2. Additionally, *Cdx4*-transduced BM cells showed a significant 1.3-fold differential upregulation of *Epb4.2*, which codes for an erythrocyte membrane skeletal protein detected in early erythroblasts and was found to be induced during erythroid differentiation (Zhu *et al.*, 1998). Like CDX2, CDX4 also induced a significant, 1.5-fold, downregulation of *Ebi2*. Amongst others the expression of *Gpnmb*, encoding a transmembrane protein highly expressed during macrophage differentiation, as well as CD36, which is expressed e.g. on macrophages or early erythroid cells, was also significantly decreased (1.3-fold and 1.7-fold, respectively). Most highly downregulated in *Cdx4*-transduced BM cells was *Sucnr1*, a gene coding for the succinate receptor GPR91. This receptor stimulates proliferation by activation of the MAPK pathway and is highly expressed in human $CD34^+$ progenitor as well as erythroid and megakaryocytic cells (Hakak *et al.*, 2009). A significant 1.3-fold decrease also

was observed in the transcript levels for the tumor necrosis factor *Tnfaip3*, a zinc finger protein inhibiting NF-κB.

When the gene expression profiles of both CDX members were compared, again signal transduction revealed to be the highest differentially regulated process with 22 affected genes followed by immunity & defense and developmental processes with 12 genes each. All of these genes were upregulated in *Cdx2*-transduced BM cells compared to *Cdx4*-transduced cells. Amongst those genes, *Irs1* was found to be 2.7-fold upregulated in the CDX2 arm, an oncogene essential for IGF-mediated proliferation and aberrantly expressed in several human cancers (Parathath *et al.*, 2008) and *Foxo1* (1.3-fold up) which was shown to be targeted by MAPK signaling (Asada *et al.*, 2007). The most deregulated signal transduction pathway however was the Wnt pathway, which was significantly upregulated in BM cells aberrantly expressing CDX2 compared to CDX4-transduced BM cells. Deregulated members of this pathway include *Wnt2* (4.1-fold upregulated in CDX2 vs. CDX4), *Fzd1* (2.6-fold up), *Tcf4* (1.6-fold up) or *Bambi* (1.4-fold up).

The (over-) expression of wild-type *Cdx2* and *Cdx4* in the transduced 5-FU BM samples was confirmed by real-time PCR and subsequent sequencing.

6. DISCUSSION

A primary feature of leukemia propagating cells is their ability to self-renew and indefinitely proliferate, acquired by genetic aberrations or epigenetic changes. Several factors conferring these abilities are members of the homeobox family, amongst others the family of *Hox* genes, which are found to be deregulated in a number of acute leukemia patients. In some of the cases, this aberrant expression can be explained by a deregulation of the *HOX* upstream regulator MLL, though in most of the cases the cause for *HOX* gene deregulation still is unclear.

One group of genes, known to be upstream regulators of *Hox* genes during embryogenesis, is the CDX family. Their role in adult normal and malignant hematopoiesis as well as their functional relevance to *HOX* gene deregulation in acute leukemia has not been well characterized thus far and is therefore the subject of this study.

6.1 CDX2 in AML

Deregulation of *HOX* genes is a common feature found in about one third of human AML. Beside those patients harboring MLL-rearrangements, *HOX* gene aberrations classically are connected to AML NK patients with NPM1 mutations (Alcalay *et al.*, 2005; Falini *et al.*, 2007). Microarray analysis of different AML subgroups of normal and aberrant karyotype performed in the course of this study show that deregulation of *HOX* cluster genes is not only present in AML NK patients with $NPMc^+$ but also in those NK patients missing this mutation. The reason for altered *HOX* gene expression in the cases of AML NK, however, is still largely unknown.

To address this question, AML patients were screened for the expression of *CDX2*, an upstream regulator of *Hox* genes during embryogenesis. The results of this test revealed that *CDX2* is aberrantly expressed in 79% of human AML patients. Hereby an aberrant expression of *CDX2* was not only more common in patients with AML NK compared to patients with abnormal karyotype (89% vs. 64%), but the expression level of *CDX2* was also significantly higher (15-fold higher) in patients with NK. The screening did not indicate any correlation of the NPM1 mutational status with the frequency and height of aberrant *CDX2*

expression. These results are consistent to the findings of Scholl *et al*. (2007) who detected aberrant expression of *CDX2* in the vast majority of analyzed AML patient samples, as well. Only the expression levels within the different AML subgroups differed slightly as Scholl *et al*. reported the highest expression of *CDX2* in patients with t(9;11) followed by AML NK and t(15;17) positive patients. In this study the highest expression was found in AML NK followed by t(9;11) and t(15;17). This, however, most probably reflects the small number of patients analyzed in both studies. Interestingly, in both screens a relatively high expression level of *CDX2* together with almost 100% positivity was detected in patients with PML-RARα translocations. PML-RARα leads to a block in differentiation, *in vivo* transgenic mice develop leukemia after a long latency and with only incomplete penetrance (Brown *et al.*, 1997; Grisolano *et al.*, 1997). Aberrant expression of *CDX2* in this case may serve as a second hit by conferring enhanced proliferation potential. In two more closely analyzed AML patients, Scholl *et al*. found *CDX2* expression levels to correlate with disease burden, underlining the importance of aberrant *CDX2* expression in acute myeloid leukemogenesis.

HOX gene deregulation was found to be present not only in $NPMc^+$ patients but also in those patients without NPM1 mutations. As high expression of *CDX2* was detected in both of these groups, it was tested if the expression pattern of *CDX2* would correlate with that of *HOX* genes. This was done by unsupervised hierarchical clustering of microarray data from AML patients and normal BM data according to *HOX* gene expression. By this analysis, two main clusters were identified: the first consisting of NK patients, which showed profound deregulation of *HOX* genes, the second cluster consisted of patients with abnormal karyotype together with normal BM samples, which showed equally low *HOX* expression levels. This suggests that not an aberrant expression of *CDX2 per se,* but rather the height of the *CDX2* expression level is of importance for deregulation *HOX* gene expression. Finding that the two NK patients with lowest *CDX2* expression of all tested NK patients fell into the abnormal karyotype cluster moreover supported this hypothesis. Immature, $CD34^+$ hematopoietic cells naturally express high levels of *HOX* genes. As $NPMc^+$ patients show less than 5% of $CD34^+$ blasts (Verhaak *et al.*, 2005), the increased *HOX* expression levels cannot be explained by an accumulation of immature blast cells. Overexpression of the *HOX* gene upstream regulator MLL

was found in only one case of a patient with NK and therefore did not influence the clustering. Also the expression level and the mutational status of *FLT3* were reported to correlate to upregulated *HOX* gene expression in AML (Roche *et al.*, 2004). However, this correlation could not be confirmed in this study. Although some possible reasons for high or deregulated *HOX* gene expression were excluded, it cannot be ruled out that other, still unknown factors contribute to *HOX* gene deregulation in AML NK. Contribution of additional regulatory mechanisms, for example, would explain the higher deregulation of *HOX* genes in AML NK with $NPMc^+$ compared to NK patients without NPM mutation, which did not show any significant differences in their *CDX2* expression levels.

To investigate if CDX2 could be functionally involved in the deregulation of *HOX* genes in AML, the ability of CDX2 to regulate *Hox* gene expression in adult hematopoiesis was tested by retroviral overexpression of CDX2 in murine hematopoietic progenitors. In this assay, CDX2 was able to significantly upregulate expression of *Hoxa5*, *Hoxa7*, *Hoxa9*, *Hoxa10* as well as *Hoxb3*, *Hoxb6* and *Hoxb8* compared to empty vector-transduced cells. All of these *Hox* genes have been reported to possess leukemic potential (Bach *et al.*, 2010, Perkins *et al.*, 1990; Thorsteinsdottir *et al.*, 2001; Fischbach *et al.*, 2005). The N-terminal transactivation domain of CDX2 is clearly important for the regulation of *Hox* gene expression (Rawat *et al.*, 2008). This data is in line with previous findings reporting CDX2 to be able to deregulate *Hox* gene expression in embryonic as well as adult nonhematopoietic tissues (Chawengsaksophak *et al.*, 2004; Liu *et al.*, 2007). Interestingly, CDX2 especially deregulated *Hox* genes of the *HoxA* and *HoxB* cluster, those clusters reported to be upregulated in $NPMc^+$ patients (Verhaak *et al.*, 2005).

To test if expression of other members of the CDX family could be responsible for the deregulation of *HOX* cluster genes, 24 AML NK patients were tested for *CDX1* and 48 AML NK patients for *CDX4* expression. However, neither *CDX1* nor *CDX4* expression was detectable in any of the samples analyzed. This is in contrast to the findings of Bansal *et al*. (2006) who reported aberrant expression of *CDX4* in 10 out of 44 analyzed AML patients. However, in this study a different primer set was used, which possibly was of a different efficiency, and the expression of *CDX4* was not tested in human normal hematopoietic tissue. Therefore, it is impossible to tell if *CDX4* in AML was actually overexpressed

compared to normal BM or detectable in their study only due to a higher overall sensitivity of the applied test. As the expression of *CDX4* in this study furthermore did not correlate to those AML subtypes where *HOX* gene deregulation can be observed, an eventual expression of CDX4 in some AML cases seems to be of only low relevance for aberrant *HOX* gene expression in AML.

As shown by Rawat *et al*. (2004), CDX2 possesses a strong leukemogenic potential in the murine BM transplantation model where it induced fully penetrant AML. This capacity, combined with its ability to deregulate *HoxA* and *HoxB* cluster genes in adult hematopoietic progenitors and its high expression in the AML subtypes with high *HOX* gene deregulation strongly support the hypothesis of an involvement of CDX2 in the leukemogenesis of AML via deregulation of *HOX* genes.

6.2 CDX2 in ALL

To test if aberrant expression of *CDX2* is a feature characteristic for AML only or if it can also be found in different types of leukemia, 57 newly diagnosed ALL patients were tested for *CDX2* expression. In this study, it was shown for the first time that *CDX2* is aberrantly expressed in the majority of ALL patients with 81% overall positivity. The overall expression level of *CDX2* in ALL exceeded that of AML patients with NK, demonstrating that aberrant expression of *CDX2* is not restricted to myeloid malignancies.

The expression level of *CDX2* in ALL significantly correlated with subtypes and survival. High expression levels were associated with high and very high risk and with an inferior overall survival. Although this study was performed with a low number of patients, *CDX2* remained an independent risk factor even after adjusting for the risk factors age and presence of molecular markers by bivariate Cox regression. This indicates aberrant *CDX2* expression is an important mechanism in the leukemogenesis of ALL. As reported by Riedt *et al*. (2009) the same is true for pediatric ALL where the vast majority of patients showed aberrant expression of *CDX2*. Also in this study, aberrant expression of *CDX2* significantly correlated to an inferior disease outcome, which was determined by linking *CDX2* expression as minimal residual disease (MRD) to treatment outcome.

Unlike AML, *HOX* gene deregulation is less common in ALL (Armstrong *et al.*, 2002; Quentmeier *et al.*, 2004). Additionally in ALL - in contrast to AML - only low correlation between the expression of *HOX* genes with the expression of *CDX2* was found. This could indicate that in ALL the leukemogenic effect of CDX2 does not depend on *HOX* gene perturbation to the same extent as in AML. The oncogenic potential of CDX2 rather seems to be mediated through different regulatory networks. Results of TaqMan LDA demonstrated that besides *Hox* deregulation aberrant CDX2 expression also led to an altered expression of a number of genes involved in lymphopoiesis. Affected for example were *Lef1*, *Tcf3* or *Id3*, genes which are frequently deregulated in lymphoid leukemia (Ferrando *et al.*, 2003; Mullighan *et al.*, 2007) or, in the case of Lef-1, lead to induction of AML and B-ALL when deregulated (Petropoulos *et al.*, 2008). An aberrant expression of CDX2 therefore may play a role in induction and/or maintenance of myeloid as well as lymphoid leukemia, possibly depending on the cell stage and type in which aberrant CDX2 expression initially occurs.

The functional relevance of CDX2 for growth of transformed lymphoid cells was confirmed by a knockdown experiment where reduced expression of CDX2 in the human pre-B cell line Nalm-6 led to an impaired growth and clonogenic potential of the cell line. The same was previously shown for different AML cell lines by Scholl *et al*. (2007) and highlights the importance of CDX2 expression for the transformation of lymphoid and myeloid hematopoietic cells in human leukemic cell lines.

This data demonstrates CDX2 is a novel proto-oncogene aberrantly expressed in the majority of adult ALL patients where it serves as an independent risk factor for inferior overall survival. In contrast to AML, aberrant expression of *CDX2* in ALL was not associated with the deregulated *HOX* gene expression. It was shown that ectopic expression of CDX2 affects several pathways involved in lymphoid commitment and differentiation and is important for the growth of the leukemic cell line Nalm-6. This hints at a functional relevance for CDX2 for initiation and/or maintenance of the lymphoblastic clone, but also at common pathways activated in both lymphoid and myeloid leukemia.

6.3 Aberrant Expression of *CDX2* in Acute Leukemia

Different to the publication of Chase *et al*. (1999) (who reported *CDX2* to be expressed in only one AML patient and absent in all other cases analyzed but used the less sensitive standard PCR) this and other studies show that aberrant expression of *CDX2* is a frequent event both in AML as well as ALL (Scholl *et al.*, 2007; Rawat *et al.*, 2008; Riedt *et al.*, 2009; Thoene *et al.*, 2009). Nevertheless, the mechanisms leading to aberrant *CDX2* expression in acute leukemia is still unclear.

As demonstrated in this study, the methylation level of the promoter region did not correspond to the expression level of *CDX2*, which is in line with previous publications (Scholl *et al.*, 2007; Pereira *et al.*, 2009). In addition, treatment of *CDX2*-negative cell lines with demethylating agents did not lead to an induction of *CDX2* expression (Hinoi *et al.*, 2003), suggesting that *CDX2* expression in leukemia is independent of promoter hypomethylation as well as the methylation level of cis-regulatory elements. Amplification of the *CDX2* locus was detected only in a small percentage of patients with complex karyotype, however not in AML patients with normal or other aberrant karyotypes (Rucker *et al.*, 2006; Scholl *et al.*, 2007). Sequencing of the coding region of *CDX2* did not – neither in the study of Scholl *et al*., nor in this study –reveal any mutations that could affect mRNA stability.

One other possibility, leading to aberrant transcription of *CDX2* could be deregulation of trans-acting pathways, which target cis-regulatory elements in the 5' region of the *CDX2* gene as suggested by Hinoi *et al.* (2003). No mutations were found in the promoter region of *CDX2,* however one cannot exclude the possibility that still unknown mutations in cis-regulatory elements of the *CDX2* gene might account for its aberrant expression. It would be interesting, therefore, to expand the sequence analysis of the *CDX2* gene beyond its coding and promoter region and to conduct a more comprehensive sequence analysis on the above-mentioned regulatory regions. For example, genetic alterations could occur in negative regulators, which Wang & Shashikant (2007) postulated to be present in an 11.4 kb sequence flanking *Cdx2*. Disruption of these elements in hematopoietic cells subsequently could lead to an aberrant expression of the generally silenced *CDX2*. Mutations within

two enhancer regions in the first intron of *CDX2*, which were demonstrated to induce ectopic expression of *Cdx2* in the murine embryo, could lead to aberrant *CDX2* expression (Wang and Shashikant, 2007). Interestingly, several binding sites for FGF and Wnt signaling were identified in these regions. Mutations in the non-coding regions of *Cdx2* therefore could possibly affect the binding of factors like FGF4, which was previously shown to target *Cdx2* (Murohashi *et al.*, 2010). Furthermore, it is probable that CDX2 not only regulates but is also targeted by WNT signaling as already shown for its paralogs CDX1 and CDX4 (Shimizu *et al.*, 2005; Pilon *et al.*, 2006). Another pathway which was described to regulate CDX2 expression is RAS/MAPK signaling (Lu *et al.*, 2008), a pathway which links extracellular stimuli, amongst others, to proliferation, differentiation and cell survival (Milella *et al.*, 2001; Lee and McCubrey, 2002; Steelman *et al.*, 2008). Both the WNT and RAS/MAPK pathway are frequently deregulated in leukemia. Their deregulation, in combination with genetic alterations in trans- or cis-regulatory elements of *Cdx2*, could possibly affect the transcription of the gene. As these two pathways are important for lymphoid and myeloid leukemogenesis, localization of *CDX2* downstream of one or more of these signaling pathways could explain the high number of *CDX2* positive cases in AML and ALL. A better investigation of the mechanisms leading to aberrant expression of *CDX2* thus might lead to a better understanding of common molecular mechanisms of leukemogenesis in both myeloid and lymphoid leukemia.

6.4 CDX4 in the Murine Transplantation Model

In contrast to the highly leukemogenic CDX2, its paralog CDX4 was reported to possess high stem cell amplificatory potential on murine embryonic hematopoietic progenitors *in vitro*, which even exceeded that of *Hoxb4* (Davidson *et al.*, 2003). The aim of this study therefore was to functionally analyze the role of CDX4 in adult hematopoiesis by use of the murine BM transplantation model.

In vitro, overexpression of CDX4 led to an enhanced proliferative as well as clonogenic capacity of the transduced cells and promoted growth, especially growth of myeloid cells. The high proliferative potential of CDX4-transduced BM cells could be due to a pronounced increase of c-Kit$^-$/ Sca1$^+$ cells in both LC

and CFC assays. This marker combination is expressed on primitive cell populations, which are shown to possess high clonogenic capacity *in vitro* (Metcalf *et al.*, 2009). This is in line with data previously published by Bansal *et al*. (2006) who demonstrated CDX4 is able to confer enhanced replating and proliferative potential to transduced murine hematopoietic cells. In addition, Davidson *et al*. (2003) and Wang *et al*. (2005) observed an expansion of particularly the progenitor population. Both publications additionally reported an increase of myeloid colonies after transduction of murine embryonic hematopoietic progenitors and ESCs, with CDX4.

Although the overall fraction of myeloid cells in LC remained stable over time, immunophenotypic analysis revealed an increase of the Gr-1$^+$/Mac-1$^-$ fraction and a decrease of the Gr-1$^-$/Mac-1$^+$ compartment in the IL-3/IL-6/SCF supplemented culture. As this effect was not observed in IL-3 only culture the shift in fraction seems to depend on the presence of IL-6 or SCF, the c-Kit ligand. This suggests an altered differentiation behavior of c-Kit$^+$ committed progenitors. A function of CDX4 particularly on the level of early hematopoietic progenitors is indicated by the expression profile of CDX4. According to the expression analysis performed in this study as well as according to the results of Bansal *et al*. (2006), *Cdx4* is highly expressed in 5-FU enriched hematopoietic progenitors and particularly high in the lineage-committed CMP population.

Overexpression of CDX4 *in vivo* initially did not lead to a block in hematopoietic differentiation. However, aberrant CDX4 expression *in vivo* conferred a short-term proliferation advantage to the transduced BM cells compared to non-transduced cells with an engraftment of almost 42% four weeks after transplantation and a decrease in the eGFP$^+$ compartment after this time point. Whereas the myeloid and T-lymphoid lineage distribution of the eGFP$^+$ compartment resembled that of the eGFP$^-$ compartment, the B-lymphoid lineage was reduced in eGFP$^+$ hematopoietic cells. As this effect of CDX4 led to a change in the lymphoid/myeloid ratio, it suggests an alteration in the differentiation behavior of the transduced stem cells. The fact that all lineages were present in the eGFP$^+$ fraction suggests that retrovirally enforced expression of CDX4 *in vivo* acts on the level of multipotent progenitor cells, which are able to differentiate into all the hematopoietic lineages. Furthermore,

it indicates that CDX4-overexpression did not block differentiation but allowed terminal differentiation of the transduced hematopoietic cells.

All mice transplanted with *Cdx4*-transduced BM died of transplantable leukemia of long latency. The median latency for primary transplanted animals was 353 days whereas secondary transplanted animals succumbed to leukemia with a median latency of 74 days. This equals the results published by Bansal *et al*. (2006) who reported primary CDX4-transplanted animals to die with a median latency of 300 days after transplantation. However, in the Balb/c mouse model of Bansal *et al.* aberrant expression of CDX4 did not lead to complete penetrance of the leukemia, only transplantation with BM cells coexpressing CDX4 and MEIS1 led to induction of disease in all experimental animals. Meis1 was shown to collaborate with certain *Hox* genes such as *Hoxa9* and *Hoxb3* (Kroon *et al.*, 1998; Thorsteinsdottir *et al.*, 2001), which in this and other studies was shown to be deregulated by overexpression of CDX4 (Davidson *et al.*, 2003; Bansal *et al.*, 2006; Yan *et al.*, 2006). This finding therefore suggests that the leukemic effect of CDX4 is, at least to a certain part, due to the induction of aberrant *Hox* gene expression (Kroon *et al.*, 1998; Thorsteinsdottir *et al.*, 2001; Davidson *et al*., 2003; Bansal *et al.*, 2006). The long latency of primary transplanted animals furthermore suggests that aberrant expression of CDX4 alone is not sufficient to induce leukemia. To investigate possible additional hits, contribution of retroviral insertions to the induction of leukemia was tested by LM-PCR. Although most of the intergenic insertions were located within a distance to genes, which could possibly affect their transcription (Bartholomew and Ihle, 1991), none of the examined integrations was inside the '*Retrovirus Tagged Cancer Gene Database*' (RTCGD), a database comprising retrovirus and transposon insertion sites. Additionally, none of the affected genes were reported to be involved in hematological malignancies. However, as it was not possible to analyze every retroviral integration site in all the mice, therefore an involvement of insertional mutagenesis in this leukemia model cannot be excluded. Nevertheless, aberrant CDX4 expression may serve as an initiating event in leukemogenesis by conferring enhanced clonogenic and proliferative capacity to hematopoietic cells. This would be supported by previous findings of Yan *et al*. (2006) who demonstrated by an *in vitro* approach that after activation of *HoxA* cluster genes, expression of CDX4 is no longer required. The group

therefore proposed that expression of CDX4 is required only in early stages of MLL-fusion gene induced transformation to induce *Hox* expression.

Histopathologically, the diseased primary and secondary transplanted mice were diagnosed with erythroleukemia in all the cases. Most of the blasts were of the erythroid lineage, but in all the cases at least 20% of MPO^+ myeloid blasts additionally were present in the histophatologically analyzed organs. The highest percentage of blasts was found in the spleen with an average blast cell count of 61%. This might be due to the induction of stress erythropoiesis, which in the mouse occurs in the spleen (Socolovsky *et al.*, 2001). A block in differentiation of erythroid cells and a thereby decreased count of differentiated RBCs leads to expansion of the erythropoietic tissue and hereby would induce splenomegaly as observed in CDX4-transplanted mice.

Taken together, these results suggest that CDX4 exerts its influence on the level of multipotent and/or very early committed progenitors and that, at least in part, this effect is due to the upregulation of *Hox* genes. The long latency of CDX4-induced leukemia, however, indicates that overexpression of this gene is not sufficient to induce leukemia on its own.

6.5 CDX4 in the Erythroid Lineage

Enforced overexpression of CDX4 in the murine BM transplantation model led to an expansion of hematopoietic progenitors and to the development of erythroleukemia in all cases indicating, that perturbed expression of CDX4 also disturbed the erythroid lineage.

The effect of CDX4 on erythroid cells was observable already *in vitro* where in liquid culture as well as in CFC assay the maintenance of a population of $Ter119^+$ erythroid cells was observed over more than three weeks of culture. This indicates that CDX4 is able to confer serial replating capacity to erythroid progenitors. Interestingly, an effect of CDX4 in particular on the erythroid lineage was already shown in embryonic development, where Wang *et al.* (2008) observed a reduction in the formation of primarily multipotent and erythroid progenitors in CDX4-deficient murine ESCs. Overexpression of CDX4 in an ES cell line on the other hand led to an increase of primitive erythroid colonies (Wang *et al.*, 2005). Wang *et al*. furthermore showed CDX4 is able to

induce strong upregulation of PU.1, which is known to block erythroid differentiation and is required for induction of erythroleukemia (Amaravadi and Klemsz, 1999; Afrikanova *et al.*, 2002). PU.1 also drives lineage specification towards macrophage differentiation (Dahl *et al.*, 2003), which may explain the increase of this lineage in *Cdx4*-transduced BM cells in the first week of LC as well as in CFC assay.

In vivo CDX4 was reported to affect the erythroid lineage, as well. Davidson *et al*. (2003) demonstrated that a loss of function mutation of *cdx4* leads to a defect in early hematopoiesis in the zebrafish embryo resulting in a severe decrease of hemoglobin-expressing erythroid cells combined with a reduction of *gata1*$^+$ erythroid precursors. An overexpression of CDX4 in contrast led to ectopic blood formation *in vivo* (Davidson *et al.*, 2003). However, the long latency of the erythroid leukemia observed in CDX4-transplanted mice indicates the need for accumulation of further genetic alterations.

The fact that CDX4-transplanted leukemic mice died of erythroleukemia may explain why no leukemic *ex vivo* cell line could be derived of those mice. For PU.1$^+$ erythroleukemia, for example, it was reported that despite their transformation permanent erythroleukemic cell lines could be obtained only by culture in Epo-supplemented conditions (Moreau-Gachelin, 2006). However, the culture conditions routinely employed in this study did not include any addition of Epo and thus may have led to an exhaustion of the leukemic erythroblast cells. This is in contrast to erythroleukemia induced by the Friend leukemia virus, which leads to aberrant activation of the erythropoietin receptor (EpoR) (Ruscetti, 1999) and would indicate that CDX4 does not lead to altered activity of EpoR, but drives transformation by alternative pathways.

The results of this study suggest a role of CDX4 in the expansion of erythroid progenitors as well as an involvement in the leukemic transformation of erythroid cells. CDX4 therefore might be a novel factor in the determination of erythroid cell fate but may also be of importance for induction of erythroid leukemia in humans. In particular, it would be interesting to investigate whether the results of the BM transplantation model can be repeated in humans and to investigate a possible involvement of CDX4 in human erythroleukemia.

6.6 Differential Effects of CDX2 and CDX4

CDX2 and CDX4 both belong to the conserved group of caudal-like group of homeobox genes and are about 45% similar at the protein level in mouse and human (see attachment, Figure 76). The homeodomain, which determines the binding to target genes and was described to be crucial for the leukemogenic effect of both CDX proteins, is highly conserved between the two genes (Rawat *et al.*, 2004; Bansal *et al.*, 2006). On the other hand, a comparatively low conservation can be observed at the N-terminal transactivation domain, which was found to be crucial for deregulation of *Hox* genes (Rawat *et al.*, 2008). Despite this weak homology, both genes were able to upregulate *HoxA* cluster genes in a similar manner. A significant difference, however, was detected in the expression levels of *Hoxb6* and *Hoxb8*. CDX2 induced an almost 7-fold higher ectopic expression of *Hoxb6* compared to CDX4 and ectopic *Hoxb8* expression was found only in *Cdx2*-transduced BM. Both *Hoxb6* and *Hoxb8* have been described to be direct targets of CDX2 before (Scholl *et al.*, 2007, McKinney-Freeman *et al.*, 2008; Wang *et al.*, 2008). Overexpression of HOXB8 *in vitro* results in immortalization of myeloid progenitors and leads to development of AML with a latency of about 8 months (Perkins *et al.*, 1990; Perkins and Cory, 1993). However, neither in AML nor in ALL was aberrant expression of *HOXB8* detected and in ALL most of the patients were negative for the *HOXB8* transcript rendering it unlikely that this *HOX* gene has a major impact on the leukemogenic potential of CDX2. Aberrant expression of HOXB6 *in vitro* can result in a differentiation block of myeloid precursors, combined with an increase of blast-like colonies (Fischbach *et al.*, 2005). The same effect was observed in this study for *Cdx4*-, and even more pronounced in *Cdx2*-transduced BM cells. In the mouse model, aberrant expression of HOXB6 leads to induction of AML with a median latency of approximately 8 months (Fischbach *et al.*, 2005). Overexpression of HOXB6 was described to inhibit erythroid maturation, and may therefore contribute to the development of erythroid leukemia in the CDX4 mouse model (Zimmermann and Rich, 1997, Shen *et al.*, 1992; Kappen, 2000). Interestingly, in AML lacking chromosomal aberrations, including NPM^+ AML – the AML subtype with highest expression of *Cdx2* – overexpression of *HOXB6* can be found in up to 60% of all the cases (Giampaolo *et al.*, 2002). Furthermore, the results of this study, showing that

HOXB6 was the only *HOX* gene correlating with the expression level of *CDX2* in ALL, suggest that aberrant *HOXB6* expression contributes to the leukemogenic potential of CDX2.

Despite the higher effect of CDX2 on expression of *Hoxb6* and *Hoxb8*, *in vitro* overexpression of CDX4 resulted in a significantly higher effect compared to CDX2 and conferred a higher proliferative potential as well as self-renewal capacity to the transduced hematopoietic progenitors. Nevertheless, BM cells overexpressing *Cdx4* still were able to differentiate to a higher extent than *Cdx2*-transduced cells. After third plating, for instance, a significantly increased number of mature macrophage colonies was observed in the CDX4 arm compared to the CDX2 arm whereas transduction with *Cdx2* led to growth of a significantly higher number of blast colonies. This was reflected by the immunophenotypic staining as well as cytomorphological analysis, demonstrating that CDX4 blocks differentiation of the transduced BM cells to a lower extent than CDX2. On the other hand, immunophenotyping of $CDX4^+$ colonies after third plating showed a significant higher percentage of cells to be c-Kit^+/Sca-1^-, a marker combination of lineage committed progenitors (Metcalf *et al.*, 2009). This suggests that CDX4 more likely acts by an expansion of lineage-restricted progenitors whereas the effect of *Cdx2* transduction most probably is due to a block of differentiation.

The fact that *Cdx2*-transduced cells derived from *in vitro* culture were able to engraft transplanted mice long-term and induce leukemia (Rawat *et al.*, 2004) demonstrates that CDX2 leads to transformation of the transduced cells *in vitro*. *Cdx4*-transduced cells in contrast did not possess this capacity, which indicates that CDX4 – unlike CDX2 – alone is not sufficient to transform hematopoietic cells *in vitro*.

In vivo, with a difference of more than 230 days in median latency compared to CDX4, CDX2 transplanted mice succumbed to transplantable leukemia significantly earlier than mice transplanted with CDX4-transduced BM. This relatively short latency of CDX2 induced leukemia suggests that aberrant CDX2 expression leads to a more advanced preleukemic stage of the transduced BM cells than overexpression of CDX4. CDX2 therefore must require less additional alterations needed for induction of full-blown leukemia. The leukemia induced by CDX2 furthermore was considerably more aggressive compared to CDX4,

as indicated by multiorgan infiltration, a significantly lower PB RBC count as well as a significantly higher spleen weight at time of death.

The results of this study indicate that both CDX2 and CDX4 are able to confer a high proliferative and clonogenic capacity to transduced BM progenitor cells. Although in *vitro*, CDX4 conferred the stronger effect overexpression of CDX4 did not block differentiation to the same extent as observed with aberrant expression of CDX2. As potent upstream regulators of *Hox* genes, the enhanced proliferative and clonogenic capacity of the two CDX members may be mainly due to the upregulated *Hox* gene expression. The reason why CDX4 is more potent in inducing proliferation *in vitro* remains to be clarified. Interestingly, McKinney-Freeman *et al*. (2008) demonstrated that during embryonic hematopoiesis, CDX2 strongly inhibits differentiation whereas CDX4 dramatically enhances the expansion of hematopoietic progenitors. Their observations resemble the results of this study and indicates the presence of additional pathways regulated by *Cdx* genes.

To investigate the role these pathways play in the different leukemogenicity of CDX2 and CDX4, the effect of their aberrant expression on global gene expression of murine BM progenitors was analyzed. In this assay, aberrant expression of CDX2 led to a clearly higher number of deregulated genes than aberrant CDX4 expression. The dataset, as analyzed by the R twilight package for example, revealed an almost 9-fold higher number of significantly deregulated genes within the CDX2 arm compared to the CDX4 arm. This result corresponds with data from Nishiyama *et al*. (2009), who reported that transduction with CDX2 amongst 50 different transcription factors resulted in the most pronounced perturbation of the transcriptome in ES cell lines. In addition, the differential expression profile of 5-FU BM cells transduced with CDX4 showed a pronounced overlap with that of CDX2 transduced BM. More than half of the genes differentially regulated by CDX4 overexpression were found to be deregulated in the CDX2 arm as well. In addition, with exception of only one gene, the deregulation of those genes was always more pronounced in CDX2-transduced cells.

In both arms, especially high upregulation of *Dlk1* was detected. *DLK1,* a member of the epidermal growth factor-like family also known as PREF-1 or FA1, belongs to the group of imprinted genes and is expressed only from the

paternal allele (Kobayashi *et al.*, 2000). During embryonic development, it is expressed predominantly in immature cells and its expression in BM stromal cells promotes expansion of primitive hematopoietic progenitors (Moore *et al.*, 1997; Floridon *et al.*, 2000). With advancing fetal development, DLK1 is downregulated and in the adult, its expression is restricted to non-hematopoietic cell types (Kim *et al.*, 2007). In 61% of AML, however, an overexpression of *DLK1* can be observed which, in 76% of the cases, is due to bi-allelic expression (Khoury *et al.*, 2010). Especially in AML M6, overexpression of *DLK1* is a frequent event (Sakajiri *et al.*, 2005) and therefore may be involved in erythroid leukemogenesis in the CDX4 mouse model. Interestingly, DLK1 was shown to activate MEK/ERK signaling by increasing ERK1/2 phosphorylation (Kim *et al.*, 2007), a pathway which was shown to be highly activated in leukemia. Furthermore, CDX2 was shown to be a target of RAS/MAPK signaling itself (Lu *et al.*, 2008), suggesting a positive feedback loop, which could be partly mediated by DLK1. This is supported by upregulation of several genes involved in MAPK signaling including MAP3K8, IRS2 or SPRY1. In contrast, no differential regulation of these MAPK signaling molecules was found in *Cdx4*-transduced cells pointing to a difference in the regulatory mechanism of the two CDX proteins. Interestingly, another transcript significantly upregulated in both CDX2- and CDX4-transduced 5-FU BM cells was *Meg3*, a non-coding RNA which is located contiguous to *Dlk1* at the imprinted region on chromosome 14q32.2 in the human and on the long arm of chromosome 12 in the mouse (Kircher *et al.*, 2008; Wallace *et al.*, 2010). The deregulation of both imprinted genes may suggest an involvement of CDX members in the co-regulation of *Dlk1* and *Meg3,* which was described for some tissues during embryonic development (da Rocha *et al.*, 2007).

In both the CDX2 and CDX4 arms, only few genes were found to be downregulated in comparison to empty vector control. For example, *Tnfaip3* was affected by aberrant expression of CDX4. A knock-down of this gene showed an enhanced clonogenicity (Honma *et al.*, 2009) and could possibly contribute to the relatively high colony forming capacity of *Cdx4*-transduced BM cells. Again, a higher number of deregulated genes was found in *Cdx2*-transduced cells compared to *Cdx4*-transduced cells. Most of the genes downregulated in the CDX2 arm encode proteins expressed mainly on/in differentiated cell types. This result therefore mirrors the effect of aberrant

expression of CDX2 on hematopoietic progenitor cells, leading to a block of differentiation and decrease of mature hematopoietic cells.

Pathways, which were significantly upregulated in *Cdx2*-transduced BM cells compared to *Cdx4*-transduced cells, were for example the PI3 kinase or the TGF-β signaling pathways, which were both upregulated in the CDX2 arm. However, the most deregulated pathway in the CDX2 arm was the WNT signaling pathway and, with a more than 4-fold difference, its member *Wnt2* was the highest differentially regulated gene when *Cdx2*-transduced BM cells were directly compared to *Cdx4*-transduced cells. Whereas CDX4 previously was shown to be targeted by WNT signaling, particularly by WNT3A (Shimizu *et al.*, 2005; Pilon *et al.*, 2006), no regulation of CDX2 by this pathway was observed so far. In contrast, recent reports suggested WNT3A to be a direct target of CDX2 (Savory *et al.*, 2009) and the results of this gene expression analysis indicate CDX2 to be able to deregulate the WNT pathway as well, by targeting *Wnt2* but also several other members such as *Fzd1* or *Tcf4*. This pathway is known to be a critical pathway involved in embryonic development and confers self-renewal properties to hematopoietic and also cancer stem cells. Deregulation of this pathway is a frequent event in various cancers (Reya *et al.*, 2003; Reya and Clevers, 2005). The ability to deregulate the WNT pathway therefore turns CDX2 into a potent oncogene and is most probably one main reason for its stronger leukemogenic effect compared to CDX4.

6.7 Role of CDX2 in Leukemia

The high oncogenic potential of CDX2 was suggested to be linked to its function as an upstream regulator of *Hox* genes. This hypothesis was supported by the finding that a deletion mutant of CDX2 missing the N-terminal transactivation domain – which was shown to be crucial for transcriptional activation of *Hox* genes (Taylor *et al.*, 1997) – did not exhibit any leukemogenic effect (Rawat *et al.*, 2008). In contrast to CDX4, aberrant expression of CDX2 led to a pronounced deregulation of the transcriptome in murine BM progenitors and an upregulation of additional pathways involved in self-renewal such as the WNT pathway. Indeed, the relevance of CDX2 for self-renewal was already shown for trophoblast stem cells, which upon withdrawal of CDX2 undergo differentiation (Niwa *et al.*, 2005). The results of this study suggest that CDX2 possesses a

similar function in transformed hematopoietic cells, as a knock down of *CDX2* in the ALL cell line Nalm-6 strongly reduced the clonogenic capacity of the cells in CFC assay, an *in vitro* surrogate for self-renewal. This finding confirmed the results of Scholl *et al*. (2007), who observed the same effect in AML cell lines and demonstrated the dependency of the leukemic clone on the expression of CDX2. As CDX2 is not expressed in normal adult hematopoietic cells, the absence of (sufficient) regulatory mechanisms controlling CDX2 induced gene transcription may contribute to its high leukemogenicity.

The high self-renewing capacity, in addition to a block of differentiation conferred by CDX2, explains the pronounced growth advantage of CDX2-transduced BM progenitors *in vivo*, as well as the high leukemogenicity of the gene in the murine BM transplantation model (Rawat *et al*. 2004). Despite the results of these *in vivo* studies in the mouse, it is not yet clear to what extent CDX2 is involved in induction and/or maintenance of human AML and ALL. An analysis of *CDX2* expression in different leukemic subpopulations would help to solve this question, as a functional involvement of CDX2 in leukemogenesis suggests expression in the $CD34^{+}/CD38^{-}$, LSC enriched compartment. A subsequent knock down of CDX2 in this compartment with analysis of the CDX2-deficient LSCs *in vivo* finally would prove the dependency of the leukemic clone on CDX2 function. If aberrant CDX2 expression is causally involved in the induction of leukemia, the leukemia subtype may also result from a different cell type targeted by CDX2 induced leukemogenesis. The kind of disease hereby would depend on whether aberrant *CDX2* expression first occurs in a myeloid or a lymphoid progenitor. To investigate this possibility, different murine hematopoietic subpopulations could be transduced with CDX2. By this approach, it would be possible to investigate if CDX2 is able to transform lymphoid progenitors in the same manner as already shown in this study where transduction of bulk BM under myeloid conditions resulted in transformation of the myeloid lineage.

Interestingly, aberrant *CDX2* expression seems to be associated with an acute stage of leukemia. Whereas more than 80% of ALL patients (Riedt *et al.*, 2009; Thoene *et al.*, 2009) and up to 90% of AML patients (Scholl *et al.*, 2007, Rawat *et al.*, 2008) were positive for the *CDX2* transcript, only a small number of patients with CML or MDS showed expression of *CDX2*. Of the 10 CML patients

tested for expression of *CDX2* by Scholl *et al*. (2007) only two patients, which were in accelerated stage or already in blast crisis, showed expression of the transcript, and one out of the two $CDX2^+$ MDS patients progressed to AML within one month after the analysis. As acute leukemias, in contrast to chronic leukemias, are associated with a block of differentiation (Rabbitts, 1991; Sell, 2005), aberrant expression of CDX2, leading to this block, therefore might be one key event associated with the induction of acute leukemias.

7. SUMMARY

In this study, it was demonstrated for the first time that aberrant expression of *CDX2* is a frequent and functionally relevant event in human ALL. In ALL, high expression of *CDX2* correlates to an inferior overall survival. It was demonstrated that *CDX2* is frequently deregulated in human AML, where its expression positively correlates with the high *HOX* expression found particularly in AML patients of normal karyotype. As CDX2 was able to deregulate *Hox* gene expression in adult murine hematopoiesis, aberrant expression of CDX2 may present an explanation for the still unknown cause of *HOX* gene deregulation in the subset of human AML of normal karyotype.

Like CDX2, aberrant expression of CDX4 induced AML in the murine BM transplantation model. While *Hox* gene deregulation contributed to the leukemogenic potential of both CDX members, CDX2 was also able to disturb additional pathways involved in self-renewal and proliferation. Particularly WNT signaling was upregulated in CDX2-overexpressing BM cells. Aberrant expression of CDX2 was able to transform murine hematopoietic cells and was essential for the enhanced proliferative and self-renewal potential of human leukemic cell lines. CDX2 therefore may be an important factor in human leukemogenesis and serve as an interesting target for the development of new agents in the therapy of acute leukemias.

The results of this study moreover indicate that CDX4 possesses a relatively low leukemogenic potential *in vivo* although it is able to confer higher proliferative and clonogenic potential compared to CDX2 *in vitro*. Overexpression of CDX4 in the murine BM transplantation model led to induction of acute erythroid leukemia. Together with its ability to expand erythroid cells *in vitro*, these results suggest that CDX4 plays a role in specification of the erythroid lineage in adult hematopoiesis and propose CDX4 to be a novel factor in the development of erythroid leukemia. Thus, the CDX4 mouse model might serve as a model system to better understand the biology of this disease with especially poor outcome.

8. ZUSAMMENFASSUNG

In dieser Arbeit konnte erstmalig gezeigt werden, dass die aberrante Expression von *CDX2* ein häufiges und funktionell relevantes Ereignis in der humanen ALL darstellt und mit einem ungünstigen Krankheitsverlauf korreliert. Auch in der Mehrheit der Patienten mit AML konnte eine Überexpression von *CDX2* nachgewiesen werden. Ein hohes Transkriptlevel von *CDX2* korrelierte in der AML mit einer erhöhten *HOX* Expression, welche insbesondere AML-Patienten mit normalem Karyotyp kennzeichnet. Es konnte gezeigt werden, dass CDX2 in der adulten murinen Hämatopoese in der Lage ist *Hox*-Gene zu deregulieren. Die aberrante Expression von CDX2 könnte damit auch in der AML mit normalem Karyotyp eine der bisher unbekannten Ursachen für die *HOX*-Überexpression dieser Subgruppe darstellen.

Ähnlich zu CDX2 induzierte auch die aberrante Expression von CDX4 AML im murinen Knochenmark-Transplantationsmodell. Die Überexpression beider *Cdx*-Gene führte zu einer verstärkten *Hox*-Expression. Zusätzlich führte CDX2 zu einer Deregulation weiterer, an Selbsterneuerung und Proliferation beteiligter Signaltransduktionswege, wie unter anderem der Aktivierung des WNT-Signalwegs. Es konnte nachgewiesen werden, dass eine aberrante Expression zu einer leukämischen Transformation muriner hämatopoetischer Zellen führt. Auch in humanen leukämischen Zelllinien ist die aberrante Expression von CDX2 für Klonogenität und Proliferation von entscheidender Bedeutung. Möglicherweise trägt CDX2 dadurch auch zur humanen Leukämogenese bei und könnte somit als potentielles Target für die Entwicklung neuartiger Krebstherapien dienen.

Die Ergebnisse dieser Arbeit zeigen weiterhin, dass eine aberrante Expression von CDX4 *in vivo* eine relativ geringe leukämogene Wirkung besitzt, obwohl CDX4 *in vitro* im Vergleich zu CDX2 ein deutlich höheres Proliferations- und Selbsterneuerungspotential verleiht. Im Mausmodell führte die Überexpression von CDX4 zu der Induktion einer akuten erythroiden Leukämie sowie *in vitro* zu einer Expansion von Zellen der erythroiden Linie. Dies deutet auf eine Rolle von CDX4 in der adulten Erythropoese hin, sowie auf eine Beteiligung von CDX4 in der Entwicklung der erythroiden Leukämie. Das CDX4-Mausmodell der erythroiden Leukämie könnte daher zum Verständnis dieses AML-Subtyps beitragen, der durch eine besonders schlechte Prognose gekennzeichnet ist.

9. REFERENCES

ADOLFSSON, J., R. MANSSON, et al. (2005). "Identification of Flt3+ lympho-myeloid stem cells lacking erythro-megakaryocytic potential a revised road map for adult blood lineage commitment." Cell **121**(2): 295-306.

AFRIKANOVA, I., E. YEH, et al. (2002). "Oncogene cooperativity in Friend erythroleukemia: erythropoietin receptor activation by the env gene of SFFV leads to transcriptional upregulation of PU.1, independent of SFFV proviral insertion." Oncogene **21**(8): 1272-1284.

AKALA, O. O. and M. F. CLARKE (2006). "Hematopoietic stem cell self-renewal." Curr Opin Genet Dev **16**(5): 496-501.

AL-HAJJ, M., M. S. WICHA, et al. (2003). "Prospective identification of tumorigenic breast cancer cells." Proc Natl Acad Sci U S A **100**(7): 3983-3988.

ALCALAY, M., E. TIACCI, et al. (2005). "Acute myeloid leukemia bearing cytoplasmic nucleophosmin (NPMc+ AML) shows a distinct gene expression profile characterized by up-regulation of genes involved in stem-cell maintenance." Blood **106**(3): 899-902.

ALMEIDA, R., E. SILVA, et al. (2003). "Expression of intestine-specific transcription factors, CDX1 and CDX2, in intestinal metaplasia and gastric carcinomas." J Pathol **199**(1): 36-40.

AMARAVADI, L. and M. J. KLEMSZ (1999). "DNA methylation and chromatin structure regulate PU.1 expression." DNA Cell Biol **18**(12): 875-884.

ARMSTRONG, S. A. and A. T. LOOK (2005). "Molecular genetics of acute lymphoblastic leukemia." J Clin Oncol **23**(26): 6306-6315.

ARMSTRONG, S. A., J. E. STAUNTON, et al. (2002). "MLL translocations specify a distinct gene expression profile that distinguishes a unique leukemia." Nat Genet **30**(1): 41-47.

ASADA, S., H. DAITOKU, et al. (2007). "Mitogen-activated protein kinases, Erk and p38, phosphorylate and regulate Foxo1." Cell Signal **19**(3): 519-527.

BACH, C., S. BUHL, et al. (2010). "Leukemogenic transformation by HOXA cluster genes." Blood **115**(14): 2910-2918.

BANSAL, D., C. SCHOLL, et al. (2006). "Cdx4 dysregulates Hox gene expression and generates acute myeloid leukemia alone and in cooperation with Meis1a in a murine model." Proc Natl Acad Sci U S A **103**(45): 16924-16929.

BARTHOLOMEW, C. and J. N. IHLE (1991). "Retroviral insertions 90 kilobases proximal to the Evi-1 myeloid transforming gene activate transcription from the normal promoter." Mol Cell Biol **11**(4): 1820-1828.

BEN-PORATH, I., M. W. THOMSON, et al. (2008). "An embryonic stem cell-like gene expression signature in poorly differentiated aggressive human tumors." Nat Genet **40**(5): 499-507.

BENNETT, J. M., D. CATOVSKY, et al. (1985). "Proposed revised criteria for the classification of acute myeloid leukemia. A report of the French-American-British Cooperative Group." Ann Intern Med **103**(4): 620-625.

BERMAN, J. N., J. P. KANKI, et al. (2005). "Zebrafish as a model for myelopoiesis during embryogenesis." Exp Hematol **33**(9): 997-1006.

BHATIA, M., J. C. WANG, et al. (1997). "Purification of primitive human hematopoietic cells capable of repopulating immune-deficient mice." Proc Natl Acad Sci U S A **94**(10): 5320-5325.

BILLETER, M., Y. Q. QIAN, et al. (1993). "Determination of the nuclear magnetic resonance solution structure of an Antennapedia homeodomain-DNA complex." J Mol Biol **234**(4): 1084-1093.

BONHOMME, C., A. CALON, et al. (2008). "Cdx1, a dispensable homeobox gene for gut development with limited effect in intestinal cancer." Oncogene **27**(32): 4497-4502.

BONNET, D. and J. E. DICK (1997). "Human acute myeloid leukemia is organized as a hierarchy that originates from a primitive hematopoietic cell." Nat Med **3**(7): 730-737.

BORROW, J., A. M. SHEARMAN, et al. (1996). "The t(7;11)(p15;p15) translocation in acute myeloid leukaemia fuses the genes for nucleoporin NUP98 and class I homeoprotein HOXA9." Nat Genet **12**(2): 159-167.

BROOKE, N. M., J. GARCIA-FERNANDEZ, et al. (1998). "The ParaHox gene cluster is an evolutionary sister of the Hox gene cluster." Nature **392**(6679): 920-922.

BROWN, D., S. KOGAN, et al. (1997). "A PMLRARalpha transgene initiates murine acute promyelocytic leukemia." Proc Natl Acad Sci U S A **94**(6): 2551-2556.

BRUHN, L., A. MUNNERLYN, et al. (1997). "ALY, a context-dependent coactivator of LEF-1 and AML-1, is required for TCRalpha enhancer function." Genes Dev **11**(5): 640-653.

BRUN, A. C., J. M. BJORNSSON, et al. (2004). "Hoxb4-deficient mice undergo normal hematopoietic development but exhibit a mild proliferation defect in hematopoietic stem cells." Blood **103**(11): 4126-4133.

BUSKE, C., M. FEURING-BUSKE, et al. (2001). "Overexpression of HOXA10 perturbs human lymphomyelopoiesis in vitro and in vivo." Blood **97**(8): 2286-2292.

CHARITE, J., W. DE GRAAFF, et al. (1998). "Transducing positional information to the Hox genes: critical interaction of cdx gene products with position-sensitive regulatory elements." Development **125**(22): 4349-4358.

CHASE, A., A. REITER, et al. (1999). "Fusion of ETV6 to the caudal-related homeobox gene CDX2 in acute myeloid leukemia with the t(12;13)(p13;q12)." Blood **93**(3): 1025-1031.

CHAWENGSAKSOPHAK, K., W. DE GRAAFF, et al. (2004). "Cdx2 is essential for axial elongation in mouse development." Proc Natl Acad Sci U S A **101**(20): 7641-7645.

CHAWENGSAKSOPHAK, K., R. JAMES, et al. (1997). "Homeosis and intestinal tumours in Cdx2 mutant mice." Nature **386**(6620): 84-87.

CHEN, A. T. and L. I. ZON (2009). "Zebrafish blood stem cells." J Cell Biochem **108**(1): 35-42.

CHOI, K., M. KENNEDY, et al. (1998). "A common precursor for hematopoietic and endothelial cells." Development **125**(4): 725-732.

CILLO, C., P. BARBA, et al. (1992). "HOX gene expression in normal and neoplastic human kidney." Int J Cancer **51**(6): 892-897.

COBALEDA, C., W. JOCHUM, et al. (2007). "Conversion of mature B cells into T cells by dedifferentiation to uncommitted progenitors." Nature **449**(7161): 473-477.

COBAS, M., A. WILSON, et al. (2004). "Beta-catenin is dispensable for hematopoiesis and lymphopoiesis." J Exp Med **199**(2): 221-229.

COZZIO, A., E. PASSEGUE, et al. (2003). "Similar MLL-associated leukemias arising from self-renewing stem cells and short-lived myeloid progenitors." Genes Dev **17**(24): 3029-3035.

DA ROCHA, S. T., M. TEVENDALE, et al. (2007). "Restricted co-expression of Dlk1 and the reciprocally imprinted non-coding RNA, Gtl2: implications for cis-acting control." Dev Biol **306**(2): 810-823.

DAHL, R., S. R. IYER, et al. (2007). "The transcriptional repressor GFI-1 antagonizes PU.1 activity through protein-protein interaction." J Biol Chem **282**(9): 6473-6483.

DAHL, R., J. C. WALSH, et al. (2003). "Regulation of macrophage and neutrophil cell fates by the PU.1:C/EBPalpha ratio and granulocyte colony-stimulating factor." Nat Immunol **4**(10): 1029-1036.

DASH, A. and D. G. GILLILAND (2001). "Molecular genetics of acute myeloid leukaemia." Best Pract Res Clin Haematol **14**(1): 49-64.

DAVIDSON, A. J., P. ERNST, et al. (2003). "cdx4 mutants fail to specify blood progenitors and can be rescued by multiple hox genes." Nature **425**(6955): 300-306.

DAVIDSON, A. J. and L. I. ZON (2006). "The caudal-related homeobox genes cdx1a and cdx4 act redundantly to regulate hox gene expression and the formation of putative hematopoietic stem cells during zebrafish embryogenesis." Dev Biol **292**(2): 506-518.

DE JONG, J. L. and L. I. ZON (2005). "Use of the zebrafish system to study primitive and definitive hematopoiesis." Annu Rev Genet **39**: 481-501.

DE VITA, G., P. BARBA, et al. (1993). "Expression of homeobox-containing genes in primary and metastatic colorectal cancer." Eur J Cancer **29A**(6): 887-893.

DEBERNARDI, R., K. PIERRE, et al. (2003). "Cell-specific expression pattern of monocarboxylate transporters in astrocytes and neurons observed in different mouse brain cortical cell cultures." J Neurosci Res **73**(2): 141-155.

DEKOTER, R. P. and H. SINGH (2000). "Regulation of B lymphocyte and macrophage development by graded expression of PU.1." Science **288**(5470): 1439-1441.

DESHPANDE, A. J., M. CUSAN, et al. (2006). "Acute myeloid leukemia is propagated by a leukemic stem cell with lymphoid characteristics in a mouse model of CALM/AF10-positive leukemia." Cancer Cell **10**(5): 363-374.

DIAS, S., W. XU, et al. (2008). "Transcriptional regulation of lymphocyte development." Curr Opin Genet Dev **18**(5): 441-448.

DUBOULE, D. (1994). "Temporal colinearity and the phylotypic progression: a basis for the stability of a vertebrate Bauplan and the evolution of morphologies through heterochrony." Dev Suppl: 135-142.

DUBOULE, D. and P. DOLLE (1989). "The structural and functional organization of the murine HOX gene family resembles that of Drosophila homeotic genes." EMBO J **8**(5): 1497-1505.

DUNCAN, A. W., F. M. RATTIS, et al. (2005). "Integration of Notch and Wnt signaling in hematopoietic stem cell maintenance." Nat Immunol **6**(3): 314-322.

DUPREY, P., K. CHOWDHURY, et al. (1988). "A mouse gene homologous to the Drosophila gene caudal is expressed in epithelial cells from the embryonic intestine." Genes Dev **2**(12A): 1647-1654.

DURAND, C., C. ROBIN, et al. (2007). "Embryonic stromal clones reveal developmental regulators of definitive hematopoietic stem cells." Proc Natl Acad Sci U S A **104**(52): 20838-20843.

DZIERZAK, E. and N. A. SPECK (2008). "Of lineage and legacy: the development of mammalian hematopoietic stem cells." Nat Immunol **9**(2): 129-136.

EDA, A., H. OSAWA, et al. (2003). "Aberrant expression of CDX2 in Barrett's epithelium and inflammatory esophageal mucosa." J Gastroenterol **38**(1): 14-22.

ERNST, P., M. MABON, et al. (2004). "An Mll-dependent Hox program drives hematopoietic progenitor expansion." Curr Biol **14**(22): 2063-2069.

FAAS, L. and H. V. ISAACS (2009). "Overlapping functions of Cdx1, Cdx2, and Cdx4 in the development of the amphibian Xenopus tropicalis." Dev Dyn **238**(4): 835-852.

FADERL, S., S. JEHA, et al. (2003). "The biology and therapy of adult acute lymphoblastic leukemia." Cancer **98**(7): 1337-1354.

FALINI, B., I. NICOLETTI, et al. (2007). "Acute myeloid leukemia carrying cytoplasmic/mutated nucleophosmin (NPMc+ AML): biologic and clinical features." Blood **109**(3): 874-885.

FALOON, P., E. ARENTSON, et al. (2000). "Basic fibroblast growth factor positively regulates hematopoietic development." Development **127**(9): 1931-1941.

FAVIER, B. and P. DOLLE (1997). "Developmental functions of mammalian Hox genes." Mol Hum Reprod **3**(2): 115-131.

FERRANDO, A. A., S. A. ARMSTRONG, et al. (2003). "Gene expression signatures in MLL-rearranged T-lineage and B-precursor acute leukemias: dominance of HOX dysregulation." Blood **102**(1): 262-268.

FISCHBACH, N. A., S. ROZENFELD, et al. (2005). "HOXB6 overexpression in murine bone marrow immortalizes a myelomonocytic precursor in vitro and causes hematopoietic stem cell expansion and acute myeloid leukemia in vivo." Blood **105**(4): 1456-1466.

FLORIDON, C., C. H. JENSEN, et al. (2000). "Does fetal antigen 1 (FA1) identify cells with regenerative, endocrine and neuroendocrine potentials? A study of FA1 in embryonic, fetal, and placental tissue and in maternal circulation." Differentiation **66**(1): 49-59.

FORSGREN, M., A. ATTERSAND, et al. (2004). "Isolation and functional expression of human COQ2, a gene encoding a polyprenyl transferase involved in the synthesis of CoQ." Biochem J **382**(Pt 2): 519-526.

FRIEDMAN, A. D. (2007). "C/EBPalpha induces PU.1 and interacts with AP-1 and NF-kappaB to regulate myeloid development." Blood Cells Mol Dis **39**(3): 340-343.

FUJIWARA, Y., C. P. BROWNE, et al. (1996). "Arrested development of embryonic red cell precursors in mouse embryos lacking transcription factor GATA-1." Proc Natl Acad Sci U S A **93**(22): 12355-12358.

FULLER, J. F., J. MCADARA, et al. (1999). "Characterization of HOX gene expression during myelopoiesis: role of HOX A5 in lineage commitment and maturation." Blood **93**(10): 3391-3400.

GALLOWAY, J. L., R. A. WINGERT, et al. (2005). "Loss of gata1 but not gata2 converts erythropoiesis to myelopoiesis in zebrafish embryos." Dev Cell **8**(1): 109-116.

GAMER, L. W. and C. V. WRIGHT (1993). "Murine Cdx-4 bears striking similarities to the Drosophila caudal gene in its homeodomain sequence and early expression pattern." Mech Dev **43**(1): 71-81.

GAUNT, S. J. (1988). "Mouse homeobox gene transcripts occupy different but overlapping domains in embryonic germ layers and organs: a comparison of Hox-3.1 and Hox-1.5." Development **103**(1): 135-144.

GAUNT, S. J., A. COCKLEY, et al. (2004). "Additional enhancer copies, with intact cdx binding sites, anteriorize Hoxa-7/lacZ expression in mouse embryos: evidence in keeping with an instructional cdx gradient." Int J Dev Biol **48**(7): 613-622.

GEKAS, C., F. DIETERLEN-LIEVRE, et al. (2005). "The placenta is a niche for hematopoietic stem cells." Dev Cell **8**(3): 365-375.

GIAMPAOLO, A., N. FELLI, et al. (2002). "Expression pattern of HOXB6 homeobox gene in myelomonocytic differentiation and acute myeloid leukemia." Leukemia **16**(7): 1293-1301.

GIAMPAOLO, A., P. STERPETTI, et al. (1994). "Key functional role and lineage-specific expression of selected HOXB genes in purified hematopoietic progenitor differentiation." Blood **84**(11): 3637-3647.

GILLILAND, D. G., C. T. JORDAN, et al. (2004). "The molecular basis of leukemia." Hematology Am Soc Hematol Educ Program: 80-97.

GILLILAND, D. G. and M. S. TALLMAN (2002). "Focus on acute leukemias." Cancer Cell **1**(5): 417-420.

GLEISSNER, B., N. GOEKBUGET, et al. (2005). "CD10- pre-B acute lymphoblastic leukemia (ALL) is a distinct high-risk subgroup of adult ALL associated with a high frequency of MLL aberrations: results of the German Multicenter Trials for Adult ALL (GMALL)." Blood **106**(13): 4054-4056.

GRAHAM, A., N. PAPALOPULU, et al. (1989). "The murine and Drosophila homeobox gene complexes have common features of organization and expression." Cell **57**(3): 367-378.

GREAVES, M. F., C. SIEFF, et al. (1983). "Monoclonal antiglycophorin as a probe for erythroleukemias." Blood **61**(4): 645-651.

GRISOLANO, J. L., R. L. WESSELSCHMIDT, et al. (1997). "Altered myeloid development and acute leukemia in transgenic mice expressing PML-RAR alpha under control of cathepsin G regulatory sequences." Blood **89**(2): 376-387.

HAKAK, Y., K. LEHMANN-BRUINSMA, et al. (2009). "The role of the GPR91 ligand succinate in hematopoiesis." J Leukoc Biol **85**(5): 837-843.

HAMMERSCHMIDT, M., F. PELEGRI, et al. (1996). "Mutations affecting morphogenesis during gastrulation and tail formation in the zebrafish, Danio rerio." Development **123**: 143-151.

HINOI, T., M. LODA, et al. (2003). "Silencing of CDX2 expression in colon cancer via a dominant repression pathway." J Biol Chem **278**(45): 44608-44616.

HOCK, H., E. MEADE, et al. (2004). "Tel/Etv6 is an essential and selective regulator of adult hematopoietic stem cell survival." Genes Dev **18**(19): 2336-2341.

HOLMES, M. L., S. CAROTTA, et al. (2006). "Repression of Flt3 by Pax5 is crucial for B-cell lineage commitment." Genes Dev **20**(8): 933-938.

HONMA, K., S. TSUZUKI, et al. (2009). "TNFAIP3/A20 functions as a novel tumor suppressor gene in several subtypes of non-Hodgkin lymphomas." Blood **114**(12): 2467-2475.

HUBER, T. L., V. KOUSKOFF, et al. (2004). "Haemangioblast commitment is initiated in the primitive streak of the mouse embryo." Nature **432**(7017): 625-630.

IWASAKI, H. and K. AKASHI (2007). "Hematopoietic developmental pathways: on cellular basis." Oncogene **26**(47): 6687-6696.

IWASAKI, H., S. MIZUNO, et al. (2003). "GATA-1 converts lymphoid and myelomonocytic progenitors into the megakaryocyte/erythrocyte lineages." Immunity **19**(3): 451-462.

IZRAELI, S. (2004). "Leukaemia -- a developmental perspective." Br J Haematol **126**(1): 3-10.

JAMES, R. and J. KAZENWADEL (1991). "Homeobox gene expression in the intestinal epithelium of adult mice." J Biol Chem **266**(5): 3246-3251.

JOHANSSON, B. M. and M. V. WILES (1995). "Evidence for involvement of activin A and bone morphogenetic protein 4 in mammalian mesoderm and hematopoietic development." Mol Cell Biol **15**(1): 141-151.

JOHNSON, G. R. and M. A. MOORE (1975). "Role of stem cell migration in initiation of mouse foetal liver haemopoiesis." Nature **258**(5537): 726-728.

KAPPEN, C. (2000). "Disruption of the homeobox gene Hoxb-6 in mice results in increased numbers of early erythrocyte progenitors." Am J Hematol **65**(2): 111-118.

KASYAN, A., L. J. MEDEIROS, et al. (2010). "Acute erythroid leukemia as defined in the World Health Organization classification is a rare and pathogenetically heterogeneous disease." Mod Pathol.

KEENAN, I. D., R. M. SHARRARD, et al. (2006). "FGF signal transduction and the regulation of Cdx gene expression." Dev Biol **299**(2): 478-488.

KESSEL, M. and P. GRUSS (1991). "Homeotic transformations of murine vertebrae and concomitant alteration of Hox codes induced by retinoic acid." Cell **67**(1): 89-104.

KHOURY, H., F. SUAREZ-SAIZ, et al. (2010). "An upstream insulator regulates DLK1 imprinting in AML." Blood.

KIM, K. A., J. H. KIM, et al. (2007). "Pref-1 (preadipocyte factor 1) activates the MEK/extracellular signal-regulated kinase pathway to inhibit adipocyte differentiation." Mol Cell Biol **27**(6): 2294-2308.

KINA, T., K. IKUTA, et al. (2000). "The monoclonal antibody TER-119 recognizes a molecule associated with glycophorin A and specifically marks the late stages of murine erythroid lineage." Br J Haematol **109**(2): 280-287.

KIRCHER, M., C. BOCK, et al. (2008). "Structural conservation versus functional divergence of maternally expressed microRNAs in the Dlk1/Gtl2 imprinting region." BMC Genomics **9**: 346.

KIRSTETTER, P., K. ANDERSON, et al. (2006). "Activation of the canonical Wnt pathway leads to loss of hematopoietic stem cell repopulation and multilineage differentiation block." Nat Immunol **7**(10): 1048-1056.

KIRSTETTER, P., M. B. SCHUSTER, et al. (2008). "Modeling of C/EBPalpha mutant acute myeloid leukemia reveals a common expression signature of committed myeloid leukemia-initiating cells." Cancer Cell **13**(4): 299-310.

KOBAYASHI, S., H. WAGATSUMA, et al. (2000). "Mouse Peg9/Dlk1 and human PEG9/DLK1 are paternally expressed imprinted genes closely located to the maternally expressed imprinted genes: mouse Meg3/Gtl2 and human MEG3." Genes Cells **5**(12): 1029-1037.

KOGAN, S. C., J. M. WARD, et al. (2002). "Bethesda proposals for classification of nonlymphoid hematopoietic neoplasms in mice." Blood **100**(1): 238-245.

KRIVTSOV, A. V., D. TWOMEY, et al. (2006). "Transformation from committed progenitor to leukaemia stem cell initiated by MLL-AF9." Nature **442**(7104): 818-822.

KROON, E., J. KROSL, et al. (1998). "Hoxa9 transforms primary bone marrow cells through specific collaboration with Meis1a but not Pbx1b." EMBO J **17**(13): 3714-3725.

KRUEGER, F., Z. MADEJA, et al. (2009). "Down-regulation of Cdx2 in colorectal carcinoma cells by the Raf-MEK-ERK 1/2 pathway." Cell Signal **21**(12): 1846-1856.

KUMARAVELU, P., L. HOOK, et al. (2002). "Quantitative developmental anatomy of definitive haematopoietic stem cells/long-term repopulating units (HSC/RUs): role of the aorta-gonad-mesonephros (AGM) region and the yolk sac in colonisation of the mouse embryonic liver." Development **129**(21): 4891-4899.

LAI, A. Y., S. M. LIN, et al. (2005). "Heterogeneity of Flt3-expressing multipotent progenitors in mouse bone marrow." J Immunol **175**(8): 5016-5023.

LAPIDOT, T., C. SIRARD, et al. (1994). "A cell initiating human acute myeloid leukaemia after transplantation into SCID mice." Nature **367**(6464): 645-648.

LAWRENCE, H. J., C. D. HELGASON, et al. (1997). "Mice bearing a targeted interruption of the homeobox gene HOXA9 have defects in myeloid, erythroid, and lymphoid hematopoiesis." Blood **89**(6): 1922-1930.

LAWSON, K. A., J. J. MENESES, et al. (1991). "Clonal analysis of epiblast fate during germ layer formation in the mouse embryo." Development **113**(3): 891-911.

LEE, J. T., JR. and J. A. MCCUBREY (2002). "The Raf/MEK/ERK signal transduction cascade as a target for chemotherapeutic intervention in leukemia." Leukemia **16**(4): 486-507.

LENGERKE, C., S. SCHMITT, et al. (2008). "BMP and Wnt specify hematopoietic fate by activation of the Cdx-Hox pathway." Cell Stem Cell **2**(1): 72-82.

LESSARD, J. and G. SAUVAGEAU (2003). "Bmi-1 determines the proliferative capacity of normal and leukaemic stem cells." Nature **423**(6937): 255-260.

LIAO, E. C., N. S. TREDE, et al. (2002). "Non-cell autonomous requirement for the bloodless gene in primitive hematopoiesis of zebrafish." Development **129**(3): 649-659.

LIU, T., D. R. BRANCH, et al. (2006). "Pbx1 is a co-factor for Cdx-2 in regulating proglucagon gene expression in pancreatic A cells." Mol Cell Endocrinol **249**(1-2): 140-149.

LIU, T., X. ZHANG, et al. (2007). "Regulation of Cdx2 expression by promoter methylation, and effects of Cdx2 transfection on morphology and gene expression of human esophageal epithelial cells." Carcinogenesis **28**(2): 488-496.

LOHNES, D. (2003). "The Cdx1 homeodomain protein: an integrator of posterior signaling in the mouse." Bioessays **25**(10): 971-980.

LU, C. W., A. YABUUCHI, et al. (2008). "Ras-MAPK signaling promotes trophectoderm formation from embryonic stem cells and mouse embryos." Nat Genet **40**(7): 921-926.

MACKAREHTSCHIAN, K., J. D. HARDIN, et al. (1995). "Targeted disruption of the flk2/flt3 gene leads to deficiencies in primitive hematopoietic progenitors." Immunity **3**(1): 147-161.

MAGLI, M. C., P. BARBA, et al. (1991). "Coordinate regulation of HOX genes in human hematopoietic cells." Proc Natl Acad Sci U S A **88**(14): 6348-6352.

MARCHESI, F., S. MINUCCI, et al. (2006). "Immunohistochemical detection of Ym1/Ym2 chitinase-like lectins associated with hyalinosis and polypoid adenomas of the transitional epithelium in a mouse with acute myeloid leukemia." Vet Pathol **43**(5): 773-776.

MARSHALL, C. J. and A. J. THRASHER (2001). "The embryonic origins of human haematopoiesis." Br J Haematol **112**(4): 838-850.

MCKINNEY-FREEMAN, S. L., C. LENGERKE, et al. (2008). "Modulation of murine embryonic stem cell-derived CD41+c-kit+ hematopoietic progenitors by ectopic expression of Cdx genes." Blood **111**(10): 4944-4953.

METCALF, D., A. P. NG, et al. (2009). "Murine hematopoietic blast colony-forming cells and their progeny have distinctive membrane marker profiles." Proc Natl Acad Sci U S A **106**(45): 19102-19107.

MILELLA, M., S. M. KORNBLAU, et al. (2001). "Therapeutic targeting of the MEK/MAPK signal transduction module in acute myeloid leukemia." J Clin Invest **108**(6): 851-859.

MILLER, B. G. and J. A. STAMATOYANNOPOULOS (2010). "Integrative meta-analysis of differential gene expression in acute myeloid leukemia." PLoS ONE **5**(3): e9466.

MOORE, K. A., B. PYTOWSKI, et al. (1997). "Hematopoietic activity of a stromal cell transmembrane protein containing epidermal growth factor-like repeat motifs." Proc Natl Acad Sci U S A **94**(8): 4011-4016.

MOREAU-GACHELIN, F. (2006). "Lessons from models of murine erythroleukemia to acute myeloid leukemia (AML): proof-of-principle of co-operativity in AML." Haematologica **91**(12): 1644-1652.

MORRISON, S. J., A. M. WANDYCZ, et al. (1997). "Identification of a lineage of multipotent hematopoietic progenitors." Development **124**(10): 1929-1939.

MORRISON, S. J. and I. L. WEISSMAN (1994). "The long-term repopulating subset of hematopoietic stem cells is deterministic and isolatable by phenotype." Immunity **1**(8): 661-673.

MULLIGHAN, C. G., S. GOORHA, et al. (2007). "Genome-wide analysis of genetic alterations in acute lymphoblastic leukaemia." Nature **446**(7137): 758-764.

MUROHASHI, M., T. NAKAMURA, et al. (2009). "An FGF4-FRS2alpha-Cdx2 Axis in Trophoblast Stem Cells Induces BMP4 to Regulate Proper Growth of Early Mouse Embryos." Stem Cells.

MUROHASHI, M., T. NAKAMURA, et al. (2010). "An FGF4-FRS2alpha-Cdx2 axis in trophoblast stem cells induces Bmp4 to regulate proper growth of early mouse embryos." Stem Cells **28**(1): 113-121.

MUTOH, H., H. HAYAKAWA, et al. (2009). "Transgenic Cdx2 induces endogenous Cdx1 in intestinal metaplasia of Cdx2-transgenic mouse stomach." FEBS J **276**(20): 5821-5831.

NISHIYAMA, A., L. XIN, et al. (2009). "Uncovering early response of gene regulatory networks in ESCs by systematic induction of transcription factors." Cell Stem Cell **5**(4): 420-433.

NIWA, H., Y. TOYOOKA, et al. (2005). "Interaction between Oct3/4 and Cdx2 determines trophectoderm differentiation." Cell **123**(5): 917-929.

NUCIFORA, G., R. A. LARSON, et al. (1993). "Persistence of the 8;21 translocation in patients with acute myeloid leukemia type M2 in long-term remission." Blood **82**(3): 712-715.

NUTT, S. L., P. URBANEK, et al. (1997). "Essential functions of Pax5 (BSAP) in pro-B cell development: difference between fetal and adult B lymphopoiesis and reduced V-to-DJ recombination at the IgH locus." Genes Dev **11**(4): 476-491.

ORKIN, S. H. and L. I. ZON (2002). "Hematopoiesis and stem cells: plasticity versus developmental heterogeneity." Nat Immunol **3**(4): 323-328.

ORKIN, S. H. and L. I. ZON (2008). "Hematopoiesis: an evolving paradigm for stem cell biology." Cell **132**(4): 631-644.

OTTERSBACH, K. and E. DZIERZAK (2005). "The murine placenta contains hematopoietic stem cells within the vascular labyrinth region." Dev Cell **8**(3): 377-387.

OTTMANN, O. G. and B. WASSMANN (2005). "Treatment of Philadelphia chromosome-positive acute lymphoblastic leukemia." Hematology Am Soc Hematol Educ Program: 118-122.

OWENS, B. M. and R. G. HAWLEY (2002). "HOX and non-HOX homeobox genes in leukemic hematopoiesis." Stem Cells **20**(5): 364-379.

PALIS, J. and M. C. YODER (2001). "Yolk-sac hematopoiesis: the first blood cells of mouse and man." Exp Hematol **29**(8): 927-936.

PAPPENHEIM, A. (1917). "Prinzipen der neuren morphologischen haematozytologie nach zytogenetischer grundlage." Folia Haematol **21**: 91-101.

PARATHATH, S. R., L. A. MAINWARING, et al. (2008). "Insulin receptor substrate 1 is an effector of sonic hedgehog mitogenic signaling in cerebellar neural precursors." Development **135**(19): 3291-3300.

PARDANAUD, L. and F. DIETERLEN-LIEVRE (1999). "Manipulation of the angiopoietic/hemangiopoietic commitment in the avian embryo." Development **126**(4): 617-627.

PARK, I. K., D. QIAN, et al. (2003). "Bmi-1 is required for maintenance of adult self-renewing haematopoietic stem cells." Nature **423**(6937): 302-305.

PASSEGUE, E. (2006). "Cancer biology: a game of subversion." Nature **442**(7104): 754-755.

PASSEGUE, E., C. H. JAMIESON, et al. (2003). "Normal and leukemic hematopoiesis: are leukemias a stem cell disorder or a reacquisition of stem cell characteristics?" Proc Natl Acad Sci U S A **100 Suppl 1**: 11842-11849.

PEREIRA, B., C. OLIVEIRA, et al. (2009). "CDX2 promoter methylation is not associated with mRNA expression." Int J Cancer **125**(7): 1739-1742.

PERKINS, A., K. KONGSUWAN, et al. (1990). "Homeobox gene expression plus autocrine growth factor production elicits myeloid leukemia." Proc Natl Acad Sci U S A **87**(21): 8398-8402.

PERKINS, A. C. and S. CORY (1993). "Conditional immortalization of mouse myelomonocytic, megakaryocytic and mast cell progenitors by the Hox-2.4 homeobox gene." EMBO J **12**(10): 3835-3846.

PETROPOULOS, K., N. ARSENI, et al. (2008). "A novel role for Lef-1, a central transcription mediator of Wnt signaling, in leukemogenesis." J Exp Med **205**(3): 515-522.

PILON, N., K. OH, et al. (2006). "Cdx4 is a direct target of the canonical Wnt pathway." Dev Biol **289**(1): 55-63.

PINEAULT, N., C. BUSKE, et al. (2003). "Induction of acute myeloid leukemia in mice by the human leukemia-specific fusion gene NUP98-HOXD13 in concert with Meis1." Blood **101**(11): 4529-4538.

POWNALL, M. E., A. S. TUCKER, et al. (1996). "eFGF, Xcad3 and Hox genes form a molecular pathway that establishes the anteroposterior axis in Xenopus." Development **122**(12): 3881-3892.

PUI, C. H., L. L. ROBISON, et al. (2008). "Acute lymphoblastic leukaemia." Lancet **371**(9617): 1030-1043.

QUENTMEIER, H., W. G. DIRKS, et al. (2004). "Expression of HOX genes in acute leukemia cell lines with and without MLL translocations." Leuk Lymphoma **45**(3): 567-574.

RABBITTS, T. H. (1991). "Translocations, master genes, and differences between the origins of acute and chronic leukemias." Cell **67**(4): 641-644.

RAFF, T., N. GOKBUGET, et al. (2007). "Molecular relapse in adult standard-risk ALL patients detected by prospective MRD monitoring during and after maintenance treatment: data from the GMALL 06/99 and 07/03 trials." Blood **109**(3): 910-915.

RAU, R. and P. BROWN (2009). "Nucleophosmin (NPM1) mutations in adult and childhood acute myeloid leukaemia: towards definition of a new leukaemia entity." Hematol Oncol **27**(4): 171-181.

RAVANDI, F. and P. KEBRIAEI (2009). "Philadelphia chromosome-positive acute lymphoblastic leukemia." Hematol Oncol Clin North Am **23**(5): 1043-1063, vi.

RAWAT, V. P., M. CUSAN, et al. (2004). "Ectopic expression of the homeobox gene Cdx2 is the transforming event in a mouse model of t(12;13)(p13;q12) acute myeloid leukemia." Proc Natl Acad Sci U S A **101**(3): 817-822.

RAWAT, V. P., S. THOENE, et al. (2008). "Overexpression of CDX2 perturbs HOX gene expression in murine progenitors depending on its N-terminal domain and is closely correlated with deregulated HOX gene expression in human acute myeloid leukemia." Blood **111**(1): 309-319.

REKHTMAN, N., K. S. CHOE, et al. (2003). "PU.1 and pRB interact and cooperate to repress GATA-1 and block erythroid differentiation." Mol Cell Biol **23**(21): 7460-7474.

REKHTMAN, N., F. RADPARVAR, et al. (1999). "Direct interaction of hematopoietic transcription factors PU.1 and GATA-1: functional antagonism in erythroid cells." Genes Dev **13**(11): 1398-1411.

RESCHAD, H. and V. SCHILLING-TORGAU (1913). "Ueber eine nue leukämie durch echte uebergangsformen und ihre bedeutung fur dies selbständigkeit dieser zellen." Munch Med Wochenschr **60**: 1981-1984.

REYA, T. and H. CLEVERS (2005). "Wnt signalling in stem cells and cancer." Nature **434**(7035): 843-850.

REYA, T., A. W. DUNCAN, et al. (2003). "A role for Wnt signalling in self-renewal of haematopoietic stem cells." Nature **423**(6938): 409-414.

REYA, T., S. J. MORRISON, et al. (2001). "Stem cells, cancer, and cancer stem cells." Nature **414**(6859): 105-111.

REYA, T., M. O'RIORDAN, et al. (2000). "Wnt signaling regulates B lymphocyte proliferation through a LEF-1 dependent mechanism." Immunity **13**(1): 15-24.

REYNIER, P., P. AMATI-BONNEAU, et al. (2004). "OPA3 gene mutations responsible for autosomal dominant optic atrophy and cataract." J Med Genet **41**(9): e110.

RIEDT, T., M. EBINGER, et al. (2009). "Aberrant expression of the homeobox gene CDX2 in pediatric acute lymphoblastic leukemia." Blood **113**(17): 4049-4051.

RILEY, J., R. BUTLER, et al. (1990). "A novel, rapid method for the isolation of terminal sequences from yeast artificial chromosome (YAC) clones." Nucleic Acids Res **18**(10): 2887-2890.

RISSOAN, M. C., T. DUHEN, et al. (2002). "Subtractive hybridization reveals the expression of immunoglobulin-like transcript 7, Eph-B1, granzyme B, and 3 novel transcripts in human plasmacytoid dendritic cells." Blood **100**(9): 3295-3303.

ROCHE, J., C. ZENG, et al. (2004). "Hox expression in AML identifies a distinct subset of patients with intermediate cytogenetics." Leukemia **18**(6): 1059-1063.

ROGNE, M., A. J. STOKKA, et al. (2009). "Mutually exclusive binding of PP1 and RNA to AKAP149 affects the mitochondrial network." Hum Mol Genet **18**(5): 978-987.

RUCKER, F. G., L. BULLINGER, et al. (2006). "Disclosure of candidate genes in acute myeloid leukemia with complex karyotypes using microarray-based molecular characterization." J Clin Oncol **24**(24): 3887-3894.

RUSCETTI, S. K. (1999). "Deregulation of erythropoiesis by the Friend spleen focus-forming virus." Int J Biochem Cell Biol **31**(10): 1089-1109.

SAKAJIRI, S., J. O'KELLY, et al. (2005). "Dlk1 in normal and abnormal hematopoiesis." Leukemia **19**(8): 1404-1410.

SAUVAGEAU, G., P. M. LANSDORP, et al. (1994). "Differential expression of homeobox genes in functionally distinct CD34+ subpopulations of human bone marrow cells." Proc Natl Acad Sci U S A **91**(25): 12223-12227.

SAUVAGEAU, G., U. THORSTEINSDOTTIR, et al. (1995). "Overexpression of HOXB4 in hematopoietic cells causes the selective expansion of more primitive populations in vitro and in vivo." Genes Dev **9**(14): 1753-1765.

SAVORY, J. G., N. BOUCHARD, et al. (2009). "Cdx2 regulation of posterior development through non-Hox targets." Development.

SAVORY, J. G., N. PILON, et al. (2009). "Cdx1 and Cdx2 are functionally equivalent in vertebral patterning." Dev Biol **330**(1): 114-122.

SCHELLER, M., J. HUELSKEN, et al. (2006). "Hematopoietic stem cell and multilineage defects generated by constitutive beta-catenin activation." Nat Immunol **7**(10): 1037-1047.

SCHOLL, C., D. BANSAL, et al. (2007). "The homeobox gene CDX2 is aberrantly expressed in most cases of acute myeloid leukemia and promotes leukemogenesis." J Clin Invest **117**(4): 1037-1048.

SELL, S. (2005). "Leukemia: stem cells, maturation arrest, and differentiation therapy." Stem Cell Rev **1**(3): 197-205.

SHEN, W. F., K. DETMER, et al. (1992). "Modulation of homeobox gene expression alters the phenotype of human hematopoietic cell lines." EMBO J **11**(3): 983-989.

SHI, W., A. KUMANOGOH, et al. (2000). "The class IV semaphorin CD100 plays nonredundant roles in the immune system: defective B and T cell activation in CD100-deficient mice." Immunity **13**(5): 633-642.

SHIMIZU, R., J. D. ENGEL, et al. (2008). "GATA1-related leukaemias." Nat Rev Cancer **8**(4): 279-287.

SHIMIZU, T., Y. K. BAE, et al. (2006). "Cdx-Hox code controls competence for responding to Fgfs and retinoic acid in zebrafish neural tissue." Development **133**(23): 4709-4719.

SHIMIZU, T., Y. K. BAE, et al. (2005). "Interaction of Wnt and caudal-related genes in zebrafish posterior body formation." Dev Biol **279**(1): 125-141.

SILBERG, D. G., J. SULLIVAN, et al. (2002). "Cdx2 ectopic expression induces gastric intestinal metaplasia in transgenic mice." Gastroenterology **122**(3): 689-696.

SINGH, S. K., I. D. CLARKE, et al. (2003). "Identification of a cancer stem cell in human brain tumors." Cancer Res **63**(18): 5821-5828.

SOCOLOVSKY, M., H. NAM, et al. (2001). "Ineffective erythropoiesis in Stat5a(-/-)5b(-/-) mice due to decreased survival of early erythroblasts." Blood **98**(12): 3261-3273.

SOULIER, J., E. CLAPPIER, et al. (2005). "HOXA genes are included in genetic and biologic networks defining human acute T-cell leukemia (T-ALL)." Blood **106**(1): 274-286.

SPELEMAN, F., B. CAUWELIER, et al. (2005). "A new recurrent inversion, inv(7)(p15q34), leads to transcriptional activation of HOXA10 and HOXA11 in a subset of T-cell acute lymphoblastic leukemias." Leukemia **19**(3): 358-366.

STARCK, J., N. COHET, et al. (2003). "Functional cross-antagonism between transcription factors FLI-1 and EKLF." Mol Cell Biol **23**(4): 1390-1402.

STEELMAN, L. S., S. L. ABRAMS, et al. (2008). "Contributions of the Raf/MEK/ERK, PI3K/PTEN/Akt/mTOR and Jak/STAT pathways to leukemia." Leukemia **22**(4): 686-707.

SUBRAMANIAN, V., B. I. MEYER, et al. (1995). "Disruption of the murine homeobox gene Cdx1 affects axial skeletal identities by altering the mesodermal expression domains of Hox genes." Cell **83**(4): 641-653.

TABARIES, S., J. LAPOINTE, et al. (2005). "Cdx protein interaction with Hoxa5 regulatory sequences contributes to Hoxa5 regional expression along the axial skeleton." Mol Cell Biol **25**(4): 1389-1401.

TAM, P. P. and R. S. BEDDINGTON (1987). "The formation of mesodermal tissues in the mouse embryo during gastrulation and early organogenesis." Development **99**(1): 109-126.

TAMAI, Y., R. NAKAJIMA, et al. (1999). "Colonic hamartoma development by anomalous duplication in Cdx2 knockout mice." Cancer Res **59**(12): 2965-2970.

TAYLOR, J. K., T. LEVY, et al. (1997). "Activation of enhancer elements by the homeobox gene Cdx2 is cell line specific." Nucleic Acids Res **25**(12): 2293-2300.

TEITELL, M. A. and P. P. PANDOLFI (2009). "Molecular genetics of acute lymphoblastic leukemia." Annu Rev Pathol **4**: 175-198.

THOENE, S., V. P. RAWAT, et al. (2009). "The homeobox gene CDX2 is aberrantly expressed and associated with an inferior prognosis in patients with acute lymphoblastic leukemia." Leukemia.

THORSTEINSDOTTIR, U., E. KROON, et al. (2001). "Defining roles for HOX and MEIS1 genes in induction of acute myeloid leukemia." Mol Cell Biol **21**(1): 224-234.

THORSTEINSDOTTIR, U., A. MAMO, et al. (2002). "Overexpression of the myeloid leukemia-associated Hoxa9 gene in bone marrow cells induces stem cell expansion." Blood **99**(1): 121-129.

THORSTEINSDOTTIR, U., G. SAUVAGEAU, et al. (1997). "Overexpression of HOXA10 in murine hematopoietic cells perturbs both myeloid and lymphoid differentiation and leads to acute myeloid leukemia." Mol Cell Biol **17**(1): 495-505.

URBANEK, P., Z. Q. WANG, et al. (1994). "Complete block of early B cell differentiation and altered patterning of the posterior midbrain in mice lacking Pax5/BSAP." Cell **79**(5): 901-912.

VAN DEN AKKER, E., S. FORLANI, et al. (2002). "Cdx1 and Cdx2 have overlapping functions in anteroposterior patterning and posterior axis elongation." Development **129**(9): 2181-2193.

VERAKSA, A., M. DEL CAMPO, et al. (2000). "Developmental patterning genes and their conserved functions: from model organisms to humans." Mol Genet Metab **69**(2): 85-100.

VERBEEK, S., D. IZON, et al. (1995). "An HMG-box-containing T-cell factor required for thymocyte differentiation." Nature **374**(6517): 70-74.

VERHAAK, R. G., C. S. GOUDSWAARD, et al. (2005). "Mutations in nucleophosmin (NPM1) in acute myeloid leukemia (AML): association with other gene abnormalities and previously established gene expression signatures and their favorable prognostic significance." Blood **106**(12): 3747-3754.

VILLEVAL, J. L., P. CRAMER, et al. (1986). "Phenotype of early erythroblastic leukemias." Blood **68**(5): 1167-1174.

WALLACE, C., D. J. SMYTH, et al. (2010). "The imprinted DLK1-MEG3 gene region on chromosome 14q32.2 alters susceptibility to type 1 diabetes." Nat Genet **42**(1): 68-71.

WALSH, J. C., R. P. DEKOTER, et al. (2002). "Cooperative and antagonistic interplay between PU.1 and GATA-2 in the specification of myeloid cell fates." Immunity **17**(5): 665-676.

WANG, K. C., J. A. HELMS, et al. (2009). "Regeneration, repair and remembering identity: the three Rs of Hox gene expression." Trends Cell Biol **19**(6): 268-275.

WANG, W. C. and C. S. SHASHIKANT (2007). "Evidence for positive and negative regulation of the mouse Cdx2 gene." J Exp Zool B Mol Dev Evol **308**(3): 308-321.

WANG, Y., Q. MENG, et al. (2009). "Role of the spleen in cyclophosphamide-induced hematosuppression and extramedullary hematopoiesis in mice." Arch Med Res **40**(4): 249-255.

WANG, Y., A. YABUUCHI, et al. (2008). "Cdx gene deficiency compromises embryonic hematopoiesis in the mouse." Proc Natl Acad Sci U S A **105**(22): 7756-7761.

WANG, Y., F. YATES, et al. (2005). "Embryonic stem cell-derived hematopoietic stem cells." Proc Natl Acad Sci U S A **102**(52): 19081-19086.

WARNER, J. K., J. C. WANG, et al. (2004). "Concepts of human leukemic development." Oncogene **23**(43): 7164-7177.

WEISSMAN, I. L. and J. A. SHIZURU (2008). "The origins of the identification and isolation of hematopoietic stem cells, and their capability to induce donor-specific transplantation tolerance and treat autoimmune diseases." Blood **112**(9): 3543-3553.

WENG, A. P., A. A. FERRANDO, et al. (2004). "Activating mutations of NOTCH1 in human T cell acute lymphoblastic leukemia." Science **306**(5694): 269-271.

WILLERT, K., J. D. BROWN, et al. (2003). "Wnt proteins are lipid-modified and can act as stem cell growth factors." Nature **423**(6938): 448-452.

WINGERT, R. A., R. SELLECK, et al. (2007). "The cdx genes and retinoic acid control the positioning and segmentation of the zebrafish pronephros." PLoS Genet **3**(10): 1922-1938.

WINNIER, G., M. BLESSING, et al. (1995). "Bone morphogenetic protein-4 is required for mesoderm formation and patterning in the mouse." Genes Dev **9**(17): 2105-2116.

WINTJENS, R. and M. ROOMAN (1996). "Structural classification of HTH DNA-binding domains and protein-DNA interaction modes." J Mol Biol **262**(2): 294-313.

WOLBER, F. M., E. LEONARD, et al. (2002). "Roles of spleen and liver in development of the murine hematopoietic system." Exp Hematol **30**(9): 1010-1019.

WONG, N. A., J. WILDING, et al. (2005). "CDX1 is an important molecular mediator of Barrett's metaplasia." Proc Natl Acad Sci U S A **102**(21): 7565-7570.

XU, F., H. LI, et al. (1999). "Cell type-specific autoregulation of the Caudal-related homeobox gene Cdx-2/3." J Biol Chem **274**(48): 34310-34316.

YAN, J., Y. X. CHEN, et al. (2006). "Cdx4 and menin co-regulate Hoxa9 expression in hematopoietic cells." PLoS ONE **1**: e47.

YUASA, Y., H. NAGASAKI, et al. (2005). "Relationship between CDX2 gene methylation and dietary factors in gastric cancer patients." Carcinogenesis **26**(1): 193-200.

ZHANG, X., K. RICE, et al. (2009). "Maternally Expressed Gene 3 (MEG3) Noncoding Ribonucleic Acid: Isoform Structure, Expression, and Functions." Endocrinology.

ZHU, L., S. B. KAHWASH, et al. (1998). "Developmental expression of mouse erythrocyte protein 4.2 mRNA: evidence for specific expression in erythroid cells." Blood **91**(2): 695-705.

ZIMMERMANN, F. and I. N. RICH (1997). "Mammalian homeobox B6 expression can be correlated with erythropoietin production sites and erythropoiesis during development, but not with hematopoietic or nonhematopoietic stem cell populations." Blood **89**(8): 2723-2735.

10. ATTACHMENTS

10.1 Patient Characteristics

10.1.1 AML

AML Subtype	Patient No.	Age	Gender	Karyotype	Other relevant markers	Treatment and outcome	CDX2 Status
t(8:21) AML1-ETO	1	48	M	n.a.	MLL-PTD-	molecular relapse after BMT	+
	2	63	M	45,X,-Y,t(8;21)(q22;q22)	AML1-ETO+, cKIT D816+, LAIP	n.a.	+
	3	70	F	45,X,-X,t(8;21)(q22;q22)	AML1-ETO+, LAIP	n.a.	+
	4	57	F	46,XX,t(8;21)(q22;q22)	AML1-ETO+	n.a.	+
	5	31	M	46,XY,t(8;21)(q22;q22)	AML1-ETO+	n.a.	+
	6	78	F	47,XX,t(8;21)(q22;q22), +13	AML1-ETO+, LAIP	n.a.	-
	7	65	M	46,XY,t(8;21)(q22;q22)	AML1-ETO+	MRD after treatment	-
	8	45	W	45,X,-X,t(8;21)(q22;q22)	AML1-ETO+, LAIP	n.a.	+
	9	38	M	46,XY,t(8;21)(q22;q22)	AML1-ETO+, LAIP	n.a.	-
	10	64	W	45,X,-X,t(8;21)(q22;q22),del(9)(q22)	AML1-ETO+, Jak-2 Mutation, LAIP	death 3 months after diagnosis without relapse	+
	11	54	W	complex aberrant	AML1-ETO+, cKIT D816+, LAIP	n.a.	-
	12	42	W	45,X,-X,t(8;21)(q22;q22)	AML1-ETO+, LAIP	n.a.	+
	13	57	W	47,XX,+8,t(8;21)(q22;q22)	AML1-ETO+, LAIP	n.a.	-
	14	78	M	45,X,-Y,t(8;21)(q22;q22)	AML1-ETO+, PML-RARA+, LAIP	n.a.	-
	15	37	W	46,XX,t(8;21)(q22;q22)	AML1-ETO+, LAIP	relapse 23 month after diagnosis, alive 29 month after diagnosis	+
	16	38	M	45,X,-Y,t(8;21)(q22;q22)	AML1-ETO+, BCR-ABL+, LAIP	n.a.	-
	17	54	M	46,XY,t(8;21)(q22;q22)	AML1-ETO+, LAIP	n.a.	-
	18	51	M	46,XY,t(8;21)(q22;q22)	AML1-ETO+, LAIP	n.a.	-
	19	41	M	46,XY,t(8;21)(q22;q22)	AML1-ETO+, LAIP	n.a.	-
	20	41	W	45,X,-X,t(8;21)(q22;q22), t(9;22)	AML1-ETO+, BCR-ABL+, NRAS-Mutation (Codon12)+, LAIP	n.a.	-
	21	41	M	46,XY,t(8;21)(q22;q22), t(1;3)	AML1-ETO+, LAIP	n.a.	+
	22	52	W	46,XX,t(8;21)(q22;q22), del9	AML1-ETO+, NRAS-Mutation (Codon61)+, LAIP	n.a.	-
	23	61	M	45,X,-Y,t(8;21)(q22;q22)	AML1-ETO+, LAIP	n.a.	-
	24	39	M	46,XY,t(8;21)(q22;q22)	AML1-ETO+, LAIP	n.a.	+
AML NK NPMc+	25	59	W	46,XX	NPM1+, LAIP	n.a.	+
	26	47	M	46,XY	NPM1+, FLT3-ITD+	n.a.	+
	27	66	W	46,XX	NPM1+, LAIP	n.a.	+
	28	53	M	46,XY	NPM1+, FLT3-ITD+	n.a.	+
	29	66	W	46,XX	NPM1+, LAIP	secondary to CMML	+
	30	77	M	46,XY	NPM1+	n.a.	+
	31	56	W	46,XX	NPM1+, LAIP	n.a.	+
	32	77	M	48,XY,+8,+8 [9]/49,idem,+8[6]/46,XY[8]	NPM1+, FLT3-ITD+, LAIP	n.a.	+

AML Subtype	Patient No.	Age	Gender	Karyotype	Other relevant markers	Treatment and outcome	CDX2 Status
	33	71	W	46,XX	NPM1+, FLT3-ITD+, LAIP	n.a.	+
	34	60	W	46,XX	NPM1+, FLT3-D835+	n.a.	+
	35	55	W	46,XX	NPM1+	n.a.	+
	36	48	M	46,XY	NPM1+, FLT3-ITD+, LAIP	n.a.	+
	37	42	W	46,XX	NPM1+, LAIP	n.a.	-
	38	58	M	46,XY	NPM1+, LAIP	n.a.	+
	39	65	W	46,XX	NPM1+, FLT3-D835+, LAIP	n.a.	+
	40	49	M	46,XY	NPM1+	n.a.	+
	41	43	M	46,XY	NPM1+, LAIP	n.a.	+
	42	65	W	46,XX	NPM1+, FLT3-ITD+, LAIP	n.a.	-
	43	63	W	46,XX	NPM1+, FLT3-D835+, LAIP	n.a.	-
	44	61	W	46,XX	NPM1+, FLT3-ITD+, LAIP	n.a.	+
	45	76	W	46,XX	NPM1+	n.a.	-
	46	69	W	46,XX	NPM1+, FLT3-ITD+	n.a.	+
	47	60	M	46,XY	NPM1+, FLT3-ITD+	n.a.	+
	48	39	W	46,XX	NPM1+, FLT3-ITD+, LAIP	n.a.	+
	49	82	M	46,XY	NPM1+, FLT3-D835+, LAIP	secondary to MDS	+
	50	49	M	46,XY	NPM1+	BMT 3 month after diagnosis, relapse and death 14 month after BMT	+
	51	47	M	46,XY	NPM1+, FLT3-ITD+	relapse 9 month after diagnosis	+
	52	71	M	46,XY	NPM1+, FLT3-ITD+, CEBPA+, LAIP	relapse 7 month after diagnosis, death 8 month after diagnosis	+
	53	80	W	46,XX	NPM1+, NRAS-Mutation (Codon12)+	death 1 month after diagnosis	+
	54	60	W	46,XX	NPM1+	n.a.	+
	55	33	M	46,XY	NPM1+, LAIP	alive 26 month after diagnosis	+
	56	58	M	46,XY	NPM1+, FLT3-ITD+, LAIP	n.a.	+
	57	60	M	46,XY	NPM1+, LAIP	n.a.	+
	58	68	M	46,XY	NPM1+, FLT3-ITD+, LAIP	relapse 7 month after diagnosis, death 9 month after diagnosis	+
	59	61	W	46,XX	NPM1+, FLT3-ITD+, LAIP	n.a.	+
	60	69	W	46,XX	NPM1+, FLT3-ITD+, LAIP	n.a.	+
	61	37	W	46,XX	NPM1+, LAIP	n.a.	+
	62	58	M	46,XY	NPM1+, NRAS-Mutation (Codon12)+, LAIP	n.a.	+
	63	57	W	46,XX	NPM1+, FLT3-D835+, LAIP	alive 6 month after diagnosis	+
	64	30	W	46,XX	NPM1+, CEBPA+, LAIP	n.a.	+
	65	81	M	46,XY	NPM1+, FLT3-ITD+, LAIP	n.a.	+
	66	39	W	46,XX	NPM1+, NRAS-Mutation (Codon12)+, LAIP	n.a.	+
	67	39	W	46,XX	NPM1+, LAIP	BMT 8 month after diagnosis, alive 9 month after diagnosis	+
	68	77	W	46,XX	NPM1+, LAIP	n.a.	+
	69	48	W	46,XX	NPM1+, FLT3-D835+, LAIP	n.a.	+

AML Subtype	Patient No.	Age	Gender	Karyotype	Other relevant markers	Treatment and outcome	CDX2 Status
AML NK NPMc-	70	79	M	46,XY	NPM1-	death 2 weeks after diagnosis	+
	71	68	M	46,XY	NPM1-	relapse 10 month after diagnosis, death 16 month after diagnosis	+
	72	59	M	46,XY	NPM1-	death 2 month after diagnosis	+
	73	76	M	46,XY	NPM1-	death 11 month after diagnosis	+
	74	65	M	46,XY	NPM1-	secondary to MDS, death 13 month after diagnosis	+
	75	58	M	46,XY	LAIP	secondary to MDS, alive 12 month after diagnosis	+
	76	70	W	46,XX	LAIP	relapse 15 month after diagnosis, death 26 month after diagnosis	+
	77	32	M	46,XY	LAIP	autologous PBSCT 5 month after diagnosis, relapse 9 month after diagnosis, BMT 12 month after diagnosis, alive 33 month after diagnosis	+
	78	63	M	46,XY	MLL-PTD+, LAIP	death 1 month after diagnosis	+
	79	39	M	46,XY	LAIP	alive 23 month after diagnosis	+
	80	69	W	46,XX	NPM1-	secondary to CMML, death 3 month after diagnosis of AML	+
	81	45	M	46,XY	LAIP	n.a.	+
	82	72	M	46,XY	LAIP	secondary to MDS, death 2 month after diagnosis of AML	+
	83	71	M	46,XY	NRAS-Mutation (Codon61)+, EVI1+	death 1 month after diagnosis	+
	84	72	M	46,XY	MLL-PTD+, LAIP	relapse 4 month after diagnosis, death 7 month after diagnosis	+
	85	72	M	46,XY	FLT3-ITD+, LAIP	n.a.	+
	86	72	M	46,XY	FLT3-ITD+, MLL-PTD+, LAIP	n.a.	+
	87	55	M	46,XY	FLT3-ITD+, LAIP	BMT 5 month after diagnosis, relapse and death 7 month after diagnosis	+
	88	61	W	46,XX	FLT3-ITD+	alive 3 month after diagnosis	+
	89	57	W	46,XX	NPM1-	alive 2 month after diagnosis	-
	90	28	M	46,XY	CEBPA+, LAIP	n.a.	+
	91	66	M	46,XY	LAIP	secondary to MDS	+
	92	75	M	46,XY	FLT3-D324+, LAIP	refractory to induction therapy, death 1 month after diagnosis	+
	93	78	M	46,XY	LAIP	alive 1 month after diagnosis	+
	94	32	W	46,XX	CEBPA+, LAIP	alive 3 month after diagnosis	+
	95	79	M	46,XY	LAIP	n.a.	+
t(15;17) PML-RARα	96	81	M	46,XY, t(15;17)(q22;q21)	PML-RARA+, LAIP	n.a.	+
	97	66	M	47,XY,+8,t(15;17)(q22;q21)	PML-RARA+, FLT3-ITD+, LAIP	n.a.	-
	98	28	W	46,XX, t(15;17)(q22;q21), der15	PML-RARA+, LAIP	n.a.	+
	99	44	W	46,XX, t(15;17)(q22;q21)	PML-RARA+, FLT3-ITD+, LAIP	n.a.	+
	100	54	W	46,XX, t(15;17)(q22;q21)	PML-RARA+, FLT3-ITD+	n.a.	-
	101	70	W	46,XX, t(15;17)(q22;q21)	PML-RARA+, FLT3-ITD+, LAIP	n.a.	+

AML Subtype	Patient No.	Age	Gender	Karyotype	Other relevant markers	Treatment and outcome	CDX2 Status
	102	38	M	46,XY, t(15;17)(q22;q21)	PML-RARA+, FLT3-ITD+, LAIP	n.a.	+
	103	64	M	46,XY, t(15;17)(q22;q21)	PML-RARA+, LAIP	n.a.	+
	104	54	W	46,XX, t(15;17)(q22;q21)	PML-RARA+, FLT3-ITD+	n.a.	+
	105	69	W	46,XX, t(15;17)(q22;q21), del9, der10	PML-RARA+, LAIP	n.a.	+
11q23 MLL-Rearr.	106	43	W	n.a.	MLL-AF9+	n.a.	-
	107	33	W	46,XX,t(6;11)(q27;q23)	MLL-AF6+, FLT3-ITD+	alive 14 months after diagnosis	+
	108	36	M	46,XY,t(9;11)(;q23)	MLL-AF9+; LAIP	after BMT AML in CR	-
	109	23	W	46,XX,t(9;11)(;q23)	MLL-AF9+; FLT3-ITD+, LAIP	n.a.	-
	110	48	W	46,XX,t(9;11)(;q23)	MLL-AF9+; MLL-PTD+, LAIP	n.a.	+
	111	25	M	47,XY,t(3;6;11)(q13;q27; q23),der(14)t(14;17)(p11; ?),+21[12]	MLL-AF6+; MLL-PTD+, LAIP	n.a.	+
inv(16)	112	82	W	46,XX,inv(16)(p13q22)	CBFβ-MYH11+, NRAS-Mutation (Codon12)+, LAIP	n.a.	+
	113	60	W	47,XX,+8,inv(16)(p13q22)	CBFβ-MYH11+, LAIP	n.a.	-
	114	37	M	46,XX,-21,+22,inv(16)(p13q22)	CBFβ-MYH11+, LAIP	n.a.	+
	115	17	M	46,XY,inv(16)(p13q22)[	CBFβ-MYH11+, LAIP	n.a.	+

10.1.2 ALL

ALL Subtype	Patient No.	Age	Gender	Karyotype	Other Relevant Markers	Treatment and Outcome	WBC [/µl]	CDX2 Status.
Pre-B/c-ALL	1	49	F	46,XX		n.a.	n.a.	+
	2	22	F	48,XX,+X,+7		n.a.	n.a.	-
	3	62	F	46,XX		n.a.	n.a.	+
	4	26	F	46,XX,del(2)(q12q14)		still in CR 56 months after diagnosis	n.a.	+
	5	34	M	44,XY,t(2;10)(p25;q24), del(5)(q13q31),dic(7;17)(p11;p11), dic(9;12)(p11;p11),del(9)(q11), der(20)t(9;20)(q21;p13)		death 9 months after diagnosis	9000	+
	6	48	M	46,XY		death 56 months after diagnosis		+
	7	40	M	46,XY		death 27 months after diagnosis	2040	-
	8	34	M	46,XY		n.a.	15900	+
	9	25	F	46,XX,+8,dic(9;12)(p13;p11)		alive 53 months after diagnosis		+
	10	21	M	46,XY		alive 19 months after diagnosis	31000	+
Ph+ ALL	11	36	M	46,XY,t(9;22)(q34;q11)	Ph+	alive 77 months after diagnosis	8800	-
	12	82	M	46,XY,t(1;4;11;8)(p11;q33;p12;p11), t(9;22)(q34;q11)	Ph+	n.a.	56500	-
	13	57	M	46,XY,der(9)t(9;22)(q34;q11)t(9;22)(p11 ;q11), der(22)t(9;22)(q34;q11)	Ph+	death 4 months after diagnosis		+
	14	38	M	45,X,-Y,t(9;22)(q34;q11),i(9)(q10), der(16)t(1;16)(q21;q13)	Ph+	death 15 months after diagnosis	26300	+

ALL Subtype	Patient No.	Age	Gender	Karyotype	Other Relevant Markers	Treatment and Outcome	WBC [/µl]	CDX2 Status.
	15	43	M	46,XY,t(9;22)(q34;q11),del(9)(p22)	Ph+	death 4 months after diagnosis	400	+
	16	66	M	46,XY,t(9;22)(q34;q11)	Ph+	alive 09/2002	47900	+
	17	83	F	46,XX,t(9;22)(q34;q11),t(9;11)(p22;q25)	Ph+	n.a.	n.a.	+
	18	58	F	51,XX,+5,+6,i(7)(q10),+8,t(9;22)(q34;q11), +15,+der(22)t(9;22)	Ph+	n.a.	n.a.	-
	19	29	F	46,XX,der(7;9)(q10;q10)t(9;22)(q34;q11), der(7;9)(p10;p10)del(7)(p?)del(9)(p?)	Ph+, FLT3 D324	CR 16 months after diagnosis, alive 44 months after diagnosis	n.a.	+
	20	62	F	46,XX,der(9)t(4;9)(q31;q34)del(9)(p13)(ABL-),del(10)(q24),der(19)t(19;22)(q13;q11)(BCR+,ABL+,BCRconABL,BCR+), der(22)t(9;22)(ABL+)	Ph+	death 7 months after diagnosis	63600	+
	21	72	F	46,XX,t(9;22)(q34;q11)	Ph+	n.a.	39510	+
	22	77	F	46,XX,t(4;11)(q21;q23)	MLL-AF4	n.a.	n.a.	+
	23	47	F	46,XX,t(4;11)(q21;q23)	MLL-AF4	alive 11/201	n.a.	+
	24	64	F	46,XX,t(4;11)(q21;q23)	MLL-AF4	CR 6 months after diagnosis, death 25 months after diagnosis	n.a.	+
Pro-B-ALL	25	40	F	46,XX,t(4;11)(q21;q23)	MLL-AF4	alive 4 months after diagnosis	48740	+
	26	53	F	n.a.	MLL-AF4	death 7 months after diagnosis	17500	+
	27	39	M	47,XY,+X,t(11;19)(q23;p13)	MLL-ENL	alive 25 months after diagnosis	124600	+
	28	62	M	46,XY,t(4;11)(q21;q23)	MLL-AF4	CR 12 months after diagnosis	n.a.	+
	29	34	M	47,XY,+X,t(4;11)(q21;q23)	MLL-AF4	n.a.	n.a.	+
	30	61	F	46,XX,t(4;11)(q21;q23)	MLL-AF4	n.a.	n.a.	+
	31	42	F	46,XX,del(2)(q31),t(8;14)(q24;q32), der(11)dup(11)(q21q25)t(2;11)(q31;q25)	IgH-cMYC-Rearr.	n.a.	n.a.	-
	32	54	M	46,XY,dup(7)(q11q36),t(8;14)(q24;q32)	IgH-cMYC-Rearr.	n.a.	n.a.	-
	33	61	F	46,XX,dup(1)(q21q44),der(1)t(1;9)(p36;q?), der(3)del(3)(p21)t(1;3)(q25;q25), der(6)t(3;6)(p21;q24),	IgH-cMYC-Rearr.	n.a.	n.a.	-
	34	34	F	46,XX,t(8;14)(q24;q32)	IgH-cMYC-Rearr.	n.a.	n.a.	-
	35	80	F	46,XX,dup(1)(q11q44),der(2)t(2;11)(p25;q23), t(3;9;14)(q27;p13;q32),t(8;14)(q24;q32), del(11)(q11q23),der(22)t(11;22)(q23;q13)	IgH-cMYC-Rearr.	n.a.	n.a.	-
B-ALL/ Burkitt	36	72	F	49,X,del(X)(q24),+7,+8,t(8;14)(q24;q32),ider(13)(q10)dup(13q?q?)t(13;14)(q34;q24) t(14;18)(q32;q21),der(14)t(X;14)(q26;q24), der(18)t(14;18)(q32;q21),+17	FLT3 D324, IgH-cMYC-Rearr., IgH-BCL2-Rearr.	n.a.	n.a.	-
	37	79	M	46,XY,t(8;14)(q24;q32)	IgH-cMYC-Rearr.	n.a.	n.a.	-
	38	40	M	47-51,XY,dup(1)(q21q44),+2,del(2)(q21), +7,t(8;14)(q24;q32),+13,+15,+16	IgH-cMYC-Rearr.	03/2002 in CR	n.a.	-
	39	27	M	48,XY,+Y,+i(7)(q10),t(8;14)(q24;q32), der(17)t(1;17)(q12;p13) [13] 49,XY,+Y, +i(7)(q10),t(8;14)(q24;q32), +der(14)t(8;14) [4]	IgH-cMYC-Rearr.	n.a.	n.a.	-

ALL Subtype	Patient No.	Age	Gender	Karyotype	Other Relevant Markers	Treatment and Outcome	WBC [/µl]	CDX2 Status.
	40	26	M	46,XY,dup(1)(q21q44),t(8;14)(q24;q32), inv(13)(p11q21)	IgH-cMYC-Rearr.	12/2006 in CR	n.a.	-
Pre-T-ALL	41	46	M	47,XY,t(10;11)(p12;q21),+13	CALM-AF10	relaps 5 months after diagnosis, death 6 months after diagnosis	n.a.	+
	42	70	F	46,XX,t(2;9)(q37;p11),t(3;7)(q27;p11), del(13)(q?)		n.a.	7020	+
	43	56	F	46,XX,der(5)t(4;5)(q25;q15)		07/2002 in CR	n.a.	+
	44	34	M	46,XY,t(10;11)(p12;q13),del(12)(p11)	CALM-AF10	n.a.	1136	-
	45	27	M	46,XY		03/2004 in CR	85000	+
	46	52	F	46,XX		08/2004 in CR	1570	-
	47	54	M	46,XY,t(2;14)(p25;q11)		BMT, 11/2004 in CR	n.a.	-
Cortical T-ALL	48	39	M	46,XY		n.a.	1120	-
	49	29	M	46,XY,t(1;14)(p34;q11),der(9)t(9;16)(p22;q22), der(16)t(7;16)(?;p13)t(9;16)(p22;q22)		01/2003 in CR	158600	-
	50	62	M	n.a.		n.a.	8250	-
	51	38	M	n.a.		BMT, 08/2004 in CR	18900	-
	52	22	F	46,XX		n.a.		-
	53	37	M	46,XY,del(6)(q21),i(9)(q10)		n.a.	73800	-
	54	46	M	46,XY,t(5;7)(q35;q22),del(9)(p13)	TLX-Rearr.	04/2005 in CR	49400	-
	55	24	M	47,XY,t(7;14)(q35;q11),+16		n.a.	310000	-
	56	42	M	46,XY,del(9)(p13),t(10;14)(q24;q11)		n.a.	101000	-
	57	29	M	46,XY	FLT3 D324	n.a.	90700	-

10.2 Alignment of CDX2 and CDX4

CDX2 and CDX4 share 46.3% and 44.6% similarity at the protein level in mouse and human, respectively (EMBOSS/needle method for pairwise global alignment, http://www.ebi.ac.uk/Tools/emboss/align/index.html). The DNA-binding homeodomain is highly conserved whereas the N- and C-termini are more divergent.

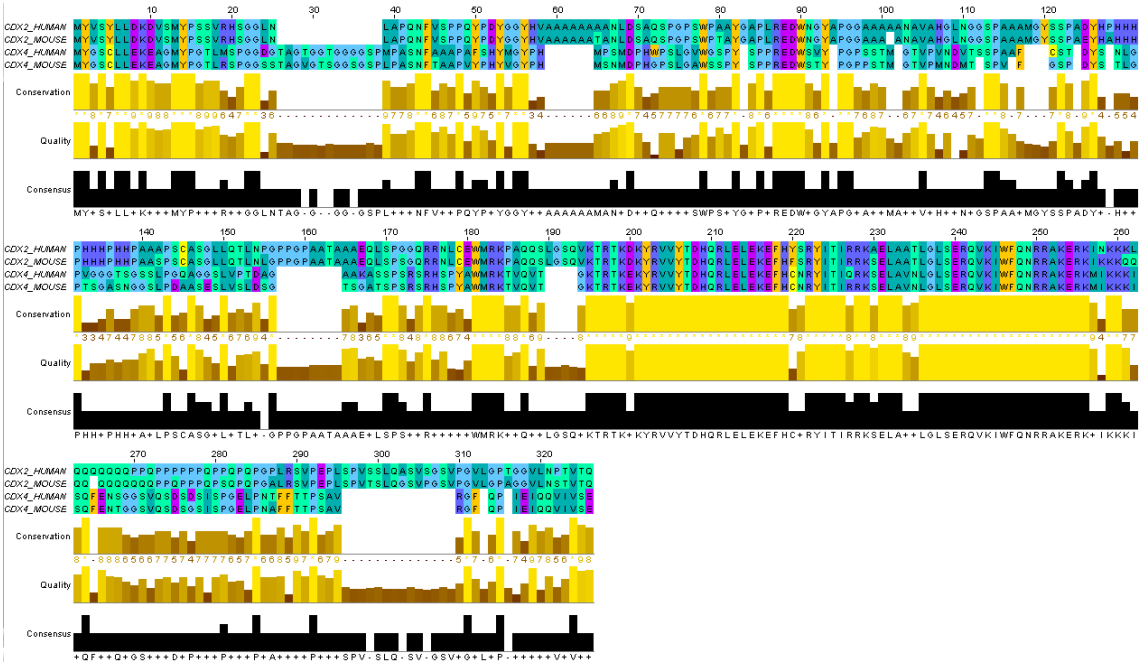

Figure 76: Alignment of human and murine protein sequences of CDX2 and CDX4.
The alignment of the protein sequences of CDX2 NM_001265, Cdx2 NM_007673, CDX4 NM_005193 and Cdx4 NM_007674 was performed using the multiple sequence alignment program T-Coffee (available on http://www.ebi.ac.uk/Tools/t-coffee/index.html) and edited by Jalview. The amino acids were colored according to their physicochemical properties: aliphatic/ hydrophobic (ILVAM) dark green, aromatic (FWY) orange, positive (KRH) dark blue, negative (DE) violet, hydrophilic (STNQ) light green, conformationally special (PG) light blue and cysteine (C) yellow.

10.3 Heatmaps of Differentially Regulated Genes in *Cdx2*- and *Cdx4*-transduced murine BM progenitors.

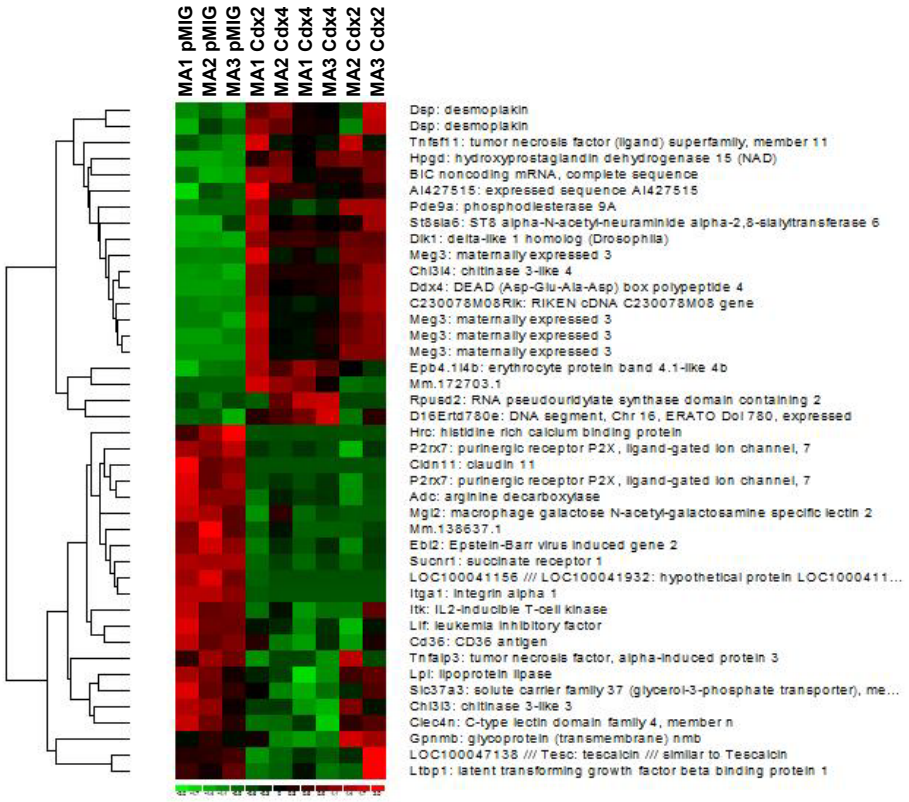

Figure 77: Genes significantly deregulated in *Cdx4*-transduced BM cells compared to empty pMIG-transduced cells.

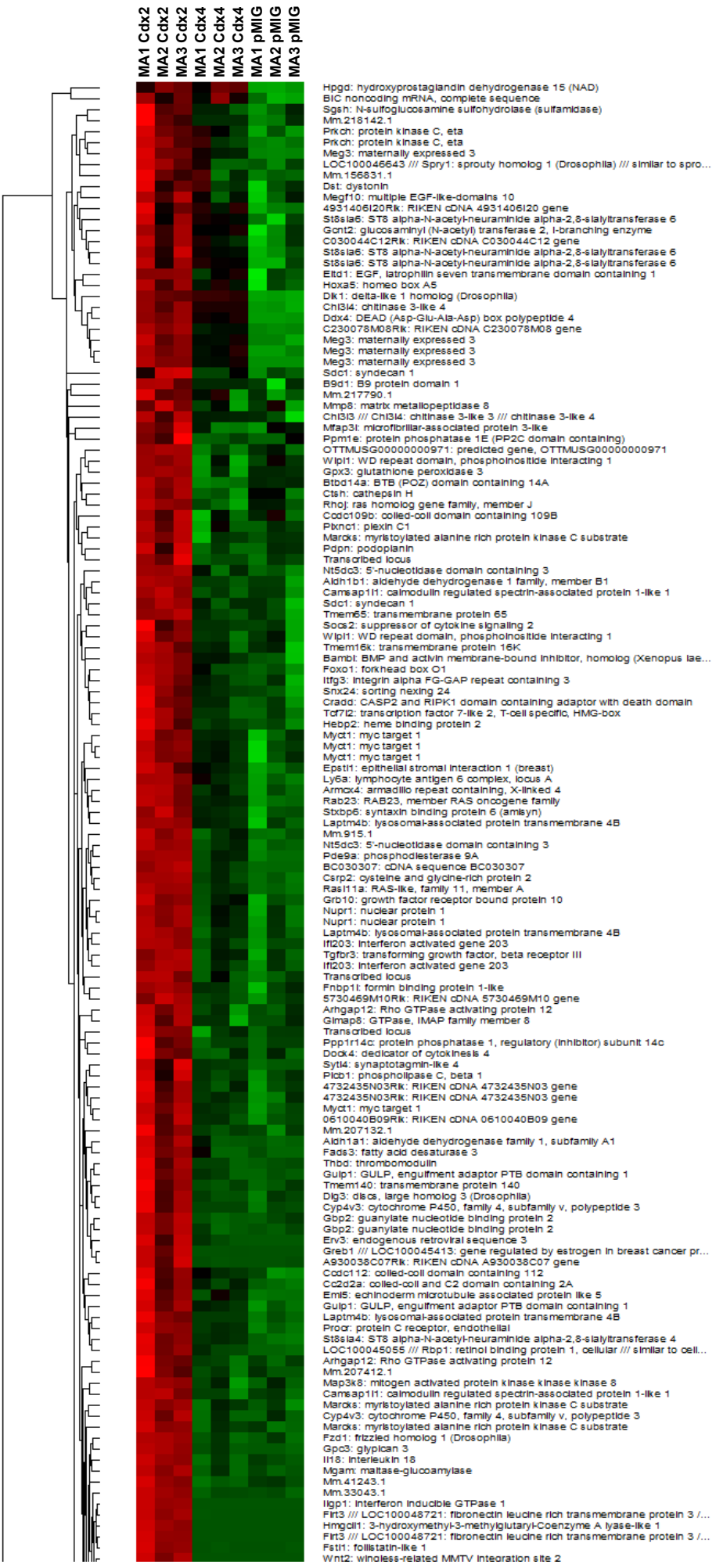
MA1 Cdx2
MA2 Cdx2
MA3 Cdx2
MA1 Cdx4
MA2 Cdx4
MA3 Cdx4
MA1 pMIG
MA2 pMIG
MA3 pMIG
Hpgd: hydroxyprostaglandin dehydrogenase 15 (NAD)
BIC noncoding mRNA, complete sequence
Sgsh: N-sulfoglucosamine sulfohydrolase (sulfamidase)
Mm.218142.1
Prkch: protein kinase C, eta
Prkch: protein kinase C, eta
Meg3: maternally expressed 3
LOC100046643 /// Spry1: sprouty homolog 1 (Drosophila) /// similar to spro...
Mm.156831.1
Dst: dystonin
Megf10: multiple EGF-like-domains 10
4931406I20Rik: RIKEN cDNA 4931406I20 gene
St8sia6: ST8 alpha-N-acetyl-neuraminide alpha-2,8-sialyltransferase 6
Gcnt2: glucosaminyl (N-acetyl) transferase 2, I-branching enzyme
C030044C12Rik: RIKEN cDNA C030044C12 gene
St8sia6: ST8 alpha-N-acetyl-neuraminide alpha-2,8-sialyltransferase 6
St8sia6: ST8 alpha-N-acetyl-neuraminide alpha-2,8-sialyltransferase 6
Eltd1: EGF, latrophilin seven transmembrane domain containing 1
Hoxa5: homeo box A5
Dlk1: delta-like 1 homolog (Drosophila)
Chi3l4: chitinase 3-like 4
Ddx4: DEAD (Asp-Glu-Ala-Asp) box polypeptide 4
C230078M08Rik: RIKEN cDNA C230078M08 gene
Meg3: maternally expressed 3
Meg3: maternally expressed 3
Meg3: maternally expressed 3
Sdc1: syndecan 1
B9d1: B9 protein domain 1
Mm.217790.1
Mmp8: matrix metallopeptidase 8
Chi3l3 /// Chi3l4: chitinase 3-like 3 /// chitinase 3-like 4
Mfap3l: microfibrillar-associated protein 3-like
Ppm1e: protein phosphatase 1E (PP2C domain containing)
OTTMUSG00000000971: predicted gene, OTTMUSG00000000971
Wipi1: WD repeat domain, phosphoinositide interacting 1
Gpx3: glutathione peroxidase 3
Btbd14a: BTB (POZ) domain containing 14A
Ctsh: cathepsin H
Rhoj: ras homolog gene family, member J
Ccdc109b: colled-coil domain containing 109B
Plxnc1: plexin C1
Marcks: myristoylated alanine rich protein kinase C substrate
Pdpn: podoplanin
Transcribed locus
Nt5dc3: 5'-nucleotidase domain containing 3
Aldh1b1: aldehyde dehydrogenase 1 family, member B1
Camsap1l1: calmodulin regulated spectrin-associated protein 1-like 1
Sdc1: syndecan 1
Tmem65: transmembrane protein 65
Socs2: suppressor of cytokine signaling 2
Wipi1: WD repeat domain, phosphoinositide interacting 1
Tmem16k: transmembrane protein 16K
Bambi: BMP and activin membrane-bound inhibitor, homolog (Xenopus lae...
Foxo1: forkhead box O1
Itfg3: integrin alpha FG-GAP repeat containing 3
Snx24: sorting nexing 24
Cradd: CASP2 and RIPK1 domain containing adaptor with death domain
Tcf7l2: transcription factor 7-like 2, T-cell specific, HMG-box
Hebp2: heme binding protein 2
Myct1: myc target 1
Myct1: myc target 1
Myct1: myc target 1
Epsti1: epithelial stromal interaction 1 (breast)
Ly6a: lymphocyte antigen 6 complex, locus A
Armcx4: armadillo repeat containing, X-linked 4
Rab23: RAB23, member RAS oncogene family
Stxbp6: syntaxin binding protein 6 (amisyn)
Laptm4b: lysosomal-associated protein transmembrane 4B
Mm.915.1
Nt5dc3: 5'-nucleotidase domain containing 3
Pde9a: phosphodiesterase 9A
BC030307: cDNA sequence BC030307
Csrp2: cysteine and glycine-rich protein 2
Rasl11a: RAS-like, family 11, member A
Grb10: growth factor receptor bound protein 10
Nupr1: nuclear protein 1
Nupr1: nuclear protein 1
Laptm4b: lysosomal-associated protein transmembrane 4B
Ifi203: interferon activated gene 203
Tgfbr3: transforming growth factor, beta receptor III
Ifi203: interferon activated gene 203
Transcribed locus
Fnbp1l: formin binding protein 1-like
5730469M10Rik: RIKEN cDNA 5730469M10 gene
Arhgap12: Rho GTPase activating protein 12
Gimap8: GTPase, IMAP family member 8
Transcribed locus
Ppp1r14c: protein phosphatase 1, regulatory (inhibitor) subunit 14c
Dock4: dedicator of cytokinesis 4
Sytl4: synaptotagmin-like 4
Plcb1: phospholipase C, beta 1
4732435N03Rik: RIKEN cDNA 4732435N03 gene
4732435N03Rik: RIKEN cDNA 4732435N03 gene
Myct1: myc target 1
0610040B09Rik: RIKEN cDNA 0610040B09 gene
Mm.207132.1
Aldh1a1: aldehyde dehydrogenase family 1, subfamily A1
Fads3: fatty acid desaturase 3
Thbd: thrombomodulin
Gulp1: GULP, engulfment adaptor PTB domain containing 1
Tmem140: transmembrane protein 140
Dlg3: discs, large homolog 3 (Drosophila)
Cyp4v3: cytochrome P450, family 4, subfamily v, polypeptide 3
Gbp2: guanylate nucleotide binding protein 2
Gbp2: guanylate nucleotide binding protein 2
Erv3: endogenous retroviral sequence 3
Greb1 /// LOC100045413: gene regulated by estrogen in breast cancer pr...
A930038C07Rik: RIKEN cDNA A930038C07 gene
Ccdc112: colled-coil domain containing 112
Cc2d2a: colled-coil and C2 domain containing 2A
Eml5: echinoderm microtubule associated protein like 5
Gulp1: GULP, engulfment adaptor PTB domain containing 1
Laptm4b: lysosomal-associated protein transmembrane 4B
Procr: protein C receptor, endothelial
St8sia4: ST8 alpha-N-acetyl-neuraminide alpha-2,8-sialyltransferase 4
LOC100045055 /// Rbp1: retinol binding protein 1, cellular /// similar to cell...
Arhgap12: Rho GTPase activating protein 12
Mm.207412.1
Map3k8: mitogen activated protein kinase kinase kinase 8
Camsap1l1: calmodulin regulated spectrin-associated protein 1-like 1
Marcks: myristoylated alanine rich protein kinase C substrate
Cyp4v3: cytochrome P450, family 4, subfamily v, polypeptide 3
Marcks: myristoylated alanine rich protein kinase C substrate
Fzd1: frizzled homolog 1 (Drosophila)
Gpc3: glypican 3
Il18: interleukin 18
Mgam: maltase-glucoamylase
Mm.41243.1
Mm.33043.1
Iigp1: interferon inducible GTPase 1
Flrt3 /// LOC100048721: fibronectin leucine rich transmembrane protein 3 /...
Hmgcll1: 3-hydroxymethyl-3-methylglutaryl-Coenzyme A lyase-like 1
Flrt3 /// LOC100048721: fibronectin leucine rich transmembrane protein 3 /...
Fstl1: follistatin-like 1
Wnt2: wingless-related MMTV integration site 2

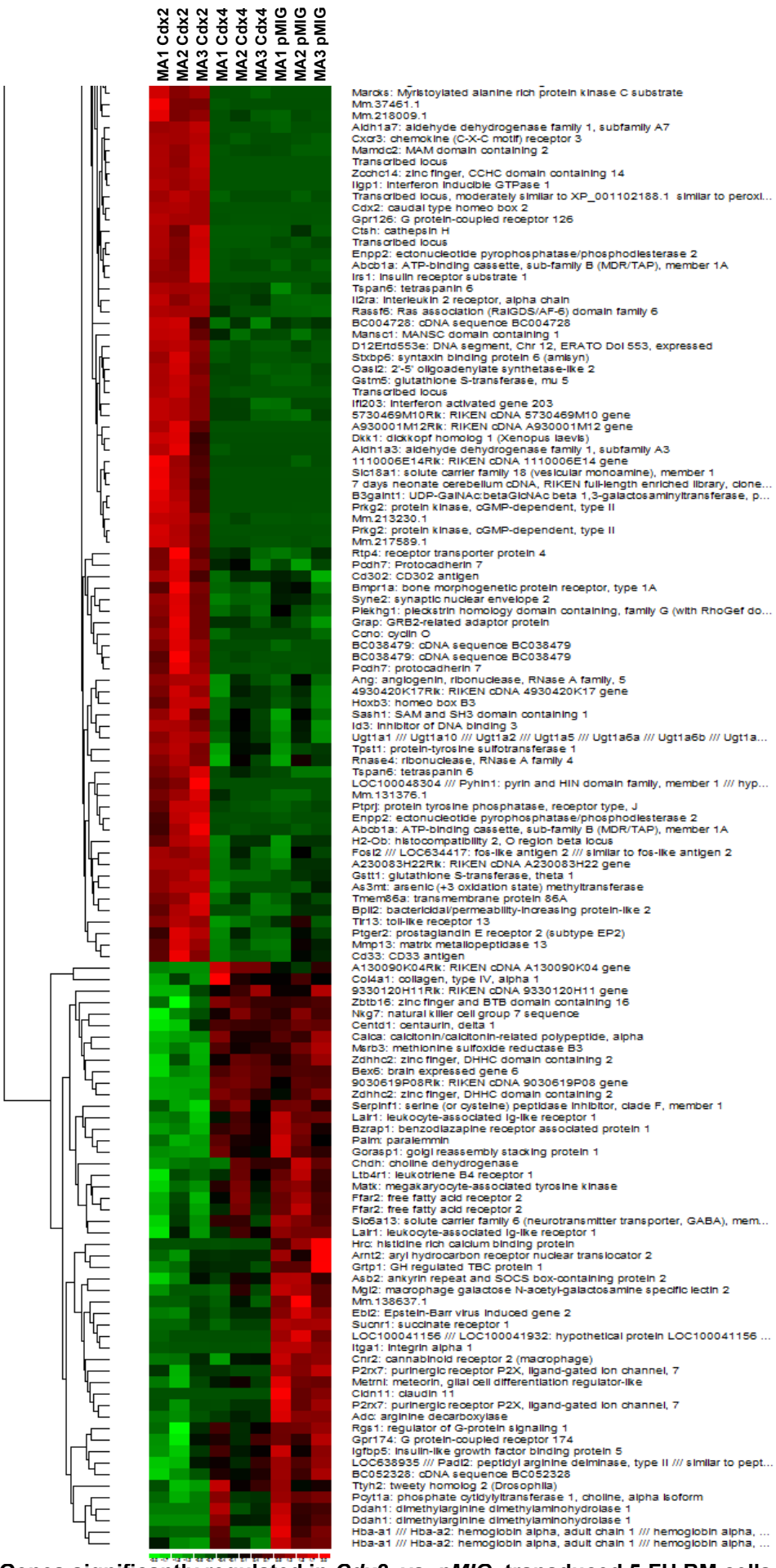

Figure 78: Genes significantly regulated in *Cdx2*- vs. *pMIG*- transduced 5-FU BM cells.

ACKNOWLEDGEMENTS

It is a pleasure to thank the many people who supported me in any respect during the completion of the project.

My sincere gratitude goes to my supervisor Prof. Dr. Christian Buske for the continuous support of my PhD study and research. His inputs and experience were extremely valuable in the completion of this thesis. Special thanks are also due to Prof. Dr. Dirk Eick for the opportunity to conduct my thesis at the Faculty of Biology and the critical reading of this manuscript.

I am deeply indebted to my colleague Jun.-Prof. Dr. Vijay Rawat whose support, valuable comments, suggestions and discussions helped me in all the time of research and writing of this thesis.

I thank my fellow labmates for stimulating discussions and for all the fun we had in the last years in the lab, on congress meetings, during birthday parties and after-work drinks. In particular, I would like to mention Naidu Vegi, who was always helpful in any way and willing to set up experiments also on short notice. I would also like to express my gratitude to our cell-sorting queen Bianka Ksziensik for her expert assistance and Heather McMurtrie for carefully reading and correcting the manuscript.

CURRICULUM VITAE

Personal Information

Name	Silvia Thoene
Birth date	13.07.1980
Birth place	Rosenheim, Germany
Nationality	German

Work Experience

since 01/2010	**PhD Student** Institute for Experimental Tumor Research, Comprehensive Cancer Center Ulm, research group of Prof. Christian Buske
11/2005 – 12/2009	**PhD Student** Clinical Cooperation Group "Leukemia" (Cooperation between Helmholtz Center Munich and University Hospital Grosshadern), research group of Prof. Christian Buske

Education

10/2003 – 08/2005	**M.Sc. Biochemistry** Technical University of Munich, Germany
10/2000 – 09/2003	**B.Sc. Biochemistry** Technical University of Munich, Germany
06/2000	**Abitur** (University Entrance Qualification) Ignaz-Guenther-Gymnasium Rosenheim, Germany

Publications

von Bubnoff N, Gorantla SP, Engh RA, Oliveira TM, **Thöne S**, Aberg E, Peschel C, Duyster J (2011) *The low frequency of clinical resistance to PDGFR inhibitors in myeloid neoplasms with abnormalities of PDGFRA might be related to the limited repertoire of possible PDGFRA kinase domain mutations in vitro*. **Oncogene** 30(8):933-43.

Rawat VPS, Arseni N, Ahmed F, Mulaw M, **Thoene S**, Heilmeier B, Sadlon T, d'Andreas R, Hiddemann W, Bohlander S, Buske C, Feuring-Buske M (2010) *The Vent-like homeobox gene VENTX promotes human myeloid development and is highly expressed in acute myeloid leukemia*. **PNAS**; 107(39):16946-51.

Thoene S, Rawat VPS, Heilmeier B, Hoster E, Metzeler KH, Herold T, Hiddemann W, Goekbuget N, Hoelzer D, Bohlander SK, Feuring-Buske M, Buske C (2009) *The homeobox gene CDX2 is aberrantly expressed and associated with an inferior prognosis in patients with acute lymphoblastic leukemia.* **Leukemia**; 23(4):649-55.

Rawat VP, **Thoene S**, Naidu VM, Arseni N, Heilmeier B, Metzeler K, Petropoulos K, Deshpande A, Quintanilla-Martinez L, Bohlander SK, Spiekermann K, Hiddemann W, Feuring-Buske M, Buske C (2008) *Overexpression of CDX2 perturbs HOX gene expression in murine progenitors depending on its N-terminal domain and is closely correlated with deregulated HOX gene expression in human acute myeloid leukemia*. **Blood**; 111(1):309-19.

von Bubnoff N, Gorantla SP, **Thöne S**, Peschel C, Duyster J (2006) *The FIP1L1-PDGFRA T674I mutation can be inhibited by the tyrosine kinase inhibitor AMN107 (nilotinib)*. **Blood**; 107(12):4970-1.

Ulbrich SE, Schoenfelder M, **Thoene S**, Einspanier R (2004) *Hyaluronan in the bovine oviduct - modulation of synthases and receptors during the estrous cycle*. **Mol Cell Endocrinol**.; 214(1-2):9-18.

Conference Presentations

10/2010	Talk: annual meeting of the *Deutsche Gesellschaft für Hämatologie* (DGHO), Berlin, Germany
09/2010	Poster: annual meeting of the *Society for Hematology and Stem Cells* (ISEH), Barcelona, Spain
06/2010	Poster: annual meeting of the *European Hematology Association* (EHA), Vienna, Austria
10/2009	Talk: annual meeting of the *Deutsche Gesellschaft für Hämatologie* (DGHO), Mannheim, Germany
09/2009	Poster: annual meeting of the *Society for Hematology and Stem Cells* (ISEH), Athens, Greece
06/2009	Poster: annual meeting of the *European Hematology Association* (EHA), Berlin, Germany
12/2008	Poster: annual meeting of the *American Society of Hematology* (ASH), San Francisco, USA
10/2008	Talk: annual meeting of the *Deutsche Gesellschaft für Hämatologie* (DGHO), Vienna, Austria
06/2008	Poster: annual meeting of the *International Society for Stem Cell Research* (ISSCR), Philadelphia, USA
02/2008	Poster: international symposium *„Acute Leukemias XII“*, Munich, Germany